BIOSYNTHESIS OF THE THIOPEPTINS AND IDENTIFICATION OF AN $F_{420}H_2$-DEPENDENT DEHYDROPIPERIDINE REDUCTASE

A Thesis Presented to The Academic Faculty

By

Hiroyuki Ichikawa

In Partial Fulfillment of the Requirements for the
Degree Doctor of Philosophy in Chemistry

Georgia Institute of Technology

August 2019

Copyright © 2019 by Hiroyuki Ichikawa

Biosynthesis of the thiopeptins and identification of an $F_{420}H_2$-dependent dehydropiperidine reductase

Approved by:

Dr. Wendy L. Kelly, Advisor
School of Chemistry and Biochemistry
Georgia Institute of Technology

Dr. Andreas S. Bommarius
School of Chemical and Biomolecular Engineering
Georgia Institute of Technology

Dr. Julia M. Kubanek
School of Biological Sciences
School of Chemistry and Biochemistry
Georgia Institute of Technology

Dr. Kirill S. Lobachev
School of Biological Sciences
Georgia Institute of Technology

Dr. Adegboyega K. Oyelere
School of Chemistry and Biochemistry
Georgia Institute of Technology

Date Approved: May 9, 2019

ACKNOWLEDGEMENTS

I would like to express my deepest gratitude for my Ph.D. advisor, Dr. Wendy Kelly, for her expertise, guidance, and patience throughout my graduate studies. Her rigor and dedication to science has taught me to apply myself more effectively to research and inspired me to complete my doctorate work. I am extremely grateful for her generosity and support in and outside the lab, especially during the last year of my tenure. I would like to thank my committee members, Dr. Andreas Bommarius, Dr. Julia Kubanek, Dr. Kirill Lobachev, and Dr. Adegboyega Oyerele, for their valuable time, understanding, and expert advice. My appreciation goes to Dr. Christy O'Mahony, Dr. Mary Peek, and Dr. Hui Zhu who have been supportive and immensely accommodating with my teaching schedule.

I am grateful for my friends and colleagues who have made my time at Georgia Institute of Technology a wonderful and memorable experience. It has been a great pleasure to work with former and present members of the Agarwal, Kelly, Oyelere, and Reddi groups. In particular, I would like to thank Dr. Bradley Carpenter, Mr. Iramofu Dominic, Ms. Verjine Khodaverdian, Ms. Osiris Martinez-Guzman, Ms. Ipsita Mohanty, Dr. Marietou Paye, Dr. Idris Raji, Mr. Daniel Sircar, Dr. Hem Thapa, Dr. Arren Washington, and Dr. Feifei Zhang for their support and encouragement.

TABLE OF CONTENTS

LIST OF TABLES

LIST OF FIGURES

LIST OF SCHEMES

LIST OF SYMBOLS AND ABBREVIATIONS

º	degrees
×	times
α	alpha
β	beta
γ	gamma
δ	chemical shift
δ	delta
ε	molar extinction coefficient
λ	lambda
σ	sigma
µg	microgram
µL	microliter
µM	micromolar
µm	micrometer
Å	angstrom
A	alanine
aac(3)IV	apramycin resistance gene
aadA	streptomycin/spectinomycin resistance gene
Abs	absorbance
ADP	adenosine-5'-diphosphate
Ala	alanine
AMP	adenosine-5'-monophosphate
amp	ampicillin
aprR	apramycin resistance gene
ATP	adenosine-5'-triphosphate
AU	absorption units
bp	base pairs
br	broad
ºC	degrees Celsius
C	cysteine
^{13}C	carbon-13
cm	centimeter
COSY	correlation spectroscopy
C q	quaternary carbon
d	doublet
Da	dalton
dd	doublet of doublets
DEPT-135	distortionless enhancement by polarization transfer with a 135º proton pulse
Dha	dehydroalanine
Dhb	dehydrobutyrine
DMSO	dimethyl sulfoxide

DMSO-d_6	deuterated DMSO
DNA	2'-deoxyribonucleic acid
dq	doublet of quartets
E. coli	*Escherichia coli*
EF-Tu	elongation factor Tu
ESI	electrospray ionization
F_0	8-hydroxy-7-desmethyl-5-deazariboflavin
F_{420}	8-hydroxy-7-desmethyl-5-deazariboflavin derivative
F_{420}-0	F_{420} with zero glutamate residues attached
F_{420}-n	F_{420} with "n" glutamate residues attached
$F_{420}H_2$	reduced F_{420}
FAD	flavin adenine dinucleotide
$FADH_2$	reduced FAD
Fbi	F_{420} biosynthetic proteins in mycobacteria
FDOR-B	flavin/deazaflavin oxidoreductase subgroup B
FGD	F_{420}-dependent glucose-6-phosphate dehydrogenase
FMN	flavin mononucleotide
$FMNH_2$	reduced FMN
g	gram
g	gravity
G6P	glucose-6-phosphate
gCOSY	gradient correlation spectroscopy
gDNA	genomic DNA
gHMBC	gradient heteronuclear multiple-bond correlation spectroscopy
gHSQC	gradient heteronuclear single quantum coherence spectroscopy
Glu	glutamic acid
GMP	guanosine-5'-monophospate
GTP	guanosine-5'-triphosphate
GTPase	guanosine-5'-triphosphate hydrolase
h	hour
^1H	proton
HEQ	4-(1-hydroxyethyl)quinoline-2-carboxylic acid
His	histidine
HMBC	heteronuclear multiple-bond correlation spectroscopy
HOMO	highest occupied molecular orbital
HPLC	high performance liquid chromatography
HPLC-MS	high performance liquid chromatography-mass spectrometry
HR	high resolution
HSQC	heteronuclear single quantum coherence spectroscopy
Hz	hertz
I	isoleucine
IC_{50}	half maximal inhibitory concentration
Ile	isoleucine

IR spectroscopy	infrared spectroscopy
J	coupling constant
K	lysine
kDa	kilodalton
kan	kanamycin
kb	kilobase pairs
kcal	kilocalorie
k_{cat}	turnover number
K_D	dissociation constant
kDa	kilodaltons
K_M	Michaelis-Menten constant
L	liter
Leu	leucine
LUMO	lowest unoccupied molecular orbital
m	multiplet
Mb	megabase pairs
mg	milligram
MHz	megahertz
MIC	minimum inhibitory concentration
min	minute
mL	milliliter
mm	millimeter
mM	millimolar
mmol	millimole
mol	mole
mRNA	messenger ribonucleic acid
MRSA	methicillin-resistant *Staphylococcus aureus*
MS	mass spectrometry
MS/MS	tandem mass spectrometry
M. smegmatis	*Mycobacterium smegmatis*
M. tuberculosis	*Mycobacterium tuberculosis*
mult	multiplicity
mV	millivolt
m/z	mass to charge ratio
NAD^+	nicotinamide adenine dinucleotide
$NADP^+$	nicotinamide adenine dinucleotide phosphate
NADPH	reduced $NADP^+$
ng	nanogram
nm	nanometer
nM	nanomolar
NMR	nuclear magnetic resonance
nt	nucleotide
OD_{600}	optical density at 600 nm
orf	open reading frame
oriT	origin of transfer
p	para

p	plasmid
PCR	polymerase chain reaction
P_i	inorganic phosphate
pip	(dehydro)piperidine
pK_a	acid dissociation constant at logarithmic scale
PLP	pyridoxal 5'-phosphate
PP_i	inorganic pyrophosphate
q	quartet
Q	quinaldic acid
RiPPs	ribosomally-synthesized and post-translationally modified peptides
RNA	ribonucleic acid
ROESY	rotating frame nuclear overhauser effect spectroscopy
rpm	revolutions per minute
S	serine
s	second
SAM	*S*-adenosyl-L-methionine
SDS-PAGE	sodium dodecyl sulfate polyacrylamide gel electrophoresis
sio	siomycin biosynthetic gene
S. laurentii	*Streptomyces laurentii* ATCC 31255
sp.	species
S. tateyamensis	*Streptomyces tateyamensis* ATCC 21389
T	threonine
t	triplet
tbt	thiomuracin biosynthetic gene
TE buffer	Tris-EDTA buffer
TES buffer	*N*-[tris(hydroxymethyl)methyl]-2-aminoethanesulfonic acid buffer
Thr	threonine
Thz	thiazole
tpn	thiopeptin biosynthetic gene
t_R	retention time
tRNA	transfer ribonucleic acid
tsr	thiostrepton biosynthetic gene
Tzn	thiazoline
UV-Vis	ultraviolet-visible
V	valine
Val	valine
VRE	vancomycin-resistant *Enterococcus faecium*
w/v	weight per volume

SUMMARY

Thiopeptins are highly decorated thiopeptide antibiotics similar in structure to thiostrepton A and harbor two unusual features. All thiopeptins contain a thioamide, a rare moiety among natural products, and a subset of thiopeptins present with a piperidine in the core macrocycle rather than the more oxidized dehydropiperidine or pyridine rings typically observed in the thiopeptides. Here, we report the identification of the thiopeptin biosynthetic gene (*tpn*) cluster in *Streptomyces tateyamensis* and the gene products, TpnLMNW.

TpnW shows sequence similarity to transaminases and is likely involved in the biosynthesis of the 4-(1-hydroxyethyl)quinoline-2-carboxylic acid (HEQ) moiety of thiopeptin. HEQ is derived from L-tryptophan and the second step of HEQ biosynthesis requires a transaminase that catalyzes the conversion of 2-methyl-L-tryptophan to 3-(2-methylindolyl)pyruvate. *In vitro* reconstitution of TpnW activity confirmed that this enzyme is a 2-methyl-L-tryptophan aminotransferase. TpnW is able to utilize 3-indolylpyruvate, *p*-hydroxyphenylpyruvate, and phenylpyruvate as α-keto acid acceptors but not pyruvate, oxaloacetate, or α-ketoglutarate.

TpnMN share homology to YcaO and TfuA proteins, respectively, responsible for thioamidation of peptidic substrates. Heterologous expression of TpnMN in the thiostrepton A producer, *Streptomyces laurentii* (*S. laurentii*), led to the production of a metabolite with a mass matching a thioamidated thiostrepton A. Structural characterization of this metabolite is still required to determine if it contains a thioamide suggested by the proposed functions of TpnMN.

TpnL shows sequence similarity to (deaza)flavin-dependent oxidoreductases. Heterologous expression of TpnL in the thiostrepton A producer, *S. laurentii*, led to the production of a piperidine-containing analog. Binding studies revealed TpnL preferentially binds the deazaflavin cofactor, coenzyme F_{420}, and *in vitro* reconstitution of TpnL activity confirmed that this enzyme is an $F_{420}H_2$-dependent dehydropiperidine reductase. The identification of TpnL and its activity establishes the basis for the piperidine-containing series *a* thiopeptides, one of the five main structural groups of this diverse family of antibiotics. This work was published in *J. Am. Chem. Soc.* in 2018.

CHAPTER 1: INTRODUCTION

1.1 Thiopeptides

Thiopeptides (examples shown in Figure 1.1 **1**-**6**), or polythiazolylpeptides, are ribosomally-synthesized and post-translationally modified peptides (RiPPs) with extensive chemical modifications that impart potent antibacterial, antimalarial, and anticancer properties.[1-3] Thiopeptides are distinguished from other peptide metabolites by their six-membered nitrogenous heterocycle that completes a rigid macrocyclic core found in all thiopeptides. The macrocyclic scaffold is decorated by azol(in)es and dehydrated amino acids such as dehydroalanine (Dha) and dehydrobutyrine (Dhb). Some thiopeptides present with a second macrocycle containing a quinaldic acid or indolic acid.

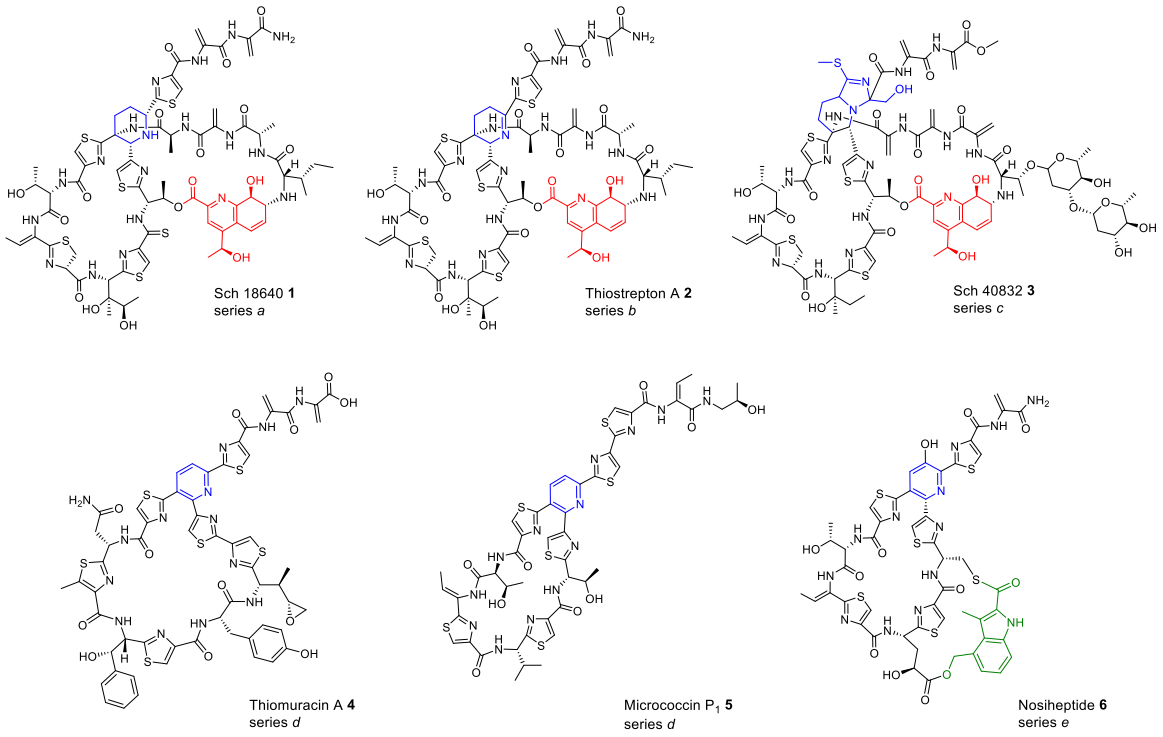

Figure 1.1: Examples of thiopeptides isolated from various Gram-positive bacteria; Sch 18640 (**1**), thiostrepton A (**2**), Sch 40832 (**3**), thiomuracin A (**4**), micrococcin P_1 (**5**), and nosiheptide (**6**).[4-10] The central nitrogenous heterocycle that completes the main macrocycle common in all thiopeptides is in blue. Some thiopeptides have a second loop that contains either a quinaldic acid (shown in red) or an indolic acid (shown in green).

Since the discovery of the first thiopeptide, micrococcin (**5**), in 1948, dozens of thiopeptides were isolated from Gram-positive bacteria of both terrestrial and marine origin.[7, 11-13] The complex structure of thiopeptides, however, has made structural characterization a difficult task. It was not until 2009, over fifty years after its discovery, that the structure of micrococcin P_1 (identical to **5,** Figure 1.1) was elucidated.[10] A total synthesis of a reference compound was shown to be spectroscopically and polarimetrically identical to **5**, enabling the assignment of the absolute configuration of micrococcin.[10] Thiostrepton A (**2**), a prototypical thiopeptide, was first isolated from *Streptomyces azureus* in 1954 and later isolated from *Streptomyces laurentii*.[8, 14-16] X-ray crystallographic

experiments and detailed NMR studies during the 1970s and 1980s, followed by multidimensional NMR methods confirmed its structural assignment in 1989.[17-20] Despite advances in spectroscopic techniques, many thiopeptides still remain uncharacterized.[1] This is in part due to difficulties in obtaining crystallographic data which has left some stereochemical and connectivity assignments ambiguous. Efforts to structurally characterize thiopeptides, however, have led to the development of more efficient methods to synthesize these complex natural products, spurred an investigation of the structural basis of its biological activities, and have bolstered the development of thiopeptide analogs.

Despite impressive biological activities of thiopeptides, clinical use of these drugs has been limited in large part due to low bioavailability caused by their low aqueous solubilities. Therefore, there is interest in the discovery, design, and production of thiopeptide analogs with improved pharmacokinetic parameters. While the chemical syntheses of thiopeptides such as promothiocin A (Figure 1.3, **8**), micrococcin P_1 **5**, and thiostrepton A **2** have been accomplished, it remains uneconomical and impractical for industrial scale use due to low net yield and the need for lengthy multistep syntheses.[10, 21-22] Nonetheless, some thiopeptides are commercially available as isolates from bacterial cultures. Accordingly, semisynthetic and biosynthetic engineering strategies appear to be viable approaches in developing and producing clinically useful thiopeptide antibiotics. For example, the semisynthetic modifications of nocathiacin I **7** (Figure 1.2), thiostrepton A **2**, and GE2270 A (Figure 1.3, **9**) have produced promising analogs.[23-27] Nocathiacin I **7**, isolated from the fermentation broth of *Norcadia* sp. ATCC 202099, was subjected to a series of modifications on the dehydroalanine tail and the hydroxypyridine core.[23-24] A structure-activity relationship study of **7** found that the dehydroalanine tail region tolerated

basic residues such as tertiary amines and tertiary amides over acidic residues such as hydroxyls.[23-24] A nocathiacin I analog (Figure 1.2, **7a**), with a terminal morpholine group and a methoxypyridine core, exhibited over ten-fold increase in water solubility while retaining comparable biological activities with **7**.[24] In addition to its antibacterial activities against *Staphylococcus aureus*, *Streptococcus pneumoniae*, and *Enterococcus faecalis*, the nocathiacin I analog **7a** retained its antituberculosis and antimalarial activities.[24, 28-29]

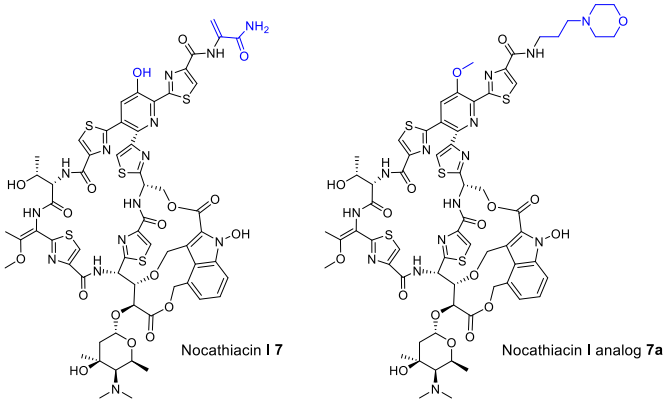

Figure 1.2: Structures of nocathiacin I (**7**) and its derivative (**7a**) with a terminal morpholine and methoxypyridine core. The modified regions are shown in blue.

The derivatization of GE2270 A **9** has led to the discovery of an analog (Figure 1.3, **9a**) with a much narrower antibiotic spectrum and the drug is currently under phase IIb clinical trials as a topical ointment effective against antibiotic-resistant strains of *Propionibacterium acnes*.[25] Meanwhile, GE37468 A (Figure 1.3, **10**), thiocillin I (Figure 1.3, **11**) and thiostrepton A **2** biosynthetic machineries appear to tolerate certain modifications on the peptide substrate (as well as the quinaldic acid moiety of thiostrepton A **2**) and a series of biosynthetic analogs have been produced.[30-36]

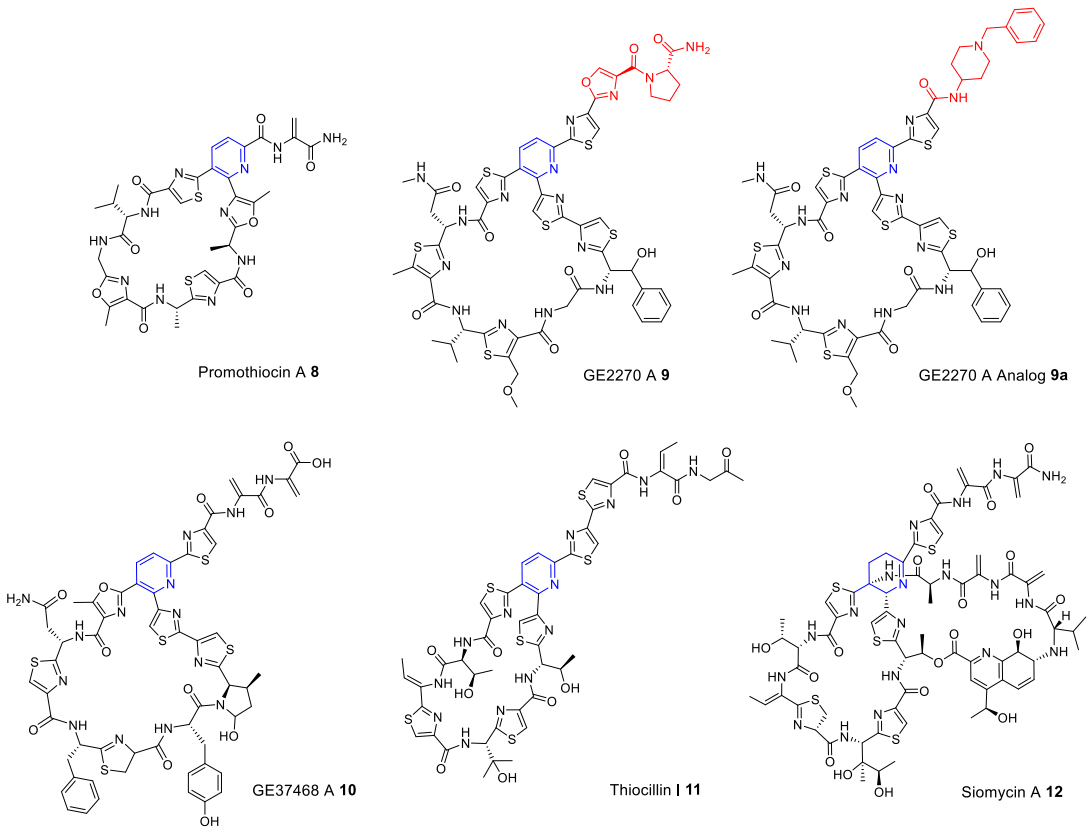

Figure 1.3: Additional examples of thiopeptides: promothiocin A (**8**), GE2270 A (**9**) and its analog (**9a**), GE37468 A (**10**), thiocillin I (**11**), and siomycin A (**12**). The central nitrogenous heterocycle that completes the main macrocycle common in all thiopeptides is in blue. The modified regions on GE2270 A **9** and **9a** are shown in red.

Both semisynthetic and biosynthetic engineering strategies depend on the isolation of thiopeptides from bacterial fermentation cultures. Therefore, our capacity to derivatize these compounds is dependent on our knowledge of the thiopeptide biosynthetic machinery and our ability to manipulate the biosyntheses of these complex metabolites. Great effort has been made in characterizing thiopeptide biosynthetic pathways since the discovery of the thiocillin **11**, thiostrepton A **2,** and siomycin (Figure 1.3, **12**) biosynthetic gene clusters in 2009.[37-39] Many aspects of thiopeptide biosyntheses remain unclear, including the formation of the central nitrogenous heterocycle integral to all thiopeptides and the timing

in which modifications are installed on the thiopeptide framework. The remainder of this chapter will introduce our current understanding of thiopeptides, with a focus on their biosyntheses.

1.2 Structural classification of thiopeptides

To date, over 100 distinct thiopeptides have been identified and are classified as structural series *a*-*e* based on the oxidation state of the central, six-membered nitrogenous ring in the core macrocycle (Figures 1.1-1.4).[1, 40] Series *a* thiopeptides such as Sch 18640 **1**, isolated from *Micromonospora arborensis,* contain a fully reduced piperidine ring while thiostrepton A **2**, isolated from *Streptomyces azureus* and *Streptomyces laurentii,* siomycin A **12**, isolated from *Streptomyces sioyaensis*, and other series *b* thiopeptides are observed with a dehydropiperidine core.[9, 41-42] The series *c* thiopeptide contains an unusual dihydroimidazopiperidine moiety and Sch 40832 **3**, isolated from *Micromonospora cabonacea* var. *africana,* is the sole known member of this structural class.[6] Thiomuracin A **4**, isolated from *Nonomuraea* sp. Bp3714-39, micrococcin P_1 **5**, isolated from *Micrococcus* and *Bacillus* species, promothiocin A **8**, isolated from *Streptomyces* sp. SF2741, GE2270 A **9**, isolated from *Planobispora rosea*, GE37468 A **10**, isolated from *Streptomyces* sp. ATCC 55365, thiocillin I **11**, isolated from *Bacillus cereus* G-15, and other series *d* thiopeptides present with an aromatic pyridine ring.[5, 10, 43-45] Nosiheptide **6**, isolated from *Streptomyces actuosus,* nocathiacin I **7**, isolated from *Nocardia* sp. ATCC 202099, and other series *e* members contain an hydroxypyridine core.[4, 46] All known members of series *a*, *b*, and *c* thiopeptides possess a second, quinaldic acid-containing macrocycle while series *e* thiopeptides present with a second, indolic acid-containing loop.[1]

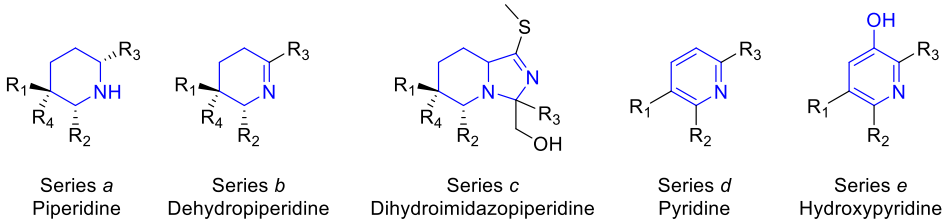

Figure 1.4: The structural classes of thiopeptides (series *a*-*e*) depend on the oxidation state of the central, six-membered nitrogenous heterocycle. R_1-R_4 represent the rest of the thiopeptide scaffold.

1.3 Biological activities of thiopeptides

Thiopeptides inhibit the growth of Gram-positive bacteria such as methicillin-resistant *Staphylococcus aureus* (MRSA) and penicillin-resistant *Streptococcus pneumoniae* by inhibiting prokaryotic ribosomal peptide synthesis.[47-49] Two separate modes of action exist. One group includes thiostrepton A **2**, nosiheptide **6**, nocathiacin I **7**, and thiocillin I **11**; these thiopeptides bind to the GTPase-associated center of the 50S ribosomal subunit.[47, 50-52] This region utilizes GTP-hydrolysis to drive translocation of the tRNA-mRNA complex during mRNA translation. When bound to the ribosome, thiopeptides interfere with the conformational changes associated with translocation to the next codon, inhibiting protein translation.[52] In a second mode of action, thiopeptides such as thiomuracin A **4**, GE2770 A **9**, and GE37468 A **10**, bind to EF-Tu and block the binding of aminoacyl-tRNA to EF-Tu.[5, 43, 53] The GTPase EF-Tu delivers aminoacyl-tRNA to the A site of the ribosome, a prerequisite for elongation of the nascent polypeptide chain on the ribosome. Thiopeptides such as **4** and **9** therefore prevent the formation of the EF-Tu-GTP-aminoacyl-tRNA complex and inhibit protein translation.[53]

Some thiopeptides, in addition to their antibacterial activity, have been shown to exhibit antiplasmodial and anticancer activity.[3, 54] Thiostrepton A **2** inhibits *Plasmodium falciparum* growth by binding to the GTPase-associated domain of the prokaryotic ribosome-like translational machinery in the apicoplasts as well as binding to the 20S proteasome to inhibit protein degradation, a necessary component for cellular upkeep.[55-57] Most apicomplexan parasites, such as *Plasmodium* species, carry an organelle called an apicoplast that is essential for the parasite's survival.[58] While it is still unclear, this organelle may be involved in fatty acid, isoprenoid, and/or heme biosyntheses that may be indispensable for *Plasmodium* parasites.[58] Apicoplasts are theorized to be vestigial prokaryotic plastids analogous to mitochondria in eukaryotic cells and the apicoplasts house their own translational machinery that is separate from the nucleus and the mitochondrion.[59] Thus, the inhibitory activity of thiostrepton A **2** on protein translation extends beyond prokaryotes to certain pathogenic eukaryotes that house prokaryotic translational machinery in the cell.

Thiostrepton A **2** exhibits its anticancer activity by binding to the Forkhead box M1 (FOXM1) transcription factor, inhibiting the binding of FOXM1 to promoter regions of genes involved in cell proliferation and cell cycles that are overexpressed in human solid cancers.[3] **2** was found to decrease expression levels of genes involved in proliferation of human breast cancer cell lines without any effect on expression of other housekeeping genes that were analyzed in the same cell line.[3] In addition, **2** inhibits proteasome activity to induce apoptosis in cancer cells.[60] The modulation of transcription factors by small molecules remain a challenge in modern medicine in part due to the difficulties of purifying transcription factors that tend to co-purify with DNA and due to a lack of known molecules

that bind to transcription factors.[61] Many of these proteins are thought to function as a "complexes within a network of interactions" and modulation of protein-protein interactions have gained interest as promising therapeutic targets to treat cancers with aberrant transcription of oncogenes.[61-62] Thiostrepton A **2** is the first known instance of a natural product binding directly to a transcription factor to inhibit transcription.[3] Sitting at the larger end of small molecules, the large, rigid, and peptidic structure of thiopeptides may be attuned to disrupt protein-protein interactions.

1.4 Thiostrepton A

Thiostrepton A **2** (Figure 1.1) is an extensively studied dehydropiperidine-containing series *b* thiopeptide produced by *Streptomyces azureus* ATCC 14921 (*S. azureus*) and *Streptomyces laurentii* ATCC 31255 (*S. laurentii*).[7-8] Like other series *a* and *b* thiopeptides, thiostrepton A **2** has a quinaldic acid-containing loop in addition to its core macrocycle. Thiostrepton A **2** has been shown to possess potent antibacterial, antiplasmodial, and anticancer activity.[3, 48, 55] While thiostrepton A **2** has been approved by the FDA as an antibiotic ointment for animal use, approval of **2** for human use has been stymied due to the low aqueous solubility that is common among all thiopeptides.

The thiostrepton biosynthetic gene (*tsr*) cluster was identified in *S. laurentii* by Kelly and coworkers and Liu and coworkers in 2009.[37-38] Soon after these publications, thiomuracin A **4**, nosiheptide **6**, GE2270 A **9**, and thiocillin I **11** biosynthetic gene clusters were identified; as a result, these studies established that thiopeptides were RiPPs, derived

from a genetically-encoded precursor peptide.[5, 39, 63] The biosyntheses of thiostrepton A **2** and other thiopeptides are discussed later in this chapter.

1.5 Thiopeptins

The thiopeptins (Figure 1.5, **13-16**) are a complex of series *a* (thiopeptins A_{1a} **13** and B_a **14**) and series *b* (thiopeptins A_{1b} **15** and B_b **16**) thiopeptides produced by *Streptomyces tateyamensis* ATCC 21389 (*S. tateyamensis*) and have structures highly similar to thiostrepton A **2**.[40, 49, 64-65] Both **2** and the thiopeptins **13-16** are 17 amino acids long, differing only in the first residue (Val in the thiopeptins and Ile in thiostrepton A **2**), and both incorporate a second, quindalic acid containing loop. The thiopeptins **13-16** are, however, distinguished from thiostrepton A **2** by a thioamide moiety in **13-16** and the piperidine ring found in thiopeptins A_{1a} **13** and B_a **14** (Figure 1.5). Like many other thiopeptides, thiopeptins inhibit prokaryotic ribosomal translation and share similar antibacterial activities to thiostrepton A **2**.[49, 66] The thiopeptin biosynthetic genes have not yet been identified, and the origins of the thioamide moiety and piperidine ring remain unclear.

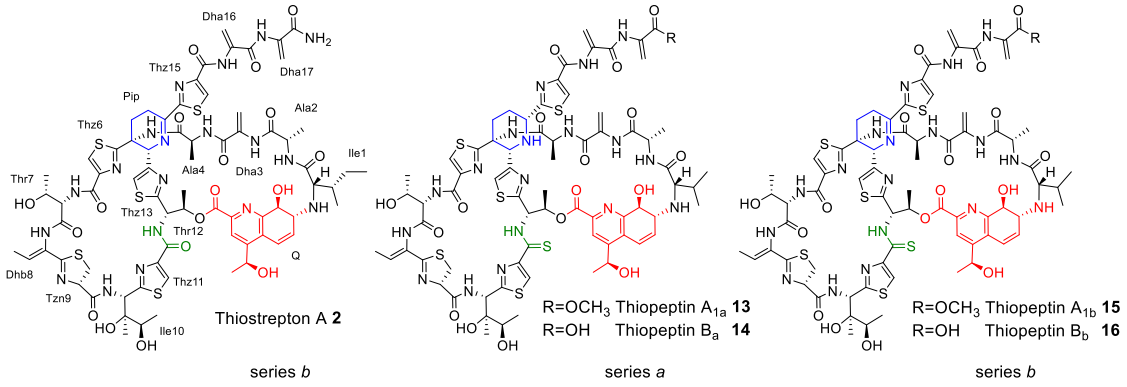

Figure 1.5: The structures of thiostrepton A **2** and the thiopeptins **13**-**16**. The (dehydro)piperidine ring is in blue, the quinaldic acid moiety in red, and the (thio)amide in green. The amino acid residue numbering system of thiostrepton A **2** is indicated on its structure. Abbreviations: dehydroalanine (Dha), dehydrobutyrine (Dhb), dehydropiperidine (Pip), quinaldic acid moiety (Q), thiazole (Thz), and thiazoline (Tzn).

1.6 Thiopeptide biosynthesis

Thiopeptides are derived from genetically-encoded precursor peptides and undergo a cascade of post-translational modifications.[2] The precursor peptide is comprised of two parts. The N-terminal leader peptide region is important for substrate recognition by much of the post-translational machinery and is cleaved during peptide maturation, and the C-terminal core peptide is the region that is transformed into the thiopeptide.[2] In addition to the precursor peptide, a minimum of six proteins (TbtB-G) corresponding to the proteins encoded by the thiomuracin A **4** biosynthetic gene (*tbt*) cluster are required for the biosynthesis of the thiopeptide scaffold, and the activities of TbtB-G have been demonstrated *in vivo* (Scheme 1.1-1.3).[67] TbtEFG work in tandem to install the thiazol(in)es that decorate the thiopeptide scaffold (Scheme 1.1). The cyclodehydration of cysteine residues to thiazolines is catalyzed by TbtF, a leader peptide binding protein, and TbtG, an F-protein dependent cyclodehydratase, via an ATP-dependent process that

activates the amide backbone.[68-69] Thiazolines are aromatized to thiazoles by the action of TbtE, an FMN-dependent thiazoline dehydrogenase.[67] A similar pair of reactions is expected to convert serines to oxazoles, found in certain thiopeptides such as GE2270 A **9** and GE37468 A **10**. Azo(lin)e formation is expected to be one of the first steps in thiopeptide biosynthesis as TbtFG accepts the unmodified precursor peptide, TbtA, as a substrate.[67, 70]

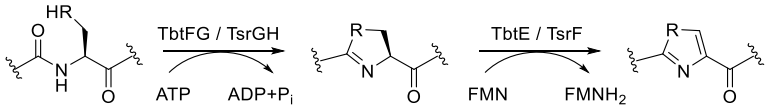

Scheme 1.1: Azoline formation of thiopeptides. Cysteines are cyclized to form thiazol(in)es. Tbt homologs that are encoded in the *tsr* cluster are shown next to the Tbt proteins.

After azol(in)e formation, TbtBC, a split LanB-type dehydratase, catalyzes the dehydration of serine residues to Dha (Scheme 1.2).[67] TbtB shows homology to the glutamylation domain of the NisB lanthipeptide dehydratase which uses glutamyl-tRNA^{Glu} to activate the serine residue as an ester, and TbtC shows homology to the glutamate elimination domain of NisB.[71] A similar reaction is expected for the dehydration of threonine residues to form Dhb. Dehydration likely occurs after azole formation as TbtBC does not accept the unmodified precursor peptide TbtA, but does accept a modified TbtA with at least one azole.[70]

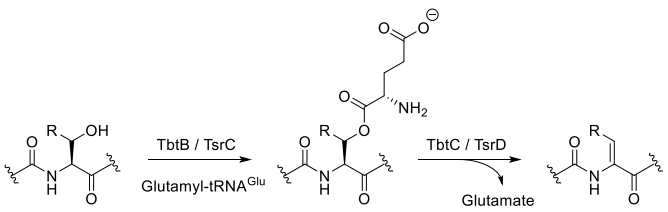

Scheme 1.2: Dehydroalanine and dehydrobutyrine formation of thiopeptides catalyzed by the split LanB-like dehydratases. Tbt homologs that are encoded in the *tsr* cluster are shown next to the Tbt proteins.

TbtD encodes a formal [4+2] cyclase that forms the series *d* pyridine core of thiomuracin **4** from two Dha residues.[67, 72] This cyclization resembles the Diels-Alder reaction utilized among synthetic chemists to introduce a substituted cyclohexene ring while controlling the stereochemistry of the substituents.[73] The regio- and stereo- selective control of the Diels-Alder reaction is particularly useful in challenging syntheses of complex natural products where only a particular diastereomer may elicit a desired biological activity. There is great interest in the biocatalysis community for enzymatic Diels-Alder reactions which may provide cleaner and more efficient pathways to synthesize natural products.

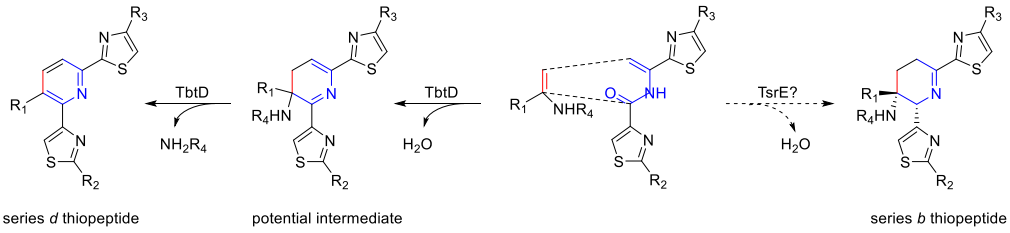

Scheme 1.3: Core macrocycle formation of thiopeptides between two Dha residues catalyzed by a [4+2] cyclase. TbtD has been shown to be a stand-alone pyridine synthase involved in thiomuracin **4** biosynthesis.[67, 72] The TbtD homolog TsrE from the *tsr* cluster is proposed to form the dehydropiperidine ring in thiostrepton A **2**. R_1-R_4 represent the rest of the thiopeptide scaffold.

There are disagreements, however, whether these [4+2] thiopeptide cyclases found in nature represent a true, pericyclic Diels-Alderase or if these reactions proceed through a different, step-wise mechanism.[74] In solution, the aza-Diels-Alder reaction between a 2-aza-1,3-butadiene and a dienophile may react readily without activation if the electronic demand of the HOMO-LUMO interaction of the two systems are small.[75] For example, the reaction may be favorable between an electron-poor diene and an electron-rich dienophile, and vice versa. Many aza-Diels-Alder cycloadditions, however, require activation by a Lewis acid catalyst to form an iminium cation at the 2-aza-1,3-butadiene and the reaction likely follows a stepwise mechanism rather than a concerted one (Figure 1.6).[75-77]

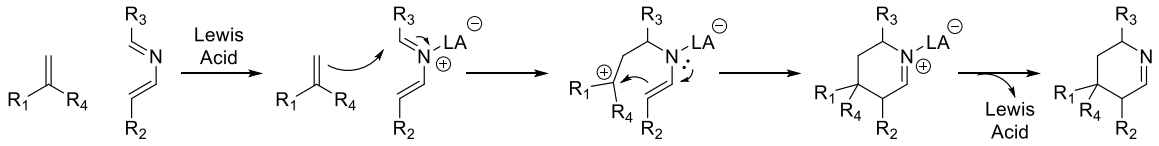

Figure 1.6: Possible stepwise mechanism of a Lewis acid (LA) catalyzed cycloaddition between 2-aza-1,3-butadiene and a dienophile.

The thiopeptide diene and dienophile are both surrounded by electron-donating substituents and this [4+2] cycloaddition likely requires activation of the dienophile or the 2-aza-1,3-butadiene for the reaction to proceed at physiological conditions, require modifications to the peptide substrate so that the cycloaddition is more favorable, or alternatively, it may proceed via a non-Diels-Alder route. In fact, many of the aza-Diels-Alder strategies employed for the total syntheses of various thiopeptides have necessitated a modified peptide substrate for the cycloaddition.[22, 78-80] If the cycloaddition proceeds without additional modifications to the peptide substrate, the thiopeptide [4+2]

cycloaddition may similarly follow an acid-catalyzed stepwise pathway that has been suggested for other aza-Diels-Alder reactions. Kelly and coworkers have proposed a general acid base catalyzed stepwise mechanism in which the neighboring thiazole functions as an electron sink (Figure 1.7).[37] Further studies of the thiopeptide [4+2] cyclases are needed to discern the exact mechanism and the substrate needed for the cycloaddition.

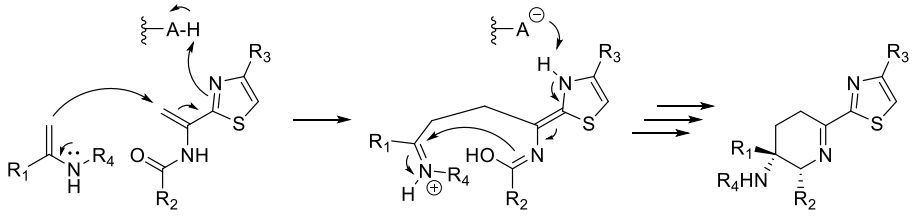

Figure 1.7: Proposed biosynthesis of the thiopeptide dehydropiperidine. R_1-R_4 represent the rest of the thiopeptide scaffold.

The TbtD-catalyzed cycloaddition of two Dha residues is followed by dehydration and elimination of the leader peptide to form the series *e* pyridine ring of thiomuracin A **4** (Scheme 1.3). It is unclear how a similar process would lead to the dehydropiperidine rings of series *b* thiopeptides whilst retaining the leader peptide. TbtABCDEFG comprise the minimum set of proteins required for the formation of the thiopeptide core scaffold.

1.7 Biosynthesis of thiostrepton A

In addition to its dehydropiperidine-containing core macrocycle, thiostrepton A **2** contains a second macrocycle that includes a quinaldic acid moiety. The *tsr* cluster encodes

homologs of TbtB-G, the minimum set of proteins encoded in the *tbt* cluster that are required for core macrocycle formation (Schemes 1.1-1.3): TsrA (the precursor peptide), along with TsrCD (the split LanB-type dehydratase), TsrE ([4+2] cyclase), TsrF (thiazoline dehydrogenase), TsrG (F-protein leader peptide binding domain), and TsrH (F-protein dependent cyclodehydratase). TsrCDEFGH are expected to transform TsrA to a thiostrepton precursor containing the core macrocycle decorated with thiazol(in)es and dehydrated amino acids.

The quinaldic acid moiety is derived from L-tryptophan and TsrMNQSV are expected to convert the amino acid into 4-(1-hydroxyethyl)quinoline-2-carboxylic acid (HEQ (**21**)) by a process that includes an oxidative ring expansion (Scheme 1.4).[34, 37, 81-82] The first step of this process is catalyzed by TsrM, a radical SAM and cobalamin-dependent methyltransferase.[81] L-Tryptophan (**17**) is converted to 2-methyl-L-tryptophan (**18**) using methyl-co(III)balamin as a methyl donor.[81] Next, TsrV, a pyridoxal 5'-phosphate (PLP)-dependent aminotransferase catalyzes the conversion of 2-methyl-L-tryptophan **18** to 3-(2-methylindolyl)pyruvate (**19**).[37] Next, TsrQ, an $FADH_2$-dependent oxygenase, initiates ring opening and rearrangement of the indole ring.[82] A *tsrS*-deletion mutant of *S. laurentii* still produced thiostrepton A, although at trace amounts, leaving the role of TsrS unclear in HEQ **21** biosynthesis.[34] TsrN, an NADPH-dependent reductase converts the ketone of 4-acetylquinoline-2-carboxylate (**20**) to an alcohol, forming HEQ **21**.[34]

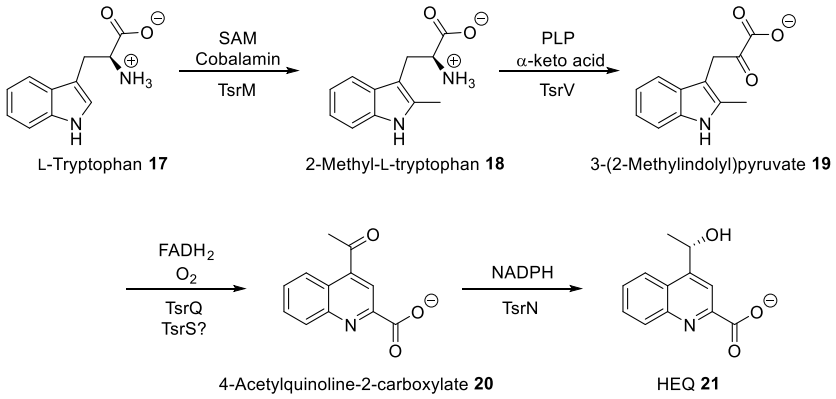

Scheme 1.4: Proposed biosynthesis of 4-(1-hydroxyethyl)quinoline-2-carboxylate (HEQ **21**) in the thiostrepton biosynthetic pathway.[34, 37, 81-82] TsrS is proposed to be involved in HEQ formation in the thiostrepton biosynthetic pathway, but the exact role is unclear.[34]

HEQ **21** is likely activated by TsrJ, an adenylyltransferase, and an ester bond is formed between the activated carboxylic acid of **21** and Thr12 of the thiostrepton A scaffold (Scheme 1.5). Once tethered to Thr12, HEQ is epoxygenated by the action of TsrI, a cytrochrome P450.[83-84] Next, TsrB catalyzes leader peptide cleavage and subsequent attack of the N-terminal amine on the HEQ epoxide to form the second macrocycle (Scheme 1.5).[85]

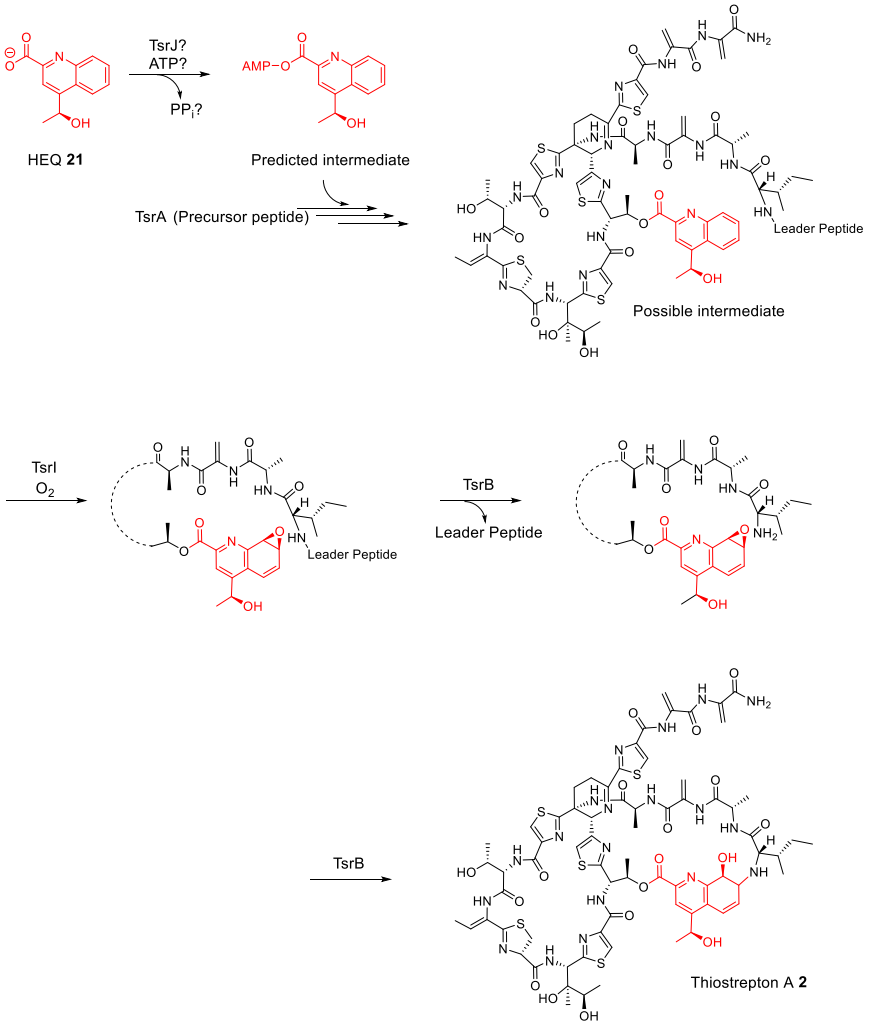

Scheme 1.5: Proposed coupling of HEQ **21** to a thiostrepton biosynthetic intermediate and the formation of the quinaldic acid-contianing loop of thiostrepton A **2**. The HEQ-derived moieties are in red while the thiostrepton scaffold is abbreviated by dashed lines in certain steps of the scheme.

Additional modifications are performed by TsrKPTU. TsrK, a cytochrome P450, catalyzes the two hydroxylations of Ile10.[84] The C-terminus of thiostrepton is likely methylated by TsrP, to from a methylester (**22**) (Scheme 1.6).[37, 86] The methylation may be important in the dehydration of the serine residue at the C-terminus (Dha17). The pK_a of the serine α hydrogen is likely between 25 and 50 when adjacent to a carboxylate but the

pK_a decreases to ~25 when adjacent to a carboxymethyl ester. The increase in acidity of the C-H bond may facilitate the elimination of water on the terminal residue. Dehydration of that serine to dehydroalanine is expected to occur early in thiostrepton biosynthesis, after azole formation on the unmodified precursor peptide.[67, 70] Therefore, methylation of the C-terminus of thiostrepton likely occurs very early in its biosynthesis, possibly on the unmodified precursor peptide or on the precursor peptide with at least one azole. The carboxymethyl ester at the C-terminus is further modified by an esterase, TsrU, that catalyzes the hydrolysis of the methylester back to a carboxylate (Scheme 1.6).[37, 86] Finally, TsrT, an amidotransferase, catalyzes the formation of the C-terminal amide (Scheme 1.6).[37, 86] Deletion mutants of TsrU accumulated a mature thiopeptide with a C-terminal methylester **22,** while a TsrT mutant accumulated a mature thiopeptide with a C-terminal carboxylic acid (**23**), suggesting that the deesterification and amidation of the C-terminus occur late in thiostrepton biosynthesis.[37, 86]

The modifications at the C-terminus affect the bioactivity and solubility of the thiostrepton analogs. While the methylester species **22** was shown to be slightly more effective against *Bacillus subtilis* than the amidated thiostrepton A **2**, the aqueous solubility of **22** was diminished.[86] On the other hand, the carboxylic acid species **23** retained comparable aqueous solubility with **2** but was slightly less effective against *Bacillus subtilis* than **2**.[86]

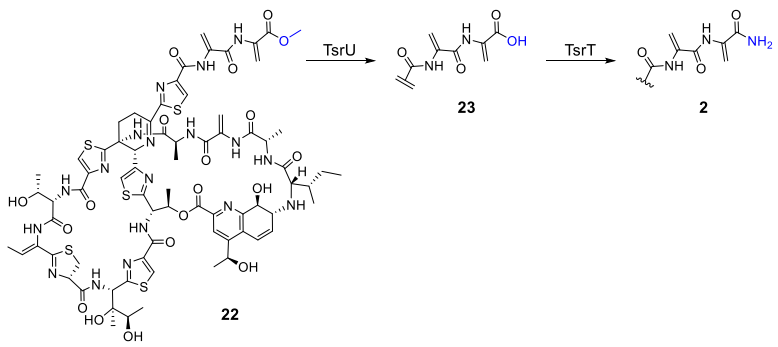

Scheme 1.6: Modifications of the thiostrepton C-terminus by TsrUT to form the amide found in the mature metabolite, thiostrepton A **2**.[37, 86] The modified region is shown in blue.

Notably, the thiazoline found in thiostrepton A **2** and many of the thiazolines found among the structurally characterized thiopeptides (Sch 18640 **1**, Sch 40832 **3**, siomycin **12**, thiopeptins **13**-**16**, and the cyclothiazomycins (Figure 1.8, **24**)) are in the D-configuration despite their origin from L-cysteine.[9, 19, 41, 87-88] Thiazolines are predicted to be formed in the L-configuration and subsequently epimerized to the D-configuration in certain thiopeptides. Though the thiostrepton **2**, siomycin **12**, and cyclothiazomycin **24** biosynthetic gene clusters have been characterized, obvious epimerase candidates have not been identified.[37-38, 89] Thus, the origin of epimerization of these thiopeptide thiazolines remain uncertain. Arndt and coworkers demonstrated that the thiostrepton A **2** thiazoline readily epimerizes under basic conditions if the second, quinaldic acid-containing ring is closed.[90] The D-configuration of the thiazoline is thermodynamically favored over the L-configuration by approximately 2 kcal mol^{-1} due to the ring strain imposed by the second macrocycle.[90] It is, however, still unclear if a dedicated enzyme catalyzes this epimerization via general-base catalysis or if the epimerization can be attributed as an additional role to an encoded product of the *tsr* cluster that already has an assigned function.

Sch 18640 **1**, thiostrepton A **2**, Sch 40832 **3**, siomycin **12**, and the thiopeptins **13**-**16** all possess a second, quinaldic acid-containing ring and, accordingly, a thiazoline in the D-configuration. Meanwhile, the cyclothiazomycins **24** do contain a second macrocycle, albeit an unusual thioether bridge between a dehydroalanine on the core macrocycle and a C-terminal cysteine thiol on the "tail" region of **24**. The cyclothiazomycins **24** contain a thiazoline in the D-configuration on the core macrocycle and a mixture of the L- and D-configurations on the second macrocycle formed by the thioether (Figure 1.8).[89] On the other hand, kocurin (Figure 1.8, **25**) does not contain a second macrocycle and, accordingly, contains a thiazoline in the L-configuration.[88] GE37468 A **10** (Figure 1.3) is highly similar in structure to kocurin **25**, but the configuration of the thiazoline in GE37468 A **10** has not been determined.

Interestingly, kocurin **25** and GE37468 A **10** are the only characterized thiopeptides that contain thiazolines in their core macrocycles without a second ring in their structures. The prolyl moiety found in the kocurin **25** and GE37468 A **10** core macrocycles likely introduces additional ring strain, and a thiazoline may better accommodate that added strain over a rigid thiazole. Further studies are required to establish the requirements for the configuration of the thiazolines found among thiopeptides.

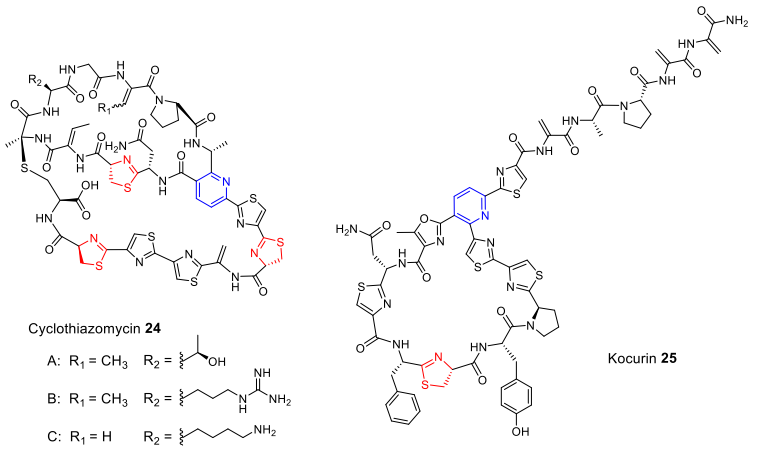

Figure 1.8: The structures of the cyclothiazomycins A-C (**24**) and kocurin (**25**). The nitrogenous heterocycle is shown in blue while the thiazolines are shown in red.

1.8 Dehydropiperidine and piperidine biosynthesis

The nitrogenous heterocycle common among thiopeptides originates from two dehydrated serine residues based on isotopic labeling studies.[44, 91-93] The pyridine of series *d* and *e* thiopeptides is derived from a dedicated pyridine synthase.[67, 72] The formal [4+2] cyclization is followed by dehydration to form a dihydropyridine intermediate, followed by elimination of the leader peptide to form the aromatic heterocycle (Figure 1.9).[72] For the series *b* thiopeptides, the pyridine, or a prior biosynthetic intermediate, needs to be reduced to the dehydropiperidine ring. There are, however, no obvious candidate reductases that can serve this role in known series *b* thiopeptide biosynthetic gene clusters.[37-38] In addition, it is unclear why the N-terminal portion of series *a-c* thiopeptides is retained after the dehydration of the core macrocycle. While the formation of the dehydropiperidine ring remains unclear, the piperidine ring of series *a* thiopeptides could be formed by the reduction of the dehydropiperidine ring. In this context, piperidine

formation may be accomplished by actions of NAD(P)H-, flavin-, or other reductive cofactor-dependent reductases utilized in secondary metabolism.

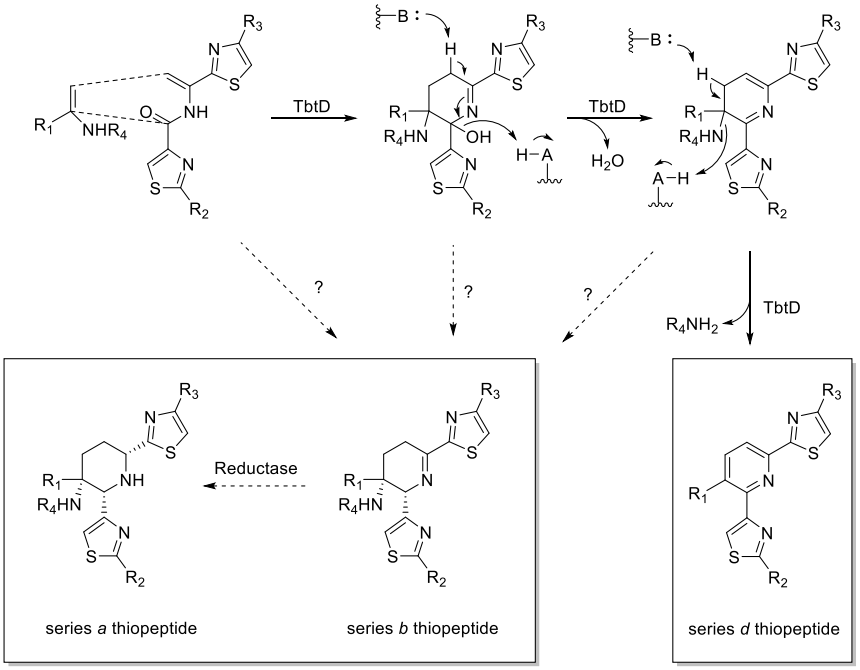

Figure 1.9: The proposed steps of the series *d* thiopeptide pyridine formation by TbtD and its possible relation to series *a* piperidine and *b* dehydropiperidine formation. R_1-R_4 represent the rest of the thiopeptide scaffold.

1.9 Reductive coenzymes

Redox coenzymes play a central role in primary and secondary metabolism across all three domains of life. Cellular processes that involve one- and two-electron redox reactions are associated with the four major energy metabolism systems in biology: aerobic respiration, denitrification, photosynthesis, and sulfur respiration.[94] While these processes depend on a number of cofactors that vary across archaea, bacteria, and eukaryotes, the niacin coenzymes nicotinamide adenine dinucleotide (phosphate) ($NAD(P)^+$ and their

reduced forms NAD(P)H), and flavin coenzymes, flavin mononucleotide (FMN and its reduced form $FMNH_2$) and flavin adenine dinucleotide (FAD and its reduced form $FADH_2$), play a central role in metabolism as electron donors and acceptors (Figure 1.10).[94-96] In addition, nicotinamide and flavin cofactors are heavily utilized in secondary metabolism of natural products with antimicrobial and anticancer activities.[97-98]

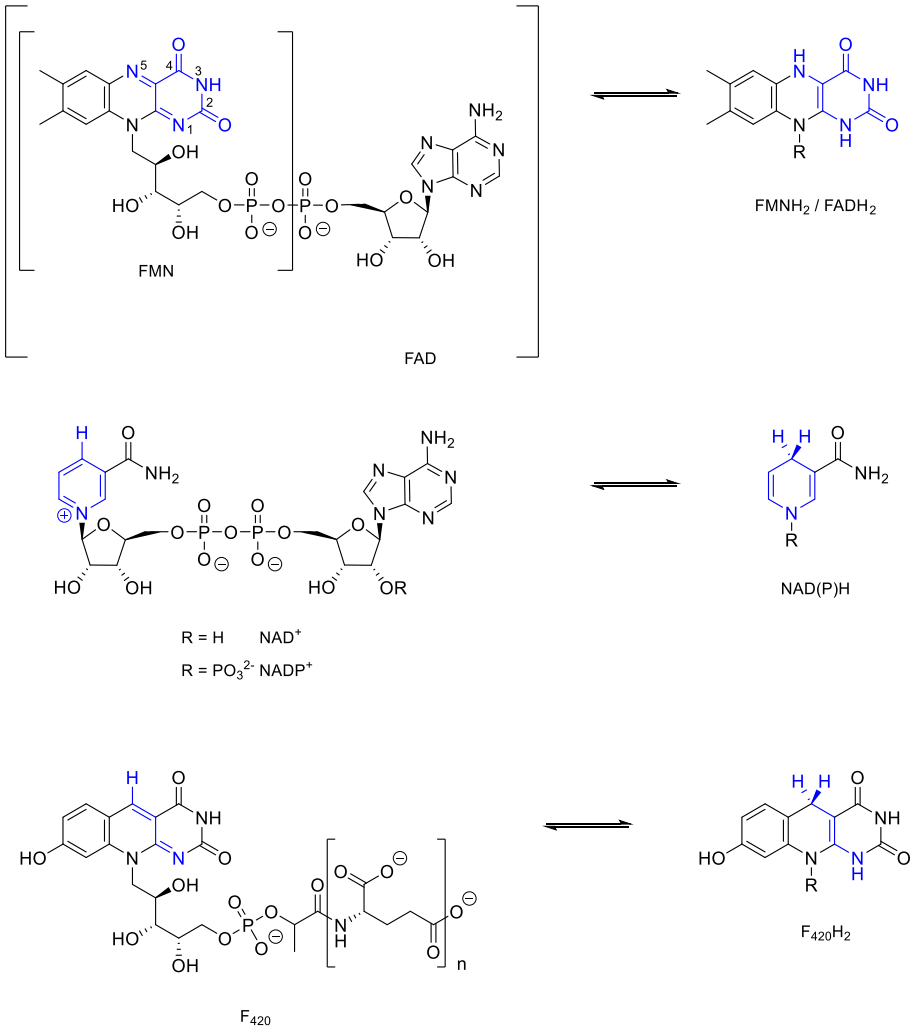

Figure 1.10: The structures of redox coenzymes FMN, FAD, $NAD(P)^+$, and F_{420}. The oxidized and reduced forms of each coenzyme are shown on the left and right, respectively. The part of the cofactor that is directly involved in two-electron transfer are in blue.

Some organisms, notably methanogens and actinobacteria, utilize a deazaflavin cofactor where the N^5 of the flavin isoalloxazine ring is replaced with a carbon. Cofactor F_{420} is an 8-hydroxy-7-desmethyl-5-deazariboflavin derivative which owes its name to a characteristically strong absorbance at 420 nm (Figure 1.10). The deazaflavin cofactor contains a polyglutamate tail and a 2-phospho-L-lactate moiety attached to the ribityl group. The number of glutamate residues tethered to the lactate moiety is species-specific and typically ranges between zero and eight. [99-100] The F_{420} produced by methanogens that do not produce cytochromes have two or three glutamate residues, F_{420} produced by methylotrophic methanogens, which are capable of producing cytochromes, have four or five glutamate residues, and actinobacteria produce F_{420} with five to seven glutamate residues tethered to the 2-phospho-L-lactyl moiety.[99-101] The physiological significance of the differences in the polyglutamate tail length are not well understood. The glutamate tail does not affect the redox potential of the cofactor and, therefore, does not affect its chemical reactivity.[102] Tail length, however, has been shown to affect the affinity of the (non-cofactor) substrate to the enzyme (K_M) and the turnover rate (k_{cat}) of certain proteins in mycobacteria.[103]

Despite its structural similarity to flavins, F_{420} acts as a two-electron (hydride) carrier like $NAD(P)^+$ (Figure 1.10).[104] Without the nitrogen at the N^5 to effectively delocalize an unpaired electron, F_{420} is unable to form a stable semiquinone species required for one-electron transfer by FMN and FAD coenzymes.[105] Moreover, the substitution of N^5 with carbon makes F_{420} a strong reductant. With a standard reduction potential of -340 mV, F_{420} is a stronger reducing agent than other common redox cofactors such as FMN (-190 mV), FAD (-220 mV), and $NAD(P)^+$ (-320 mV).[102, 106-107] In

accordance with its reductive strength, F_{420}-dependent enzymes are involved in challenging reactions such as the reduction of methenyltetrahydromethanopterin to methyltetrahydromethanopterin during methanogenesis, sulfite reduction, and the reduction of the imidazole of nitroimidazole (Scheme 1.7). [108-111]

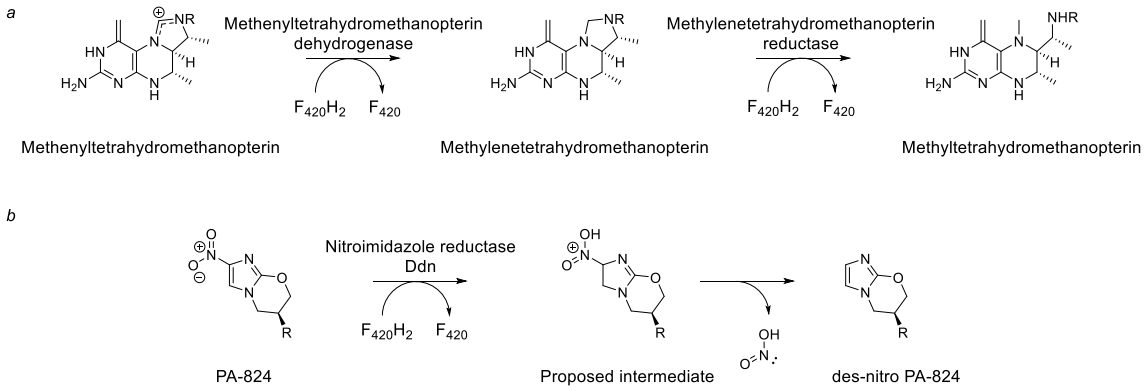

Scheme 1.7: The $F_{420}H_2$-dependent reduction of (*a*) methenyltetrahydromethanopterin to methyltetrahydromethanopterin by archaea and (*b*) potential antituberculosis drug PA-824 to a des-nitro form of PA-824 by a nitroimidazole reductase Ddn in *Mycobacterium tuberculosis*.[108, 111]

F_{420}-dependent pathways are widely found in actinobacteria species such as *Mycobacterium tuberculosis* (*M. tuberculosis)* and *Mycobacterium smegmatis* (*M. smegmatis),* yet little is known about the role of the deazaflavin cofactor in the metabolism of actinobacteria. Conservation of F_{420}-dependent genes in *Mycobacterium leprae*, the causative agent of leprosy with a heavily reduced genome, may suggest a significant role of F_{420} in *Mycobacterium* metabolism.[112] Although F_{420} is not essential to mycobacteria, F_{420} production is linked to the ability of pathogenetic mycobacteria to withstand oxidative and nitrosative stress.[113-115] In fact, *in vitro* studies have found that

F_{420}-deficient *M. smegmatis* strains were two- to four-times more sensitive to first-line antimycobacterial drugs such as isoniazid, rifampin, and ethambutol and over 100-times more sensitive to other antimicrobial agents such as nalidixic acid and malachite green.[114] Thus, F_{420}-dependent pathways have garnered attention as an attractive drug target for the selective inhibition of pathogenic *Mycobacterium* that are notoriously difficult to treat.

1.10 Biosynthesis of cofactor F_{420}

F_{420} biosynthesis diverges from the early steps of the flavin biosynthetic pathway. L-Tyrosine and 5-amino-6-ribitylamino-2,4(1*H*,3*H*)-pyrimidinedione, a biosynthetic intermediate of riboflavin, is condensed by F_0 synthase to form F_0, a biosynthetic precursor to F_{420} (Scheme 1.8).[116] F_0 synthase marks the first dedicated step in F_{420} biosynthesis and is encoded as two polypeptides (CofG and CofH) in archaea and a single polypeptide (FbiC) in bacteria.[116-117] Both domains contain a radical SAM active site. CofH initiates the reaction by abstracting a hydrogen atom from the amine of L-tyrosine to form a *p*-hydroxybenzyl radical which is then coupled to the 5-position of the pyrimidine moiety of 5-amino-6-ribitylamino-2,4(1*H*,3*H*)-pyrimidinedione to form a *p*-hydroxybenzylated pyrimidinedione adduct.[118] Next, CofG abstracts a hydrogen from the *p*-hydroxybenzyl moiety to facilitate ring closure with the pyrimidinedione moiety to form F_0.[118]

Next, a 2-phospho-L-lactate transferase (CofD in archaea and FbiA in bacteria) attaches a phospho-L-lactyl moiety on to F_0 to form F_{420}-0.[119-120] The final step in F_{420} biosynthesis is the polyglutamylation of F_{420}-0 catalyzed by a γ-glutamyl ligase (CofE in archaea and FbiB in bacteria). CofE and the N-terminal domain of FbiB are homologous

to each other, but the bacterial γ-glutamyl ligase, FbiB, contains an additional C-terminal domain that is not present in the γ-glutamyl ligases of archaea.[121-122] While both domains of FbiB are required for activity, the CofE-like N-terminal domain of FbiB appears to contain the active site. The C-terminal domain of FbiB contains a groove of positively charged residues which may be involved in binding the polyglutamate-tail observed in F_{420} produced by bacteria. FbiB from *M. tuberculosis* produced cofactor F_{420} containing a mixture of glutamate tail lengths, with seven being the most common.[122] It is not yet known how the number of glutamates attached to F_{420} are regulated by FbiB between different species.

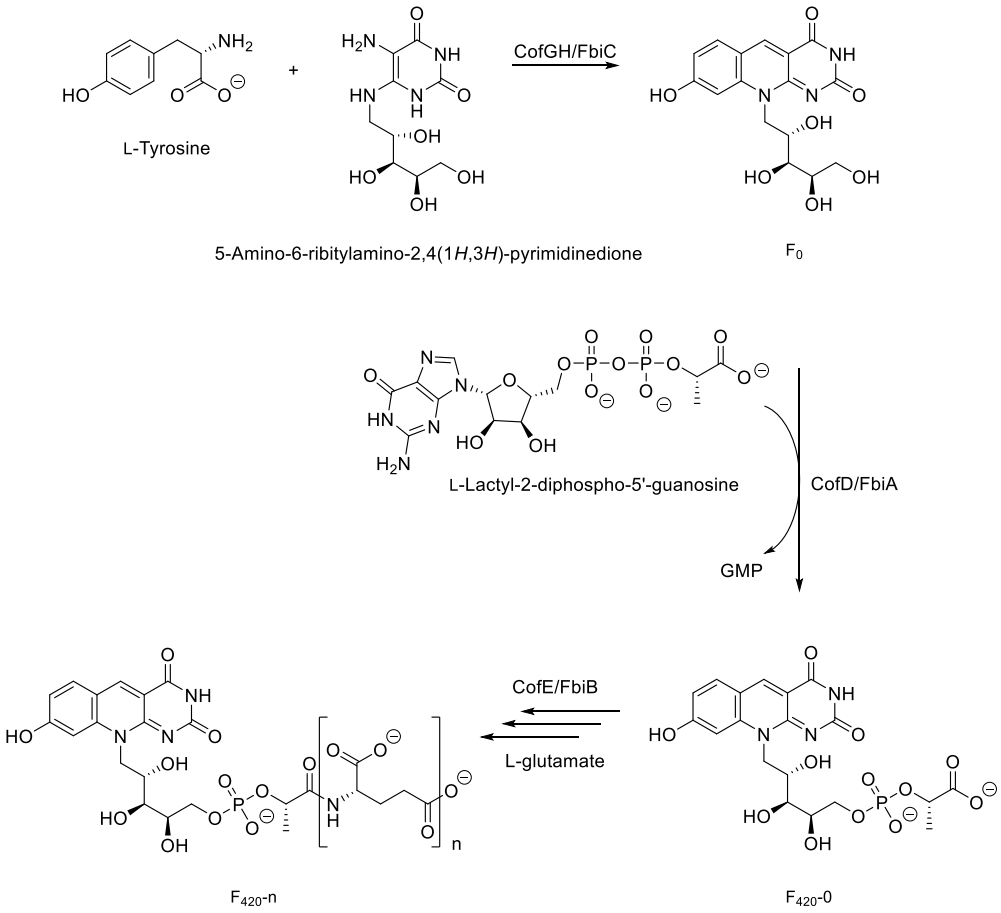

Scheme 1.8: The proposed biosynthetic pathway of coenzyme F_{420} in archaea (CofEDGH) and in actinobacteria (FbiABC).[116, 119, 122]

1.11 Scope of this work

At least fifteen thiopeptide biosynthetic gene clusters have been identified since 2009, and the functions of many proteins involved in thiopeptide biosynthesis have been described.[35, 37-39, 44, 63, 67, 89, 123-130] Thiopeptides, however, are a diverse family of natural products with an abundance of interesting chemical modifications for which the biosynthetic origins remain unclear. In particular, the formation of the central nitrogenous heterocycle in series *a-b* remains enigmatic. The thiopeptins are a complex of thiopeptides

with either a piperidine (series *a*) or a dehydropiperidine (seires *b*) ring in the core macrocycle and an unusual thioamide moiety. In this work, the thiopeptin biosynthetic gene cluster is identified along with two enzymes of this pathway: TpnW, a L-tryptophan transaminase and TpnL, an unusual $F_{420}H_2$-dependent dehydropiperidine reductase. The characterization of TpnL as a dehydropiperidine reductase establishes the basis for the piperidine-containing series *a* thiopeptides. These insights expand our understanding of complex chemical transformations in biological systems and provide us with biosynthetic tools that may be useful in the discovery of analogs with improved biological activities.

1.12 References

1. Bagley, M. C.; Dale, J. W.; Merritt, E. A.; Xiong, X., Thiopeptide antibiotics. *Chem. Rev.* **2005**, *105*, 685-714.

2. Arnison, P. G.; Bibb, M. J.; Bierbaum, G.; Bowers, A. A.; Bugni, T. S.; Bulaj, G.; Camarero, J. A.; Campopiano, D. J.; Challis, G. L.; Clardy, J.; Cotter, P. D.; Craik, D. J.; Dawson, M.; Dittmann, E.; Donadio, S.; Dorrestein, P. C.; Entian, K. D.; Fischbach, M. A.; Garavelli, J. S.; Goransson, U.; Gruber, C. W.; Haft, D. H.; Hemscheidt, T. K.; Hertweck, C.; Hill, C.; Horswill, A. R.; Jaspars, M.; Kelly, W. L.; Klinman, J. P.; Kuipers, O. P.; Link, A. J.; Liu, W.; Marahiel, M. A.; Mitchell, D. A.; Moll, G. N.; Moore, B. S.; Muller, R.; Nair, S. K.; Nes, I. F.; Norris, G. E.; Olivera, B. M.; Onaka, H.; Patchett, M. L.; Piel, J.; Reaney, M. J.; Rebuffat, S.; Ross, R. P.; Sahl, H. G.; Schmidt, E. W.; Selsted, M. E.; Severinov, K.; Shen, B.; Sivonen, K.; Smith, L.; Stein, T.; Sussmuth, R. D.; Tagg, J. R.; Tang, G. L.; Truman, A. W.; Vederas, J. C.; Walsh, C. T.; Walton, J. D.; Wenzel, S. C.; Willey, J. M.; van der Donk, W. A., Ribosomally synthesized and post-translationally modified peptide natural products: overview and recommendations for a universal nomenclature. *Nat. Prod. Rep.* **2013**, *30*, 108-160.

3. Hegde, N. S.; Sanders, D. A.; Rodriguez, R.; Balasubramanian, S., The transcription factor FOXM1 is a cellular target of the natural product thiostrepton. *Nat. Chem.* **2011**, *3*, 725-731.

4. Mocek, U.; Chen, L. C.; Keller, P. J.; Houck, D. R.; Beale, J. M.; Floss, H. G., ^{1}H and ^{13}C NMR assignments of the thiopeptide antibiotic nosiheptide. *J. Antibiot.* **1989**, *42*, 1643-1648.

5. Morris, R. P.; Leeds, J. A.; Naegeli, H. U.; Oberer, L.; Memmert, K.; Weber, E.; LaMarche, M. J.; Parker, C. N.; Burrer, N.; Esterow, S.; Hein, A. E.; Schmitt, E. K.; Krastel, P., Ribosomally synthesized thiopeptide antibiotics targeting elongation factor Tu. *J. Am. Chem. Soc.* **2009**, *131*, 5946-5955.

6. Puar, M. S.; Chan, T. M.; Hegde, V.; Patel, M.; Bartner, P.; Ng, K. J.; Pramanik, B. N.; MacFarlane, R. D., Sch 40832: a novel thiostrepton from *Micromonospora carbonacea*. *J. Antibiot.* **1998**, *51*, 221-224.

7. Dutcher, J. D.; Vandeputte, J., Thiostrepton, a new antibiotic. II. Isolation and chemical characterization. *Antibiot. Annu.* **1955**, *3*, 560-561.

8. Trejo, W. H.; Dean, L. D.; Pluscec, J.; Meyers, E.; Brown, W. E., *Streptomyces laurentii*, a new species producing thiostrepton. *J. Antibiot.* **1977**, *30*, 639-643.

9. Puar, M. S.; Ganguly, A. K.; Afonso, A.; Brambilla, R.; Mangiaracina, P.; Sarre, O.; MacFarlane, R. D., Sch 18640. A new thiostrepton-type antibiotic. *J. Am. Chem. Soc.* **1981**, *103*, 5231-5233.

10. Ciufolini, M. A.; Lefranc, D., Micrococcin P_1: structure, biology and synthesis. *Nat. Prod. Rep.* **2010**, *27*, 330-342.

11. Su, T. L., Micrococcin, an antibacterial substance formed by a strain of *Micrococcus*. *Br. J. Exp. Pathol.* **1948**, *29*, 473-481.

12. Nagai, K.; Kamigiri, K.; Arao, N.; Suzumura, K.; Kawano, Y.; Yamaoka, M.; Zhang, H.; Watanabe, M.; Suzuki, K., YM-266183 and YM-266184, novel thiopeptide antibiotics produced by *Bacillus cereus* isolated from a marine sponge. I. Taxonomy, fermentation, isolation, physico-chemical properties and biological properties. *J. Antibiot.* **2003**, *56*, 123-128.

13. Pascard, C.; Ducruix, A.; Lunel, J.; Prange, T., Highly modified cysteine-containing antibiotics. Chemical structure and configuration of nosiheptide. *J. Am. Chem. Soc.* **1977**, *99*, 6418-6423.

14. Jambor, W. P.; Steinberg, B. A.; Suydam, L. O., Thiostrepton, a new antibiotic. III. *In vivo* studies. *Antibiot. Annu.* **1955**, *3*, 562-565.

15. Dutcher, J. D.; Vandeputte, J., Thiostrepton, a new antibiotic. II. Isolation and chemical characterization. *Antibiot. Annu.* **1955**, *3*, 560-561.

16. Donovick, R.; Pagano, J. F.; Stout, H. A.; Weinstein, M. J., Thiostrepton, a new antibiotic. I. *In vitro* studies. *Antibiot. Annu.* **1955**, *3*, 554-559.

17. Anderson, B.; Hodgkin, D. C.; Viswamitra, M. A., The structure of thiostrepton. *Nature* **1970**, *225*, 233-235.

18. Mocek, U.; Beale, J. M.; Floss, H. G., Reexamination of the ^{1}H and ^{13}C NMR spectral assignments of thiostrepton. *J. Antibiot.* **1989**, *42*, 1649-1652.

19. Tori, K.; Tokura, K.; Okabe, K.; Ebata, M.; Otsuka, H.; Lukacs, G., Carbon-13 NMR studies of peptide antibiotics, thiostrepton and siomycin A: the structure relationship. *Tetrahedron Lett.* **1976**, *17*, 185-188.

20. Hensens, O. D.; Albers-Schonberg, G., ^{13}C NMR study of thiostrepton and thiopeptin components. *J. Antibiot.* **1983**, *36*, 832-845.

21. Bagley, M. C.; Bashford, K. E.; Hesketh, C. L.; Moody, C. J., Total Synthesis of the Thiopeptide Promothiocin A. *J. Am. Chem. Soc.* **2000**, *122*, 3301-3313.

22. Nicolaou, K. C.; Safina, B. S.; Zak, M.; Lee, S. H.; Nevalainen, M.; Bella, M.; Estrada, A. A.; Funke, C.; Zecri, F. J.; Bulat, S., Total synthesis of thiostrepton. Retrosynthetic analysis and construction of key building blocks. *J. Am. Chem. Soc.* **2005**, *127*, 11159-11175.

23. Xu, L.; Farthing, A. K.; Dropinski, J. F.; Meinke, P. T.; McCallum, C.; Leavitt, P. S.; Hickey, E. J.; Colwell, L.; Barrett, J.; Liu, K., Nocathiacin analogs: Synthesis and antibacterial activity of novel water-soluble amides. *Bioorg. Med. Chem. Lett.* **2009**, *19*, 3531-3535.

24. Naidu, B. N.; Sorenson, M. E.; Matiskella, J. D.; Li, W.; Sausker, J. B.; Zhang, Y.; Connolly, T. P.; Lam, K. S.; Bronson, J. J.; Pucci, M. J.; Yang, H.; Ueda, Y., Synthesis and antibacterial activity of nocathiacin I analogues. *Bioorg. Med. Chem. Lett.* **2006**, *16*, 3545-3549.

25. Fabbretti, A.; He, C. G.; Gaspari, E.; Maffioli, S.; Brandi, L.; Spurio, R.; Sosio, M.; Jabes, D.; Donadio, S., A derivative of the thiopeptide GE2270A highly selective against *Propionibacterium acnes*. *Antimicrob. Agents Chemother.* **2015**, *59*, 4560-4568.

26. Myers, C. L.; Hang, P. C.; Ng, G.; Yuen, J.; Honek, J. F., Semi-synthetic analogues of thiostrepton delimit the critical nature of tail region modifications in the control of protein biosynthesis and antibacterial activity. *Bioorg. Med. Chem.* **2010**, *18*, 4231-4237.

27. Jonker, H. R.; Baumann, S.; Wolf, A.; Schoof, S.; Hiller, F.; Schulte, K. W.; Kirschner, K. N.; Schwalbe, H.; Arndt, H. D., NMR structures of thiostrepton derivatives for characterization of the ribosomal binding site. *Angew. Chem. Int. Ed. Engl.* **2011**, *50*, 3308-3312.

28. Singh, S. B.; Xu, L.; Meinke, P. T.; Kurepina, N.; Kreiswirth, B. N.; Olsen, D. B.; Young, K., Thiazomycin, nocathiacin and analogs show strong activity against

clinical strains of drug-resistant *Mycobacterium tuberculosis*. *J. Antibiot.* **2017**, *70*, 671-674.

29. Sharma, I.; Sullivan, M.; McCutchan, T. F., *In vitro* antimalarial activity of novel semisynthetic nocathiacin I antibiotics. *Antimicrob. Agents Chemother.* **2015**, *59*, 3174-3179.

30. Zhang, F.; Kelly, W. L., Saturation mutagenesis of TsrA Ala4 unveils a highly mutable residue of thiostrepton A. *ACS Chem. Biol.* **2015**, *10*, 998-1009.

31. Zhang, F.; Li, C.; Kelly, W. L., Thiostrepton variants containing a contracted quinaldic acid macrocycle result from mutagenesis of the second residue. *ACS Chem. Biol.* **2016**, *11*, 415-424.

32. Bowers, A. A.; Acker, M. G.; Young, T. S.; Walsh, C. T., Generation of thiocillin ring size variants by prepeptide gene replacement and *in vivo* processing by *Bacillus cereus*. *J. Am. Chem. Soc.* **2012**, *134*, 10313-10316.

33. Acker, M. G.; Bowers, A. A.; Walsh, C. T., Generation of thiocillin variants by prepeptide gene replacement and *in vivo* processing by *Bacillus cereus*. *J. Am. Chem. Soc.* **2009**, *131*, 17563-17565.

34. Duan, L.; Wang, S.; Liao, R.; Liu, W., Insights into quinaldic acid moiety formation in thiostrepton biosynthesis facilitating fluorinated thiopeptide generation. *Chem. Biol.* **2012**, *19*, 443-448.

35. Young, T. S.; Walsh, C. T., Identification of the thiazolyl peptide GE37468 gene cluster from *Streptomyces* ATCC 55365 and heterologous expression in *Streptomyces lividans*. *Proc. Natl. Acad. Sci. U.S.A.* **2011**, *108*, 13053-13058.

36. Li, C.; Zhang, F.; Kelly, W. L., Mutagenesis of the thiostrepton precursor peptide at Thr7 impacts both biosynthesis and function. *Chem. Commun.* **2012**, *48*, 558-560.

37. Kelly, W. L.; Pan, L.; Li, C., Thiostrepton biosynthesis: prototype for a new family of bacteriocins. *J. Am. Chem. Soc.* **2009**, *131*, 4327-4334.

38. Liao, R.; Duan, L.; Lei, C.; Pan, H.; Ding, Y.; Zhang, Q.; Chen, D.; Shen, B.; Yu, Y.; Liu, W., Thiopeptide biosynthesis featuring ribosomally synthesized precursor peptides and conserved posttranslational modifications. *Chem. Biol.* **2009**, *16*, 141-147.

39. Wieland Brown, L. C.; Acker, M. G.; Clardy, J.; Walsh, C. T.; Fischbach, M. A., Thirteen posttranslational modifications convert a 14-residue peptide into the antibiotic thiocillin. *Proc. Natl. Acad. Sci. U.S.A.* **2009**, *106*, 2549-2553.

40. Hensens, O. D.; Albers-Schonberg, G., Total structure of the highly modified peptide antibiotic components of thiopeptin. *J. Antibiot.* **1983**, *36*, 814-831.

41. Anderson, B.; Hodgkin, D. C.; Viswamitra, M. A., The structure of thiostrepton. *Nature* **1970**, *225*, 233-235.

42. Ebata, M.; Miyazaki, K.; Otsuka, H., Studies on siomycin. I. Physicochemical properties of siomycins A, B and C. *J. Antibiot.* **1969**, *22*, 364-368.

43. Stella, S.; Montanini, N.; Le Monnier, F.; Ferrari, P.; Colombo, L.; Marinelli, F.; Landini, P.; Ciciliato, I.; Goldstein, B. P.; Selva, E.; et al., Antibiotic GE37468 A: a new inhibitor of bacterial protein synthesis. I. Isolation and characterization. *J. Antibiot.* **1995**, *48*, 780-786.

44. De Pietro, M. T.; Marazzi, A.; Sosio, M.; Donadio, S.; Lancini, G., Biosynthesis of the thiazolylpeptide antibiotic GE2270. *J. Antibiot.* **2001**, *54*, 1066-1071.

45. Yun, B. S.; Hidaka, T.; Furihata, K.; Seto, H., Promothiocins A and B novel thiopeptides with a tipA promoter inducing activity produced by *Streptomyces* sp. SF2741. *J. Antibiot.* **1994**, *47*, 510-514.

46. Leet, J. E.; Li, W.; Ax, H. A.; Matson, J. A.; Huang, S.; Huang, R.; Cantone, J. L.; Drexler, D.; Dalterio, R. A.; Lam, K. S., Nocathiacins, new thiazolyl peptide antibiotics from *Nocardia* sp. II. Isolation, characterization, and structure determination. *J. Antibiot.* **2003**, *56*, 232-242.

47. Pucci, M. J.; Bronson, J. J.; Barrett, J. F.; DenBleyker, K. L.; Discotto, L. F.; Fung-Tomc, J. C.; Ueda, Y., Antimicrobial evaluation of nocathiacins, a thiazole peptide class of antibiotics. *Antimicrob. Agents Chemother.* **2004**, *48*, 3697-3701.

48. Kelly, J.; Kutscher, A. H.; Tuot, I. F., Thiostrepton, a new antibiotic: tube dilution sensitivity studies. *Oral Surg. Oral Med. Oral Pathol.* **1959**, *12*, 1334-1339.

49. Miyairi, N.; Miyoshi, T.; Aoki, H.; Kosaka, M.; Ikushima, H., Thiopeptin, a new feed additive antibiotic: microbiological and chemical studies. *Antimicrob. Agents Chemother.* **1972**, *1*, 192-196.

50. Lentzen, G.; Klinck, R.; Matassova, N.; Aboul-ela, F.; Murchie, A. I., Structural basis for contrasting activities of ribosome binding thiazole antibiotics. *Chem. Biol.* **2003**, *10*, 769-778.

51. Bausch, S. L.; Poliakova, E.; Draper, D. E., Interactions of the N-terminal domain of ribosomal protein L11 with thiostrepton and rRNA. *J. Biol. Chem.* **2005**, *280*, 29956-29963.

52. Harms, J. M.; Wilson, D. N.; Schluenzen, F.; Connell, S. R.; Stachelhaus, T.; Zaborowska, Z.; Spahn, C. M. T.; Fucini, P., Translational regulation via L11: molecular switches on the ribosome turned on and off by thiostrepton and micrococcin. *Mol. Cell* **2008**, *30*, 26-38.

53. Heffron, S. E.; Jurnak, F., Structure of an EF-Tu complex with a thiazolyl peptide antibiotic determined at 2.35 Å resolution: atomic basis for GE2270A inhibition of EF-Tu. *Biochemistry* **2000**, *39*, 37-45.

54. Clough, B.; Rangachari, K.; Strath, M.; Preiser, P. R.; Wilson, R. J., Antibiotic inhibitors of organellar protein synthesis in *Plasmodium falciparum*. *Protist.* **1999**, *150*, 189-195.

55. Clough, B.; Strath, M.; Preiser, P.; Denny, P.; Wilson, I. R., Thiostrepton binds to malarial plastid rRNA. *FEBS Lett.* **1997**, *406*, 123-125.

56. Aminake, M. N.; Schoof, S.; Sologub, L.; Leubner, M.; Kirschner, M.; Arndt, H. D.; Pradel, G., Thiostrepton and derivatives exhibit antimalarial and gametocytocidal activity by dually targeting parasite proteasome and apicoplast. *Antimicrob. Agents Chemother.* **2011**, *55*, 1338-1348.

57. Fichera, M. E.; Roos, D. S., A plastid organelle as a drug target in apicomplexan parasites. *Nature* **1997**, *390*, 407-409.

58. Lim, L.; McFadden, G. I., The evolution, metabolism and functions of the apicoplast. *Philos. Trans. R. Soc. Lond. B. Biol. Sci.* **2010**, *365*, 749-763.

59. Gupta, A.; Shah, P.; Haider, A.; Gupta, K.; Siddiqi, M. I.; Ralph, S. A.; Habib, S., Reduced ribosomes of the apicoplast and mitochondrion of *Plasmodium* spp. and predicted interactions with antibiotics. *Open Biol.* **2014**, *4*, 140045.

60. Pandit, B.; Bhat, U. G.; Gartel, A. L., Proteasome inhibitory activity of thiazole antibiotics. *Cancer Biol. Ther.* **2011**, *11*, 43-47.

61. Fontaine, F.; Overman, J.; Francois, M., Pharmacological manipulation of transcription factor protein-protein interactions: opportunities and obstacles. *Cell Regen.* **2015**, *4*, 2.

62. Hopkins, A. L.; Groom, C. R., The druggable genome. *Nat. Rev. Drug Discov.* **2002**, *1*, 727-730.

63. Yu, Y.; Duan, L.; Zhang, Q.; Liao, R.; Ding, Y.; Pan, H.; Wendt-Pienkowski, E.; Tang, G.; Shen, B.; Liu, W., Nosiheptide biosynthesis featuring a unique indole side ring formation on the characteristic thiopeptide framework. *ACS Chem. Biol.* **2009**, *4*, 855-864.

64. Mine, K.; Miyairi, N.; Takano, N.; Mori, S.; Watanabe, N., Thiopeptin, a new feed-additive antibiotic: biological studies and field trials. *Antimicrob. Agents Chemother.* **1972**, *1*, 496-503.

65. Miyairi, N.; Miyoshi, T.; Aoki, H.; Kosaka, M.; Ikushima, H., Studies on thiopeptin antibiotics. I. Characteristics of thiopeptin B. *J. Antibiot.* **1970**, *23*, 113-119.

66. Liou, Y. F.; Kinoshita, T.; Tanaka, N., Inhibition by thiopeptin of bacterial protein synthesis. *J. Microbiol.* **1976**, *20*, 233-240.

67. Hudson, G. A.; Zhang, Z.; Tietz, J. I.; Mitchell, D. A.; van der Donk, W. A., *In vitro* biosynthesis of the core scaffold of the thiopeptide thiomuracin. *J. Am. Chem. Soc.* **2015**, *137*, 16012-16015.

68. Dunbar, K. L.; Tietz, J. I.; Cox, C. L.; Burkhart, B. J.; Mitchell, D. A., Identification of an auxiliary leader peptide-binding protein required for azoline formation in ribosomal natural products. *J. Am. Chem. Soc.* **2015**, *137*, 7672-7677.

69. Dunbar, K. L.; Melby, J. O.; Mitchell, D. A., YcaO domains use ATP to activate amide backbones during peptide cyclodehydrations. *Nat. Chem. Biol.* **2012**, *8*, 569-575.

70. Zhang, Z.; Hudson, G. A.; Mahanta, N.; Tietz, J. I.; van der Donk, W. A.; Mitchell, D. A., Biosynthetic timing and substrate specificity for the thiopeptide thiomuracin. *J. Am. Chem. Soc.* **2016**, *138*, 15511-15514.

71. Garg, N.; Salazar-Ocampo, L. M.; van der Donk, W. A., *In vitro* activity of the nisin dehydratase NisB. *Proc. Natl. Acad. Sci. U.S.A.* **2013**, *110*, 7258-7263.

72. Cogan, D. P.; Hudson, G. A.; Zhang, Z.; Pogorelov, T. V.; van der Donk, W. A.; Mitchell, D. A.; Nair, S. K., Structural insights into enzymatic [4+2] aza-cycloaddition in thiopeptide antibiotic biosynthesis. *Proc. Natl. Acad. Sci. U.S.A.* **2017**, *114*, 12928-12933.

73. Brieger, G.; Bennett, J. N., The intramolecular Diels-Alder reaction. *Chem. Rev.* **1980**, *80*, 63-97.

74. Klas, K.; Tsukamoto, S.; Sherman, D. H.; Williams, R. M., Natural Diels-Alderases: elusive and irresistable. *J. Org. Chem.* **2015**, *80*, 11672-11685.

75. Tietze, L. F.; Kettschau, G., Hetero Diels-Alder reactions in organic chemistry. In *Stereoselective Heterocyclic Synthesis I*, Metz, P., Ed. Springer Berlin Heidelberg: Berlin, Heidelberg, **1997**, 1-120.

76. Linkert, F.; Laschat, S.; Kotila, S.; Fox, T., Evidence for a stepwise mechanism in formal hetero-Diels-Alder reactions of *N*-arylimines. *Tetrahedron* **1996**, *52*, 955-970.

77. Lock, R.; Waldmann, H., Asymmetric synthesis of highly functionalized tetracyclic indole bases embodying the basic skeleton of yohimbine- and reserpine-type alkaloids. *Tetrahedron Lett.* **1996**, *37*, 2753-2756.

78. Nicolaou, K. C.; Dethe, D. H.; Chen, D. Y., Total syntheses of amythiamicins A, B and C. *Chem. Commun.* **2008**, 23, 2632-2634.

79. Moody, C. J.; Hughes, R. A.; Thompson, S. P.; Alcaraz, L., Biosynthesis inspired Diels-Alder route to pyridines: synthesis of the 2,3-dithiazolylpyridine core of the thiopeptide antibiotics. *Chem. Commun.* **2002**, 16, 1760-1761.

80. Nicolaou, K. C.; Dethe, D. H.; Leung, G. Y. C.; Zou, B.; Chen, D. Y.-K., Total synthesis of thiopeptide antibiotics GE2270A, GE2270T, and GE2270C1. *Chem. Asian J.* **2008**, *3*, 413-429.

81. Benjdia, A.; Pierre, S.; Gherasim, C.; Guillot, A.; Carmona, M.; Amara, P.; Banerjee, R.; Berteau, O., The thiostrepton A tryptophan methyltransferase TsrM catalyses a cob(II)alamin-dependent methyl transfer reaction. *Nat. Commun.* **2015**, *6*, 8377.

82. Lin, Z.; Ji, J.; Zhou, S.; Zhang, F.; Wu, J.; Guo, Y.; Liu, W., Processing 2-methyl-L-tryptophan through tandem transamination and selective oxygenation initiates indole ring expansion in the biosynthesis of thiostrepton. *J. Am. Chem. Soc.* **2017**, *139*, 12105-12108.

83. Ryan, P. C.; Lu, M.; Draper, D. E., Recognition of the highly conserved GTPase center of 23 S ribosomal RNA by ribosomal protein L11 and the antibiotic thiostrepton. *J. Mol. Biol.* **1991**, *221*, 1257-1268.

84. Zheng, Q.; Wang, S.; Liao, R.; Liu, W., Precursor-directed mutational biosynthesis facilitates the functional assignment of two cytochromes P450 in thiostrepton biosynthesis. *ACS Chem. Biol.* **2016**, *11*, 2673-2678.

85. Zheng, Q.; Wang, S.; Duan, P.; Liao, R.; Chen, D.; Liu, W., An α/β-hydrolase fold protein in the biosynthesis of thiostrepton exhibits a dual activity for endopeptidyl hydrolysis and epoxide ring opening/macrocyclization. *Proc. Natl. Acad. Sci. U.S.A.* **2016**, *113*, 14318-14323.

86. Liao, R.; Liu, W., Thiostrepton maturation involving a deesterification-amidation way to process the C-terminally methylated peptide backbone. *J. Am. Chem. Soc.* **2011**, *133*, 2852-2855.

87. Aoki, M.; Ohtsuka, T.; Itezono, Y.; Yokose, K.; Furihata, K.; Seto, H., Structure of cyclothiazomycin, a unique polythiazole-containing peptide with renin inhibitory activity. Part 2. Total structure. *Tetrahedron Lett.* **1991**, *32*, 221-224.

88. Martin, J.; da, S. S. T.; Crespo, G.; Palomo, S.; Gonzalez, I.; Tormo, J. R.; de la Cruz, M.; Anderson, M.; Hill, R. T.; Vicente, F.; Genilloud, O.; Reyes, F., Kocurin, the true structure of PM181104, an anti-methicillin-resistant *Staphylococcus aureus* (MRSA) thiazolyl peptide from the marine-derived bacterium *Kocuria palustris*. *Mar. Drugs* **2013**, *11*, 387-398.

89. Wang, J.; Yu, Y.; Tang, K.; Liu, W.; He, X.; Huang, X.; Deng, Z., Identification and analysis of the biosynthetic gene cluster encoding the thiopeptide antibiotic cyclothiazomycin in *Streptomyces hygroscopicus* 10-22. *Appl. Environ. Microbiol.* **2010**, *76*, 2335-2344.

90. Schoof, S.; Arndt, H.-D., D-Cysteine occurrence in thiostrepton may not necessitate an epimerase. *Chem. Commun.* **2009**, 46, 7113-7115.

91. Fate, G. D.; Benner, C. P.; Grode, S. H.; Gilbertson, T. J., The biosynthesis of sulfomycin elucidated by isotopic labeling studies. *J. Am. Chem. Soc.* **1996**, *118*, 11363-11368.

92. Mocek, U.; Knaggs, A. R.; Tsuchiya, R.; Nguyen, T.; Beale, J. M.; Floss, H. G., Biosynthesis of the modified peptide antibiotic nosiheptide in *Streptomyces actuosus*. *J. Am. Chem. Soc.* **1993**, *115*, 7557-7568.

93. Mocek, U.; Zeng, Z. P.; Ohagan, D.; Zhou, P.; Fan, L. D. G.; Beale, J. M.; Floss, H. G., Biosynthesis of the modified peptide antibiotic thiostrepton in *Streptomyces azureus* and *Streptomyces laurentii*. *J. Am. Chem. Soc.* **1993**, *115*, 7992-8001.

94. Tomiki, T.; Saitou, N., Phylogenetic analysis of proteins associated in the four major energy metabolism systems: photosynthesis, aerobic respiration, denitrification, and sulfur respiration. *J. Mol. Evol.* **2004**, *59*, 158-176.

95. Schäfer, G.; Engelhard, M.; Müller, V., Bioenergetics of the archaea. *Microbiol. Mol. Biol. Rev.* **1999**, *63*, 570-620.

96. Anraku, Y., Bacterial electron transport chains. *Annu. Rev. Biochem.* **1988**, *57*, 101-132.

97. Walsh, C. T.; Wencewicz, T. A., Flavoenzymes: versatile catalysts in biosynthetic pathways. *Nat. Prod. Rep.* **2013**, *30*, 175-200.

98. Běhal, V., Enzymes of secondary metabolism in microorganisms. *Trends Biochem. Sci.* **1986**, *11*, 88-91.

99. Gorris, L. G.; van der Drift, C., Cofactor contents of methanogenic bacteria reviewed. *BioFactors* **1994**, *4*, 139-145.

100. Bair, T. B.; Isabelle, D. W.; Daniels, L., Structures of coenzyme F_{420} in *Mycobacterium* species. *Arch. Microbiol.* **2001**, *176*, 37-43.

101. Enzmann, F.; Mayer, F.; Rother, M.; Holtmann, D., Methanogens: biochemical background and biotechnological applications. *AMB Express* **2018**, *8*, 1.

102. Jacobson, F.; Walsh, C., Properties of 7,8-didemethyl-8-hydroxy-5-deazaflavins relevant to redox coenzyme function in methanogen metabolism. *Biochemistry* **1984**, *23*, 979-988.

103. Ney, B.; Carere, C. R.; Sparling, R.; Jirapanjawat, T.; Stott, M. B.; Jackson, C. J.; Oakeshott, J. G.; Warden, A. C.; Greening, C., Cofactor tail length modulates catalysis of bacterial F_{420}-dependent oxidoreductases. *Front. Microbiol.* **2017**, *8*, 1902.

104. Walsh, C., Naturally occurring 5-deazaflavin coenzymes: biological redox roles. *Acc. Chem. Res.* **1986**, *19*, 216-221.

105. Edmondson, D. E.; Barman, B.; Tollin, G., On the importance of the N^5 position in flavin coenzymes. Properties of free and protein-bound 5-deaza analogs. *Biochemistry* **1972**, *11*, 1133-1138.

106. Thauer, R. K.; Jungermann, K.; Decker, K., Energy conservation in chemotrophic anaerobic bacteria. *Bacteriol. Rev.* **1977**, *41*, 100-180.

107. Herrmann, G.; Jayamani, E.; Mai, G.; Buckel, W., Energy conservation via electron-transferring flavoprotein in anaerobic bacteria. *J. Bacteriol.* **2008**, *190*, 784-791.

108. Hagemeier, C. H.; Shima, S.; Thauer, R. K.; Bourenkov, G.; Bartunik, H. D.; Ermler, U., Coenzyme F_{420}-dependent methylenetetrahydromethanopterin dehydrogenase (Mtd) from *Methanopyrus kandleri*: a methanogenic enzyme with an unusual quarternary structure. *J. Mol. Biol.* **2003**, *332*, 1047-1057.

109. Cellitti, S. E.; Shaffer, J.; Jones, D. H.; Mukherjee, T.; Gurumurthy, M.; Bursulaya, B.; Boshoff, H. I.; Choi, I.; Nayyar, A.; Lee, Y. S.; Cherian, J.; Niyomrattanakit, P.; Dick, T.; Manjunatha, U. H.; Barry, C. E., 3rd; Spraggon, G.; Geierstanger, B. H., Structure of Ddn, the deazaflavin-dependent nitroreductase from *Mycobacterium tuberculosis* Involved in bioreductive activation of PA-824. *Structure* **2013**, *21*, 101-112.

110. Johnson, E. F.; Mukhopadhyay, B., A new type of sulfite reductase, a novel coenzyme F_{420}-dependent enzyme, from the methanarchaeon *Methanocaldococcus jannaschii*. *J. Biol. Chem.* **2005**, *280*, 38776-38786.

111. Singh, R.; Manjunatha, U.; Boshoff, H. I.; Ha, Y. H.; Niyomrattanakit, P.; Ledwidge, R.; Dowd, C. S.; Lee, I. Y.; Kim, P.; Zhang, L.; Kang, S.; Keller, T. H.; Jiricek, J.; Barry, C. E., 3rd, PA-824 kills nonreplicating *Mycobacterium tuberculosis* by intracellular NO release. *Science* **2008**, *322*, 1392-1395.

112. Selengut, J. D.; Haft, D. H., Unexpected abundance of coenzyme F_{420}-dependent enzymes in *Mycobacterium tuberculosis* and other actinobacteria. *J. Bacteriol.* **2010**, *192*, 5788-5798.

113. Purwantini, E.; Mukhopadhyay, B., Conversion of NO_2 to NO by reduced coenzyme F_{420} protects mycobacteria from nitrosative damage. *Proc. Natl. Acad. Sci. U.S.A.* **2009**, *106*, 6333-6338.

114. Jirapanjawat, T.; Ney, B.; Taylor, M. C.; Warden, A. C.; Afroze, S.; Russell, R. J.; Lee, B. M.; Jackson, C. J.; Oakeshott, J. G.; Pandey, G.; Greening, C., The redox cofactor F_{420} protects mycobacteria from diverse antimicrobial compounds and mediates a reductive detoxification system. *Appl. Environ. Microbiol.* **2016**, *82*, 6810-6818.

115. Gurumurthy, M.; Rao, M.; Mukherjee, T.; Rao, S. P.; Boshoff, H. I.; Dick, T.; Barry, C. E., 3rd; Manjunatha, U. H., A novel F_{420}-dependent anti-oxidant mechanism protects *Mycobacterium tuberculosis* against oxidative stress and bactericidal agents. *Mol. Microbiol.* **2013**, *87*, 744-755.

116. Decamps, L.; Philmus, B.; Benjdia, A.; White, R.; Begley, T. P.; Berteau, O., Biosynthesis of F_0, precursor of the F_{420} cofactor, requires a unique two radical-SAM domain enzyme and tyrosine as substrate. *J. Am. Chem. Soc.* **2012**, *134*, 18173-18176.

117. Choi, K. P.; Kendrick, N.; Daniels, L., Demonstration that *fbiC* is required by *Mycobacterium bovis* BCG for coenzyme F_{420} and F_0 biosynthesis. *J. Bacteriol.* **2002**, *184*, 2420-2428.

118. Philmus, B.; Decamps, L.; Berteau, O.; Begley, T. P., Biosynthetic versatility and coordinated action of 5'-deoxyadenosyl radicals in deazaflavin biosynthesis. *J. Am. Chem. Soc.* **2015**, *137*, 5406-5413.

119. Graupner, M.; Xu, H.; White, R. H., Characterization of the 2-phospho-L-lactate transferase enzyme involved in coenzyme F_{420} biosynthesis in *Methanococcus jannaschii*. *Biochemistry* **2002**, *41*, 3754-3761.

120. Forouhar, F.; Abashidze, M.; Xu, H.; Grochowski, L. L.; Seetharaman, J.; Hussain, M.; Kuzin, A.; Chen, Y.; Zhou, W.; Xiao, R.; Acton, T. B.; Montelione, G. T.; Galinier, A.; White, R. H.; Tong, L., Molecular insights into the biosynthesis of the F_{420} coenzyme. *J. Biol. Chem.* **2008**, *283*, 11832-11840.

121. Li, H.; Graupner, M.; Xu, H.; White, R. H., CofE catalyzes the addition of two glutamates to F_{420}-0 in F_{420} coenzyme biosynthesis in *Methanococcus jannaschii*. *Biochemistry* **2003**, *42*, 9771-9778.

122. Bashiri, G.; Rehan, A. M.; Sreebhavan, S.; Baker, H. M.; Baker, E. N.; Squire, C. J., Elongation of the poly-γ-glutamate tail of F_{420} requires both domains of the F_{420}:γ-glutamyl ligase (FbiB) of *Mycobacterium tuberculosis*. *J. Biol. Chem.* **2016**, *291*, 6882-6894.

123. Hayashi, S.; Ozaki, T.; Asamizu, S.; Ikeda, H.; Omura, S.; Oku, N.; Igarashi, Y.; Tomoda, H.; Onaka, H., Genome mining reveals a minimum gene set for the biosynthesis of 32-membered macrocyclic thiopeptides lactazoles. *Chem. Biol.* **2014**, *21*, 679-688.

124. Malcolmson, S. J.; Young, T. S.; Ruby, J. G.; Skewes-Cox, P.; Walsh, C. T., The posttranslational modification cascade to the thiopeptide berninamycin generates linear forms and altered macrocyclic scaffolds. *Proc. Natl. Acad. Sc.i U.S.A.* **2013**, *110*, 8483-8488.

125. Engelhardt, K.; Degnes, K. F.; Zotchev, S. B., Isolation and characterization of the gene cluster for biosynthesis of the thiopeptide antibiotic TP-1161. *Appl. Environ. Microbiol.* **2010**, *76*, 7093-7101.

126. Cox, C. L.; Tietz, J. I.; Sokolowski, K.; Melby, J. O.; Doroghazi, J. R.; Mitchell, D. A., Nucleophilic 1,4-additions for natural product discovery. *ACS Chem. Biol.* **2014**, *9*, 2014-2022.

127. Ding, Y.; Yu, Y.; Pan, H.; Guo, H.; Li, Y.; Liu, W., Moving posttranslational modifications forward to biosynthesize the glycosylated thiopeptide nocathiacin I in *Nocardia* sp. ATCC202099. *Mol. Biosyst.* **2010**, *6*, 1180-1185.

128. Schwalen, C. J.; Hudson, G. A.; Kille, B.; Mitchell, D. A., Bioinformatic expansion and discovery of thiopeptide antibiotics. *J. Am. Chem. Soc.* **2018**, *140*, 9494–9501.

129. Bennallack, P. R.; Bewley, K. D.; Burlingame, M. A.; Robison, R. A.; Miller, S. M.; Griffitts, J. S., Reconstitution and minimization of a micrococcin biosynthetic pathway in *Bacillus subtilis*. *J. Bacteriol.* **2016**, *198*, 2431-2438.

130. Kaweewan, I.; Komaki, H.; Hemmi, H.; Kodani, S., Isolation and structure determination of a new thiopeptide globimycin from *Streptomyces globisporus* subsp. globisporus based on genome mining. *Tetrahedron Lett.* **2018**, *59*, 409-414.

CHAPTER 2: IDENTIFICATION OF THE THIOPEPTIN BIOSYNTHETIC GENE CLUSTER AND CHARACTERIZATION OF TpnW, A 2-METHYL-L-TRYPTOPHAN AMINOTRANSFERASE

Adapted from: Ichikawa, H.; Bashiri, G.; Kelly, W.L. Biosynthesis of the thiopeptins and the identification of an $F_{420}H_2$-dependent dehydropiperidine reductase. *J. Am. Chem. Soc.* **2018**, *140*, 10749-10756.

The work described in this chapter was performed by Ichikawa, H.

2.1 Introduction

All members of the thiopeptins (**13-16**) contain an unusual thioamide moiety and thiopeptins A_{1a} **13** and B_a **14** contain a piperidine ring in the core macrocycle (Figure 2.1). The biosynthetic gene cluster responsible for the production of the thiopeptins has not yet been identified and the biosyntheses of the thioamide and piperidine ring are not well understood.

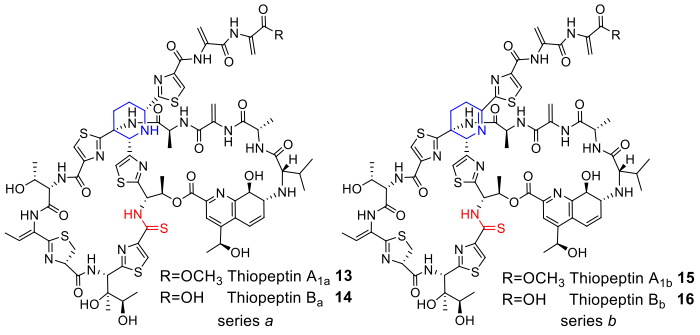

Figure 2.1: The structures of the thiopeptins. The (dehydro)piperidine ring is in blue and the thioamide is in red.

The thioamide is of particular interest as it is a rare modification in naturally-occurring metabolites. In addition to the thiopeptins, methanobactin, closthioamide, and thioviridamide are among the few examples that have been identified and the biological significance of the thioamide moieties of these compounds is not well understood (Figures 2.1 and 2.2).[1-3] The hexaoxa analog of the antibiotic closthioamide, closamide, lost activity against test bacterial strains, suggesting the thioamides are critical for its activity and this significance may extend to other thioamidated metabolites.[2]

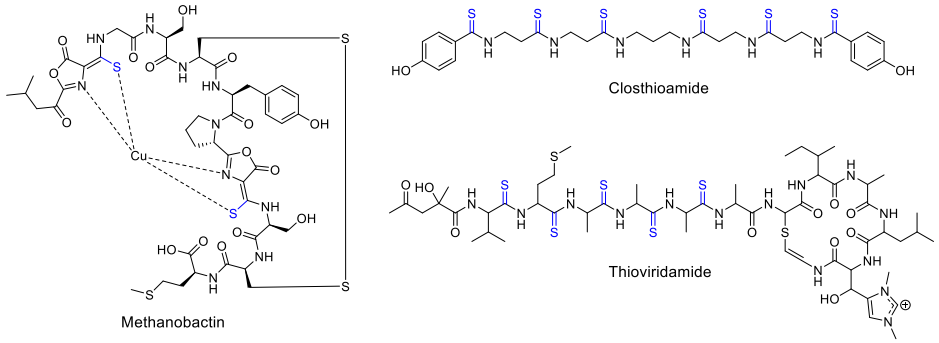

Figure 2.2: Examples of thioamide-containing natural products. The thioamide is in blue.[1-3]

In contrast to the rarity of thioamides in nature, thioamides have been utilized in medicinal chemistry to improve resistance of some peptidic drugs to proteolytic degradation over their amide counterparts.[4] In addition, certain thioamidated drugs have been shown to increase the potency of a drug compared to its parent compound.[5] The polythioamide analog of an opioid neuropeptide Leu-enkephalin is ten-fold more active over its amide equivalent and the affinity of the thioamidated Leu-enkephalin for the σ-opioid receptor is increased by more than five-fold.[6] Thioamide-containing drugs have

also been used to treat tuberculosis. Ethionamide and prothionamide are thioamide analogs of isoniazid (Figure 2.3). All three drugs are thought to inhibit InhA, the NADH-dependent enoyl-ACP reductase involved in mycolic acid biosynthesis, by strongly binding an isonicotinyl-NAD adduct that is formed in the cell (Figure 2.4).[7] While similar in structure, isoniazid and the thioamidated prodrugs are activated by different pathways. Heme-dependent catalase-peroxidase KatG abstracts the hydrazine moiety of isoniazid to form an isonicotinyl radical that reacts with NAD^+ to form an isonicotinyl-NAD adduct (Figure 2.4).[8] Certain mutations in *katG* confer resistance to isoniazid but not to ethionamide, suggesting either a different binding mode of the thioamidated analogs with KatG or a different activator of the analogs.[9] Ethionamide has been shown to be activated by an NADPH- and O_2-dependent flavin monooxygenase, EtaA, via formation of an *S*-oxide intermediate that is possibly oxidized to a sulfinic acid-containing reactive species.[7, 10] The ethionamide-derived NAD adduct has been shown to bind to InhA and mutations in *inhA* have been linked to ethionamide resistance by *Mycobacterium tuberculosis* (*M. tuberculosis*).[7, 11]

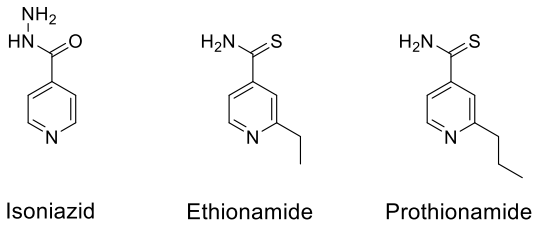

Figure 2.3: The structures of isonicotinic acid drugs used for treating tuberculosis.

While isoniazid is still an important antituberculosis drug today, it is ineffective against many other mycobacteria species such as *Mycobacterium leprae* (*M. leprae*), the causative agent of leprosy.[12] *M. leprae* and other isoniazid-resistant mycobacteria either lack *katG* or have a truncated *katG* homolog encoded in its genome and it is thought *M. leprae* is unable to activate isoniazid to form the isonicotinyl-NAD adduct that inhibits InhA.[13] Ethionamide and prothionamide, however, are effective against *M. leprae*. The formation of a prothionamide-derived NAD adduct was detected in the presence of prothionamide, NAD^+, and an EtaA-homolog in *M. leprae* and the NAD adduct showed strong inhibition of InhA in *M. leprae* (Figure 2.4).[11] The case of isoniazid and its thioamide derivatives shows how a simple modification of the chemical structure, such as the replacement of an amide with a thioamide, can alter how the drug is activated in the cell, enhancing its biological activity.

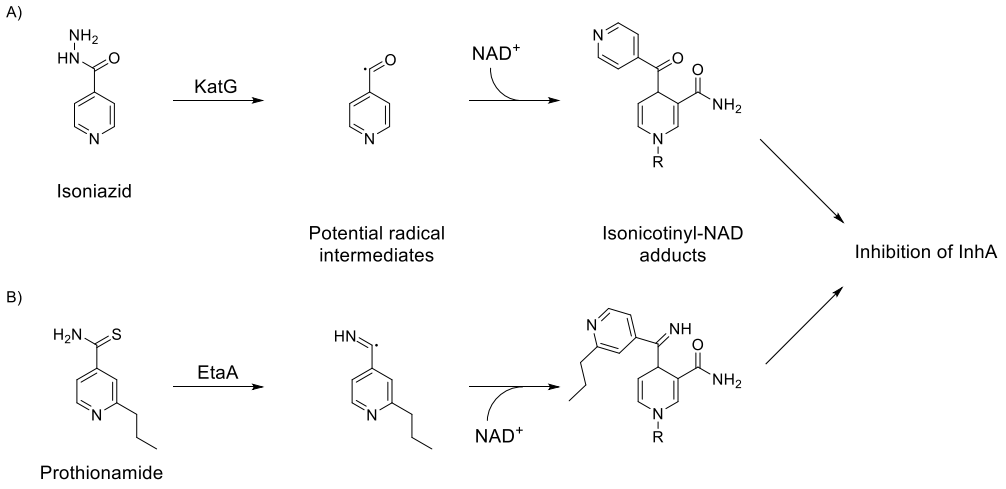

Figure 2.4: Possible pathways of InhA inhibition by prodrugs isoniazid and prothionamide. A) KatG-dependent activation of isoniazid, and B) EtaA-dependent activation of prothionamide, both which leads to the formation of an isonicotinyl-NAD adduct that inhibits InhA in certain mycobacteria species.

Detailed understanding of the biological activities associated with structural features in natural products and the biosynthetic machinery that installs these moieties are useful in the design, discovery, and production of novel metabolites with improved activities. Thiopeptides, like the thiopeptins, contain a wealth of unusual and complex chemical moieties installed on a peptidic substrate by a cascade of post-translational modifications.[14-17] The biosynthetic role of each enzyme that installs a novel modification onto a thiopeptide may be elucidated by a series of gene inactivation, heterologous expression, and *in vitro* enzyme activity reconstitution experiments. Characterization of these enzymes may lead to a development of useful biological tools to modify thiopeptides and other peptidic substrates. In addition, evaluation of the biological activities of thiopeptide analogs and biosynthetic intermediates produced in these experiments may provide us with insight to the structure-activity relationships of the thiopeptides.

In the interest of uncovering how the unusual piperidine and thioamide structural features are installed on thiopeptins and the potential biological effects of these modifications, we report the identification of the thiopeptin biosynthetic gene (*tpn*) cluster, and the putative functions of each open reading frame (*orf*). Based on bioinformatic analysis of 23 *orf*s of the *tpn* cluster, we propose that the thioamide is likely installed by the combined actions of TpnM, a YcaO-like protein, and TpnN, a TfuA-like protein, while the piperidine is installed by TpnL, a flavin/deazaflavin-dependent oxidoreductase. In support of the involvement of the *tpn* cluster in thiopeptin production, we present the initial characterization of TpnW, a transaminase that is involved in the biosynthesis of 4-(1-hydroxyethyl)quinoline-2-carboxylic acid (HEQ), a critical feature of the quinaldic acid-containing loop found in series *a-c* thiopeptides. The bioinformatic analysis of the *tpn*

cluster and the identification of TpnW as a 2-methyl-L-tryptophan transaminase present the basis for thiopeptin production in *S. tateyamensis*.

2.2 Materials and methods

2.2.1 General

All reagents, unless otherwise specified, were purchased from standard commercial sources and used as provided. 2-Methyl-L-tryptophan was enzymatically synthesized from 2-methylindole and L-serine according to previously described methods.[18] High-performance liquid chromatography (HPLC) analyses were performed on a Beckman Coulter System Gold HPLC using an analytical Phenomenex Luna 5μm C18(2) 250 x 4.6 mm column (Torrance, CA). All mass spectrometry analyses were performed at the Georgia Institute of Technology Bioanalytical Mass Spectrometry Facility. High-performance liquid chromatography-mass spectrometry (HPLC-MS) analyses were performed on a Micromass Quattro LC using a Phenomenex Synergi 4 μm MAX-RP 80 Å C18 250 x 2.00 mm column (Torrance, CA). Oligonucleotides were purchased from Integrated DNA Technologies, Inc. (Coralville, IA). DNA sequencing analyses were performed by Eurofins MWG Operon USA (Louisville, KY).

2.2.2 Bacterial strains, plasmids, and growth medium

All primers used are listed in Table A.1 and strains and plasmids used are listed in Table A.2. *Streptomyces tateyamensis* ATCC 21389 (*S. tateyamensis*) was purchased from American Type Culture Collection. *Escherichia coli* (*E. coli*) strains were cultured in Luria-Bertani medium supplemented with 100 μg/mL ampicillin, 50 μg/mL apramycin, 12.5 μg/mL chloramphenicol, 50 μg/mL kanamycin, or 50 μg/mL streptomycin. *Streptomyces* strains were cultured in medium supplemented with 50 μg/mL apramycin or 40 μg/mL streptomycin.

2.2.3 Growth of *S. tateyamensis* and analysis of thiopeptin production

A glycerolic mycelium stock of *S. tateyamensis* was used to inoculate 50 mL potato starch-based medium (40 g/L potato starch, 20 g/L cotton seed meal, 10 g/L corn steep liquor, 10 g/L yeast extract, 3 g/L $CaCO_3$, 21.8 g/L KH_2PO_4, 14.3 g/L $Na_2HPO_4 \cdot 12H_2O$, 1.7 g/L *N*-acetyl-DL-methionine) in a 250 mL Erlenmeyer flask. After incubation at 28 °C and 220 rpm for 72 hours, 2.5 mL of the starter culture was used to inoculate 50 mL potato starch-based medium in a 250 mL Erlenmeyer flask and grown at 28 °C and 220 rpm for 72 hours. Next, 5 mL of this seed culture was used to inoculate 100 mL potato starch-based medium in a 500 mL Erlenmeyer flask, and incubated at 28 °C at 220 rpm for 7 days. The whole culture was extracted twice with an equal volume of chloroform. The chloroform layers were pooled together, filtered, and the solvent was removed *in vacuo*. The solid residue was dissolved in 4 mL of chloroform. Samples were analyzed by HPLC and HPLC-MS.

2.2.4 Construction of the *S. tateyamensis* fosmid library and screening for selected sequences

S. tateyamensis genomic DNA was prepared according to the wizard DNA isolation kit (Promega, Madison, WI) protocol. *De novo* genome sequencing was performed at Macrogen Korea using a HiSeq 2000 sequencing system. The draft genome was partially sequenced to 6.92 Mb on 2,838 contiguous fragments and scanned for a nucleotide sequence encoding the thiopeptin core peptide (VASASCTTCICTCSCSS) using VectorNTI Advance 11. One match was identified, named as *tpnA*, and neighboring genes shared sequence similarity to thiostrepton (*tsr*) and siomycin (*sio*) biosynthetic genes.[14, 16] To facilitate fully assembling the sequence around *tpnA*, an *S. tateyamensis* genomic fosmid library was constructed using the CopyControl Fosmid Library Production Kit (Lucigen, Middleton, WI). 2,304 clones were isolated and stored according to manufacturer instructions. The *S. tateyamensis* fosmid library was screened by polymerase chain reaction (PCR) for the desired *tpn* sequences using the primer pairs HI-1F/HI-1R (for *tpnD*), HI-2F/HI-2R (for *tpnO*), and HI-3F/HI-3R (for *tpnU*). Two fosmids, HI2B7 and HI2G2, were found to harbor the *tpn* cluster and shotgun libraries of these two fosmids were prepared according to the TOPO Shotgun Subcloning Kit (Life Technologies, Carlsbad, CA) protocol. Sequencing of the shotgun libraries was performed at Functional Biosciences (Madison, WI). Additional DNA sequencing analysis was used to close any remaining gaps in the sequences of the fosmids by primer walking. The *tpn* cluster was included within a combined span of ~53 kb.

2.2.5 Bioinformatics analyses of the *tpn* gene cluster

Open reading frames (*orf*s) were determined using FramePlot 4.0 and the *orf*s were compared to other entries in the NCBI database using the protein Basic Local Alignment Search Tool (BLAST).

2.2.6 Sporulation of *S. tateyamensis*

A glycerolic mycelium stock of *S. tateyamensis* was used to inoculate 50 mL ATCC 172 medium in a 250 mL Erlenmeyer flask. After incubation at 28 °C and 220 rpm for 72 hours, 400 µL of the culture was inoculated on ISP3 agar. Colonies were observed after 1 day at incubation at 28 °C and spores were harvested after 10-25 days.

2.2.7 Intergeneric conjugation in *S. tateyamensis*

S. tateyamensis spores were collected from sporulating colonies that were 10-25 days old from four ISP3 agar plates and a spore suspension was prepared according to protocol with a few modifications.[19] To each ISP3 agar plate, 9 mL of sterile water was added and the surface of the solid culture was gently rubbed with an inoculation loop to suspend the spores in the water. The aqueous suspension of spores and mycelium from all four plates were pooled together and transferred to a 15 mL conical tube and vortexed for 1 min to break up spore aggregates. The spore-mycelium mixture was filtered twice through a cotton wool column and the isolated spores were checked by examination under an optical microscope. The spores were collected by centrifugation at 1000 x *g* for 10 min

at 4 °C. The supernatant was discarded and the spores were resuspended in ~100 μL of residual liquid. Intergeneric conjugation with *S. tateyamensis* spores was performed according to protocol.[19] An *E. coli* (ET12567/pUZ80002) strain harboring the appropriate pGM160HKss-derived vector was used as the donor for conjugation.

2.2.8 Disruption of *tpnA*

The *tpnA* gene and its flanking regions was amplified by PCR as a 2.5 kb fragment from fosmid HI2B7 using the primer pair HI-4F/HI-4R. The amplicon was cloned into pSC-B-amp/kan (Agilent, Santa Clara, CA) to yield pTpnA, and the vector was confirmed by DNA sequence analysis. pTpnA was digested with *Hin*dIII and the resulting 2.5 kb fragment was ligated into pGM160HKss to form pGM-tpnA. A 1.4 kb fragment containing the *aac(3)IV/oriT* cassette, amplified from pIJ773 using the primer pair HI-5F/HI-5R, was inserted into pGM-tpnA by λ Red-mediated recombination in *E. coli* BW25113/pKD46 to generate pGM-dtpnA. The resulting construct was confirmed by DNA sequence analysis and transformed into *E. coli* ET12567/pUZ8002.

S. tateyamensis protoplasts were prepared according to protocol with a few modifications.[19] A glycerolic mycelium stock of *S. tateyamensis* was used to inoculate 50 mL of ATCC 172 medium in a 250 mL Erlenmeyer flask. After incubation at 28 °C and 220 rpm for 72 hours, 1 mL of the starter culture was used to inoculate 50 mL of ATCC 172 medium containing 0.25% glycine in a 250 mL Erlenmeyer flask. After incubation at 28 °C and 220 rpm for 16 hours, the mycelium was harvested at 1000 x *g* for 10 min. Next, the mycelium was washed twice with 15 mL 10.3% (w/v) D-sucrose and resuspended in

4 mL lysis (L) buffer (9.09% (w/v) D-sucrose, 0.50% TES buffer pH 7.2, 0.02% (w/v) K_2SO_4, 1.76 x 10^{-3}% (w/v) trace metals solution (40 mg/L $ZnCl_2$, 200 mg/L $FeCl_3 \cdot 6H_2O$, 10 mg/L $CuCl_2 \cdot 2H_2O$, 10 mg/L $MnCl_2 \cdot 4H_2O$, 10 mg/L $Na_2B_4O_7 \cdot 10H_2O$, and 10 mg/L $(NH_4)_6Mo_7O_{24} \cdot 10H_2O$), 4.41 x 10^{-3}% (w/v) KH_2PO_4, 2.20 mM $MgCl_2 \cdot 6H_2O$, 2.20 mM $CaCl_2$) with 1.5 mg/mL lysozyme. The suspension was incubated at 30 °C for 30 min, gently mixed, and then incubated for 15 min at 30 °C. At this time, 5 mL of L buffer (without lysozyme) was added, and the mixture was incubated for another 15 min at 30 °C. The protoplast-mycelium mixture was filtered twice through a cotton wool column and the isolated protoplasts were checked by examination under an optical microscope. Protoplasts were harvested at 1000 x *g* for 7 min at 4 °C. The supernatant was removed and protoplasts were suspended in residual buffer. To 50 µL of protoplast suspension, 10 µL of a 100 ng/µL solution of pGM-dtpnA in TE buffer (10 mM Tris pH 8.0 and 1 mM ethylenediaminetetraacetic acid (EDTA)) isolated from *E. coli* ET12567/pUZ8002 was added, followed immediately by the addition of 0.5 mL room-temperature transformation buffer (2.37% (w/v) D-sucrose, 1.8 x 10^{-3}% (w/v) trace metals solution, 0.02% (w/v) K_2SO_4, 0.10 M $CaCl_2$, 50 mM Tris-maleic acid buffer pH 8.0, and 40% (w/v) polyethylene glycol 1000). To this mixture, 5 mL of room-temperature protoplast (P) buffer (103 g/L D-sucrose, 0.25 g/L K_2SO_4, 2.02 g/L $MgCl_2 \cdot 6H_2O$, 2 mL/L trace metals solution, 0.5 x 10^{-3}% (w/v) KH_2PO_4, 3.68 x 10^{-2}% (w/v) $CaCl_2 \cdot 2H_2O$, and 5.73 x 10^{-2}% (w/v) TES buffer pH 7.2) was immediately added. The protoplasts were harvested at 700 x *g* for 7 min at 4 °C. After removing the supernatant, the protoplasts were suspended in residual buffer and were diluted serially with room-temperature protoplast buffer. The transformation mixture was plated on ISP3 agar that was supplemented with 10 mM $MgCl_2$ and had dried in a laminar

flow hood for 6 hours. After incubation at 28 °C for 18 hours, the agar was overlaid with 1.25 mg apramycin in 1 mL of water. Plates were incubated at 28 °C for 3-5 days.

Mycelia of apramycin-resistant colonies were inoculated in 50 mL of ATCC 172 medium supplemented with 50 μg/mL apramycin in a 250 mL Erlenmeyer flask and incubated at 28 °C and 220 rpm for 72 hours. Whole-cell PCR was used to identify transformants harboring pGM-dtpnA using the primer pair HI-4F/HI-4R. A 2.5 kb amplicon was expected from wild-type *S. tateyamensis*, while a 3.7 kb amplicon was expected from the transformant. Forced homologous recombination at 39 °C provided the *tpnA* disruption mutant, *S. tateyamensis* HI1. The *tpnA* disruption (double crossover) mutant was confirmed by PCR analysis. A 2588 bp amplicon was expected from *S. tateyamensis* HI1 using primer pairs HI-26F/HI-26R and a 1871 bp amplicon was expected using primer pairs HI-27F/HI-27R. Together, the two amplified regions comprise a 4.4 kb region on the *S. tateyamensis* HI1 chromosome, including the 3.7 kb region involved in the disruption of *tpnA*. Amplicons were not expected from the wild-type *S. tateyamensis* using either primer pairs HI-26F/HI-26R or HI-27F/HI-27R. The amplicons from *S. tateyamensis* HI1 were cloned into pSC-B-kan/amp and the inserts were confirmed by DNA sequence analysis.

2.2.9 Additional conditions for *S. tateyamensis* protoplast preparation

In addition to the optimized condition for protoplast preparation described in section 2.3.8, other buffers were utilized during protocol development (Table 2.2). P_{R5} buffer (103 g/L D-sucrose, 0.25 g/L K_2SO_4, 2.03 g/L $MgCl_2 \cdot 6H_2O$, 2 mL/L trace metals

solution, 0.5 x 10^{-3}% (w/v) KH_2PO_4, 3.70 x 10^{-2}% (w/v) $CaCl_2 \cdot 2H_2O$, and 0.57% (w/v) TES buffer pH 7.2), and P_{R6} buffer (200 g/L D-sucrose, 0.10 g/L K_2SO_4, 2 mL/L trace metals solution, 7.0 x 10^{-2}% (w/v) $CaCl_2 \cdot 2H_2O$, 0.21% (w/v) 3-(*N*-morpholino)propanesulfonic acid **(**MOPS) buffer pH 7.2, and 10 g/L filter-sterilized bovine serum albumin) were used instead of the P buffer (described in Section 2.2.8) in certain conditions.[20] R2YE medium was used in certain conditions in place of the ISP3 medium as the regeneration medium.

2.2.10 Towards the disruption of *tpnL*

The *tpnL* gene and flanking regions was amplified by PCR as a 2.7 kb fragment from fosmid HI2G2 using the primer pair HI-8F/HI-8R. The amplicon was cloned into pSC-B-amp/kan (Agilent, Santa Clara, CA) to yield pTpnL, and the vector was confirmed by DNA sequence analysis. pTpnL was digested with *Hin*dIII, and the resulting 2.5 kb fragment was ligated into pGM160HKss to form pGM-tpnL. A 1.4 kb fragment containing the *aac(3)IV/oriT* cassette, amplified from pIJ773 using the primer pair HI-9F/HI-9R, was inserted into pGM-tpnL by λ Red-mediated recombination in *E. coli* BW25113/pKD46 to generate pGM-dtpnL. The resulting construct was confirmed by DNA sequence analysis and transformed into *E. coli* ET12567/pUZ8002.

S. tateyamensis protoplast preparation and transformation with pGM-dtpnL into *S. tateyamensis* were performed according to the methods described for the disruption of *tpnA*. Mycelia of apramycin-resistant colonies were inoculated in 50 mL of ATCC 172 medium supplemented with 50 μg/mL apramycin in a 250 mL Erlenmeyer flask and

incubated at 28 °C and 220 rpm for 72 hours. Whole-cell PCR was used to identify transformants harboring pGM-dtpnL using the primer pair HI-8F/HI-8R. From the wild-type strain, a 2.7 kb amplicon was expected while a 3.6 kb amplicon was expected from the transformant.

2.2.11 Towards the disruption of *tpnM*

The *tpnM* gene and flanking regions was amplified by PCR as a 2.7 kb fragment from fosmid HI2G2 using the primer pair HI-10F/HI-10R. The amplicon was cloned into pSC-B-amp/kan (Agilent, Santa Clara, CA) to yield pTpnM, and the vector was confirmed by DNA sequence analysis. pTpnM was digested with *Hin*dIII, and the resulting 2.7 kb fragment was ligated into pGM160HKss to form pGM-tpnM. A 1.4 kb fragment containing the *aac(3)IV/oriT* cassette, amplified from pIJ773 using the primer pair HI-11F/HI-11R, was inserted into pGM-tpnM by λ Red-mediated recombination in *E. coli* BW25113/pKD46 to generate pGM-dtpnM. The resulting construct was confirmed by DNA sequence analysis and transformed into *E. coli* ET12567/pUZ8002.

S. tateyamensis protoplast preparation and transformation with pGM-dtpnM were performed according to the methods described for the disruption of *tpnA*. Mycelia of apramycin-resistant colonies were inoculated in 50 mL of ATCC 172 medium supplemented with 50 μg/mL apramycin in a 250 mL Erlenmeyer flask and incubated at 28 °C and 220 rpm for 72 hours. Whole-cell PCR was used to identify transformants harboring pGM-dtpnM using the primer pair HI-10F/HI-10R. From the wild-type strain, a 2.7 kb amplicon was expected while a 3.1 kb amplicon was expected from the transformant.

2.2.12 Towards the disruption of *tpnN*

The *tpnN* gene and flanking regions was amplified by PCR as a 3.2 kb fragment from fosmid HI2G2 using the primer pair HI-12F/HI-12R. The amplicon was cloned into pSC-B-amp/kan (Agilent, Santa Clara, CA) to yield pTpnN, and the vector was confirmed by DNA sequence analysis. pTpnN was digested with *Hin*dIII, and the resulting 3.2 kb fragment was ligated into pGM160HKss to form pGM-tpnN. A 1.4 kb fragment containing the *aac(3)IV/oriT* cassette, amplified from pIJ773 using the primer pair HI-13F/HI-13R, was inserted into pGM-tpnN by λ Red-mediated recombination in *E. coli* BW25113/pKD46 to generate pGM-dtpnN. The resulting construct was confirmed by DNA sequence analysis and transformed into *E. coli* ET12567/pUZ8002.

S. tateyamensis protoplast preparation and transformation with pGM-dtpnN were performed according to the methods described for the disruption of *tpnA*. Mycelia of apramycin-resistant colonies were inoculated in 50 mL of ATCC 172 medium supplemented with 50 μg/mL apramycin in a 250 mL Erlenmeyer flask and incubated at 28 °C and 220 rpm for 72 hours. Whole-cell PCR was used to identify transformants harboring pGM-dtpnN using the primer pair HI-12F/HI-12R. From the wild-type strain, a 3.2 kb amplicon was expected while a 3.8 kb amplicon was expected from the transformant.

2.2.13 Towards the disruption of *tpnR*

The *tpnR* gene and flanking regions was amplified by PCR as a 3.1 kb fragment from fosmid HI2G2 using the primer pair HI-14F/HI-14R. The amplicon was cloned into pSC-B-amp/kan (Agilent, Santa Clara, CA) to yield pTpnR, and the vector was confirmed

by DNA sequence analysis. pTpnR was digested with *Hin*dIII, and the resulting 3.1 kb fragment was ligated into pGM160HKss to form pGM-tpnR. A 1.4 kb fragment containing the *aac(3)IV/oriT* cassette, amplified from pIJ773 using the primer pair HI-15F/HI-15R, was inserted into pGM-tpnR by λ Red-mediated recombination in *E. coli* BW25113/pKD46 to generate pGM-dtpnR. The resulting construct was confirmed by DNA sequence analysis and transformed into *E. coli* ET12567/pUZ8002.

S. tateyamensis protoplast preparation and transformation with pGM-dtpnR were performed according to the methods described for the disruption of *tpnA*. Mycelia of apramycin-resistant colonies were inoculated in 50 mL of ATCC 172 medium supplemented with 50 μg/mL apramycin in a 250 mL Erlenmeyer flask and incubated at 28 °C and 220 rpm for 72 hours. Whole-cell PCR was used to identify transformants harboring pGM-dtpnR using the primer pair HI-14F/HI-14R. From the wild-type strain, a 3.1 kb amplicon was expected while a 3.8 kb amplicon was expected from the transformant.

2.2.14 Towards the genetic complementation *of S. tateyamensis* HI1

The *tpnA* gene was amplified from fosmid HI2B7 by PCR using the primer pair HI-16F/HI16R. The amplicon was digested with *Nde*I and *Eco*RI and ligated into pSET1520ss to give pSET1520ss-TpnA. The resulting plasmid was confirmed by DNA sequencing analysis. After the isolation of pSET1520ss-TpnA from *E. coli* ET12567/pUZ8002, the plasmid was used to transform protoplasts of *S. tateyamensis* HI1. *S. tateyamensis* HI1 protoplast preparation and transformation with pSET1520ss-TpnA were performed according to the methods described for the disruption of *tpnA* with one

exception. After the transformant was plated on ISP3 plates, the agar was overlaid with 1.25 mg streptomycin and 1.25 mg apramycin in 2 mL of H_2O. Mycelia of streptomycin- and apramycin-resistant colonies were inoculated into 50 mL of ATCC 172 medium supplemented with 50 µg/mL streptomycin and 50 µg/mL apramycin in a 250 mL Erlenmeyer flask and incubated at 28 °C and 220 rpm for 72 hours. Whole-cell PCR was used to identify transformants harboring pSET1520ss-TpnA using the primer pair HI-16F/HI-16R. A 198 bp amplicon was expected from the transformants while an amplicon was not expected from *S. tateyamensis* HI1.

2.2.15 Expression and purification of TpnW

The *tpnW* gene and its flanking regions was amplified from HI2B7 by primer pairs HI-17F/HI-17R. The amplicon was ligated into pSC-B-amp/kan (Agilent, Santa Clara, CA) to form ptpnW and the vector confirmed by DNA sequence analysis. The gene *tpnW* was amplified by PCR from ptpnW using the primer pair HI-18F/HI-18R. The amplicon was ligated into pSC-B-amp/kan to yield ptpnW2 and the insert was confirmed by DNA sequence analysis. The plasmid was digested with *Nde*I and *Eco*RI, and the resulting *tpnW* fragment ligated into pET28b(+) to form pET28b-tpnW. The construct was confirmed by DNA sequence analysis. *E. coli* BL21(DE3) containing pET28b-tpnW was incubated overnight at 37 °C and 220 rpm in 10 mL of Luria-Bertani medium supplemented with 50 µg/mL kanamycin. 20 mL of the overnight culture was used to inoculate 2 L of Luria-Bertani medium supplemented with 50 µg/mL kanamycin. The culture was incubated at 37 °C and 220 rpm until the optical density at 600 nm (OD_{600}) = 0.6, at which point the temperature was decreased to 15 °C and TpnW expression was induced with the addition

of 0.4 mM isopropyl-*β*-D-thiogalactopyranoside (IPTG). Cultures were incubated for an additional 48 hours. Harvested cells were resuspended in 50 mL of lysis buffer (20 mM Tris pH 8.0, 500 mM NaCl, 2 mM imidazole, 10% glycerol, 1 mg/mL lysozyme, 10 µg/mL deoxyribonuclease, 2 mM $MgCl_2$). Cells were disrupted by sonication (10 rounds of 10 s pulses followed by a 60 s pause) and the lysate clarified by centrifugation at 14,000 x *g* for 30 min at 4 °C. The cell-free extract was incubated with 1.5 mL of Ni-NTA (Qiagen, Germantown, MD) slurry for 20 min. The slurry was poured into a column, and the resin was washed with 15 mL wash buffer (20 mM Tris pH 8.0, 500 mM NaCl, 20 mM imidazole, 10% glycerol, 2 mM $MgCl_2$). Next, the resin was washed with 15 mL wash buffer with 40 mM imidazole. Protein was eluted with 15 mL elution buffer (20 mM Tris pH 8.0, 500 mM NaCl, 300 mM imidazole, 10% glycerol, 2 mM $MgCl_2$) collecting 5 mL fractions. Fractions containing the protein were pooled together and dialyzed against 2 x 2 L storage buffer (50 mM Tris pH 8.0, 300 mM NaCl, 10% glycerol, 2 mM $MgCl_2$, 2 mM dithiothreitol). TpnW was concentrated with a 10,000 Da molecular weight cut-off Amicon Ultra centrifugal filter (Millipore, Burlington, MA). Protein concentration was determined by the method of Bradford using bovine serum albumin as a standard.[21] Purified TpnW was flash frozen in liquid nitrogen and stored at –80 °C.

2.2.16 *In vitro* reconstitution of TpnW activity

A 200 µL reaction mixture containing 1.5 µM TpnW, 1 mM 2-methyl-L-tryptophan **18** (Scheme 2.1), 1 mM of an α-keto acid acceptor (pyruvate, oxaloacetate, α-ketoglutarate, phenylpyruvate, *p*-hydroxyphenylpyruvate, or 3-indolylpyruvate **30**), 100 µM pyridoxal 5'-phosphate, 100 mM potassium phosphate buffer pH 7.8, and 3% DMSO

(2-methyl-L-tryptophan and the α-keto acid were added from stock solutions in DMSO) was prepared in an HPLC-MS vial. The reaction mixture was incubated under argon in the dark at 25 °C for 30 min, quenched with liquid nitrogen, and stored at –80 °C until ready for analysis. 100 µL of each sample was analyzed by HPLC or HPLC-MS. An HPLC gradient was developed from 5% acetonitrile in water with 0.1% formic acid to 95% acetonitrile in water with 0.1% formic acid over 30 min. Absorbance was monitored at 280 nm.

2.3 Results and discussion

2.3.1 Production of thiopeptins by *S. tateyamensis*

To verify that *S. tateyamensis* produces the thiopeptin complex, the strain was cultivated in a manner similar to a previously described method.[22] Metabolites that matched the mass of thiopeptins A_{1a}, B_a, A_{1b}, and B_b (Figure 2.1, **13**-**16**) were identified in the crude culture extract of *S. tateymanesis* by HPLC-MS analysis (Figure B.1). A similar mixture of thiopeptin congeners was identified from the culture extract in previous reports. Initially, Miyairi and coworkers identified thiopeptin B as the major component of the complex with minor components A_1-A_4, based on separation of thiopeptin components by silica gel, UV-visible and IR spectroscopy, and mass characterization by gas chromatography vapor pressure method.[23] No structural characterization was provided at this stage and the "*a*" and "*b*" designations that indicate the oxidation state of the nitrogenous heterocycle were applied later in a detailed structural characterization of the thiopeptins by Hensens (Figures 2.1, **13**-**16** and 2.5, **26**-**29**).[17] It is unclear if the numerical designations of thiopeptins A_1-

A_4 given by Miyairi match the thiopeptin designations $A_{1a/b}$-$A_{4a/b}$ given by Hensens. The masses of thiopeptins A_1-A_4 or their relative trend in mass differences among the congeners do not match $A_{1a/b}$-$A_{4a/b}$. In addition, thiopeptin B was separated in two distinct fractions, B_a and B_b in later sutides.[17, 23] Miyairi and coworkers did not characterize thiopeptin A_2 due to insufficient yield, and this derivative was not observed by Hensens in later studies.[17] Thiopeptins A_{3a}, A_{4a}, A_{3b}, and A_{4b} (**26**-**29**) are truncated at the C-terminus relative to **13**-**16** and they may be artifacts of the purification process or caused by degradation upon storage. During the course of siomycin structure elucidation, a truncated analog was observed from acid hydrolysates, and **26**-**29** may have resulted from thiopeptins $A_{1a/b}$-$A_{2a/b}$ in a similar manner during purification, storage, or analysis.[24] The thiopeptin congener designations given by Hensens is used in this work.

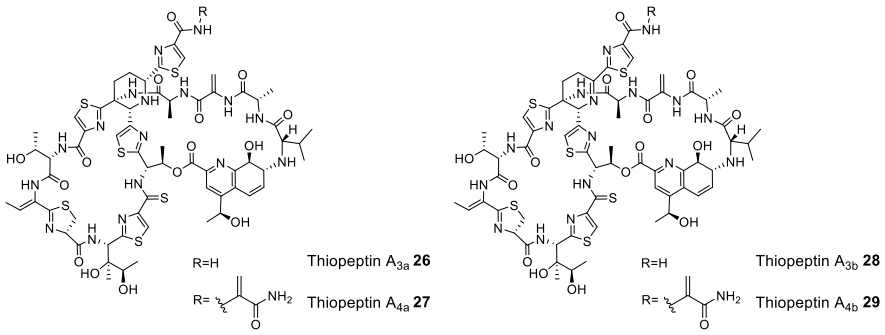

Figure 2.5: Structures of minor components of the thiopeptin complex A_3-A_4 (**26**-**29**).[17]

Isolation and characterization of each thiopeptin derivative would be essential and are needed as standards for thiopeptin production and biosynthetic studies. For example, a gene deletion study of a thiopeptin biosynthetic gene that is responsible for piperidine

formation may result in abolishment of production of piperidine-containing **13** and **14** and an accumulation of dehydropiperidine-containing **15** and **16** by the mutant strain. The availability of standards would be key in identifying the exact mixture of metabolites. Additionally, compounds produced by the mutants may be highly similar in structure and difficult to distinguish from **13-16** in a crude culture extract. A co-injection of a crude culture extract from a mutant with a thiopeptin standard may accelerate identification of new metabolites and intermediates. Furthermore, thiopeptides have complex MS and NMR spectra. The availability of reference spectra would facilitate the structural characterization of a potential thiopeptin derivative.

Thiopeptin production by *S. tateyamensis*, however, was difficult to reproduce. Despite repeated efforts to maintain cell stocks that produced thiopeptin, its production ceased periodically. The loss of thiopeptin production in *S. tateyamensis* may be due to mutations and deletions in the chromosome. Genetic instability has been observed in certain streptomycetes, and is markedly prevalent among genes involved in sporulation, pigment production, antibiotic resistance, and antibiotic production.[25-27] *Streptomyces glaucescens* strain GLA0 (*S. glaucescens*), for example, is naturally resistant to streptomycin. Antibiotic-sensitive *S. glaucescens* strains, however, can arise spontaneously at a frequency of 0.2 to 1.4% by growth on agar media alone or after cold storage.[28] Reversion to wild-type streptomycin resistance levels was observed at a frequency of 10^{-5}, and the cause of its reversion is not understood. Chromosome rearrangements may have led to polar effects on the expression of the *S. glaucescens* streptomycin resistance gene or point mutations may be contributors.[29] Mutations of genes involved in aerial mycelium formation and sporulation have been implicated in the drastic loss of secondary metabolite

production.[30-34] The products of *bldABCDFGH* are required for aerial mycelium formation in *Streptomyces*, and *bldA* mutations are associated with a "bald" non-sporulating phenotype and abolishment of secondary metabolite production.[35-37] *BldA* encodes for a $tRNA^{Leu}$ and *bldA* mutants are unable to translate genes with the rare *Streptomyces* leucine codon TTA.[34] In fact, only 145 of 7825 genes (< 2%) identified in the *Streptomyces coelicolor* genome contain a TTA codon.[38] This rare codon, however, is frequently found in regulatory genes that control cell differentiation and antibiotic production.[33] "Bald" mutants of *S. coelicolor* are unable to produce the antibiotics actinorhodin and undecylprodigosin as the biosyntheses of these two metabolites are dependent on the expression of transcription factors ActII and RedZ, respectively, that contain the rare codon TTA.[32, 39] Site-directed mutagenesis of the TTA codon of *actII* to TTG restored actinorhodin production in the "bald" mutants, establishing the relationship between the use of the rare TTA codon and antibiotic production.[33] Genes that regulate *Streptomyces* morphology, such as *whiABCDEFGHI* involved in sporulation, may also be involved in a regulatory cascade of secondary metabolism.[35] Strains that contain a *whi* mutation are known as "white" mutants as aerial mycelia and spores lose their pigmentation and appear white.[40] "Bald" and "white" mutants of *Streptomyces avermitilis*, the producer of the anthelmintic avermectins, were found to appear at a frequency of 2.4% from the wild-type strain under growth on solid media.[41] These "bald" and "white" strains showed reduction or the complete loss of avermectin production.[41]

When grown on ISP3 agar, *S. tateyamensis* initially appeared dusty and pinkish-grey. *S. tateyamensis*, however, often displayed characteristics of "bald" and "white" colonies that may carry a *bldA* or *whi* mutation. Colonies that were both "white" and "bald",

those that were “white” but not “bald”, and even the colonies that retained a dusty, pinkish-grey appearance all lost its ability to produce the thiopeptin complex (Figure 2.6). Only the glycerolic mycelium stock prepared from the lyophilized stock purchased from ATCC retained some thiopeptin production (Figure 2.6). Despite repeated efforts, thiopeptide production diminished or was lost over time. Comparison of DNA sequences of the *bld* and *whi* genes of *S. tateyamensis* colonies that have lost the ability to produce the thiopeptins may reveal mutations and or deletions in the aforementioned genes that are not present in *S. tateyamensis* colonies that produce the thiopeptins. Genomic analysis may reveal chromosomal rearrangements and other alterations to the *S. tateyamensis* genome and shed light to why thiopeptin production was abolished in *S. tateyamensis*. Although we were unable to develop a reproducible thiopeptin production protocol and to obtain thiopeptin standards, *S. tateyamensis* is a known producer of the thiopeptins and efforts to identify the biosynthetic genes continued.[17, 22-23, 42]

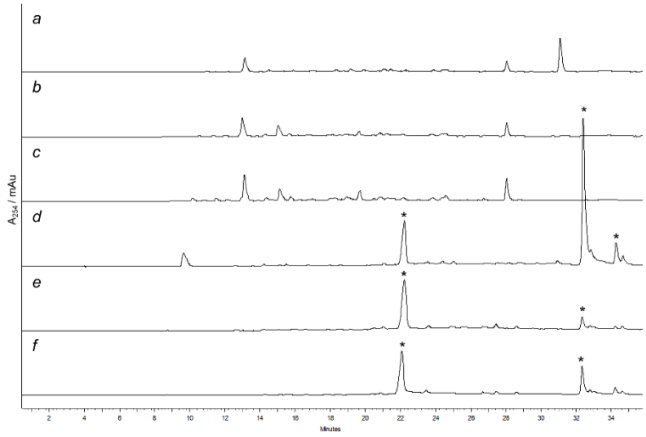

Figure 2.6: HPLC analyses of crude culture extracts from (*a-c*) *S. tateyamensis* colonies that presented with a pink pigment on solid media and crude culture extracts of (*d-f*) *S. tateyamensis* prepared from a glycerolic mycelium stock from the lyophilized ATCC sample. Compounds suspected to be thiopeptins based on the UV-vis absorbance profile are indicated by asterisks. Absorbance was monitored at 254 nm.

2.3.2 Identification of the thiopeptin biosynthetic gene cluster

To pinpoint the genes responsible for **13-16** biosyntheses, the *S. tateyamensis* genome was partially sequenced to 6.92 Mb on 2,838 contiguous fragments and scanned for a nucleotide sequence that could encode the core peptide (VASASCTTCICTCSCSS). The gene encoding the thiopeptin precursor peptide, *tpnA*, was identified but the *tpn* locus included gaps in the sequence and ambiguous sequences in the draft genome assembly. To assist in sequencing of the *tpn* cluster, an *S. tateyamensis* genomic fosmid library was prepared. While a fosmid can accommodate an insert up to ~40 kb, an entire thiopeptide gene cluster, it is more likely that overlapping fragments of the *tpn* gene cluster will be found on multiple fosmids. Based on the draft genome sequence, the boundaries of the *tpn* locus appeared to be around *tpnU* (similar to *tsrQ* of the thiostrepton biosynthetic gene cluster) on the 5' end of the gene cluster and near *tpnO* (similar to *tsrM*) on the 3' end. Therefore, the fosmid library was screened for the 5'-end (*tpnU*), 3'-end (*tpnO*), and a central region (*tpnD,* similar to *tsrE*) of the *tpn* gene cluster in order to identify any fosmids that contained, at minimum, a partial *tpn* locus. Fosmid HI2B7 was found to contain *tpnD* and *tpnU* (Figure 2.7 and 2.8) while HI2G2 was found to contain *tpnO* (Figure 2.9 and 2.10). Fosmids HI2B7 and HI2G2 were sequenced and, together, found to span the entire *tpn* locus. The *tpn* cluster encompasses 23 open reading frames (*tpnA-W*) very similar in composition and organization to the thiostrepton biosynthetic gene (*tsr*) cluster (Figure 2.11 and Table 2.1).

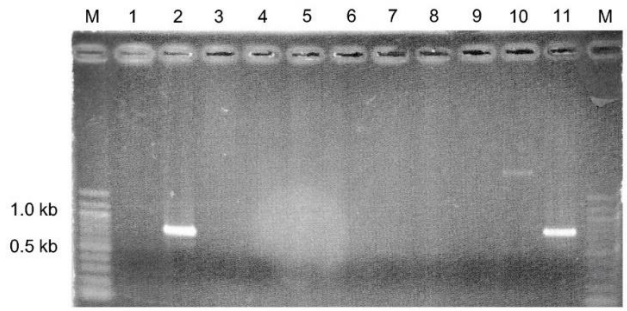

Figure 2.7: PCR screen of the *S. tateyamensis* genomic fosmid library for *tpnD*. Fosmids from the *S. tateyamensis* genomic fosmid library are named "HIxxx". JP8D9 is a fosmid from the *S. laurentii* genomic fosmid library and is used as a control. Primer pairs HI-1F/HI-1R were used for amplification. (M) 100 bp molecular weight ladder, (1) HI2A7, (2) HI2B7, (3) HI2C7, (4) HI2D7, (5) HI2E7, (6) HI2F7, (7) HI2G7, (8) HI2H7, (9) JP8D9, (10) pCC1FOS, and (11) *S. tateyamensis* gDNA. A 0.7 kb amplicon was expected from *S. tateyamensis* gDNA.

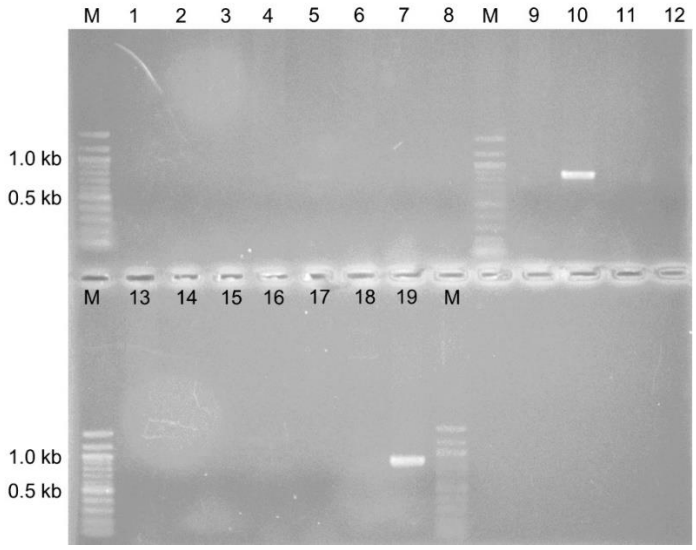

Figure 2.8: PCR screen of the *S. tateyamensis* genomic fosmid library for *tpnU*. Fosmids from the *S. tateyamensis* genomic fosmid library are named "HIxxx". JP8D9 is a fosmid from the *S. laurentii* genomic fosmid library and used as a control. Primer pairs HI-3F/HI-3R were used for amplification. (M) 100 bp molecular weight ladder, (1) HI2A6, (2) HI2B6, (3) HI2C6, (4) HI2D6, (5) HI2E6, (6) HI2F6, (7) HI2G6, (8) HI2H6, (9) HI2A7, (10) HI2B7, (11) HI2C7, (12) HI2D7, (13) HI2E7, (14) HI2F7, (15) HI2G7, (16) HI2H7, (17) JP8D9, (18) pCC1FOS, and (19) *S. tateyamensis* gDNA. A 0.8 kb amplicon was expected from *S. tateyamensis* gDNA.

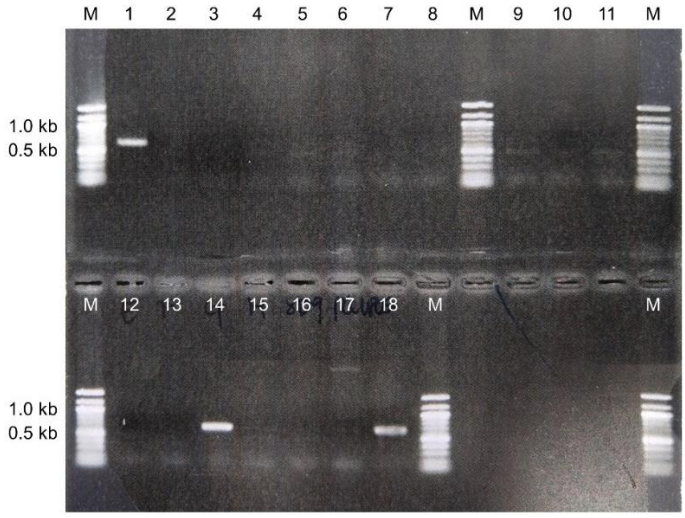

Figure 2.9: PCR screen of the *S. tateyamensis* genomic fosmid library for *tpnO*. Fosmids from the *S. tateyamensis* genomic fosmid library are named "HIxxx". JP8D9 is a fosmid from the *S. laurentii* genomic fosmid library and used as a control. Primer pairs HI-2F/HI-2R were used for amplification. (M) 100 bp molecular weight ladder, (1) HI2A5, (2) HI2B5, (3) HI2C5, (4) HI2D5, (5) HI2E5, (6) HI2F5, (7) HI2G5, (8) HI2H5, (9) HI2B2, (10) HI2C2, (11) HI2D2, (12) HI2E2, (13) HI2F2, (14) HI2G2, (15) HI2H2, (16) JP8D9, (17) pCC1FOS, and (18) *S. tateyamensis* gDNA. A 0.6 kb amplicon was expected from *S. tateyamensis* gDNA.

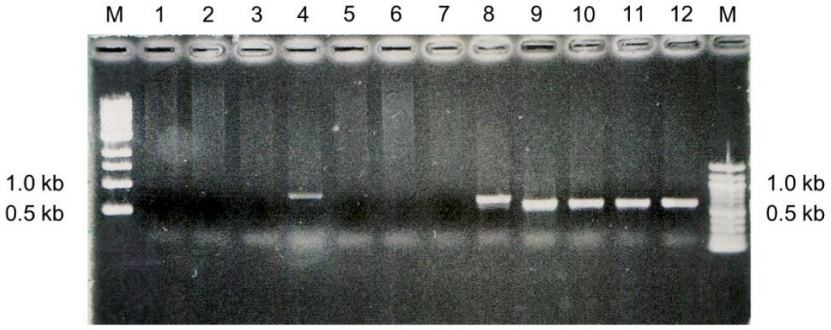

Figure 2.10: PCR amplification of *tpnDOU* from fosmid HI2G2. (M) 100 bp molecular weight ladder, (1-3) amplification of *tpnU* from HI2G2, (4) amplification of *tpnD* from *S. tateyamensis* gDNA, (5-7) amplification of *tpnD* from HI2G2, (8) amplification of *tpnU* from *S. tateyamensis* gDNA, (9-11) amplification of *tpnO* from HI2G2, (12) amplification of *tpnO* from *S. tateyamensis* gDNA. The expected amplicon sizes: 0.8 kb for *tpnU*, 0.7 kb for *tpnD*, and 0.6 kb for *tpnO*.

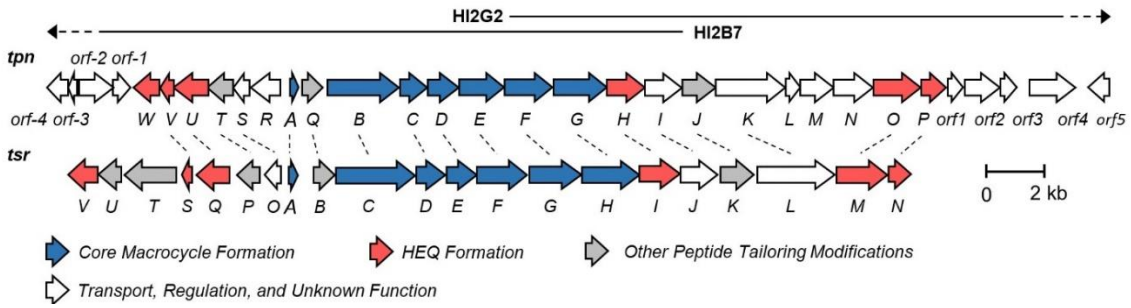

Figure 2.11: The organization of the thiopeptin (*tpn*) and thiostrepton (*tsr*) biosynthetic gene clusters. Homologous genes are indicated by dashed lines. Gene products that are likely involved in core macrocycle formation are in blue, those involved in HEQ formation are in red, those involved in other modifications to the thiopeptide scaffold are in grey, and those with either unknown, transport, or regulatory functions are in white. The span of the fosmid inserts that contain a partial *tpn* locus (HI2B7 and HI2G2) are indicated by solid and dashed lines above the gene cluster depiction.

2.3.3 The deduced functions of the *tpn* cluster

The gene products of the *tpn* cluster were compared to proteins from the NCBI database using protein BLAST to identify their proposed functions (Table 2.1). Based on sequence similarity to proteins encoded in the *tsr* and other thiopeptide biosynthetic gene clusters, the predicted thiopeptin precursor peptide TpnA, together with TpnBCDEFG, comprise the minimum set of proteins expected to assemble the core thiopeptide scaffold. The thiazol(in)es are likely installed by TpnEFG. TpnF and TpnG are similar to leader peptide binding proteins and YcaO domain-containing cyclodehydratases, respectively, that operate in concert to form thiazoline rings from the amide backbone and cysteine residues of the thiopeptide.[15, 43-44] The dehydrogenase TpnE is expected to oxidize the intermediate thiazoline to the thiazole.[15, 45] A split LanB-type dehydratase appears to be encoded by *tpnBC*, and likely catalyzes the dehydrations to generate the Dha and

dehydrobutyrine residues.[15] Two Dha residues are likely coupled together by a putative [4+2] cyclase, TpnD, to form a dehydropiperidine and the thiopeptin core macrocycle.

Table 2.1: Deduced functions of the open reading frames in the *tpn* cluster.

Gene Product	Description of Deduced Protein	Tsr Homolog[a]	Closest Homolog[a]
Orf-5	Transporter	---	Arsenic transporter (WP_030553753.1; 85/90); *Kitasatospora aureofaciens*
Orf-4	ABC transporter permease	---	ABC transporter permease (WP_035847761.1; 69/79); *Kitasatospora azatica*
Orf-3	ABC transporter ATP-binding protein	---	ATP transporter ATP-binding protein (WP_083977627.1; 84/92); *Kitasatospora azatica*
Orf-2	Sensor histidine kinase	---	Hypothetical protein (WP_083977629.1; 69/75); *Kitasatospora azatica*
Orf-1	LuxR family transcriptional regulator	---	DNA-binding response regulator (WP_035847766.1; 90/95); *Kitasatospora azatica*
TpnW	2-Methyl-L-tryptophan aminotransferase	---	Hypothetical protein (WP_091614342.1; 63/72); *Amycolatopsis saalfeldensis*
TpnV	SnoaL-like cyclase	TsrS (ACN52308.1; 66/78)	SnoaL-like polyketide cyclase (SEO89837.1; 79/84); *Amycolatopsis saalfeldensis*
TpnU	3-(2-Methylindolyl)pyruvate dehydrogenase	TsrQ (ACN52307.1; 65/79)	Acyl-CoA dehydrogenase (SEO89852.1; 79/88); *Amycolatopsis saalfeldensis*
TpnT	Carboxymethyltransferase	TsrP (ACN52306.1; 62/70)	Leucine carboxylmethyltransferase (SEO89872.1; 76/81); *Amycolatopsis saalfeldensis*
TpnS	Hypothetical protein	TsrO (ACN52305.1; 45/62)	DUF2867 domain-containing protein (WP_091614353.1; 72/85); *Amycolatopsis saalfeldensis*
TpnR	α/β-Hydrolase fold family protein	---	Pimeloyl-ACP methyl ester carboxylesterase (SEO89904.1; 62/74); *Amycolatopsis saalfeldensis*
TpnA	Thiopeptin precursor peptide	TsrA (ACN52291.1; 66/77)	Thiocillin/thiostrepton family thiazolyl peptide (WP_091614358.1; 81/88); *Amycolatopsis saalfeldensis*
TpnQ	Thiopeptin macrocyclase	TsrB (ACN52292.1; 58/72)	Pimeloyl-ACP methyl ester carboxylesterase (SEO89930.1; 73/82); *Amycolatopsis saalfeldensis*
TpnB	LanB-type dehydratase glutamylation domain subunit	TsrC (ACN52293.1; 52/63)	Hypothetical protein (WP_091614364.1; 67/75); *Amycolatopsis saalfeldensis*
TpnC	LanB-type dehydratase glutamate elimination domain subunit	TsrD (ACN52294.1; 62/74)	Hypothetical protein (WP_091614367.1; 71/81); *Amycolatopsis saalfeldensis*

Table 2.1 (continued)

TpnD	Thiopeptide [4+2] cyclase	TsrE (ACN52295.1; 74/85)	Hypothetical protein (WP_091614370.1; 85/92); *Amycolatopsis saalfeldensis*
TpnE	Thiazoline dehydrogenase	TsrF (ACN52296.1; 58/65)	Hypothetical protein (WP_091614372.1; 72/78); *Amycolatopsis saalfeldensis*
TpnF	F-protein-leader peptide binding protein	TsrG (ACN52297.1; 53/61)	Hypothetical protein (WP_091614375.1; 68/75); *Amycolatopsis saalfeldensis*
TpnG	F-protein-dependent cyclodehydratase	TsrH (ACN52298.1; 59/67)	Ribosomal protein S12 methylthiotransferase accessory factor (SEO90054.1; 73/78); *Amycolatopsis saalfeldensis*
TpnH	4-(1-Hydroxyethyl)quinoline-2-carboxylic acid epoxygenase	TsrI (ACN52299.1; 61/69)	Cytochrome P450 (SEO90075.1; 72/80); *Amycolatopsis saalfeldensis*
TpnI	Adenylyltransferase	TsrJ (ACN52300.1; 61/70)	Long-chain fatty acid-CoA ligase (WP_091614382.1; 79/87); *Amycolatopsis saalfeldensis*
TpnJ	Isoleucine hydroxylase	TsrK (ACN52301.1; 55/66)	Cytochrome P450 (WP_091614385.1; 73/81); *Amycolatopsis saalfeldensis*
TpnK	LanB-type dehydratase glutamylation domain subunit	TsrL (ACN52302.1; 41/50)	Hypothetical protein (WP_091614387.1; 60/69); *Amycolatopsis saalfeldensis*
TpnL	Flavin/deazaflavin oxidoreductase	---	Pyridoxamine 5'-phosphate oxidase (SEO90151.1; 70/78); *Amycolatopsis saalfeldensis*
TpnM	YcaO domain-containing protein	---	Hypothetical protein (WP_091614389.1; 78/84); *Amycolatopsis saalfeldensis*
TpnN	TfuA-like protein	---	Hypothetical protein (WP_091614392.1; 72/79); *Amycolatopsis saalfeldensis*
TpnO	Tryptophan methyltransferase	TsrM (ACN52303.1; 65/73)	Tryptophan-2-*C*-methyltransferase (WP_091614395.4; 85/91); *Amycolatopsis saalfeldensis*
TpnP	4-Acetylquinoline-2-carboxylic acid reductase	TsrN (ACN52304.1; 62/71)	SDR family NAD(P)-dependent oxidoreductase (WP_091614398.1; 74/82); *Amycolatopsis saalfeldensis*
Orf1	Universal stress protein	---	Universal stress protein (WP_097239522.1; 77/84); *Streptomyces* sp. 1331.2
Orf2	β-Lactamase	---	Serine hydrolase (WP_030274042.1; 67/75); *Streptomyces* sp. NRRL B-24484
Orf3	Hypothetical protein	---	Hypothetical protein (WP_053175376.1; 40/57); *Streptomyces virginiae*
Orf4	Major facilitator superfamily transporter	---	MFS transporter (WP_100887175.1; 85/92); *Kitasatospora* sp. OK780
Orf5	DNA-binding response regulator	---	DNA-binding response regulator (WP_042413556.1; 97/98); *Streptacidiphilus anmyonenis*

[a] NCBI accession numbers and % identity/similarity are given in parentheses.

The quinaldic acid moiety of **2**, and likely of **13-16** (Figure 2.1), is derived from L-tryptophan. TpnOPUVW are expected to convert the amino acid into 4-(1-hydroxyethyl)quinoline-2-carboxylic acid (HEQ **21**) by a process that includes an oxidative ring expansion (Scheme 1.4).[14, 46-47] TpnO is similar to TsrM, a radical SAM and cobalamin-dependent methyltransferase that generates 2-methyl-L-tryptophan as the first step in this process.[48] The second step is catalyzed by an aminotransferase.[14] TpnW shares homology with histidinol-phosphate transaminases but demonstrates only 40% identity (50% similarity) with the thiostrepton pathway transaminase, TsrV.[14] Since there is no other open reading frame in the *tpn* locus that shows homology to an aminotransferase, TpnW is a candidate 2-methyl-L-tryptophan transaminase. TpnU shows homology to the $FADH_2$-dependent oxygenase, TsrQ, that initiates ring opening and rearrangement of the indole ring.[47] TpnV shows homology to TsrS, a SnoaL-like cyclase suggested to be involved in HEQ **21** biosynthesis, although its function is unclear.[46] TpnP shows sequence homology to the NADPH-dependent reductase TsrN that reduces the ketone of 4-acetylquinoline-2-carboxylate to the alcohol of HEQ.[46]

The quinaldic acid-containing macrocycle is likely installed in the thiopeptin scaffold by the actions of TpnHIQ.[49-51] TpnI is similar to adenylyltransferases and is expected to attach HEQ **21** to Thr12 of the peptide, likely followed by TpnH-catalyzed epoxygenation.[14, 49, 51] TpnQ, similar to the macrocyclase TsrB, is a candidate to mediate macrocyclization of the quinaldic acid-containing loop through attack of the core peptide's N-terminus upon the epoxide.[50] The thiopeptins from *S. tateyamensis* possess either a methylester (Figure 2.1, **13** and **15**) or a carboxylic acid (Figure 2.1, **14** and **16**) at their C-termini; none containing the C-terminal amide observed in **2** have been reported.

Accordingly, a homolog encoding the thiostrepton amidotransferase, TsrT, is absent.[14] TpnT is similar to TsrP and may function as a carboxymethyltransferase to produce the C-terminal methyl ester.[14, 52] A homolog of the methylesterase TsrU is not present in the *tpn* cluster.[52] Instead, TpnR, with similarity to other α/β-hydrolases likely serves this role.

Three genes of the *tpn* cluster, *tpnLMN*, do not share homology with known thiopeptide biosynthetic genes and are therefore candidates for the thioamide and piperidine features unique to **13**-**16**. TpnMN show sequence similarity to YcaO proteins and TfuA-like proteins, respectively, and are similar to the TvnHI pair encoded in the thioviridamide gene cluster, another thioamidated metabolite.[53] Involvement of a YcaO-TfuA pair in the posttranslational thioamidation of methyl-coenzyme A reductase in *Methanosarcina acetivorans* was recently established.[54-55] The YcaO protein activates the peptide backbone in an ATP-dependent manner similar to the YcaO-domain containing cyclodehydratases involved in thiazoline formation.[55] Although the function of the TfuA protein is unclear, both the YcaO and TfuA proteins are required for the thioamidation of the peptide substrate.[55] It is therefore likely that TpnM (YcaO protein) and TpnN (TfuA protein) work together to install the thiopeptin thioamide.

TpnL, on the other hand, shares homology to proteins annotated as FMN-dependent pyridoxine/pyridoxamine 5'-phosphate oxidases and other enzymes of the flavin/deazaflavin oxidoreductase subgroup B (FDOR-B).[56] The only remaining thiopeptin modification unaccounted for is a reduction to produce the piperidine ring of the series *a* thiopeptins **13** and **14**, and an oxidoreductase is a candidate enzyme for that step.

2.3.4 Disruption of open reading frames of the *tpn* cluster

To confirm the involvement of the *tpn* cluster in thiopeptin biosynthesis, insertional mutants of *tpnALMNR* in *S. tateyamensis* were pursued. Inactivation of a gene essential to thiopeptin biosynthesis would abolish its production and affirm the involvement of the *tpn* cluster in the pathway. In addition, accumulation of any biosynthetic intermediates would shed light on the role and timing of a particular modification mediated by the inactivated gene. A λ Red-mediated recombination strategy was used to insert the *aac(3)IV/oriT* cassette in *E. coli* into each *tpn* gene being targeted for disruption.[57] The *aac(3)IV* gene confers resistance to apramycin and is used to apply selective pressure for the bacterium to retain the plasmid while *oriT* is required for intergeneric conjugation between *E. coli* and *Streptomyces*. The disrupted gene would then be incorporated into the *S. tateyamensis* chromosome through homologous recombination. The *tpnA* insertional mutant *S. tateyamensis* HI1, for example, was constructed using the λ Red-mediated recombination strategy (Figure 2.12). To rule out polar effects on thiopeptide production that may have been caused by modifications to the *S. tateyamensis* chromosome, we attempted to genetically complement the *tpnA* insertional mutant with a functional copy of the inactivated gene expressed under the constitutive promoter *erm*E*.[58]

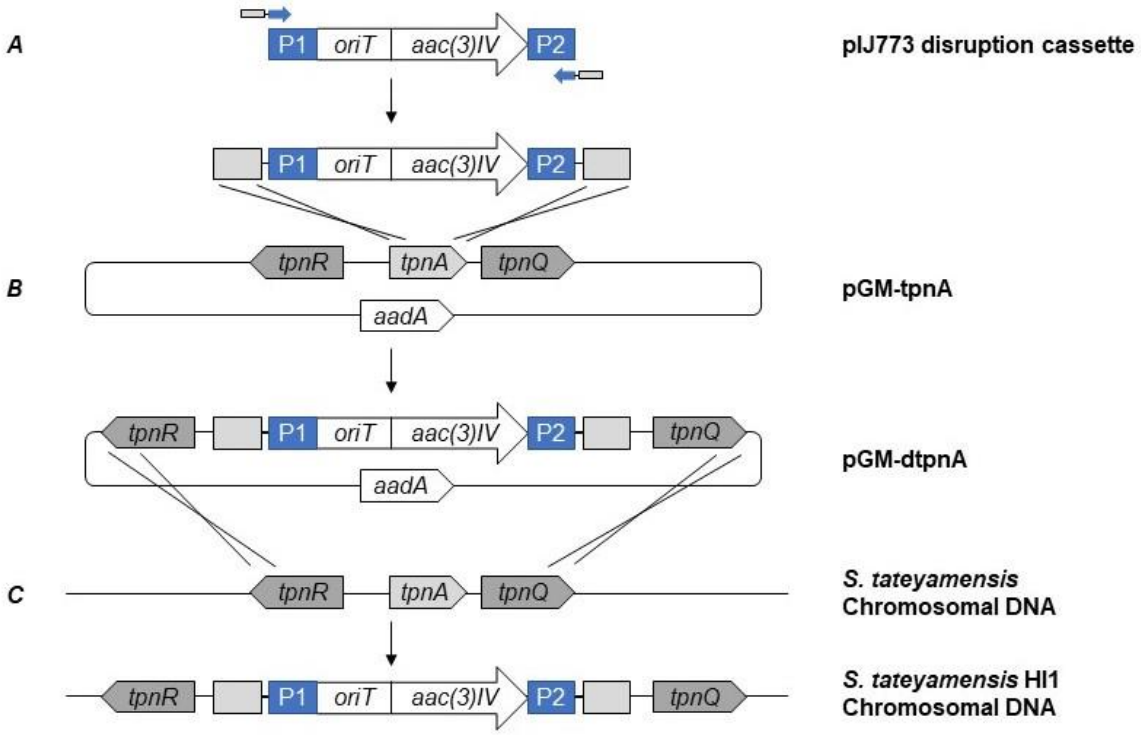

Figure 2.12: Strategy used to construct the *tpnA* mutant, *S. tateyamensis* HI1. (*A*) The pIJ773 disruption cassette was amplified by PCR with primer pair HI-5F/HI-5R containing a 39 nt region around *tpnA* at the 5' ends of the primers and a 20 nt P1 or P2 sequence at the 3' ends of the primers. (*B*) Homologous recombination between the PCR product and pGM-tpnA generated pGM-dtpnA. (*C*) Homologous recombination between pGM-dtpnA and the chromosomal DNA of *S. tateyamensis* yielded *S. tateyamensis* HI1.

While many methods exist to introduce DNA into *Streptomyces*, intergeneric conjugation of plasmids from *E. coli* into streptomycetes is frequently used for its simplicity in protocol over protoplast transformation, which requires species-specific protocol optimization.[19] For conjugation experiments, *Streptomyces* spore germlings are used so that a homogeneous cell population can be subjected to genetic manipulation under more consistent and reproducible conditions. Due to the complex life cycle of *Streptomyces* species, physiological homogeneity is difficult to achieve and even a young mycelium culture can contain a heterogeneous population.[19]

A variety of conditions were explored to generate *S. tateyamensis* spores suitable for intergeneric conjugation with *E. coli*. Sporulation of *S. tateyamensis* was assayed on ISP4, ATCC 184, ISP7, and calcium-malate agar, but robust spore formation was not observed. ISP3 solid media produced thick, dusty, and gray growth and the spores were harvested after 10, 15, 20, and 25 days. Mycelium heat shocked at 50 °C for 10 min did not grow on either ISP3 or MS agar, allowing us to confirm the presence of *S. tateyamensis* spores and their viability. Both heat-shocked and untreated spores germinated on ISP3 agar, but seemed to grow quicker on ISP3 medium supplemented with 10 mM $MgCl_2$. Spores also germinated on maltose sugar (MS) solid medium supplemented with 10 mM $MgCl_2$. Spores harvested after 10-25 days were used for conjugation with *E. coli* harboring a pGM160HKss plasmid. Unfortunately, our protocols were not successful in introducing foreign DNA into *S. tateyamensis* spores.

S. tateyamensis protoplast transformation was also pursued. Protoplasts are bacterial cells that lack a cell wall, leaving the plasma membrane as the outermost barrier. The lack of a rigid, secondary outer cell wall is thought to make the transfer of genetic material into the cell more efficient. Protoplast generation of Gram-positive bacteria has been demonstrated as the cell wall is easily removed with lysozyme treatment and may be an applicable method in producing *S. tateyamensis* protoplasts.[59] To complement lysozyme treatment, bacteria may be cultured in media containing penicillin or glycine to weaken the integrity of the cell wall by preventing optimal cross-linking in the peptidoglycan. Penicillin irreversibly inhibits DD-transpeptidase, which catalyzes cross-link formation in peptidoglycan.[60-61] Glycine weakens the bacterial cell wall at high concentrations (0.5-3.0%), by competing with D-alanine for incorporation into peptidoglycan; D-alanine is

involved in cross-linking in the cell wall of all bacteria, and the replacement of D-alanine with glycine disrupts the integrity of the cell wall.[62-63] The age and/or physiological state of the mycelium used to prepare the protoplasts can have an effect on transformation frequencies in individual species.[57] *Streptomyces lividans* protoplasts prepared from late exponential phase of the mycelium stage (36-40 h) were found to yield transformants, whereas younger mycelium (18 h) of *Streptomyces parvulus* was found to be viable for transformation.[19, 64] In addition to the importance of the growth phase of the mycelium at the time of protoplast transformation, several factors can greatly influence transformation efficiencies, including the temperature at which the mycelium and protoplasts are kept during preparation and transformation, the concentration of protoplasts, the composition and dryness of the regeneration medium, the organism from which the plasmid is isolated, and the temperature at which protoplasts are regenerated.[19, 57, 65]

S. tateyamensis protoplasts were prepared at various growth phases of the mycelium, glycine concentrations, and cell wall lysis buffers (Table 2.2). Cultures incubated for 16 and 24 hours with 0.25% glycine did provide protoplasts which regenerated on dried ISP3 solid medium. Conditions 18 and 19 (Table 2.2) were selected for protoplast transformation as these conditions yielded a homogeneous sample of protoplasts in initial transformation efforts. In later trials, however, condition 21 and 22 yielded better results for protoplasts regeneration (Table 2.2).

Table 2.2: Conditions used to prepare *S. tateyamensis* protoplasts. The protoplasts used for transformation are highlighted in orange.

Protoplast Preparation Condition	Age of Culture[a]	Glycine Concentration (% w/v)	Lysis Buffer	Lysis Time	Morphology under Microscope	Regeneration Media (solid)	Protoplast Regeneration[b]
1	40 hours	0.5 %	P + 1 mg/mL lysozyme	30 min	Mostly mycelium	R2YE	No growth
2	40 hours	0.5 %	P + 1 mg/mL lysozyme	30 min	Mostly mycelium	Dried ISP3	No growth
3	40 hours	0.5 %	P + 1 mg/mL lysozyme	30 min	Mostly mycelium	ISP3	No growth
4	40 hours	0.5 %	P + 1 mg/mL lysozyme	60 min	Mostly mycelium	R2YE	No growth
5	40 hours	0.5 %	P + 1 mg/mL lysozyme	60 min	Mostly mycelium	Dried ISP3	No growth
6	40 hours	0.5 %	P + 1 mg/mL lysozyme	60 min	Mostly mycelium	ISP3	No growth
7	40 hours	0.5 %	L + 1 mg/mL lysozyme	60 min	Mixture of mycelium and protoplasts	R2YE	No growth
8	40 hours	0.5 %	L + 1 mg/mL lysozyme	60 min	Mixture of mycelium and protoplasts	ISP3	No growth
9	40 hours	0.5 %	L + 1 mg/mL lysozyme	60 min	Mixture of mycelium and protoplasts	Dried ISP3	Some growth after 2 days
10	40 hours	0.5 %	L + 1.5 mg/mL lysozyme	60 min	Mostly protoplasts	R2YE	No growth
11	40 hours	0.5 %	L + 1.5 mg/mL lysozyme	60 min	Mostly protoplasts	Dried ISP3	No growth
12	40 hours	0.5 %	L + 2.0 mg/mL lysozyme	60 min	Mostly protoplasts	R2YE	No growth
13	40 hours	0.5 %	L + 2.0 mg/mL lysozyme	60 min	Mostly protoplasts	Dried ISP3	No growth
14	30 hours	0.5 %	L + 1.5 mg/mL lysozyme	60 min	Mostly protoplasts	Dried ISP3	Some growth
15	30 hours	0.75 %	L + 1.5 mg/mL lysozyme	60 min	Cell debris	Dried ISP3	No growth
16	30 hours	1.0 %	L + 1.5 mg/mL lysozyme	60 min	Cell debris	Dried ISP3	No growth
17	24 hours	0.5 %	L + 1.5 mg/mL lysozyme	60 min	Mixture of mycelium and protoplasts	Dried ISP3	No growth
18	24 hours	0.25 %	L + 1.5 mg/mL lysozyme	60 min	Protoplasts	Dried ISP3	Growth after 2 days
19	24 hours	0.25 %	L + 1.5 mg/mL lysozyme	45 min	Protoplasts	Dried ISP3	Growth after 2 days
20	24 hours	0.25 %	L + 1.5 mg/mL lysozyme	30 min	Mostly Protoplasts	Dried ISP3	Growth after 2 days

Table 2.2 (continued)

21	16 hours	0.25 %	L + 1.5 mg/mL lysozyme	45 min	Protoplasts	Dried ISP3	Growth after 2 days
22	16 hours	0.25 %	P + 1.5 mg/mL lysozyme	60 min	Protoplasts	Dried ISP3	Growth after 2 days
23	16 hours	0.25 %	P_{R5} + 1.5 mg/mL lysozyme	60 min	Protoplasts	Dried ISP3	No growth
24	16 hours	0.25 %	P_{R6} + 1.5 mg/mL lysozyme	60 min	Protoplasts	Dried ISP3	No growth

[a] The time of culture incubated at 28 °C after inoculation.
[b] Protoplast regeneration was distinguished from mycelial growth by overlaying a second, identical plate with 0.01% sodium dodecyl sulfate (SDS). SDS inhibits the growth of protoplasts but does not significantly affect mycelium growth. The number of colonies on plates with and without SDS were compared to determine if protoplasts had regenerated on solid media. Protoplasts were regenerated at 28 °C.

Protoplasts of many *Streptomcyes* species are transformed by plasmid DNA at high frequency in the presence of polyethylene glycol (PEG).[66] The *w*/*v* of the PEG solution seems to influence transformation frequency rather than the molecular weight of the PEG used.[19] While the exact mechanism of PEG-mediated DNA transformation is not known, DNA collapses into a globular form in PEG solutions and compacted DNA may be more efficiently taken up by a cell via endocytosis over its coiled counterpart.[67] *S. tateyamensis* protoplast transformation was performed under various conditions (Table 2.3) and transformation was successful using conditions 2 and 21 (Table 2.3). In later trials to transform *S. tateyamensis*, neither condition yielded transformants. Protoplast transformation using 10% PEG1000 and 100 mM $MgCl_2$ in the transformation buffer with pGM-dtpnL did yield apramycin-resistant colonies, suggesting the transfer of a plasmid with an apramycin resistance gene (such as *aac3(IV)* in pGM-dtpnL) into *S. tateyamensis*. However, a PCR-based screen for pGM-dtpnL in the candidate transformants did not identify any harboring the plasmid.

Transformation of *Streptomyces* may be significantly impacted by the presence of restriction-modification (RM) systems in the organism.[68] Protoplasts are fragile and may leak nucleases that degrade foreign DNA introduced during transformation. The addition of calf thymus DNA before, but not after, the addition of plasmid DNA was found to increase the transformation frequency 10-fold in *Streptomyces ambofaciens* (*S. ambofaciens*).[65] Calf thymus DNA may provide competitive protection against endonucleolytic cleavage of plasmid DNA. In addition, transformation frequency was increased by 10^3 in *S. ambofaciens* and in *Streptomyces griseus* (*S. griseus*) using plasmid DNA isolated from *S. ambofaciens* and *S. griseus*, respectively.[65, 68] Many *Streptomyces* species have species-specific methyltransferases that methylate their own DNA and protect themselves from endonucleases that cleave incoming bacteriophage DNA.[69-70] For example, plasmids isolated from *E. coli* were unable to be introduced into *S. griseus* until the plasmid was methylated *in vitro* with *Hpa*II and *Sss*I.[68] The transformation efficiency increased by 10^5 using *Hpa*II-methylated plasmid DNA, comparable to transformation levels observed using plasmids isolated from *S. griseus*.[68] Dam-methylated plasmids are cleaved by restriction endonucleases of many *Streptomcyes* species and accordingly, the plasmids used to transform *S. tateyamensis* were isolated from a Dam-deficient *E. coli* strain (*E. coli* ET12567).[68, 71] This method by MacNeil and coworkers was successful in introducing a plasmid into *Streptomyces avermitilis*, later shown to be applicable for *Streptomyces laurentii* by Kelly and coworkers, but not for *S. tateyamensis*.[14, 72] DNA introduced to *S. tateyamensis* may require a different methylation pattern than those generated in *E. coli* ET12567 to overcome RM systems present in *S. tateyamensis*. RM systems can be a great obstacle for interspecies DNA transfer.

Table 2.3: Transformation conditions for *S. tateyamensis* protoplasts. Conditions that resulted in transformants are in orange.

Transformation Condition	Protoplast Preparation Condition[a]	PEG1000 Concentration[b] (% w/v)	Transformation Temperature (°C)	DNA used in Transformation (µg)	Protoplast Regeneration	Transformants Observed
1	18	20	25	0.5	yes	no
2	18	20	25	1	yes	yes
3	18	20	4	0.5	yes	no
4	18	20	4	1	yes	no
5	21	10	25	0.5	yes	no
6	21	10	25	1	yes	no
7	21	10	25	10	yes	no
8	21	20	25	0.5	yes	no
9	21	20	25	1	yes	yes
10	21	20	25	10	yes	yes
11	21	20	4	0.5	yes	no
12	21	20	4	1	yes	no
13	21	20	4	10	yes	no
14	21	40	25	0.5	yes	no
15	21	40	25	1	yes	no
16	21	40	25	10	yes	no
17	21	55	25	0.5	yes	no
18	21	55	25	1	yes	no
19	21	55	25	10	yes	no
20	21	10 + 100 mM $MgCl_2$	25	1	yes	no[c]
21	21	10 + 100 mM $MgCl_2$	25	10	yes	no[c]
22	21	20 + 100 mM $MgCl_2$	25	1	yes	no
23	21	20 + 100 mM $MgCl_2$	25	10	yes	no
24	21	40 + 100 mM $MgCl_2$	25	1	yes	no
25	21	40 + 100 mM $MgCl_2$	25	10	yes	no
26	22	20	25	1	yes	no
27	22	20	25	5	yes	no
28	22	20	25	10	yes	no
29	22	40	25	1	yes	no
30	22	40	25	5	yes	no
31	22	40	25	10	yes	no
32	22	55	25	1	yes	no
33	22	55	25	5	yes	no
34	22	55	25	10	yes	no

[a] Protoplast preparation conditions shown in Table 2.2.
[b] PEG1000 concentration in the transformation buffer along with other additives.
[c] Apramycin-resistant transformants were observed, suggesting the acquisition of pGM-dtpnL. The presence of the plasmid in these strains, however, was not able to be confirmed by PCR amplification of the insert in pGM-dtpnL.

Conditions to transform *S. tateyamensis* were unable to be optimized. Only the *tpnA* mutant was successfully produced. *S. tateyamensis* transformants that harbored pGM-dtpnA were screened by whole cell culture PCR and the double crossover mutant, *S. tateyamensis* HI1, was confirmed by PCR and DNA sequencing analysis (Figures 2.13

and 2.14). The crude culture extract of the *tpnA* mutant, *S. tateyamensis* HI1, seemed to lack many of the compounds suspected to be the thiopeptins (Figure 2.15 and B.2). To rule out polar effects on thiopeptin production that may have been caused by the modifications on the *S. tateyamensis* chromosome, we attempted to genetically complement *S. tateyamensis* HI1 with a functional copy of *tpnA* expressed under the constitutive promotor *erm*E*.[58] A direct relationship between the expression of *tpnA* and thiopeptin production can be demonstrated if thiopeptin production is restored in *S. tateyamensis* HI1 by *in trans* expression of *tpnA*. Genetic complementation of *S. tateyamensis* HI1, however, was unsuccessful. In addition, thiopeptin production was difficult to reproduce in *S. tateyamensis*, as mentioned earlier in this chapter, causing the results of these genetic experiments to be difficult to interpret. Therefore, alternate strategies to assess the involvement of the *tpn* genes were considered.

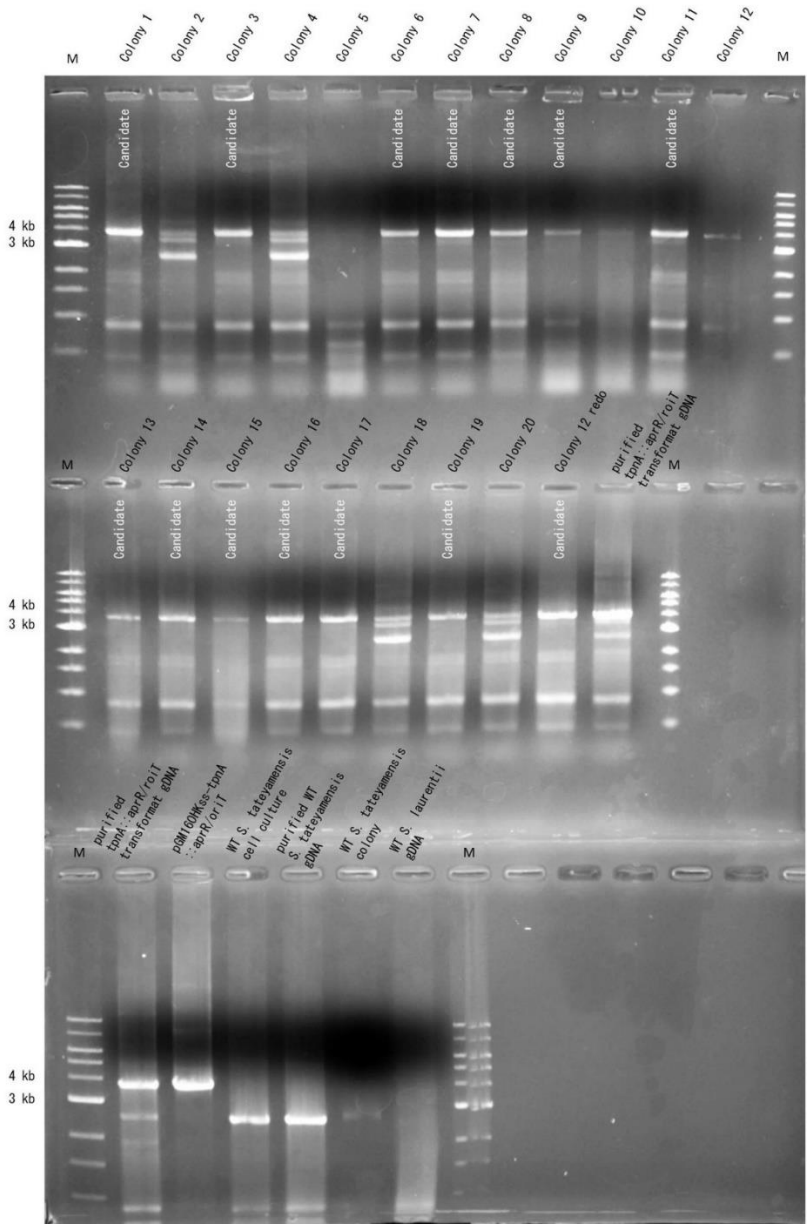

Figure 2.13: Whole cell culture PCR analysis of potential *S. tateyamensis* pGM-dtpnA transformants. (M) 1 kb molecular weight ladder and (Colonies 1-20) potential *S. tateyamensis* pGM-dtpnA transformants. A 3625 bp product was amplified from *S. tateyamensis* pGM-dtpnA (*tpnA::aprR/oriT*) transformants and pGM-dtpnA (pGM160HKss-*tpnA::aprR/oriT*) while a 2469 bp product was amplified from wild-type *S. tateyamensis*. *S. laurentii* was used as a control. Primer pair HI-4F/HI-4R was used for amplification. *S. tateyamensis* transformants that appear to harbor pGM-dtpnA are labeled as "Candidate".

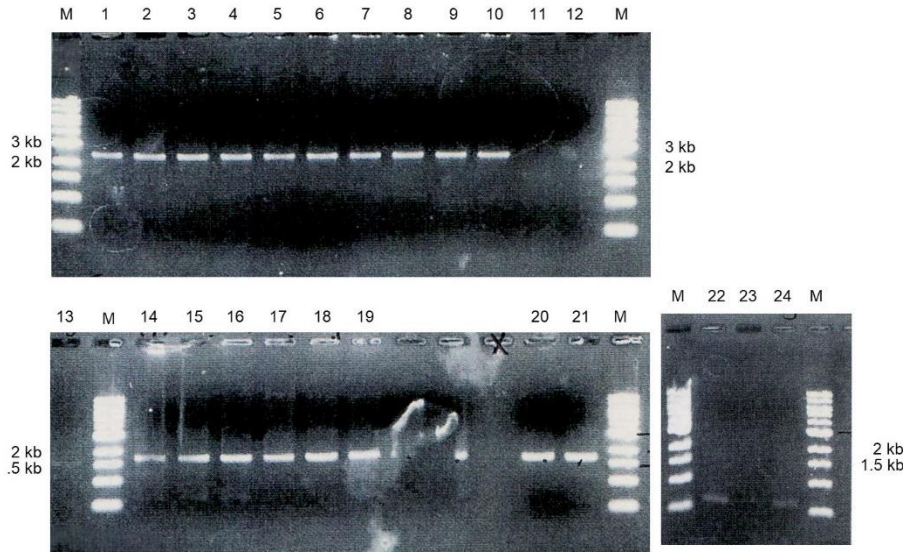

Figure 2.14: PCR analysis of the *tpnA* mutant, *S. tateyamensis* HI1. (M) 1 kb molecular weight ladder. (1-10) *S. tateyamensis* HI1 (11) wild-type *S. tateyamensis* (12) *S. laurentii* (13) wild-type *S. tateyamensis* gDNA (14-21) *S. tateyamensis* HI1 (22) wild-type *S. tateyamensis* (23) *S. laurentii* (24) wild-type *S. tateyamensis* gDNA. A 2588 bp product was amplified from (1-10) using primer pair HI-26F/HI-26R and a 1871 bp product was amplified from (14-21) using primer pair HI-27F/HI-27R from *S. tateyamensis* HI1. No product was expected to be amplified from either (11-13) using primer pair HI-26F/HI-26R or (22-24) using primer pair HI-27F/HI-27R. An amplicon (~600 bp) is observed in some reactions (14-15, 22, and 24) with primer pair HI-27F/HI-27R which likely resulted from nonspecific primer interactions during PCR.

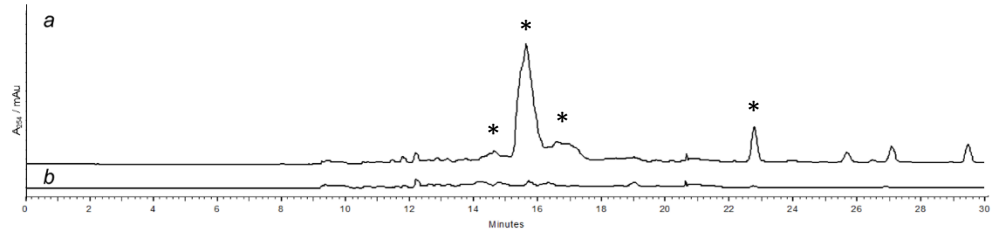

Figure 2.15: HPLC analysis of (*a*) *S. tateyamensis* and (*b*) *S. tateyamensis* HI1 crude culture extracts. Absorbance was monitored at 254 nm. Compounds suspected to be thiopeptins based on the UV-vis absorbance profiles are indicated by asterisks.

2.3.5 Transaminase activity of TpnW

Transamination of 2-methyl-L-tryptophan (**17**) is a required step in the biosynthesis of the HEQ **21** moiety of the thiopeptins.[14] TpnW shares homology with histidinol-phosphate transaminases but shows only modest homology with the thiostrepton pathway transaminase, TsrV.[14] To determine if TpnW could be involved in **13**-**16** biosynthesis, we expressed TpnW in *E. coli*, purified the protein (Figure 2.16), and reconstituted its activity *in vitro*. TpnW does convert 2-methyl-L-tryptophan **18** to 3-(2-methylindolyl)pyruvate (**19**) in the presence of aromatic α-keto acid acceptors 3-indolylpyruvate (**30**), *p*-hydroxyphenylpyruvate, and phenylpyruvate, but not in the presence of pyruvate, oxaloacetate, or α-ketoglutarate (Scheme 2.1 and Figures 2.17-2.18). Similar preferences for α-keto acid acceptors were observed with TsrV.[14, 47] These results indicate that TpnW is a 2-methyl-L-tryptophan aminotransferase involved in HEQ **21** biosynthesis for **13**-**16** and supports the involvement of the *tpn* gene cluster in thiopeptin biosynthesis. It is not clear if TpnW has a preferred α-keto acid acceptor or if TpnW has a relaxed substrate preference. Further biochemical studies, such as substrate binding and kinetic experiments, are needed to better characterize TpnW.

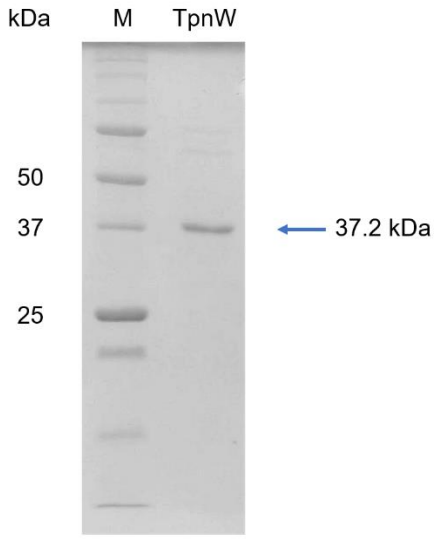

Figure 2.16: SDS-PAGE analysis of purified TpnW.

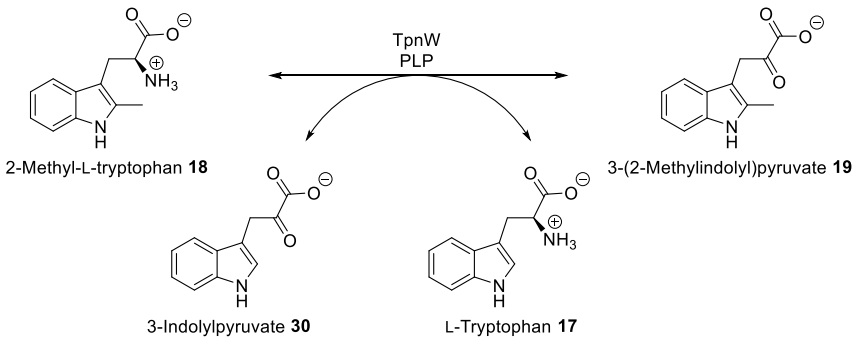

Scheme 2.1: Transamination of 2-methyl-L-tryptophan **18** with 3-indolylpyruvate **30** and TpnW to form L-tryptophan **17** and 3-(2-methylindolyl)pyruvate **19**.

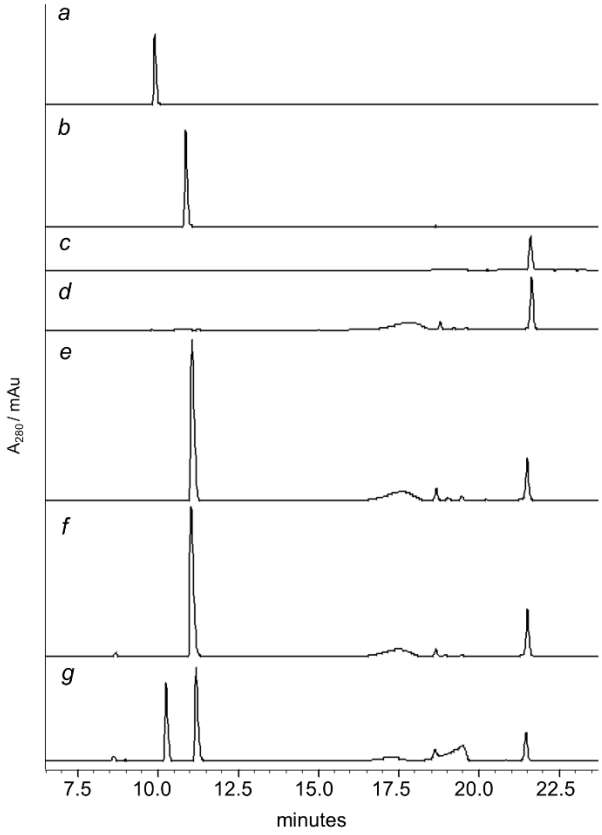

Figure 2.17: HPLC analyses of TpnW transamination activity after a 30 minute reaction time. (*a*) L-Tryptophan **17** standard; (*b*) 2-methyl-L-tryptophan **18** standard; (*c*) 3-indolylpyruvate **30** standard; (*d*) **30** after 30 min incubation in phosphate buffer; (*e*) **18** and **30**; (f) **18**, **30**, and PLP; (g) **18**, **30**, PLP, and TpnW. Absorbance was monitored at 280 nm. A new metabolite presumed to correspond to 3-(2-methylindolyl)pyruvate **19** was observed at t_R ~19.5 min and the product **17** was observed at t_R ~10.2 min in the intact reaction. The presence of an ion corresponding to the expected *m/z* of **19** in the reaction mixture was confirmed by HPLC-MS (Figure B.3).

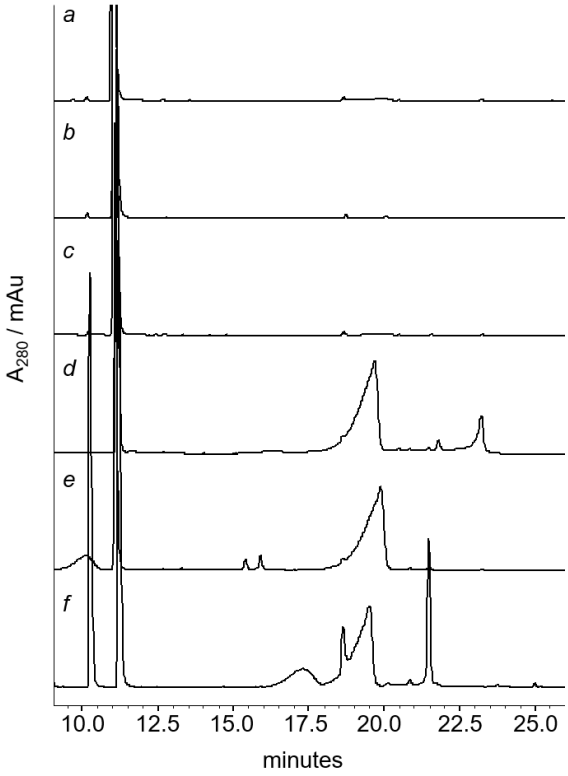

Figure 2.18: HPLC analyses of TpnW transamination activity with various α-keto acids. Transamination of 2-methyl-L-tryptophan **18** was performed with various α-keto acid acceptors: (*a*) pyruvate, (*b*) oxaloacetate, (*c*) α-ketoglutarate, (*d*) phenylpyruvate, (*e*) *p*-hydroxyphenylpyruvate, and (*f*) 3-indolylpyruvate **30**. The formation of a new metabolite at t_R ~19.5 min presumed to be 3-(2-methylindolyl)pyruvate **19** was observed in the presence of the aromatic α-keto acids phenylpyruvate, *p*-hydroxyphenylpyruvate, and 3-indolylpyruvate **30**. Absorbance was monitored at 280 nm.

2.4 Conclusions

The thiopeptin biosynthetic gene (*tpn*) cluster was identified in *S. tateyamensis* based on *in silico* comparisons of encoded products of the *tpn* cluster to homologous proteins found on the NCBI database, as well as to other known thiopeptide biosynthetic genes. The structure of thiostrepton A **2** and the thiopeptins **13**-**16** are highly similar and, accordingly, many of the encoded products of the *tpn* cluster show amino acid sequence similarities to thiostrepton biosynthetic proteins. In support of the involvement of the *tpn* cluster in thiopeptin biosynthesis, TpnW was shown to catalyze the transamination of 2-methyl-L-tryptophan **18** to 3-(2-methylindolyl)pyruvate **19**, the second step in HEQ **21** biosynthesis from L-tryptophan **17**.

Homologs of the thiostrepton biosynthetic gene cluster that are present in the *tpn* cluster can account for nearly all modification to the thiopeptin scaffold. TpnLMN, however, do not show sequence homology to known thiopeptide biosynthetic proteins. TpnL shows homology to flavin/deazaflavin oxidoreductases and is a candidate for piperidine formation. TpnMN show homology to YcaO domain-containing proteins and TfuA-like proteins, respectively, that effect thioamidation and are proposed to have similar activities in thiopeptin biosynthesis. The roles of TpnLMN in thiopeptin biosynthesis will be investigated through heterologous expression of TpnLMN in a host organism that produces a thiopeptide similar to thiopeptin and, for TpnL, *in vitro* biochemical assays that demonstrate enzyme activity.

2.5 References

1. Kim, H. J.; Graham, D. W.; DiSpirito, A. A.; Alterman, M. A.; Galeva, N.; Larive, C. K.; Asunskis, D.; Sherwood, P. M., Methanobactin, a copper-acquisition compound from methane-oxidizing bacteria. *Science* **2004**, *305*, 1612-1615.

2. Lincke, T.; Behnken, S.; Ishida, K.; Roth, M.; Hertweck, C., Closthioamide: an unprecedented polythioamide antibiotic from the strictly anaerobic bacterium *Clostridium cellulolyticum*. *Angew. Chem. Int. Ed. Engl.* **2010**, *49*, 2011-2013.

3. Hayakawa, Y.; Sasaki, K.; Nagai, K.; Shin-ya, K.; Furihata, K., Structure of thioviridamide, a novel apoptosis inducer from *Streptomyces olivoviridis*. *J. Antibiot.* **2006**, *59*, 6-10.

4. Mock, W. L.; Chen, J. T.; Tsang, J. W., Hydrolysis of a thiopeptide by cadmium carboxypeptidase A. *Biochem. Biophys. Res. Commun.* **1981**, *102*, 389-396.

5. Zacharie, B.; Lagraoui, M.; Dimarco, M.; Penney, C. L.; Gagnon, L., Thioamides: synthesis, stability, and immunological activities of thioanalogues of Imreg. Preparation of new thioacylating agents using fluorobenzimidazolone derivatives. *J. Med. Chem.* **1999**, *42*, 2046-2052.

6. Clausen, K.; Spatola, A. F.; Lemieux, C.; Schiller, P. W.; Lawesson, S. O., Evidence of a peptide backbone contribution toward selective receptor recognition for leucine enkephalin thioamide analogs. *Biochem. Biophys. Res. Commun.* **1984**, *120*, 305-310.

7. Morlock, G. P.; Metchock, B.; Sikes, D.; Crawford, J. T.; Cooksey, R. C., *EthA*, *inhA*, and *katG* loci of ethionamide-resistant clinical *Mycobacterium tuberculosis* isolates. *Antimicrob. Agents Chemother.* **2003**, *47*, 3799-3805.

8. Singh, R.; Wiseman, B.; Deemagarn, T.; Donald, L. J.; Duckworth, H. W.; Carpena, X.; Fita, I.; Loewen, P. C., Catalase-peroxidases (KatG) exhibit NADH oxidase activity. *J. Biol. Chem.* **2004**, *279*, 43098-43106.

9. Quemard, A.; Sacchettini, J. C.; Dessen, A.; Vilcheze, C.; Bittman, R.; Jacobs, W. R., Jr.; Blanchard, J. S., Enzymatic characterization of the target for isoniazid in *Mycobacterium tuberculosis*. *Biochemistry* **1995**, *34*, 8235-8241.

10. Vannelli, T. A.; Dykman, A.; Ortiz de Montellano, P. R., The antituberculosis drug ethionamide is activated by a flavoprotein monooxygenase. *J. Biol. Chem.* **2002**, *277*, 12824-12829.

11. Wang, F.; Langley, R.; Gulten, G.; Dover, L. G.; Besra, G. S.; Jacobs, W. R., Jr.; Sacchettini, J. C., Mechanism of thioamide drug action against tuberculosis and leprosy. *J. Exp. Med.* **2007**, *204*, 73-78.

12. Ramasesh, N.; Krahenbuhl, J. L.; Hastings, R. C., *In vitro* effects of antimicrobial agents on *Mycobacterium leprae* in mouse peritoneal macrophages. *Antimicrob. Agents Chemother.* **1989**, *33*, 657-662.

13. Nakata, N.; Matsuoka, M.; Kashiwabara, Y.; Okada, N.; Sasakawa, C., Nucleotide sequence of the *Mycobacterium leprae katG* region. *J. Bacteriol.* **1997**, *179*, 3053-3057.

14. Kelly, W. L.; Pan, L.; Li, C., Thiostrepton biosynthesis: prototype for a new family of bacteriocins. *J. Am. Chem. Soc.* **2009**, *131*, 4327-4334.

15. Hudson, G. A.; Zhang, Z.; Tietz, J. I.; Mitchell, D. A.; van der Donk, W. A., *In vitro* biosynthesis of the core scaffold of the thiopeptide thiomuracin. *J. Am. Chem. Soc.* **2015**, *137*, 16012-16015.

16. Liao, R.; Duan, L.; Lei, C.; Pan, H.; Ding, Y.; Zhang, Q.; Chen, D.; Shen, B.; Yu, Y.; Liu, W., Thiopeptide biosynthesis featuring ribosomally synthesized precursor peptides and conserved posttranslational modifications. *Chem. Biol.* **2009**, *16*, 141-147.

17. Hensens, O. D.; Albers-Schonberg, G., Total structure of the highly modified peptide antibiotic components of thiopeptin. *J. Antibiot.* **1983**, *36*, 814-831.

18. Goss, R. J.; Newill, P. L., A convenient enzymatic synthesis of L-halotryptophans. *Chem. Commun.* **2006**, 47, 4924-4925.

19. Kieser, T. B., M.J.; Buttner, M.J.; Chater, K.F.; Hopwood, D.A., *Practical Streptomyces Genetics*. John Innes Centre, Norwich Research Park, 2000.

20. Illing, G. T.; Normansell, I. D.; Peberdy, J. F., Protoplast isolation and regeneration in *Streptomyces clavuligerus*. *J. Gen. Microbiol.* **1989**, *135*, 2289-2297.

21. Bradford, M. M., A rapid and sensitive method for the quantitation of microgram quantities of protein utilizing the principle of protein-dye binding. *Anal. Biochem.* **1976**, *72*, 248-254.

22. Miyairi, N.; Miyoshi, T.; Aoki, H.; Kosaka, M.; Ikushima, H., Studies on thiopeptin antibiotics. I. Characteristics of thiopeptin B. *J. Antibiot.* **1970**, *23*, 113-119.

23. Miyairi, N.; Miyoshi, T.; Aoki, H.; Kosaka, M.; Ikushima, H., Thiopeptin, a new feed additive antibiotic: microbiological and chemical studies. *Antimicrob. Agents Chemother.* **1972**, *1*, 192-196.

24. Ebata, M.; Miyazaki, K.; Otsuka, H., Studies on siomycin. 3. Structural features of siomycin A. *J. Antibiot.* **1969**, *22*, 434-441.

25. Leblond, P.; Demuyter, P.; Moutier, L.; Laakel, M.; Decaris, B.; Simonet, J. M., Hypervariability, a new phenomenon of genetic instability, related to DNA amplification in *Streptomyces ambofaciens*. *J. Bacteriol.* **1989**, *171*, 419-423.

26. Birch, A.; Hausler, A.; Hutter, R., Genome rearrangement and genetic instability in *Streptomyces* spp. *J. Bacteriol.* **1990**, *172*, 4138-4142.

27. Fischer, G.; Decaris, B.; Leblond, P., Occurrence of deletions, associated with genetic instability in *Streptomyces ambofaciens*, is independent of the linearity of the chromosomal DNA. *J. Bacteriol.* **1997**, *179*, 4553-4558.

28. Crameri, R.; Kieser, T.; Ono, H.; Sanchez, J.; Hutter, R., Chromosomal instability in *Streptomyces glaucescens*: mapping of streptomycin-sensitive mutants. *J. Gen. Microbiol.* **1983**, *129*, 519-527.

29. Birch, A.; Hausler, A.; Ruttener, C.; Hutter, R., Chromosomal deletion and rearrangement in *Streptomyces glaucescens*. *J. Bacteriol.* **1991**, *173*, 3531-3538.

30. Cai, X.; Teta, R.; Kohlhaas, C.; Crusemann, M.; Ueoka, R.; Mangoni, A.; Freeman, M. F.; Piel, J., Manipulation of regulatory genes reveals complexity and fidelity in hormaomycin biosynthesis. *Chem. Biol.* **2013**, *20*, 839-846.

31. den Hengst, C. D.; Tran, N. T.; Bibb, M. J.; Chandra, G.; Leskiw, B. K.; Buttner, M. J., Genes essential for morphological development and antibiotic production in *Streptomyces coelicolor* are targets of BldD during vegetative growth. *Mol. Microbiol.* **2010**, *78*, 361-379.

32. White, J.; Bibb, M., BldA dependence of undecylprodigiosin production in *Streptomyces coelicolor* A3(2) involves a pathway-specific regulatory cascade. *J. Bacteriol.* **1997**, *179*, 627-633.

33. Fernandez-Moreno, M. A.; Caballero, J. L.; Hopwood, D. A.; Malpartida, F., The *act* cluster contains regulatory and antibiotic export genes, direct targets for translational control by the *bld*A tRNA gene of *Streptomyces*. *Cell* **1991**, *66*, 769-780.

34. Piret, J. M.; Chater, K. F., Phage-mediated cloning of *bld*A, a region involved in *Streptomyces coelicolor* morphological development, and its analysis by genetic complementation. *J. Bacteriol.* **1985**, *163*, 965-972.

35. Hopwood, D. A., The Leeuwenhoek lecture, 1987. Towards an understanding of gene switching in *Streptomyces*, the basis of sporulation and antibiotic production. *Proc. R. Soc. Lond. B. Biol. Sci.* **1988**, *235*, 121-138.

36. Hopwood, D. A., Genetic analysis and genome structure in *Streptomyces coelicolor*. *Bacteriol. Rev.* **1967**, *31*, 373-403.

37. Merrick, M. J., A morphological and genetic mapping study of bald colony mutants of *Streptomyces coelicolor*. *J. Gen. Microbiol.* **1976**, *96*, 299-315.

38. Bentley, S. D.; Chater, K. F.; Cerdeno-Tarraga, A. M.; Challis, G. L.; Thomson, N. R.; James, K. D.; Harris, D. E.; Quail, M. A.; Kieser, H.; Harper, D.; Bateman, A.; Brown, S.; Chandra, G.; Chen, C. W.; Collins, M.; Cronin, A.; Fraser, A.; Goble, A.; Hidalgo, J.; Hornsby, T.; Howarth, S.; Huang, C. H.; Kieser, T.; Larke, L.; Murphy, L.; Oliver, K.; O'Neil, S.; Rabbinowitsch, E.; Rajandream, M. A.; Rutherford, K.; Rutter, S.; Seeger, K.; Saunders, D.; Sharp, S.; Squares, R.; Squares, S.; Taylor, K.; Warren, T.; Wietzorrek, A.; Woodward, J.; Barrell, B. G.; Parkhill, J.; Hopwood, D. A., Complete genome sequence of the model actinomycete *Streptomyces coelicolor* A3(2). *Nature* **2002**, *417*, 141-147.

39. Passantino, R.; Puglia, A.-M.; Chater, K., Additional copies of the *act*II regulatory gene induce actinorhodin production in pleiotropic *bld* mutants of *Streptomyces coelicolor* A3(2). *Microbiology* **1991**, *137*, 2059-2064.

40. Chater, K. F., A morphological and genetic mapping study of white colony mutants of *Streptomyces coelicolor*. *J. Gen. Microbiol.* **1972**, *72*, 9-28.

41. Chen, W.; He, F.; Zhang, X.; Chen, Z.; Wen, Y.; Li, J., Chromosomal instability in *Streptomyces avermitilis*: major deletion in the central region and stable circularized chromosome. *BMC Microbiol.* **2010**, *10*, 198.

42. Mine, K.; Miyairi, N.; Takano, N.; Mori, S.; Watanabe, N., Thiopeptin, a new feed-additive antibiotic: biological studies and field trials. *Antimicrob. Agents Chemother.* **1972**, *1*, 496-503.

43. Dunbar, K. L.; Tietz, J. I.; Cox, C. L.; Burkhart, B. J.; Mitchell, D. A., Identification of an auxiliary leader peptide-binding protein required for azoline formation in ribosomal natural products. *J. Am. Chem. Soc.* **2015**, *137*, 7672-7677.

44. Dunbar, K. L.; Melby, J. O.; Mitchell, D. A., YcaO domains use ATP to activate amide backbones during peptide cyclodehydrations. *Nat. Chem. Biol.* **2012**, *8*, 569-575.

45. Dunbar, K. L.; Chekan, J. R.; Cox, C. L.; Burkhart, B. J.; Nair, S. K.; Mitchell, D. A., Discovery of a new ATP-binding motif involved in peptidic azoline biosynthesis. *Nat. Chem. Biol.* **2014**, *10*, 823-829.

46. Duan, L.; Wang, S.; Liao, R.; Liu, W., Insights into quinaldic acid moiety formation in thiostrepton biosynthesis facilitating fluorinated thiopeptide generation. *Chem. Biol.* **2012**, *19*, 443-448.

47. Lin, Z.; Ji, J.; Zhou, S.; Zhang, F.; Wu, J.; Guo, Y.; Liu, W., Processing 2-methyl-L-tryptophan through tandem transamination and selective oxygenation initiates

indole ring expansion in the biosynthesis of thiostrepton. *J. Am. Chem. Soc.* **2017**, *139*, 12105-12108.

48. Benjdia, A.; Pierre, S.; Gherasim, C.; Guillot, A.; Carmona, M.; Amara, P.; Banerjee, R.; Berteau, O., The thiostrepton A tryptophan methyltransferase TsrM catalyses a cob(II)alamin-dependent methyl transfer reaction. *Nat. Commun.* **2015**, *6*, 8377.

49. Priestley, N. D.; Smith, T. M.; Shipley, P. R.; Floss, H. G., Studies on the biosynthesis of thiostrepton: 4-(1-hydroxyethyl)quinoline-2-carboxylate as a free intermediate on the pathway to the quinaldic acid moiety. *Bioorg. Med. Chem.* **1996**, *4*, 1135-1147.

50. Zheng, Q.; Wang, S.; Duan, P.; Liao, R.; Chen, D.; Liu, W., An α/β-hydrolase fold protein in the biosynthesis of thiostrepton exhibits a dual activity for endopeptidyl hydrolysis and epoxide ring opening/macrocyclization. *Proc. Natl. Acad. Sci. U.S.A.* **2016**, *113*, 14318-14323.

51. Zheng, Q.; Wang, S.; Liao, R.; Liu, W., Precursor-directed mutational biosynthesis facilitates the functional assignment of two cytochromes P450 in thiostrepton biosynthesis. *ACS Chem. Biol.* **2016**, *11*, 2673-2678.

52. Liao, R.; Liu, W., Thiostrepton maturation involving a deesterification-amidation way to process the C-terminally methylated peptide backbone. *J. Am. Chem. Soc.* **2011**, *133*, 2852-2855.

53. Izawa, M.; Kawasaki, T.; Hayakawa, Y., Cloning and heterologous expression of the thioviridamide biosynthesis gene cluster from *Streptomyces olivoviridis*. *Appl. Environ. Microbiol.* **2013**, *79*, 7110-7113.

54. Nayak, D. D.; Mahanta, N.; Mitchell, D. A.; Metcalf, W. W., Post-translational thioamidation of methyl-coenzyme M reductase, a key enzyme in methanogenic and methanotrophic Archaea. *eLife* **2017**, *6*.

55. Mahanta, N.; Liu, A.; Dong, S.; Nair, S. K.; Mitchell, D. A., Enzymatic reconstitution of ribosomal peptide backbone thioamidation. *Proc. Natl. Acad. Sci. U.S.A.* **2018**, *115*, 3030-3035.

56. Ahmed, F. H.; Carr, P. D.; Lee, B. M.; Afriat-Jurnou, L.; Mohamed, A. E.; Hong, N. S.; Flanagan, J.; Taylor, M. C.; Greening, C.; Jackson, C. J., Sequence-structure-function classification of a catalytically diverse oxidoreductase superfamily in mycobacteria. *J. Mol. Biol.* **2015**, *427*, 3554-3571.

57. Gust, B. K., T.; Chater, K. F. PCR targeting system in *Streptomyces coelicolor* A3(2) 2002. http://streptomyces.org.uk/redirect/.

58. Bibb, M. J.; Janssen, G. R.; Ward, J. M., Cloning and analysis of the promoter region of the erythromycin resistance gene *ermE* of *Streptomyces erythraeus*. *Gene* **1985**, *38*, 215-226.

59. Okanishi, M.; Hamana, K.; Umezawa, H., Factors affecting infection of protoplasts with deoxyribonucleic acid of actinophage PK-66. *J. Virol.* **1968**, *2*, 686-691.

60. Tipper, D. J.; Strominger, J. L., Mechanism of action of penicillins: a proposal based on their structural similarity to acyl-D-alanyl-D-alanine. *Proc. Natl. Acad. Sci. U.S.A.* **1965**, *54*, 1133-1141.

61. Sagara, Y.; Fukui, K.; Ota, F.; Yoshida, N.; Kashiyama, T., Rapid formation of protoplasts of *Streptomyces griseoflavus* and their fine structure. *Jpn. J. Microbiol.* **1971**, *15*, 73-84.

62. Hopwood, D. A.; Wright, H. M.; Bibb, M. J.; Cohen, S. N., Genetic recombination through protoplast fusion in *Streptomyces*. *Nature* **1977**, *268*, 171-174.

63. Hammes, W.; Schleifer, K. H.; Kandler, O., Mode of action of glycine on the biosynthesis of peptidoglycan. *J. Bacteriol.* **1973**, *116*, 1029-1053.

64. Ochi, K.; Hitchcock, M. J.; Katz, E., High-frequency fusion of *Streptomyces parvulus* or *Streptomyces antibioticus* protoplasts induced by polyethylene glycol. *J. Bacteriol.* **1979**, *139*, 984-992.

65. Matsushima, P.; Baltz, R. H., Efficient plasmid transformation of *Streptomyces ambofaciens* and *Streptomyces fradiae* protoplasts. *J. Bacteriol.* **1985**, *163*, 180-185.

66. Bibb, M. J.; Ward, J. M.; Hopwood, D. A., Transformation of plasmid DNA into *Streptomyces* at high frequency. *Nature* **1978**, *274*, 398-400.

67. Biswas, N.; Ichikawa, M.; Datta, A.; Sato, Y. T.; Yanagisawa, M.; Yoshikawa, K., Phase separation in crowded micro-spheroids: DNA–PEG system. *Chem. Phys. Lett.* **2012**, *539-540*, 157-162.

68. Kwak, J.; Jiang, H.; Kendrick Kathleen, E., Transformation using *in vivo* and *in vitro* methylation in *Streptomyces griseus*. *FEMS Microbiol. Lett.* **2006**, *209*, 243-248.

69. Zotchev, S. B.; Schrempf, H.; Hutchinson, C. R., Identification of a methyl-specific restriction system mediated by a conjugative element from *Streptomyces bambergiensis*. *J. Bacteriol.* **1995**, *177*, 4809-4812.

70. MacNeil, D. J., Characterization of a unique methyl-specific restriction system in *Streptomyces avermitilis*. *J. Bacteriol.* **1988**, *170*, 5607-5612.

71. Gonzalez-Ceron, G.; Miranda-Olivares, O. J.; Servin-Gonzalez, L., Characterization of the methyl-specific restriction system of *Streptomyces coelicolor* A3(2) and of the role played by laterally acquired nucleases. *FEMS Microbiol. Lett.* **2009**, *301*, 35-43.

72. MacNeil, D. J.; Gewain, K. M.; Ruby, C. L.; Dezeny, G.; Gibbons, P. H.; MacNeil, T., Analysis of *Streptomyces avermitilis* genes required for avermectin biosynthesis utilizing a novel integration vector. *Gene* **1992**, *111*, 61-68.

CHAPTER 3: HETEROLOGOUS EXPRESSION OF TPNLMNR IN *STREPTOMYCES LAURENTII*

Adapted from: Ichikawa, H.; Bashiri, G.; Kelly, W.L. Biosynthesis of the thiopeptins and the identification of an $F_{420}H_2$-dependent dehydropiperidine reductase. *J. Am. Chem. Soc.* **2018**, *140*, 10749-10756.

The work described in this chapter was performed by Ichikawa, H.

3.1 Introduction

The thiopeptin biosynthetic gene (*tpn*) cluster contains 23 open reading frames (*orfs*), *tpnA-W*, and *tpnLMN* do not share homology to other known thiopeptide biosynthetic genes. These three *orfs* are candidates for their involvement in thioamide and piperidine formation, the two distinguishing features of the thiopeptins. In addition, *tpnR* encodes a predicted α/β-hydrolase that does not show homology to other known thiopeptide biosynthetic genes and may serve as an esterase that hydrolyzes the C-terminus carboxymethyl of a thiopeptin biosynthetic intermediate. To investigate the roles of *tpnLMNR* in thiopeptin biosynthesis, we attempted to inactivate each gene in *Streptomyces tateyamensis* ATCC 21389 (*S. tateyamensis*) and examine the effects of the gene inactivations on the biosynthesis of thiopeptin. Despite repeated efforts, conditions to reliably modify the *S. tateyamensis* genome were unable to be optimized.

Instead, an alternate approach was taken to investigate the roles of *tpnLMNR*. Thiostrepton A **2**, a thiopeptide produced by *Streptomyces laurentii* ATCC 31255 (*S. laurentii*), is highly similar in structure to the thiopeptins and we hypothesized that the

products of *tpnLMNR* may intercept the appropriate thiostrepton biosynthetic intermediate in *S. laurentii* as a substrate, generating a new metabolite, and shedding light on the function of these proteins. Thiostrepton A **2** production by *S. laurentii* has been shown to be reproducible in the Kelly lab.[1-3] In addition, the genomic manipulation of *S. laurentii* has been demonstrated and conditions previously reported by Kelly and coworkers.[4-6] Together, these two capabilities offer a separate strategy to examine *tpn* genes. Thus, TpnLMNR were heterologously expressed in *S. laurentii.* The *S. laurentii* strain that heterologously expressed TpnL produced a new piperidine-containing metabolite, thiostrepton A_a. This thiostrepton analog was structurally characterized and was evaluated for its aqueous solubility and antibacterial properties.

3.2 Materials and methods

3.2.1 General

All reagents, unless otherwise specified, were purchased from standard commercial sources and used as provided. High-performance liquid chromatography (HPLC) analyses were performed on a Beckman Coulter System Gold HPLC using an analytical Phenomenex Luna 5µm C18(2) 250 x 4.6 mm column (Torrance, CA). All mass spectrometry analyses were performed at the Georgia Institute of Technology Bioanalytical Mass Spectrometry Facility. High-performance liquid chromatography-mass spectrometry (HPLC-MS) analyses were performed on a Micromass Quattro LC using a Phenomenex Synergi 4 µm MAX-RP 80 Å C18 250 x 2.00 mm column (Torrance, CA). High resolution electrospray ionization mass spectrometry (HR-ESI-MS) and subsequent MS/MS analyses

were performed on a Thermo Fisher Scientific LTQ Orbitrap XL ETD with flow injection analysis. NMR analyses were performed on a Bruker Avance IIIHD 800 at the Georgia Institute of Technology NMR Center. Oligonucleotides were purchased from Integrated DNA Technologies, Inc. (Coralville, IA). DNA sequencing analyses were performed by Eurofins MWG Operon USA (Louisville, KY).

3.2.2 Bacterial strains, plasmids, and growth medium

All primers used are listed in Table A.1 and strains and plasmids used are listed in Table A.2. *Streptomyces tateyamensis* ATCC 21389 (*S. tateyamensis*) and *Streptomyces laurentii* ATCC 31255 (*S. laurentii*) were purchased from American Type Culture Collection. *Escherichia coli* (*E. coli*) strains were cultured in Luria-Bertani medium supplemented with 100 μg/mL ampicillin, 50 μg/mL apramycin, 12.5 μg/mL chloramphenicol, 50 μg/mL kanamycin, or 50 μg/mL streptomycin. *S. laurentii* strains containing pSET1520-derived vectors were cultured in media supplemented with 50 μg/mL apramycin.

3.2.3 Growth of *S. laurentii* and analysis of thiostrepton production

Growth of *S. laurentii* strains were carried out in a three step process as previously described.[2] First, a glycerolic mycelium stock was used to inoculate 50 mL of tryptic soy broth in a 250 mL Erlenmeyer flask, and the resulting culture was incubated at 28 °C and 220 rpm for 72 hours. 2.5 mL of this culture was used to inoculate 50 mL of seed medium (15 g/L D-glucose, 15 g/L soybean flour, 15 g/L soluble starch) in a 250 mL Erlenmeyer

flask and cultured at 28 °C and 220 rpm for 72 hours. Next, 5 mL of the seed medium was used to inoculate 100 mL of fermentation medium (50 g/L D-glucose, 11 g/L yeast extract, 15 g/L tryptic soy broth, 1 mL/L trace elements solution (5 g/L $CoCl_2 \cdot 6H_2O$, 0.5 g/L Na_2MoO_4, 0.5 g/L H_3BO_3, 1.0 g/L $CuSO_4 \cdot 2H_2O$, 1.0 g/L $ZnSO_4 \cdot 7H_2O$)) in a 500 mL Erlenmeyer flask. The culture was incubated at 28 °C and 220 rpm for 5 days for the initial studies of the *S. laurentii* heterologous expression strains HI0-HI7 and 8 days for latter studies involving *S. laurentii* HI0 and HI1. The whole culture was extracted twice with an equal volume of chloroform. The chloroform layers were pooled together, filtered, and the solvent was removed *in vacuo*. The solid residue was dissolved in 4 mL of chloroform. Samples were analyzed by HPLC and developed with a gradient of 0 to 100% acetonitrile in water over 30 min at a flow rate of 1 mL/min. Absorbance was monitored at 254 nm.

3.2.4 Transformation of *S. laurentii* with pSET1520 and cultivation of *S. laurentii* HI0

The plasmid pSET1520 was transformed into *E. coli* ET12567/pUZ8002, and introduced into *S. laurentii* by intergeneric conjugation.[2, 7] Colonies resistant to apramycin were selected, gDNA was isolated from each colony, and *S. laurentii* HI0 (*S. laurentii* harboring pSET1520) was confirmed by PCR analysis (Figure 3.1) using the primer pair HI-19F/HI-19R and sequencing analysis of the amplified product. *S. laurentii* HI0 was cultured and evaluated for thiostrepton production as described in 3.2.3.

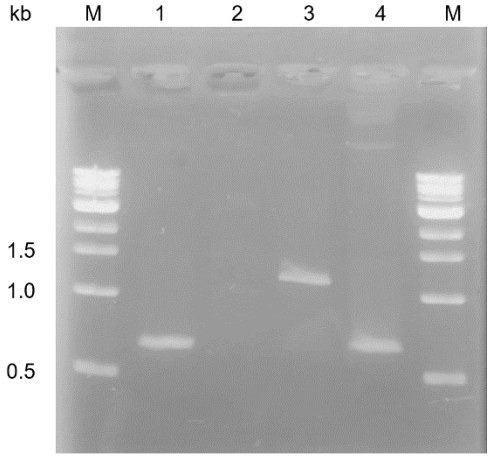

Figure 3.1: Confirmation of *S. laurentii* HI0 by PCR. The primers used were HI-19F and HI-19R, which anneal to sites on either side of the pSET1520 multiple cloning site. (M) 1 kb molecular weight ladder; (1) *S. laurentii* HI0; (2) *S. laurentii*; (3) *S. laurentii* HI1; (4) pSET1520. The expected 659 bp products were amplified from *S. laurentii* HI0 and pSET1520. The expected product from pSET1520-tpnL in *S. laurentii* HI1 is 1172 bp.

3.2.5 Expression of TpnL in *S. laurentii*

The gene encoding TpnL was amplified by PCR from HI2G2 using the primer pair HI-20F/HI-20R. The PCR product was ligated into pSC-B-amp/kan to form pSC-B-tpnL, and the genomic insert was confirmed by DNA sequence analysis. The vector was digested with *Eco*RI and *Nde*I, the insert ligated into pSET1520 to form pSET1520-tpnL, and the insert was confirmed by DNA sequence analysis. Following transformation into *E. coli* ET12567/pUZ8002, pSET1520-tpnL was introduced into *S. laurentii* by intergeneric conjugation.[2, 7] Colonies resistant to apramycin were selected, gDNA was isolated from each colony, and *S. laurentii* HI1 (*S. laurentii* harboring pSET1520-tpnL) was confirmed by PCR analysis (Figure 3.2) using the primer pair HI-20F/HI-20R and sequencing analysis of the amplified product. *S. laurentii* HI1 was cultured and evaluated for thiostrepton production as described in 3.2.3.

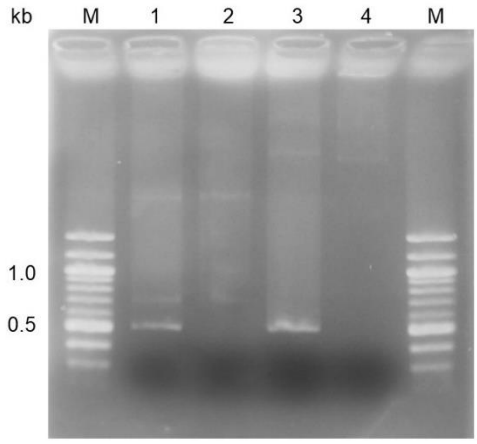

Figure 3.2: Confirmation of *S. laurentii* HI1 by PCR. The primers used were HI-20F and HI-20R, which anneal to *tpnL*. (M) 1 kb molecular weight ladder; (1) *S. laurentii* HI1; (2) *S. laurentii*; (3) pSET1520-tpnL; (4) pSET1520. The expected 519 bp products were amplified from *S. laurentii* HI1 and pSET1520-tpnL.

3.2.6 Expression of TpnM in *S. laurentii*

The gene encoding TpnM was amplified by PCR from HI2G2 using the primer pair HI-21F/HI-21R. The PCR product was ligated into pSC-B-amp/kan to form pSC-B-tpnM, and the genomic insert was confirmed by DNA sequence analysis. The vector was digested with *Eco*RI and *Nde*I, the insert ligated into pSET1520 to form pSET1520-tpnM, and the insert was confirmed by DNA sequence analysis. Following transformation into *E. coli* ET12567/pUZ8002, pSET1520-tpnM was introduced into *S. laurentii* by intergeneric conjugation.[2, 7] Colonies resistant to apramycin were selected, gDNA was isolated from each colony, and *S. laurentii* HI2 (*S. laurentii* harboring pSET1520-tpnM) was confirmed by PCR analysis (Figure 3.3) using the primer pair HI-21F/HI-21R and sequencing analysis of the amplified product. *S. laurentii* HI2 was cultured and evaluated for thiostrepton production as described in 3.2.3.

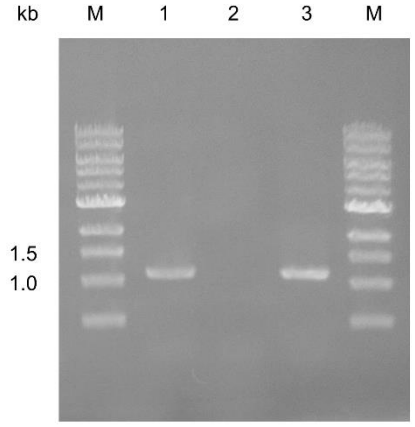

Figure 3.3: Confirmation of *S. laurentii* HI2 by PCR. The primers used were HI-21F and HI-21R, which anneal to *tpnM*. (M) 1 kb molecular weight ladder; (1) *S. laurentii* HI2; (2) *S. laurentii*; (3) pSET1520-tpnM. The expected 1.2 kb products were amplified from *S. laurentii* HI2 and pSET1520-tpnM.

3.2.7 Expression of TpnN in *S. laurentii*

The gene encoding TpnN was amplified by PCR from HI2G2 using the primer pair HI-22F/HI-22R. The PCR product was ligated into pSC-B-amp/kan to form pSC-B-tpnN, and the genomic insert was confirmed by DNA sequence analysis. The vector was digested with *Eco*RI and *Nde*I, the insert ligated into pSET1520 to form pSET1520-tpnN, and the insert was confirmed by DNA sequence analysis. Following transformation into *E. coli* ET12567/pUZ8002, pSET1520-tpnN was introduced into *S. laurentii* by intergeneric conjugation.[2, 7] Colonies resistant to apramycin were selected, gDNA was isolated from each colony, and *S. laurentii* HI3 (*S. laurentii* harboring pSET1520-tpnN) was confirmed by PCR analysis (Figure 3.4) using the primer pair HI-22F/HI-22R and sequencing analysis of the amplified product. *S. laurentii* HI3 was cultured and evaluated for thiostrepton production as described in 3.2.3.

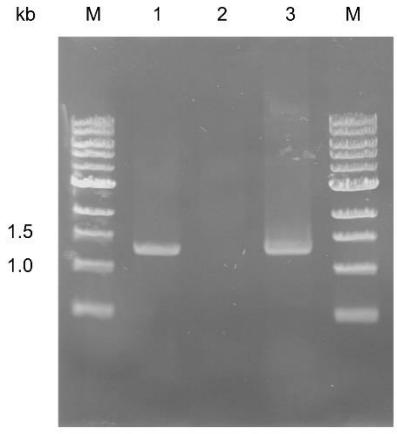

Figure 3.4: Confirmation of *S. laurentii* HI3 by PCR. The primers used were HI-22F and HI-22R, which anneal to *tpnN*. (M) 1 kb molecular weight ladder; (1) *S. laurentii* HI3; (2) *S. laurentii*; (3) pSET1520-tpnN. The expected 1.3 kb products were amplified from *S. laurentii* HI3 and pSET1520-tpnN.

3.2.8 Expression of TpnR in *S. laurentii* and cultivation of *S. laurentii* HI4

The gene encoding TpnR was amplified by PCR from HI2B7 using the primer pair HI-23F/HI-23R. The PCR product was ligated into pSC-B-amp/kan to form pSC-B-tpnR, and the genomic insert was confirmed by DNA sequence analysis. The vector was digested with *Eco*RI, the insert ligated into pSET1520 to form pSET1520-tpnR, and the insert was confirmed by DNA sequence analysis. Following transformation into *E. coli* ET12567/pUZ8002, pSET1520-tpnR was introduced into *S. laurentii* by intergeneric conjugation.[2, 7] Colonies resistant to apramycin were selected, gDNA was isolated from each colony, and *S. laurentii* HI4 (*S. laurentii* harboring pSET1520-tpnR) was confirmed by PCR analysis (Figure 3.5) using the primer pair HI-23F/HI-23R and sequencing analysis of the amplified product. *S. laurentii* HI4 was cultured and evaluated for thiostrepton production as described in 3.2.3.

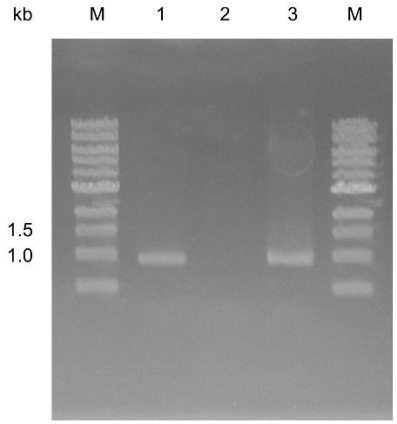

Figure 3.5: Confirmation of *S. laurentii* HI4 by PCR. The primers used were HI-23F and HI-23R, which anneal to *tpnR*. (M) 1 kb molecular weight ladder; (1) *S. laurentii* HI4; (2) *S. laurentii*; (3) pSET1520-tpnR. The expected 1.0 kb products were amplified from *S. laurentii* HI4 and pSET1520-tpnR.

3.2.9 Expression of TpnLM in *S. laurentii*

The genes encoding TpnLM were amplified by PCR from HI2G2 using the primer pair HI-20F/HI-21R. The PCR product was ligated into pSC-B-amp/kan to form pSC-B-tpnLM, and the genomic insert was confirmed by DNA sequence analysis. The vector was digested with *Eco*RI and *Nde*I, the insert ligated into pSET1520 to form pSET1520-tpnLM, and the insert was confirmed by DNA sequence analysis. Following transformation into *E. coli* ET12567/pUZ8002, pSET1520-tpnLM was introduced into *S. laurentii* by intergeneric conjugation.[2, 7] Colonies resistant to apramycin were selected, gDNA was isolated from each colony, and *S. laurentii* HI5 (*S. laurentii* harboring pSET1520-tpnLM) was confirmed by PCR analysis (Figure 3.6) using the primer pair HI-20F/HI-21R and sequencing analysis of the amplified product. *S. laurentii* HI5 was cultured and evaluated for thiostrepton production as described in 3.2.3.

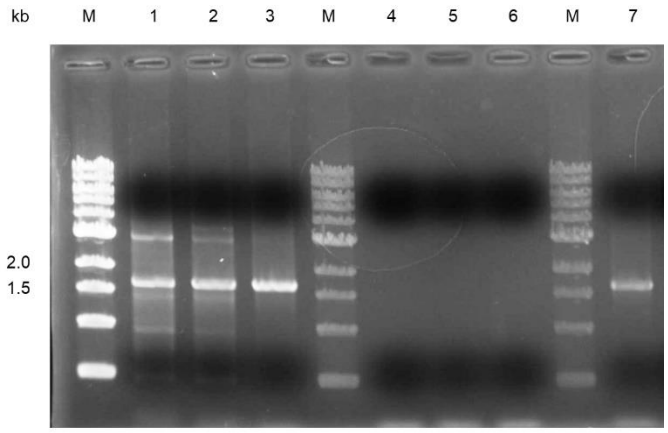

Figure 3.6: Confirmation of *S. laurentii* HI5 by PCR. The primers used were HI-20F and HI-21R, which anneal to the 5'-end of *tpnL* and the 3'-end of *tpnM*, respectively. (M) 1 kb molecular weight ladder; (1-3) *S. laurentii* HI5; (4-6) *S. laurentii*; (7) pSET1520-tpnLM. The expected 1.7 kb products were amplified from *S. laurentii* HI5 and pSET1520-tpnLM.

3.2.10 Expression of TpnMN in *S. laurentii*

The genes encoding TpnMN were amplified by PCR from HI2G2 using the primer pair HI-21F/HI-22R. The PCR product was ligated into pSC-B-amp/kan to form pSC-B-tpnMN, and the genomic insert was confirmed by DNA sequence analysis. The vector was digested with *Eco*RI and *Nde*I, the insert ligated into pSET1520 to form pSET1520-tpnMN, and the insert was confirmed by DNA sequence analysis. Following transformation into *E. coli* ET12567/pUZ8002, pSET1520-tpnMN was introduced into *S. laurentii* by intergeneric conjugation.[2, 7] Colonies resistant to apramycin were selected, gDNA was isolated from each colony, and *S. laurentii* HI6 (*S. laurentii* harboring pSET1520-tpnMN) was confirmed by PCR analysis (Figure 3.7) using the primer pair HI-21F/HI-22R and sequencing analysis of the amplified product. *S. lasurentii* HI6 was cultured and evaluated for thiostrepton production as described in 3.2.3.

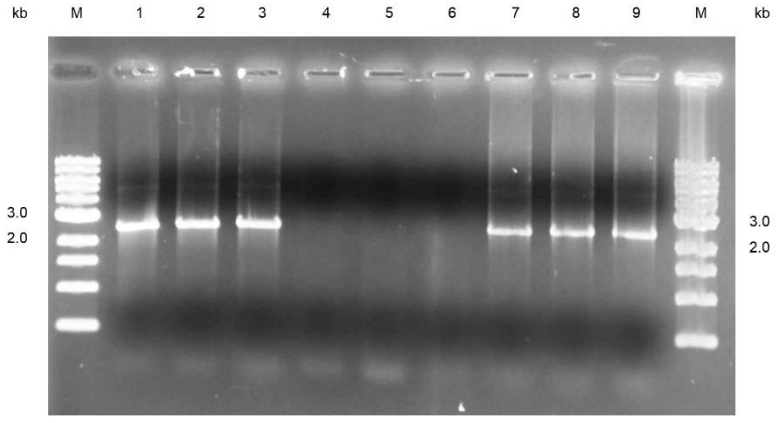

Figure 3.7: Confirmation of *S. laurentii* HI6 by PCR. The primers used were HI-21F and HI-22R, which anneal to the 5'-end of *tpnM* and the 3'-end of *tpnN*, respectively. (M) 1 kb molecular weight ladder; (1-3) *S. laurentii* HI6; (4-6) *S. laurentii*; (7-9) pSET1520-tpnMN. The expected 2.5 kb products were amplified from *S. laurentii* HI5 and pSET1520-tpnMN.

3.2.11 Expression of TpnLMN in *S. laurentii*

The genes encoding TpnLMN were amplified by PCR from HI2G2 using the primer pair HI-20F/HI-22R. The PCR product was ligated into pSC-B-amp/kan to form pSC-B-tpnLMN, and the genomic insert was confirmed by DNA sequence analysis. The vector was digested with *Eco*RI and *Nde*I, the insert ligated into pSET1520 to form pSET1520-tpnLMN, and the insert was confirmed by DNA sequence analysis. Following transformation into *E. coli* ET12567/pUZ8002, pSET1520-tpnLMN was introduced into *S. laurentii* by intergeneric conjugation.[2, 7] Colonies resistant to apramycin were selected, gDNA was isolated from each colony, and *S. laurentii* HI7 (*S. laurentii* harboring pSET1520-tpnLMN) was confirmed by PCR analyses (Figure 3.8) using the primer pair HI-20F/HI-22R and sequencing analysis of the amplified product. *S. laurentii* HI7 was evaluated for thiostrepton production as described in 3.2.3.

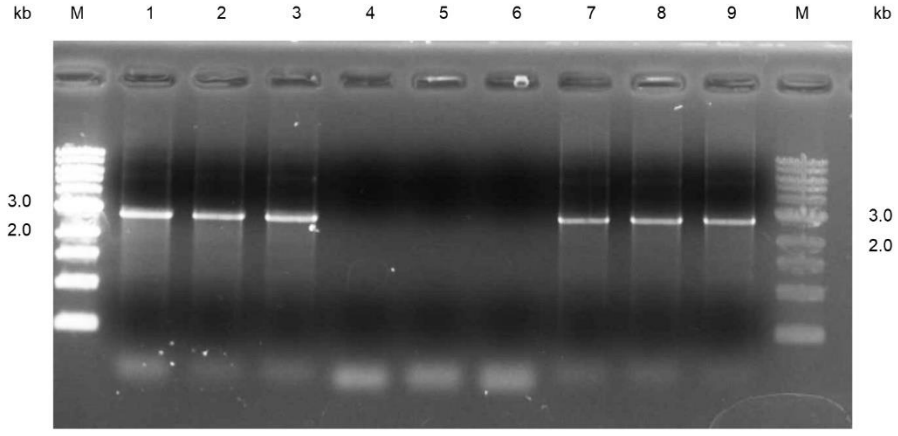

Figure 3.8: Confirmation of *S. laurentii* HI7 by PCR. The primers used were HI-20F and HI-22R, which anneal to the 5'-end of *tpnL* and the 3'-end of *tpnN*, respectively. (M) 1 kb molecular weight ladder; (1-3) *S. laurentii* HI7; (4-6) *S. laurentii*; (7-9) pSET1520-tpnLMN. The expected 3.0 kb products were amplified from *S. laurentii* HI7 and pSET1520-tpnLMN.

3.2.12 Purification and characterization of thiostrepton A_a (**31**)

From 1 L of *S. laurentii* HI1 culture, 3 mL of crude extract was prepared and thiostrepton A_a **31** was purified by HPLC. A Phenomenex 5µm C18(2) Luna 250 x 10.00 mm column was used to develop a gradient of 0% to 50% acetonitrile in water over 60 min at 7 mL/min. The purified metabolite was analyzed by HR-ESI-MS (observed: *m/z* 1666.5157 $[M+H]^+$, calculated: *m/z* 1666.5158), ESI-MS/MS, and NMR (Figures B.13-B.23 and Tables B.1-B.3).

3.2.13 Determination of thiostrepton A_a (**31**) solubility

The solubility of thiostrepton A_a **31** was determined following a previously described method.[5] A 100 µL mixture containing 50 µM thiostrepton A **2** or thiostrepton A_a **31**, 50 mM Tris pH 7.5, and 10% DMSO was incubated at 25 °C for 2 hours with rotary shaking. Samples were prepared in triplicate. The mixtures were centrifuged at 14,000 x g for 10 min at 4 °C. The absorbance of the supernatant was analyzed at 280 nm. Thiostrepton remaining in solution was quantified using the molar absorptivity of thiostrepton at 280 nm, 0.027 $\mu M^{-1}cm^{-1}$.[8]

3.2.14 Antimicrobial activity of thiostrepton A_a (**31**)

The minimum inhibitory concentrations (MICs) of thiostreptons A **2** and A_a **31** against *Bacillus* sp. ATCC 27859 (*Bacillus* sp.), vancomycin-resistant *Enterococcus faecium* ATCC 12952 (VRE), methicillin-resistant *Staphylococcus aureus* ATCC 33591

(MRSA), and *Escherichia coli* ATCC 27856 (*E. coli*) were determined using previously described methods.[4] Cell growth was monitored by comparing the OD_{600} at the time of treatment and after 18 hours incubation at 37 °C. A difference in OD_{600} was considered growth. DMSO was used as a control in all assays. To determine the relative inhibition of cell growth, the difference in OD_{600} was normalized against the DMSO control. MIC was defined as the lowest concentration at which no difference in OD_{600} was observed.

3.2.15 *In vitro* coupled transcription-translation assay

The half maximum inhibitory concentration (IC_{50}) of thiostrepton A **2** and thiostrepton A_a **31** against prokaryotic ribosomal translation was determined using the *E. coli* S30 Extract System for Circular DNA and the Luciferase Assay System (Promega, Madison, WI) according to a previously described method with one modification.[5] The concentration of the template DNA, pBEST*luc*, was reduced from 50 ng/μL to 5 ng/μL in the reaction mixture.

3.3 Results and Discussion

3.3.1 Heterologous expression of TpnLMNR in *S. laurentii*

TpnLMNR were heterologously expressed, either individually or coexpressed in combination with the others, in *S. laurentii* under the control of the constitutive *ermE** promotor of the pSET1520 plasmid (Table 3.1).[9-10] The strains were cultured in liquid media and the crude culture extracts were analyzed by HPLC and HPLC-MS for a piperidine-containing analog of thiostrepton A (**31**) ($[M+2H]^{2+}$ calculated *m/z* 834), a thioamide-containing analog of thiostrepton A (**32**) ($[M+2H]^{2+}$ calculated *m/z* 841), or a piperidine- and thioamide-containing analog (**33**) ($[M+2H]^{2+}$ calculated *m/z* 842) (Table 3.1, Figures 3.9-3.20, and B.5-B.12). Wild-type *S. laurentii*, *S. laurentii* HI0, and *S. laurentii* HI4 each produced **2** and the proposed analogs **31**-**33** were not detected (Figures 3.10-3.11, 3.14 and Figures B.4-B.5, B.9). *S. laurentii* HI0 is a negative control and alterations to thiostrepton production are not expected. *S. laurentii* HI4 expresses TpnR, a predicted α/β-hydrolase that may hydrolyze the C-terminal methyl ester of a thiopeptin/thiostrepton biosynthetic intermediate. Wild-type *S. laurentii* already expresses the thiostrepton methylesterase, TsrU.[2] If our prediction about TpnR function is correct, it is not surprising that no new thiostrepton analogs were observed in *S. laurentii* HI4. All other *S. laurentii* strains still produced thiostrepton A **2**, but strains that expressed TpnL (*S. laurentii* HI1, *S. laurentii* HI5, and *S. laurentii* HI7) also produced a new metabolite (**31** $[M+2H]^{2+}$ calculated *m/z* 834) with a mass increased by 2 Da relative to **2** and a slightly earlier HPLC retention time compared to **2** (Table 3.2, Figure 3.11, 3.15, 3.17 and Figures B.6, B.10, and B.12). *S. laurentii* HI1 produced **31** at 76.97 ± 40.87 mg/L and **2** at 4.82 ± 3.03 mg/L, nearly 9-fold less than the titer of **2** produced by the wild-type strain at 41.63

± 22.26 mg/L. HPLC co-injection of the crude culture extracts of *S. laurentii* HI1, *S. laurentii* HI5, and *S. laurentii* HI7 resulted in a co-elution of **31**, suggesting that all three strains produced the same metabolite (Figures 3.18-3.20). *S. laurentii* HI6, which expresses both TpnMN but not TpnL, did not produce **31** (Figure 3.15 and B.11). The only common gene expressed in all three strains that produced **31** is *tpnL*, and therefore *tpnL* is likely to be responsible for this new metabolite.

The strain that coexpressed TpnM and TpnN (*S. laurentii* HI6) produced a compound with a mass matching a thioamidated thiostrepton analog **32** (Figure B.11, t_R ~ 21.84 min, observed *m/z* 840.9 $[M+2H]^+$, calculated *m/z* 840.7), but *S. laurentii* HI6 did not produce either of the piperidine-containing analogs **31** or **33**. The strain that coexpressed TpnLMN (*S. laurentii* HI7) produced a compound with a mass similar to a piperidine- and thioamide-containing thiostrepton analog **33** (Figure B.12, t_R ~ 29.01 min, observed *m/z* 842.4 $[M+2H]^+$, calculated *m/z* 841.8). The proposed thiostrepton A analogs detected in *S. laurentii* strains that expressed TpnMN and TpnLMN match predicted functions of the proteins. The YcaO-TfuA pair, TpnM and TpnN, is predicted to work in concert to thioamidate the peptidic substrate, and accordingly, a new metabolite with a mass matching a thioamide-containing thiostrepton analog **32** was observed in *S. laurentii* HI6, which coexpresses TpnMN (Figure B.11), but not in *S. laurentii* HI2, *S. laurentii* HI3, or *S. laurentii* HI5 which express TpnM, TpnN, or TpnLM, respectively (Figure B.7-B.8). In addition, TpnL appears to mediate formation of a piperidine-containing thiostrepton analog **31**. Accordingly, a new metabolite with a mass matching a piperidine- and thioamide-containing thiostrepton analog **33** was observed in *S. laurentii* HI7 which coexpresses TpnLMN but not in other strains which either lacked the expression of TpnL

or a TpnMN pair. Compounds presumed to be **32** and **33** need to be isolated and structurally characterized to confirm if they contain a thioamide moiety suggested by the proposed functions of TpnMN.

Table 3.1. *S. laurentii* strains evaluated in this chapter

Strain Name	Expression Vector	Gene(s) Expressed	New Metabolite Observed	HPLC	HPLC-MS
S. laurentii					Figure B.4
S. laurentii HI0	pSET1520			Figure 3.10	Figure B.5
S. laurentii HI1	pSET1520-TpnL	*tpnL*	Thiostrepton A_a **31**	Figure 3.11	Figure B.6
S. laurentii HI2	pSET1520-TpnM	*tpnM*		Figure 3.12	Figure B.7
S. laurentii HI3	pSET1520-TpnN	*tpnN*		Figure 3.13	Figure B.8
S. laurentii HI4	pSET1520-TpnR	*tpnR*		Figure 3.14	Figure B.9
S. laurentii HI5	pSET1520-TpnLM	*tpnLM*	**31** (unconfirmed)[a]	Figure 3.15	Figure B.10
S. laurentii HI6	pSET1520-TpnMN	*tpnMN*	**32?** (unconfirmed)[a]	Figure 3.16	Figure B.11
S. laurentii HI7	pSET1520-TpnLMN	*tpnLMN*	**31, 33?** (unconfirmed)[a]	Figure 3.17	Figure B.12

[a]Compound presumed to be **31** produced by *S. laurentii* HI5 and *S. laurentii* HI7 co-elutes with **31**, which was isolated from *S. laurentii* HI1 and structurally characterized. **32** and **33** were not isolated and the structures were not confirmed.

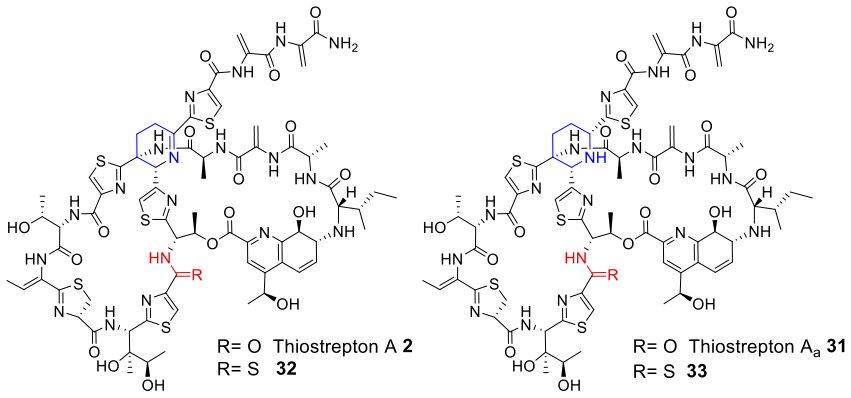

Figure 3.9: The structures of potential thiostrepton analogs (**2**, **31**-**33**) that could be produced by *S. laurentii* HI0-HI7. The dehydro(piperidine) ring is in blue and the (thio)amide is in red.

Table 3.2: *S. laurentii* strains which produced thiostrepton A_a **31**

Strain Name	HPLC	HPLC Retention Time of 31	HPLC-MS	HPLC-MS Retention Time of 31
S. laurentii HI1	Figure 3.11	22.85 min	Figure B.6	24.91 min
S. laurentii HI5	Figure 3.15	27.60 min	Figure B.10	25.42 min
S. laurentii HI7	Figure 3.17	27.60 min	Figure B.12	25.50 min

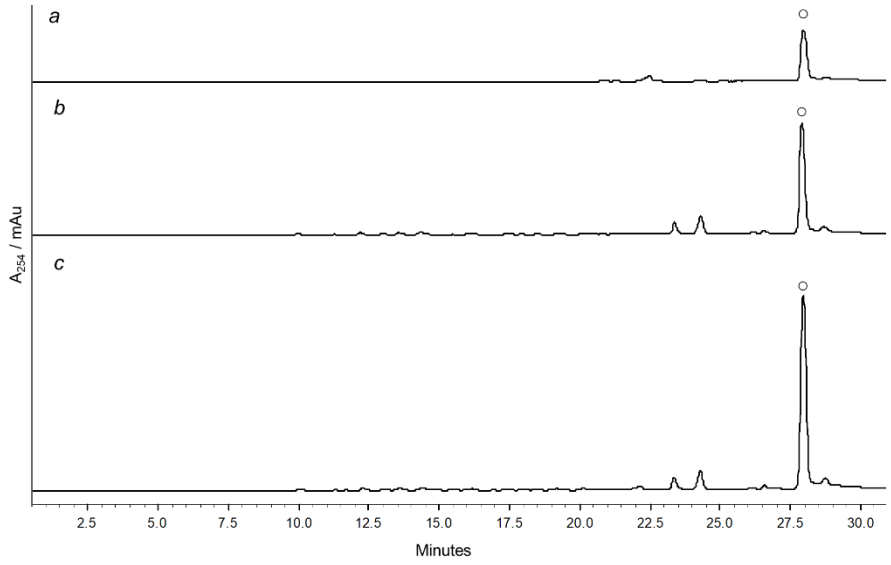

Figure 3.10: HPLC analyses of (*a*) thiostrepton A **2**, (*b*) culture extract of *S. laurentii* HI0, and (*c*) co-injection of **2** and the culture extract of *S. laurentii* HI0. Absorbance was monitored at 254 nm. Thiostrepton A **2** is indicated by (○).

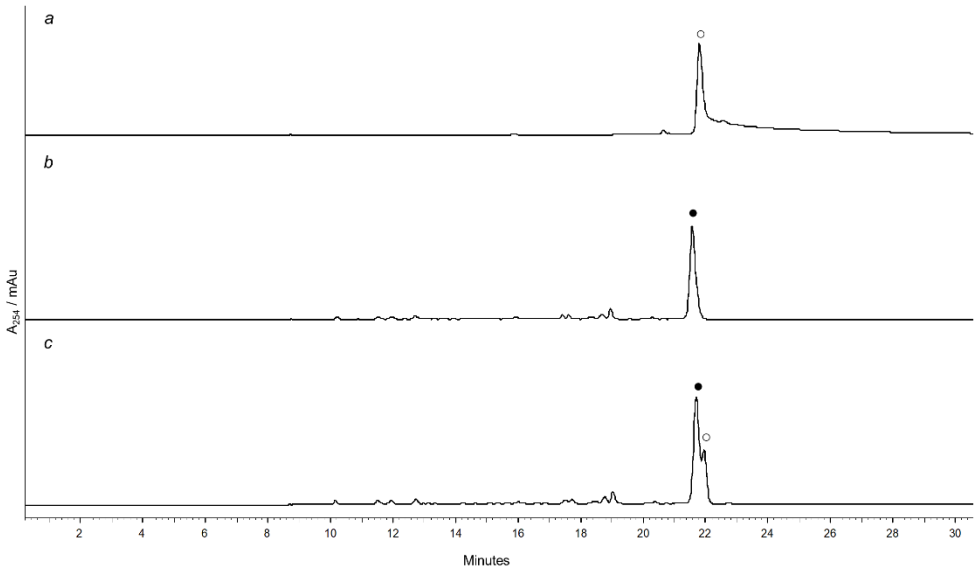

Figure 3.11: HPLC analyses of (*a*) thiostrepton A **2**, (*b*) culture extract of *S. laurentii* HI1, and (*d*) co-injection of **2** and the culture extract of *S. laurentii* HI1. Absorbance was monitored at 254 nm. Thiostrepton A **2** is indicated by (○) and Thiostrepton A_a **31** is indicated by (●).

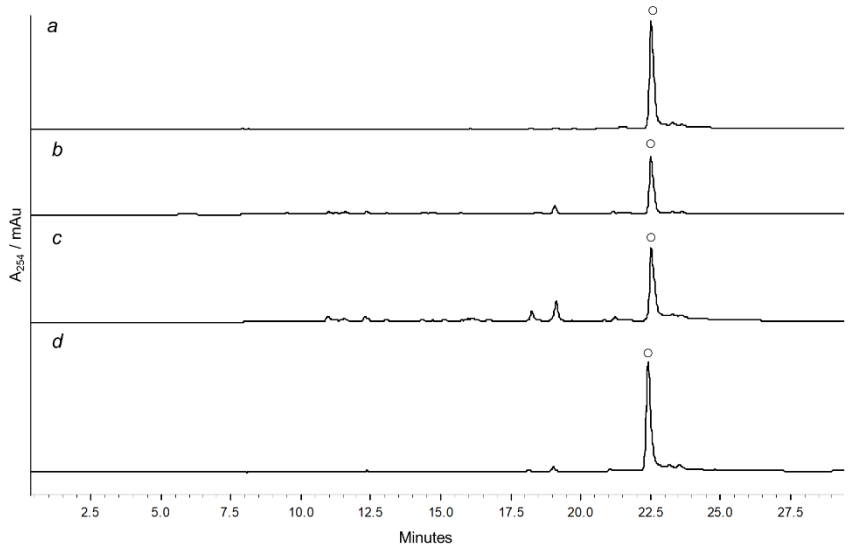

Figure 3.12: HPLC analyses of (*a*) thiostrepton A **2**, (*b*) culture extract of *S. laurentii*, (*c*) culture extract of *S. laurentii* HI2, and (*d*) co-injection of **2** and the culture extract of *S. laurentii* HI2. Absorbance was monitored at 254 nm. Thiostrepton A **2** is indicated by (○).

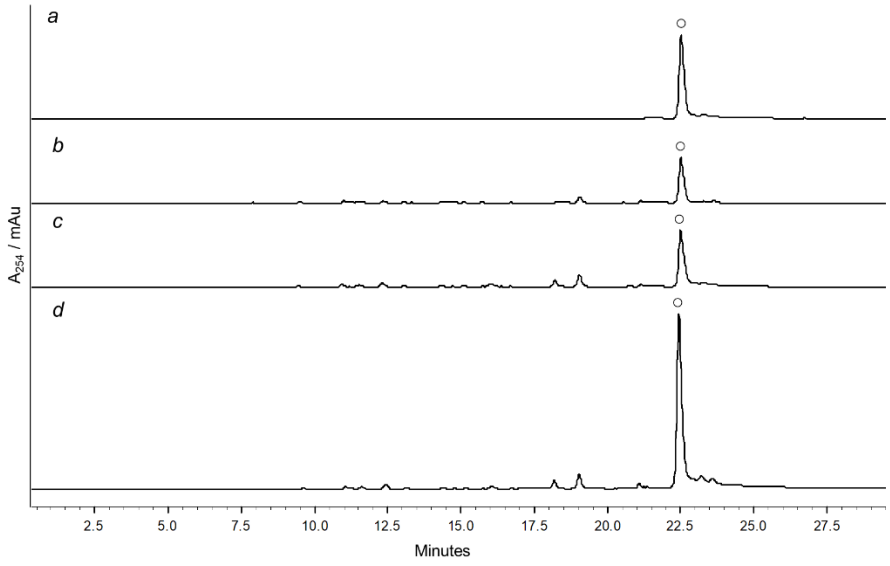

Figure 3.13: HPLC analyses of (*a*) thiostrepton A **2**, (*b*) culture extract of *S. laurentii*, (*c*) culture extract of *S. laurentii* HI3, and (*d*) co-injection of **2** and the culture extract of *S. laurentii* HI3. Absorbance was monitored at 254 nm. Thiostrepton A **2** is indicated by (○).

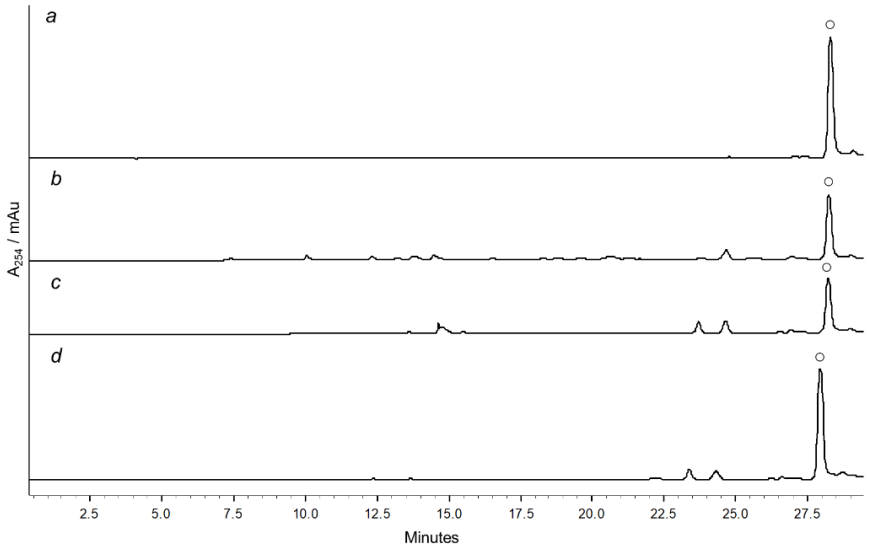

Figure 3.14: HPLC analyses of (*a*) thiostrepton A **2**, (*b*) culture extract of *S. laurentii*, (*c*) culture extract of *S. laurentii* HI4, and (*d*) co-injection of **2** and the culture extract of *S. laurentii* HI4. Absorbance was monitored at 254 nm. Thiostrepton A **2** is indicated by (○).

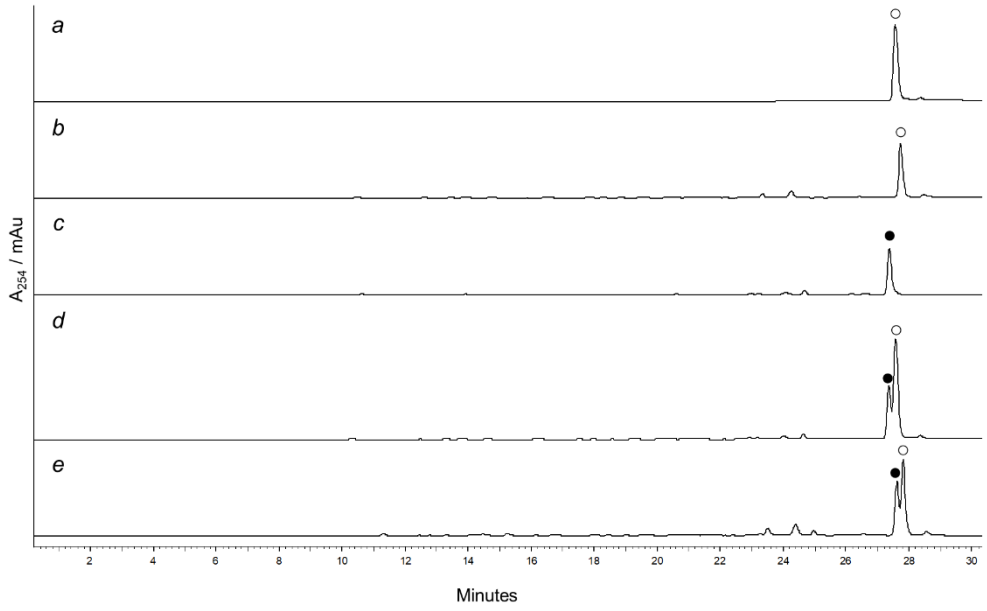

Figure 3.15: HPLC analyses of (*a*) thiostrepton A **2**, (*b*) culture extract of *S. laurentii*, (*c*) culture extract of *S. laurentii* HI5, (*d)* co-injection of **2** and the culture extract of *S. laurentii* HI5, and (*e*) co-injection of the culture extracts of *S. laurentii* and *S. laurentii* HI5. Absorbance was monitored at 254 nm. Thiostrepton A **2** is indicated by (○) and **31** is indicated by (●).

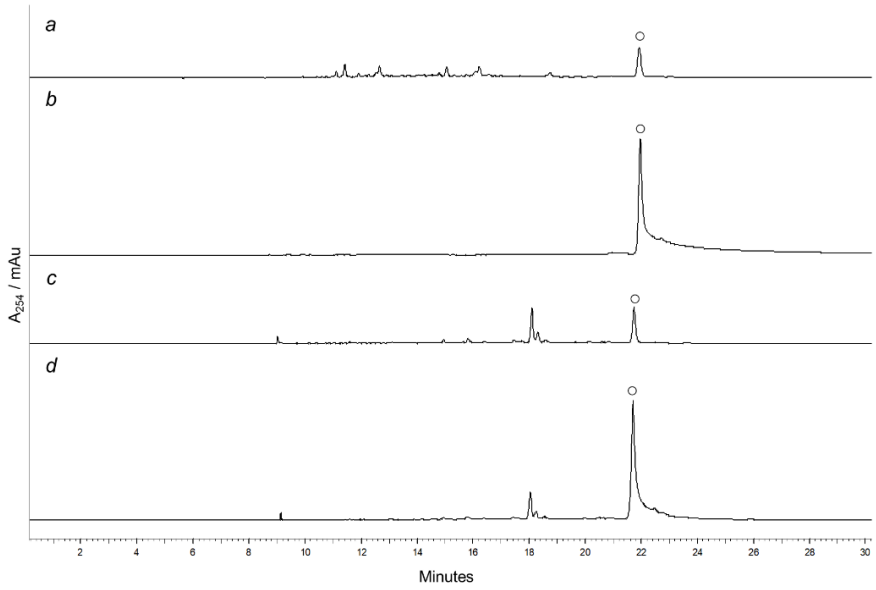

Figure 3.16: HPLC analyses of (*a*) culture extract of *S. laurentii*, (*b*) thiostrepton A **2**, (*c*) culture extract of *S. laurentii* HI6, and (*d)* co-injection of **2** and the culture extract of *S. laurentii* HI6. Absorbance was monitored at 254 nm. Thiostrepton A **2** is indicated by (○) and **31** is indicated by (●).

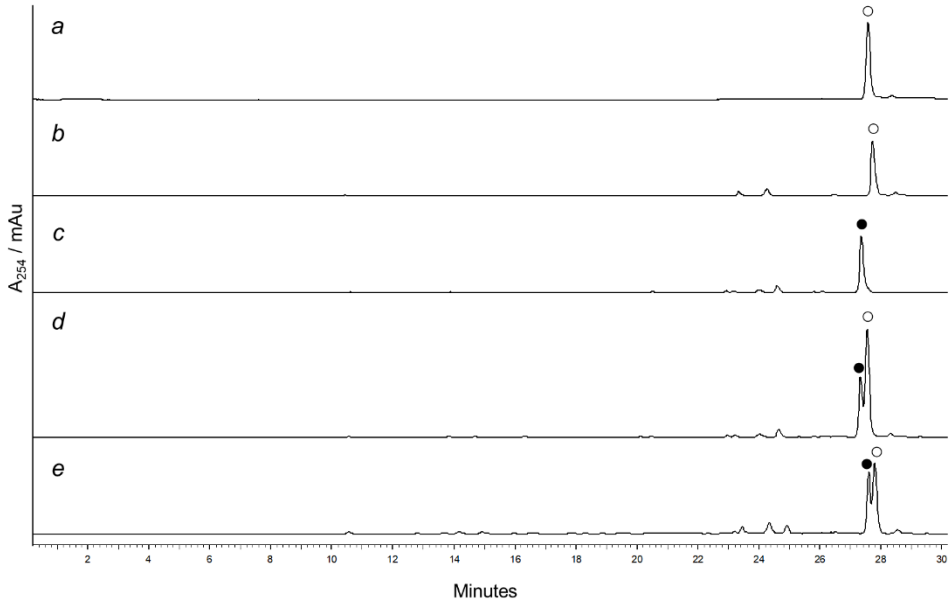

Figure 3.17: HPLC analyses of (*a*) thiostrepton A **2**, (*b*) culture extract of *S. laurentii*, (*c*) culture extract of *S. laurentii* HI7, (*d)* co-injections of **2** and the culture extract of *S. laurentii* HI7, and (*e*) co-injection of the culture extracts of *S. laurentii* and *S. laurentii* HI7. Absorbance was monitored at 254 nm. Thiostrepton A **2** is indicated by (○) and **31** is indicated by (●).

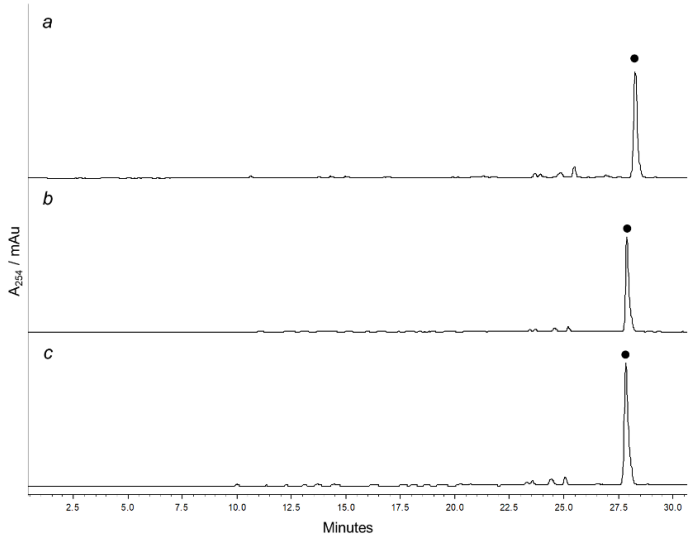

Figure 3.18: HPLC analyses of (*a*) culture extract of *S. laurentii* HI1, (*b*) culture extract of *S. laurentii* HI5, and (*c*) co-injection of the culture extracts of *S. laurentii* HI1 and *S. laurentii* HI5. The metabolite **31** observed in *S. laurentii* HI1 and HI5 strains is indicated by (●).

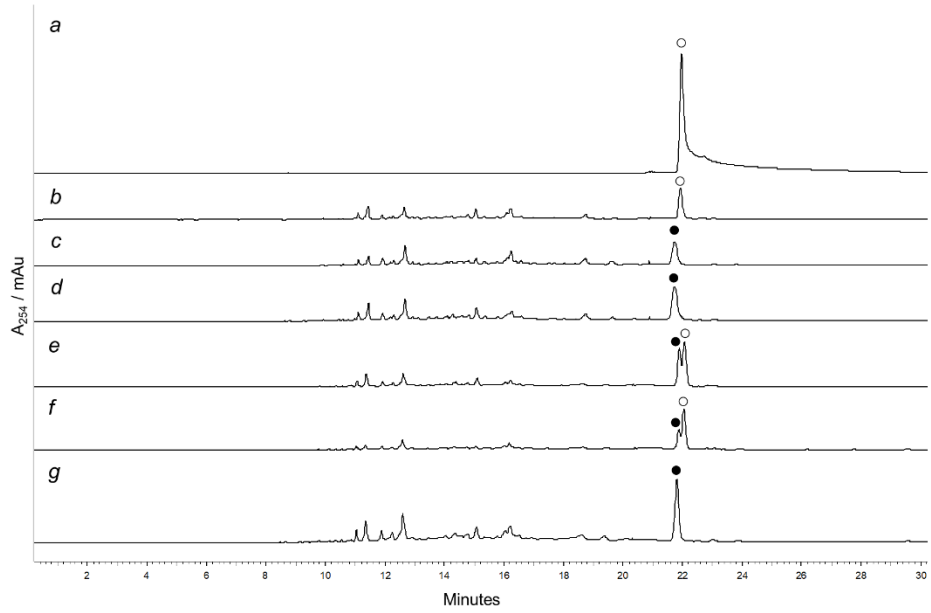

Figure 3.19: HPLC analyses of (*a*) thiostrepton A **2**, (*b*) culture extract of *S. laurentii*, (*c*) culture extract of *S. laurentii* HI1, (*d)* culture extract of *S. laurentii* HI7, (*e*) co-injection of **2** and the culture extract of *S. laurentii* HI7, (*f*) co-injection of the culture extracts of *S. laurentii* and *S. laurentii* HI7 and (*g*) co-injection of the culture extracts of *S. laurentii* HI1 and *S. laurentii* HI7. Absorbance was monitored at 254 nm. Thiostrepton A **2** is indicated by (○) and **31** is indicated by (●).

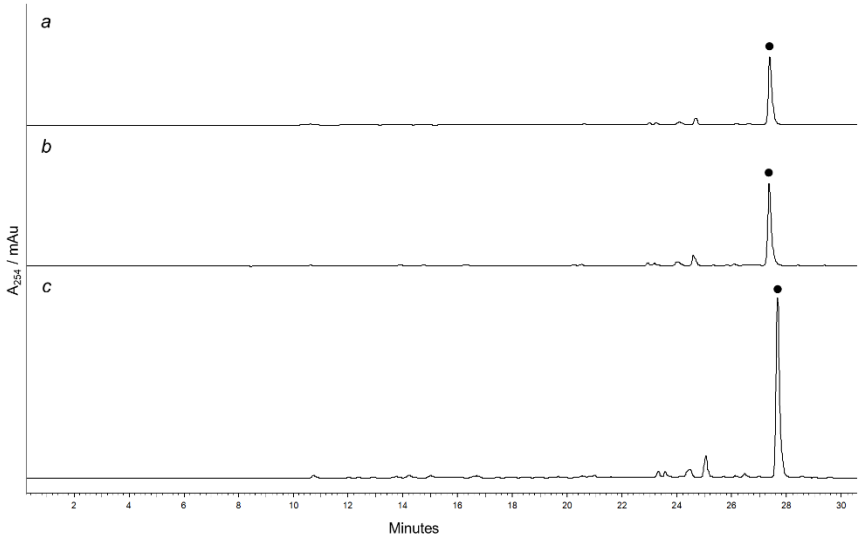

Figure 3.20: HPLC analyses of (*a*) culture extract of *S. laurentii* HI5, (*b*) culture extract of *S. laurentii* HI7, and (*c*) co-injection of the culture extracts of *S. laurentii* HI5 and *S. laurentii* HI7. The metabolite **31** observed in *S. laurentii* HI5 and HI7 strains is indicated by (●).

3.3.2 Structural characterization of thiostrepton A_a (**31**)

31 was isolated from *S. laurentii* HI1 (Figure 3.21) and a molecular formula of $C_{72}H_{88}N_{19}O_{18}S_5$ was determined by HR-ESI-MS (observed *m/z* 1666.5157 $[M+H]^+$, calculated *m/z* 1666.5158) which suggests the addition of 2 hydrogen atoms to thiostrepton A **2** (Figure B.13a). Additional MS/MS and NMR analyses (COSY, HSQC, HMBC, DEPT-135, and ROESY) were used to elucidate the structure of **31** (Figures B.13-B.23 and Table B.1-B.3). A ^1H chemical shift at δ_H = 4.68-4.66 ppm (Pip-2) is obscured by other resonances, but its COSY correlations with two piperidine protons (Pip-3-H_A δ_H = 2.12-2.08 ppm and Pip-3-H_B δ_H = 1.70-1.65 ppm) suggest a newly introduced proton on the nitrogenous heterocycle that is unobserved in the dehydropiperidine-containing thiostrepton A **2**. In addition, a broad singlet at δ_H = 4.05 ppm (Pip-5-NH) does not show an HSQC correlation, but does reveal COSY correlations to the protons of the piperidine

ring at the 2, 3, and 6 positions (Pip-2-H δ_H = 4.68-4.66 ppm, Pip-3-H_A δ_H = 2.12-2.08 ppm, and Pip-6-H δ_H = 4.76 ppm, respectively) suggesting the presence of an amine proton in the ring. The Pip-5 amine and Pip-3 protons likely adopt a "W" conformation within the ring and long-range $^4J_{HH}$ COSY correlation is expected due to the favorable overlap of molecular orbitals in this conformation.[11] Taken together, the NMR analyses indicate that the dehydropiperidine ring of **2** was reduced by TpnL to form a piperidine ring in **31** (Scheme 3.1). To determine the configuration of the newly introduced stereocenter at the Pip-2 carbon, a ROESY analysis of **31** was conducted (Figures B.22-B.23 and Tables B.2-B.3). ^{1}H-^{1}H ROESY correlations between Pip-6-H and Pip-4-H_B (δ_H = 2.63-2.58 ppm) and between Pip-4-H_B and Pip-2-H of **31** suggest these three atoms are all in axial positions of the six-membered piperidine ring (Figures B.22-B.23 and Tables B.2-B.3). Based on the previously determined structure of **2**, we propose that the newly introduced stereocenter in **31** presents with the same absolute configuration as is observed in the other series *a* thiopeptide metabolites **13** and **14**.[12-13]

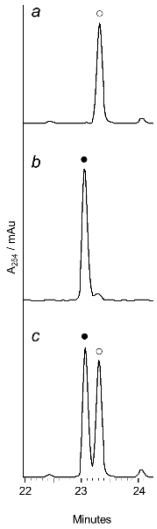

Figure 3.21: HPLC analysis of (*a*) thiostrepton A **2**, (*b*) thiostrepton A_a **31** isolated from *S. laurentii* HI1, and (*c*) co-injection of **2** and **31**. **2** is indicated by (○) and **31** is indicated by (●).

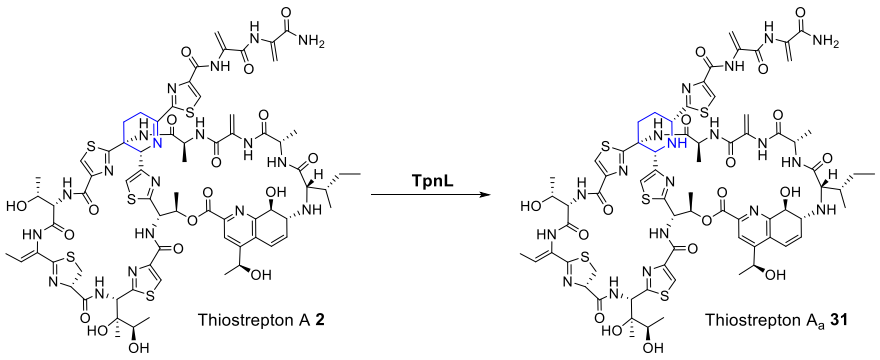

Scheme 3.1: TpnL-mediated conversion of thiostrepton A **2** to thiostrepton A_a **31**.

3.3.3 Aqueous solubility and antibacterial activity of thiostrepton A_a (**31**)

Despite the potent antibacterial activities of thiostrepton A **2** and other thiopeptides, their low aqueous solubility has dampened the development of thiopeptide antibiotics for clinical use.[6, 14-15] We made initial investigations of the biological activities of the piperidine-containing analog **31** by comparing the solubility and biological activity of **31**

with thiostrepton A **2**. The aqueous solubility of **31** in 10% DMSO (26.01 ± 0.05 μM) is slightly improved relative to 21.88 ± 0.05 μM of **2**.[5] The antibacterial activities of **31** are comparable to **2,** demonstrating minimum inhibitory concentrations of 0.018-0.098 μg/mL against Gram-positive strains (Table 3.3 and Figures B.24-B.26) and, as expected, **31** is ineffective against *E. coli*, a Gram-negative bacterium (Table 3.3).

Table 3.3: Antibiotic activities of thiostrepton A **2** and thiostrepton A_a **31**.

	MIC[a] (μg/mL)			
Compound	**MRSA[b]**	**VRE[c]**	***Bacillus*[d]**	***E. coli*[e]**
Thiostrepton A 2	0.061	0.017	0.023	>0.500
Thiostrepton A_a 31	0.098	0.018	0.040	>0.500
Vancomycin	0.78	ND[f]	ND	ND
Chloramphenicol	ND	3.9	0.97	3.9

[a]Minimum inhibitory concentration.
[b]*Staphylococcus aureus* ATCC 33591.
[c]*Enterococcus faecium* ATCC 12952.
[d]*Bacillus* sp. ATCC 27859.
[e]*Escherichia coli* ATCC 27859.
[f]Not Determined.

Since **2**, and presumably **13**-**16**, bind to the ribosome and impair its activity, inhibition of prokaryotic protein synthesis by **31** was determined using an *in vitro* transcription-translation assay.[5, 16] A cell-free *E. coli* extract containing the cellular components necessary for transcription and translation was coupled to a luciferase/luciferin reporter system. Luciferin fluorescence was measured in the presence of DMSO (negative control), vancomycin (negative control), **2**, and **31**. A relative decrease in fluorescence compared to the negative control suggests inhibition of ribosomal translation activity. Under these conditions, the half-maximal inhibitory concentration of **31** was

0.26 ± 0.04 μM, similar to 0.50 ± 0.04 μM for **2** and consistent with the activities of the two metabolites against the indicator bacterial strains (Figure B.27) The piperidine modification does not significantly alter the antibacterial properties of **31** under conditions tested, consistent with prior examination of a semisynthetic piperidine-containing **2** analog.[17]

The introduction of a piperidine ring in **31** alters the orientation of the tail (Thz15, Dha16, and Dha17) of the thiostrepton analog.[17] The crystal structure of thiostrepton A **2** bound to the L11 ribosomal protein subunit and 23S rRNA subunit of the 50S large ribosomal subunit of *Deinococcus radiodurans* (*D. radiodurans*) shows the Thz15 of thiostrepton A involved in electrostatic interactions with Pro26 of the ribosomal protein L11 subunit. In addition, the interaction of L11 and the tail region of thiostrepton appear to prevent conformational changes in the L11 subunit required for stable interactions of L11 and the L7 ribosomal subunit with EF-G.[16] Docking studies of the piperidine-containing thiostrepton analog **31** with the L11-RNA complex of *D. radiodurans* performed by Arndt and coworkers suggest that **31** may have a similar binding mode as **2** to the L11 ribosomal subunit and the tail region of **31** may provide an additional hydrogen bond interaction with the protein backbone of L11.[17] In addition, Arndt and coworkers found the K_D of a piperidine-containing thiostrepton analog to the L11-RNA subunit of *Thermus thermophilus* to be nearly two-fold less than the K_D of **2** to the L11-RNA subunit.[17]

A slight increase in binding affinity of thiostrepton A_a **31** to the ribosomal subunit may explain its modest increase in inhibition of prokaryotic translation over **2**. It is, however, not clear why **31** shows a slightly diminished activity against MRSA and *Bacillus*

compared to **2** while **31** retained similar activity against VRE with **2** (Table 3.3). The efficacy of many antibiotics not only depend on their activity against their target, but their ability to cross the cellular wall and membrane.[18] Most hydrophobic antibiotics, like thiopeptides, are thought to permeate the Gram-positive bacterial cell membrane and enter the cytoplasm by passive diffusion.[19] A slight increase in aqueous solubility may affect how **31** passes through the cell membrane of certain bacteria to its biological target.

3.4 Conclusions

To shed light on the roles of encoded proteins that may be associated with thioamide and piperdine formation in the *tpn* cluster, as well as to circumvent difficulties encountered with the genetic modification of *S. tateyamensis*, *tpnLMNR* were expressed in *S. laurentii*, a producer of thiostrepton A **2**. Heterologous expression of TpnL in *S. laurentii* resulted in the production of a new metabolite thiostrepton A_a **31**, a piperidine-containing analog of thiostrepton A **2**. TpnL appears to be involved in the reduction of the dehydropiperidine moiety of thiostrepton A **2** to a piperidine ring. The newly introduced stereocenter at the piperidine carbon (Pip-2) is consistent with the configuration reported for the series *a* thiopeptins and suggests a similar enzymatic origin. The piperidine modification of thiostrepton A_a **31** did not significantly alter either its aqueous solubility or antibacterial activities against the strains evaluated. In addition, possible thioamidated thiostrepton analogs were detected in *S. laurentii* strains that coexpressed TpnMN, but not in strains the expressed TpnM or TpnN separately, consistent with our predictions that this YcaO-TfuA pair is required for thioamidation. Isolation and structural characterization of these metabolites are needed to confirm the presence of the thioamide.

3.5 References

1. Trejo, W. H.; Dean, L. D.; Pluscec, J.; Meyers, E.; Brown, W. E., *Streptomyces laurentii*, a new species producing thiostrepton. *J. Antibiot.* **1977**, *30*, 639-643.

2. Kelly, W. L.; Pan, L.; Li, C., Thiostrepton biosynthesis: prototype for a new family of bacteriocins. *J. Am. Chem. Soc.* **2009**, *131*, 4327-4334.

3. Suzuki, T.; Yamane, T.; Shimizu, S., Mass production of thiostrepton by fed-batch culture of *Streptomyces laurentii* with pH-stat modal feeding of multi-substrate. *Appl. Microbiol. Biotechnol.* **1987**, *25*, 526-531.

4. Li, C.; Zhang, F.; Kelly, W. L., Heterologous production of thiostrepton A and biosynthetic engineering of thiostrepton analogs. *Mol. BioSyst.* **2011**, *7*, 82-90.

5. Zhang, F.; Kelly, W. L., Saturation mutagenesis of TsrA Ala4 unveils a highly mutable residue of thiostrepton A. *ACS Chem. Biol.* **2015**, *10*, 998-1009.

6. Li, C.; Zhang, F.; Kelly, W. L., Mutagenesis of the thiostrepton precursor peptide at Thr7 impacts both biosynthesis and function. *Chem. Commun.* **2012**, *48*, 558-560.

7. Gust, B.; Challis, G. L.; Fowler, K.; Kieser, T.; Chater, K. F., PCR-targeted *Streptomyces* gene replacement identifies a protein domain needed for biosynthesis of the sesquiterpene soil odor geosmin. *Proc. Natl. Acad. Sci. U.S.A.* **2003**, *100*, 1541-1546.

8. Ryan, P. C.; Lu, M.; Draper, D. E., Recognition of the highly conserved GTPase center of 23 S ribosomal RNA by ribosomal protein L11 and the antibiotic thiostrepton. *J. Mol. Biol.* **1991**, *221*, 1257-1268.

9. Bibb, M. J.; Janssen, G. R.; Ward, J. M., Cloning and analysis of the promoter region of the erythromycin resistance gene *erm*E of *Streptomyces erythraeus*. *Gene* **1985**, *38*, 215-226.

10. Palaniappan, N.; Alhamadsheh, M. M.; Reynolds, K. A., *cis*-$\Delta^{2,3}$-double bond of phoslactomycins is generated by a post-PKS tailoring enzyme. *J. Am. Chem. Soc.* **2008**, *130*, 12236-12237.

11. Rubiralta, M. G., E.; Diez, A., In *Studies in organic chemistry. Piperidine structure, preparation, reactivity, and synthetic applications of piperidine and its derivatives.*, 1991; Vol. 43, pp 34-87.

12. Hensens, O. D.; Albers-Schonberg, G., Total structure of the highly modified peptide antibiotic components of thiopeptin. *J. Antibiot.* **1983**, *36*, 814-831.

13. Hensens, O. D.; Albers-Schonberg, G.; Anderson, B. F., The solution conformation of the peptide antibiotic thiostrepton: a ^{1}H NMR study. *J. Antibiot.* **1983**, *36*, 799-813.

14. Just-Baringo, X.; Albericio, F.; Alvarez, M., Thiopeptide engineering: a multidisciplinary effort towards future drugs. *Angew. Chem. Int. Ed. Engl.* **2014**, *53*, 6602-6616.

15. LaMarche, M. J.; Leeds, J. A.; Amaral, A.; Brewer, J. T.; Bushell, S. M.; Deng, G.; Dewhurst, J. M.; Ding, J.; Dzink-Fox, J.; Gamber, G.; Jain, A.; Lee, K.; Lee, L.; Lister, T.; McKenney, D.; Mullin, S.; Osborne, C.; Palestrant, D.; Patane, M. A.; Rann, E. M.; Sachdeva, M.; Shao, J.; Tiamfook, S.; Trzasko, A.; Whitehead, L.; Yifru, A.; Yu, D.; Yan, W.; Zhu, Q., Discovery of LFF571: an investigational agent for *Clostridium difficile* infection. *J. Med. Chem.* **2012**, *55*, 2376-2387.

16. Harms, J. M.; Wilson, D. N.; Schluenzen, F.; Connell, S. R.; Stachelhaus, T.; Zaborowska, Z.; Spahn, C. M. T.; Fucini, P., Translational regulation via L11: molecular switches on the ribosome turned on and off by thiostrepton and micrococcin. *Mol. Cell* **2008**, *30*, 26-38.

17. Jonker, H. R.; Baumann, S.; Wolf, A.; Schoof, S.; Hiller, F.; Schulte, K. W.; Kirschner, K. N.; Schwalbe, H.; Arndt, H. D., NMR structures of thiostrepton derivatives for characterization of the ribosomal binding site. *Angew. Chem. Int. Ed. Engl.* **2011**, *50*, 3308-3312.

18. Lipinski, C. A.; Lombardo, F.; Dominy, B. W.; Feeney, P. J., Experimental and computational approaches to estimate solubility and permeability in drug discovery and development settings. *Adv. Drug. Deliv. Rev.* **2001**, *46*, 3-26.

19. Lambert, P. A., Cellular impermeability and uptake of biocides and antibiotics in Gram-positive bacteria and mycobacteria. *Symp. Ser. Soc. Appl. Microbiol.* **2002**, 46S-54S.

CHAPTER 4: CHARACTERIZATION OF TPNL, A $F_{420}H_2$-DEPENDENT DEHYDROPIPERIDINE REDUCTASE

Adapted from: Ichikawa, H.; Bashiri, G.; Kelly, W.L. Biosynthesis of the thiopeptins and the identification of an $F_{420}H_2$-dependent dehydropiperidine reductase. *J. Am. Chem. Soc.* **2018**, *140*, 10749-10756. The production and purification of cofactor F_{420} and F_{420}-dependent glucose-6-phosphate dehydrogenase was performed by Bashiri, G. Other work in this chapter was performed by Ichikawa, H.

4.1 Introduction

TpnL is an encoded product of the thiopeptin biosynthetic gene (*tpn*) cluster that shows homology to proteins of the flavin/deazaflavin-dependent oxidoreductase subgroup B (FDOR-B). The FDOR-B family is a diverse group of small proteins that bind flavin mononucleotide (FMN), flavin adenine dinucleotide (FAD), deazaflavin cofactor F_{420}, or heme.[1] The members of this family share low sequence similarity with each other (~30%) but all are predicted to adopt a split β-barrel fold.[1-5] These proteins are found in a wide range of bacterial phyla and include the ubiquitous pyridoxal 5'-phosphate oxidase (PPNOx) involved in vitamin B_6 metabolism.[1, 6] Notably, some FDOR-Bs found in actinobacteria are thought to bind the unusual cofactor F_{420} (Figure 4.1) and participate in a wide range of redox reactions.[1, 7-10]

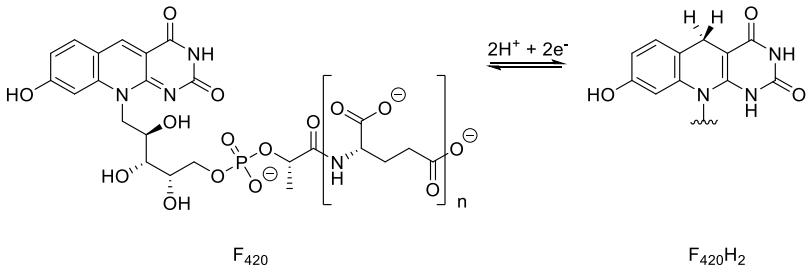

Figure 4.1. The structures of cofactor F_{420} and $F_{420}H_2$.

Only a handful of FDOR-Bs have been biochemically and structurally characterized, and many of those that have been characterized thus far are closely involved in mycobacterial heme catabolism and virulence. MSMEG_6519 from *Mycobacterium smegmatis* (*M. smegmatis*) and HugZ from *Heliobacter pylori* bind and oxidize heme to biliverdin, a linear tetrapyrrole (Figure 4.2).[1, 3, 11] Both proteins adopt a split β-barrel fold and a strictly conserved histidine residue coordinates the propionate side chain of the heme molecule.[1, 3] In addition to the split β-barrel fold-containing domain, a secondary domain is found in heme-binding members of the FDOR-B family.[1, 3] The role of this secondary domain is unclear as the heme-oxidizing activity of HugZ appears to be contained on the split β-barrel fold-containing domain.[1, 3] A truncated HugZ mutant lacking the secondary domain was catalytically active, and this mutant showed higher turnover rate than the wild-type HugZ.[3]

In addition to the heme-oxidizing enzymes, other FDOR-B proteins have been implicated in other aspects of heme catabolism and mycobacterial virulence. MSMEG_3880 from *M. smegmatis*, Rv2074 and Rv1155 from *M. tuberculosis* reduce biliverdin-IX_α to bilirubin-IX_α using cofactor $F_{420}H_2$ as a hydride source (Figure 4.2).[1, 12] These three proteins adopt a split β-barrel fold, forming a cofactor F_{420} binding cleft at the

dimer interface.[4-5, 13] While there are no strictly conserved motifs or residues, a highly conserved lysine residue coordinates the phosphate moiety of FMN, FAD, and F_{420} among certain FDOR-Bs.[1] The F_{420} binding site contains additional basic residues that interact with the polyglutamate tail of the cofactor.[5] These positively charged residues are unique to F_{420}-binding FDOR-Bs and not found in FDOR-B proteins that bind FMN, FAD, or heme.[1]

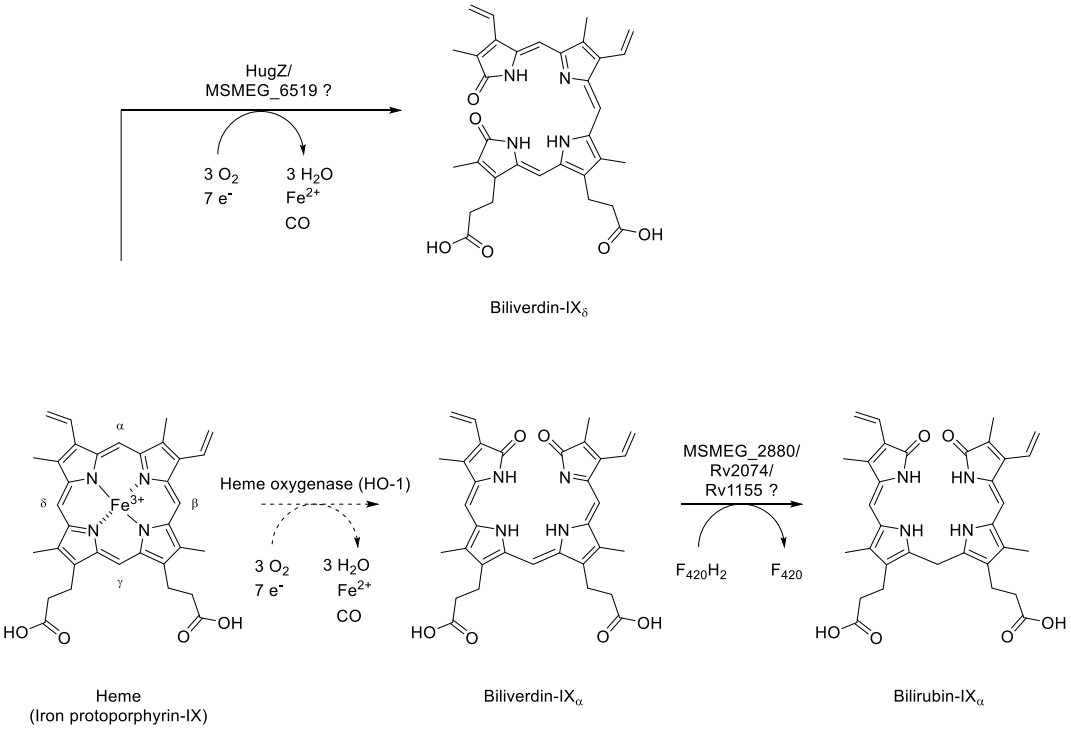

Figure 4.2: The degradation of heme in mycobacteria and in *Helicobacter pylori* are mediated by proteins of the FDOR-B family. In most organisms, the first step of heme catabolism involves heme oxygenase (HO-1), a protein unrelated to FDOR-Bs.

Homologs of these $F_{420}H_2$-dependent biliverdin reductases are widely distributed among actinobacteria and demonstrate high sequence similarity to each other, suggesting an important physiological role.[12] Biliverdin reductases are notably overexpressed in *M. tuberculosis* and the product bilirubin is a powerful antioxidant.[14] 10 nM of bilirubin-IX_α reversed cell death induced by a 10,000-fold excess concentration of H_2O_2 in HeLa cells and brain cultures.[15-16] It has been shown that disruption of bilirubin production leads to greater levels of reactive oxygen species in *M. tuberculosis* in non-pathogenic environments and higher rates of bacterial cell death.[14] Therefore, the $F_{420}H_2$-dependent reduction of biliverdin-IX_α to bilirubin-IX_α may play a critical role not only in the virulence of pathogenic mycobacteria but for the general survival of mycobacteria by reducing oxidative stress on the bacterium.

The involvement of FDOR-B proteins in mycobacterial heme degradation pathways and the use of an unusual cofactor F_{420} by biliverdin reductases in *M. tuberculosis* virulence has added interest in F_{420}-dependent pathways and the proteins that bind F_{420} towards treatment of pathogenic mycobacteria. Little is known, however, about FDOR-B proteins in other actinomycetes, especially the proteins involved in secondary metabolism. One of the few characterized examples of an F_{420}-dependent FDOR-B protein is OxyR, a reductase from *Streptomyces rimosus* that is involved in the biosynthesis of tetracycline (Figure 4.3).[9] Characterization of proteins in the FDOR-B family, such as TpnL in the thiopeptin biosynthetic gene (*tpn*) cluster, will expand our understanding of this diverse protein family.

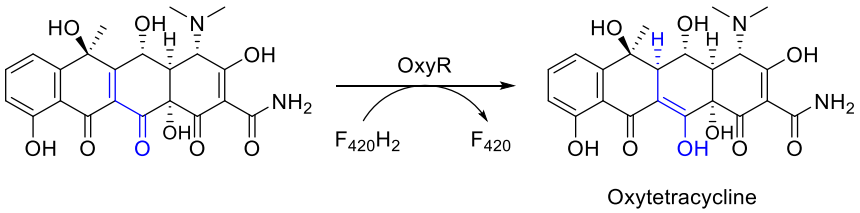

Figure 4.3: The terminal step of oxytetracycline biosynthesis catalyzed by OxyR.

Heterologous expression of TpnL in the dehydropiperidine-containing series *b* thiopeptide thiostrepton A **2** producer, *S. laurentii*, resulted in the production of thiostrepton A_a **31**, a piperidine-containing series *a* analog of **2**. Therefore, TpnL is likely to mediate the reduction of the dehydropiperidine ring of thiostrepton A **2**, and, presumably, the dehydropiperidine-containing intermediate of the thiopeptin biosynthetic pathway. To establish the role of this protein, TpnL was subjected to a series of bioinformatic and biochemical analyses to determine the cofactor necessary for activity, to reconstitute TpnL activity, and to demonstrate formation of **31** *in vitro*.

4.2 Materials and methods

4.2.1 General

All reagents, unless otherwise specified, were purchased from standard commercial sources and used as provided. All primers used are listed in Table A.1 and strains and plasmids used are listed in Table A.2. *Streptomyces laurentii* ATCC 31255 (*S. laurentii*) and *Streptomyces tateyamensis* ATCC 21389 (*S. tateyamensis*) were purchased from American Type Culture Collection. *Escherichia coli* (*E. coli*) strains were cultured in Luria-Bertani medium supplemented with 100 µg/mL ampicillin, 50 µg/mL apramycin,

12.5 μg/mL chloramphenicol, 50 μg/mL kanamycin, or 50 μg/mL streptomycin. *S. laurentii* containing pSET1520-derived vectors were cultured in media supplemented with 50 μg/mL apramycin. High-performance liquid chromatography (HPLC) analyses were performed on a Beckman Coulter System Gold HPLC using an analytical Phenomenex Luna 5μm C18(2) 250 x 4.6 mm column (Torrance, CA). All mass spectrometry analyses were performed at the Georgia Institute of Technology Bioanalytical Mass Spectrometry Facility. High-performance liquid chromatography-mass spectrometry (HPLC-MS) analyses were performed on a Micromass Quattro LC using a Phenomenex Synergi 4 μm MAX-RP 80 Å C18 250 x 2.00 mm column (Torrance, CA). Oligonucleotides were purchased from Integrated DNA Technologies, Inc. (Coralville, IA). DNA sequencing analyses were performed by Eurofins MWG Operon USA (Louisville, KY). Cofactor F_{420} and F_{420}-dependent glucose-6-phosphate dehydrogenase (FGD) were purified as previously described by Ghader Bashiri.[17-18]

4.2.2 Bioinformatics analyses of TpnL, its homologs and other proteins of the FDOR-B family, and cofactor F_{420} biosynthetic enzymes FbiABC

The proteins were compared to other entries in the NCBI database using the protein Basic Local Alignment Search Tool (BLAST). Multiple sequence alignments and phylogenetic analyses were performed using Clustal Omega multiple sequence alignment and the EMBOSS-Needle tool on the European Bioinformatics Institute (EMBL-EBI) server was used for pairwise sequence alignments. The phylogenetic tree of TpnL and homologs was constructed with ClustalW2 - Phylogeny (Simple Phylogeny) tool on the EMBL-EBI server using a neighbor-joining algorithm to construct trees from the distance

matrix and visualized using the Interactive Tree of Life (iTOL) v4.2.3. Accession numbers of the protein sequences used to construct the phylogenetic tree of TpnL homologs are listed in Table A.3.

4.2.3 Expression and purification of TpnL

The gene encoding TpnL was amplified by PCR from fosmid HI2G2 using the primer pair HI-23F/HI-23R. The amplicon was digested with *Hin*dIII and *Nde*I, ligated into pET28b(+) to form pET28b-tpnL, and confirmed by DNA sequence analysis. *E. coli* BL21(DE3) containing pET28b-tpnL was incubated overnight at 37 °C and 220 rpm in 10 mL of Luria-Bertani medium supplemented with 50 µg/mL kanamycin. 10 mL of the overnight culture was used to inoculate 1 L of Luria-Bertani medium supplemented with 50 µg/mL kanamycin. The culture was incubated at 37 °C and 220 rpm until $OD_{600} = 0.6$, at which point the temperature was decreased to 15 °C, and TpnL expression was induced with the addition of 0.4 mM IPTG. Cultures were incubated for an additional 48 hours. Harvested cells were resuspended in 50 mL of lysis buffer (20 mM Tris pH 8.0, 500 mM NaCl, 2 mM imidazole, 10% glycerol, 1 mg/mL lysozyme, 10 µg/mL deoxyribonuclease, 2 mM $MgCl_2$). Cells were disrupted by sonication (10 rounds of 10 s pulses followed by a 60 s pause) and the lysate clarified by centrifugation at 14,000 x *g* for 30 min at 4 °C. The cell-free extract was incubated with 1 mL of Ni-NTA (Qiagen, Germantown, MD) slurry for 20 min. The slurry was poured into a column, and the resin was washed with 10 mL wash buffer (20 mM Tris pH 8.0, 500 mM NaCl, 20 mM imidazole, 10% glycerol, 2 mM $MgCl_2$). Protein was eluted with 15 mL elution buffer (20 mM Tris pH 8.0, 500 mM NaCl, 150 mM imidazole, 10% glycerol, 2 mM $MgCl_2$) collecting 5 mL fractions. Fractions

containing the protein were pooled together and dialyzed against 2 x 2 L storage buffer (50 mM Tris pH 8.0, 300 mM NaCl, 10% glycerol, 2 mM $MgCl_2$, 2 mM dithiothreitol). TpnL was concentrated with a 10,000 Da molecular weight cut-off Amicon Ultra centrifugal filter. Protein concentration was determined by the method of Bradford using bovine serum albumin as a standard.[19] Purified TpnL was flash frozen in liquid nitrogen and stored at -80 °C.

4.2.4 Cofactor binding assays

A 100 µL reaction mixture containing 2 µM TpnL, 100 mM NaCl, 50 mM Tris pH 7.0 and 0-2 mM cofactor FAD, FMN, or F_{420} was incubated in the dark at 25 °C for 15 min. The samples were excited at 285 nm and the emission wavelength at 340 nm was monitored in a 75 µL quartz cuvette by a Shimadzu RF-530/PC spectrofluorophotometer. The fluorescence of each sample was collected as an average of 3 scans at high sensitivity, and each ligand concentration was repeated in triplicate. The fraction of protein bound to the cofactor was derived by $1 - F/F_0$, where F is the fluorescence of $tryptophan_{TpnL}$ in the presence of a particular concentration of cofactor and F_0 is the fluorescence of $tryptophan_{TpnL}$ in the absence of cofactor. To calculate the K_D of the ligands, the data was fit into a hyperbolic function using Kaleidagraph 4.0.

4.2.5 *In vitro* reconstitution of FGD activity

A 100 µL reaction mixture containing 50 mM Tris pH 7.0, 300 mM NaCl, 1 mM β-mercaptoethanol, 1 mM EDTA, 100 nM FGD, 20 µM F_{420}, and 1 mM glucose-

6-phosphate (G6P) were incubated at room temperature. FGD was omitted in the negative control. The absorbance spectra were taken every 30 seconds over the course of 5 min.

4.2.6 *In vitro* reconstitution of TpnL activity

A 200 µL reaction mixture containing 10 µL DMSO, 10 µL of 500 µM thiostrepton A **2** in DMSO (25 µM final concentration), 10 µL of 1 M Tris pH 7.5 (50 mM final concentration), 144.5 µL of deionized water, 4 µL of 500 µM F_{420} (10 µM final concentration), 5 µL of 100 mM G6P (2.5 mM final concentration), and 14.5 µL of 6.2 µM FGD (0.45 µM final concentration), and 2 µL 100 µM TpnL (1 µM final concentration) was prepared. Reagents were added in the order described. Before the addition of TpnL, however, the 198 µL mixture was pre-incubated at 25 °C for 5 min. Reactions were initiated with either TpnL or 2 µL of 50 mM Tris pH 7.5 and incubated at 25 °C for 0-6 hours. Reactions were quenched with trifluoroacetic acid (1% final concentration), flash frozen with liquid nitrogen, and stored at –80 °C until ready for analysis. 100 µL of each sample was analyzed by HPLC using an isocratic condition of 42.5% acetonitrile in water over 30 min at 2 mL/min. Absorbance was monitored at 254 nm. For kinetic assays, the concentration of TpnL was decreased to 25 nM, the concentration of thiostrepton A **2** used was between 0.5-10 µM, the volume of DMSO added was adjusted to maintain 10% final concentration, and the reactions were quenched after 5 min. In one set of the activity assays, the concentration of F_{420} was increased to 20 µM and 2 µM FGD. Samples were analyzed by HPLC as described above. To quantify thiostrepton A **2** and thiostrepton A_a **31** present in a reaction mixture by HPLC, the areas under the peaks were compared to a calibration

curve prepared for thiostrepton A **2**, assuming **2** and **31** have comparable molar absorptivities at 254 nm.

4.2.7 PCR amplification of a putative F_0 synthase from *S. tateyamensis*

A gene fragment encoding a putative F_0 synthase was amplified from *S. tateyamensis* using the primer pair HI-24F/HI-24R. The 2.5 kb amplicon was ligated into pSC-B-amp/kan and the DNA sequence of the product was determined.

4.3 Results and discussion

4.3.1 TpnL cofactor determination

TpnL shows sequence homology to enzymes of the flavin/deazaflavin oxidoreductase subgroup B (FDOR-B). An amino acid alignment of TpnL with other characterized members of this protein family indicated that TpnL has a conserved lysine residue (K55) that is present in most F_{420}-dependent FDOR-Bs (Figure 4.4).[1] In addition, K55 is adjacent to several basic residues, a characteristic of the cofactor binding region in F_{420}-dependent FDOR-Bs, that are not observed in FDOR-Bs that bind FMN and FAD.[13, 20]

Figure 4.4: Alignment of the amino acid sequences of TpnL and proteins of the flavin/deazaflavin oxidoreductase subgroup B (FDOR-B) that bind cofactor F_{420}. Rv1155 (WP_003898745.1),[13] Rv2074 (WP_003899157.1),[12] and Rv2991 (NP_217507.1)[13] are proteins from *Mycobacterium tuberculosis* H37Rv. MSMEG_3800 (YP_888093.1)[21] is a protein from *Mycobacterium smegmatis* MC^2 155. The highly conserved lysine residue present in most F_{420}-dependent proteins of the FDOR-B subgroup is highlighted in green. The motif around the conserved lysine residue contains positively charged residues that facilitate the binding of the F_{420} polyglutamate tail and is highlighted in yellow in the Rv1155 sequence.[13]

To determine if TpnL preferentially binds cofactor F_{420} over other flavins, a fluorescence binding experiment was performed. TpnL was heterologously expressed in *E. coli* with an N-terminal His_6-tag. The purified protein (Figure 4.5) was colorless, suggesting it does not copurify with the flavins present in *E. coli*, a microorganism that does not produce F_{420}. Tryptophan fluorescence quenching in the presence of F_{420} or the flavins was used to indicate cofactor binding to TpnL (Figure 4.6).[8] The K_D of F_{420} for TpnL (8.5 ± 1.4 μM) is ten times lower than those for FAD and FMN (88.3 ± 24.4 μM and

105.9 ± 13.2 μM, respectively). In addition, other common cofactors were analyzed for their binding affinities to TpnL. ATP, NADH, and NADPH did not appear to show binding affinity towards TpnL, and K_D values for these cofactors were not calculated. Although the reduced form, $F_{420}H_2$, is most likely the native cofactor for TpnL, this protein does preferentially bind F_{420} over FAD or FMN.

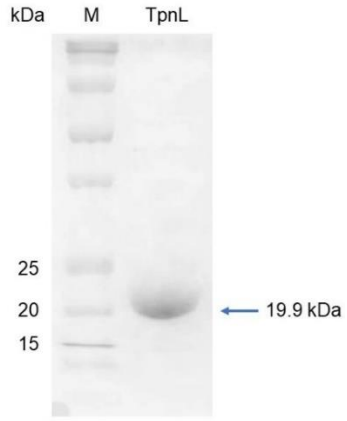

Figure 4.5: SDS-PAGE analysis of purified TpnL.

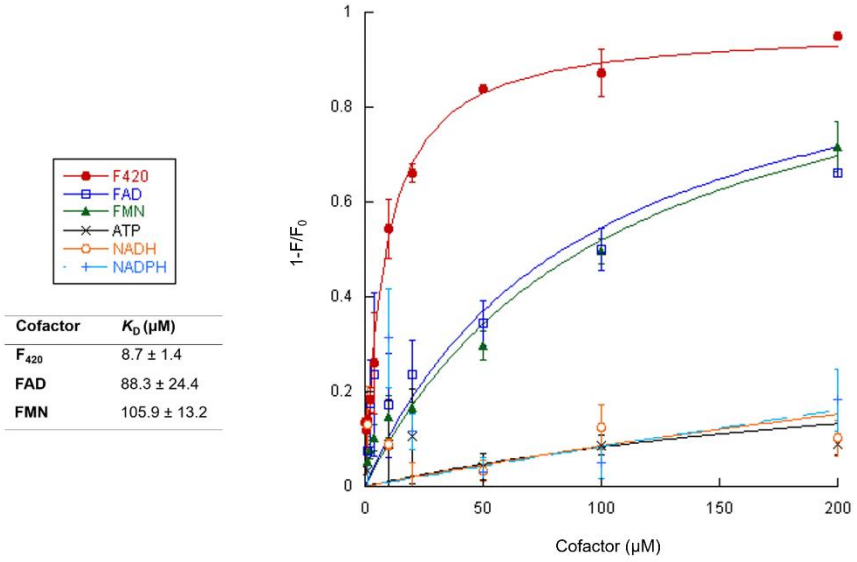

Cofactor	K_D (μM)
F_{420}	8.7 ± 1.4
FAD	88.3 ± 24.4
FMN	105.9 ± 13.2

Figure 4.6: Binding of cofactors to TpnL as measured by tryptophan fluorescence. Cofactor binding was quantified by monitoring the quenching of tryptophan fluorescence. F_{420} binding is indicated by red closed circles (●), FAD by blue open squares (□), FMN by green closed triangles (▲), ATP by black x's (X), NADH by orange open circles (○), and NADPH by blue plus signs (+). The excitation wavelength was 280 nm and the emission wavelength was 340 nm.

4.3.2 Reconstitution of TpnL activity

To determine the appropriate substrate for TpnL, we considered the TpnL-mediated formation of a piperidine-containing thiostrepton A_a **31** in *S. laurentii* HI1 (Chapter 3). Piperidine formation in series *a* thiopeptides likely results from the reduction of the dehydropiperidine ring of series *b* thiopeptides. This dehydropiperidine reduction is expected to be among the latter maturation steps as the [4+2] condensation that assembles the dehydropiperidine-containing core macrocycle occurs after many of the post-translational modifications on the precursor peptide.[22-23] We therefore reasoned that **2**, a dehydropiperidine-containing series *b* thiopeptide, may be a substrate of TpnL and the hydride source for a reduction may be supplied by cofactor F_{420} (Scheme 4.1). TpnL shows

affinity towards F_{420} (Figure 4.6) but $F_{420}H_2$, the reduced form of the cofactor is most likely the required for TpnL activity. $F_{420}H_2$, however, readily oxidizes in the presence of O_2.[24] To generate the reduced coenzyme $F_{420}H_2$ *in situ*, F_{420}-dependent glucose-6-phosphate dehydrogenase (FGD) and glucose-6-phosphate (G6P) were included in the assay mixture with TpnL and **2** (Scheme 4.1).[8] The presence of F_{420} can be determined by its diagnostic absorbance at 420 nm and the formation of $F_{420}H_2$ can be observed by an increase in absorbance at 320 nm.[24-25] Initial studies reconstituting FGD activity show a decrease in absorbance at 420 nm and an increase in absorbance at 320 nm, which corresponds to a reduction of F_{420} (Figure 4.7).

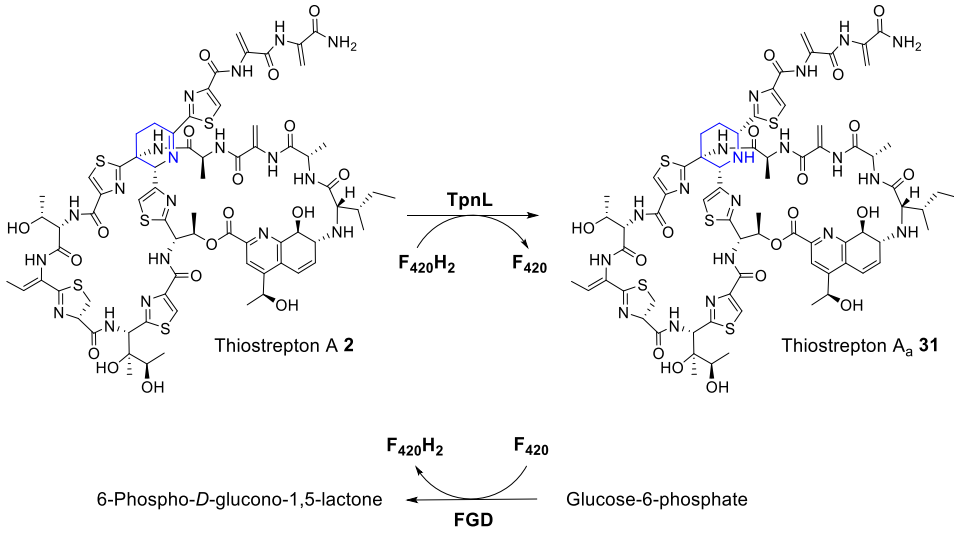

Scheme 4.1: Dehydropiperidine reduction catalyzed by TpnL and the coupled reaction that regenerates cofactor $F_{420}H_2$.

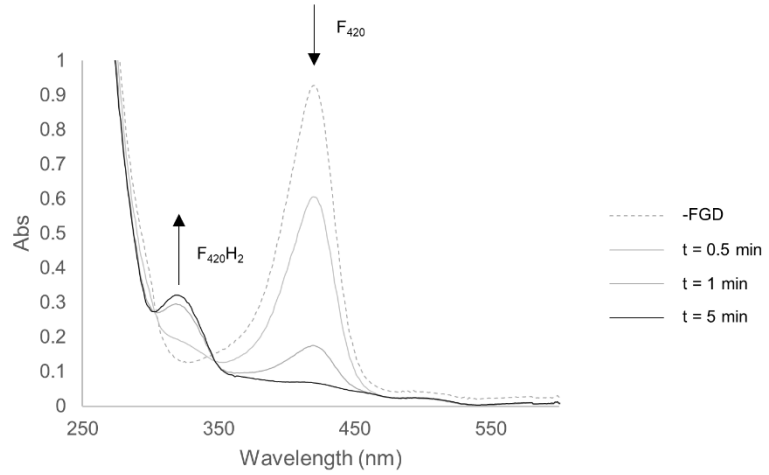

Figure 4.7: UV-visible absorbance spectra of the FGD-catalyzed reduction of 20 μM F_{420} to $F_{420}H_2$ by 100 nM FGD over the course of 5 min after the addition of FGD to the reaction mixture. The negative control reaction (-FGD) omitted FGD and the absorbance was measured after 5 min incubation. The absorbance at 420 nm (indicated by a down arrow) is diagnostic for the presence of F_{420}. The absorbance at 320 nm (indicated by an up arrow) is characteristic for the presence of $F_{420}H_2$.

To confirm that TpnL reduces the thiostrepton dehydropiperidine, we reconstituted its activity *in vitro*. In the absence of either F_{420} or FGD, conversion of thiostrepton A **2** to thiostrepton A_a **31** was not observed (Figure 4.8, *a*-*b*). Similarly, in a reaction with both F_{420} and FGD, but lacking TpnL, **31** was not observed (Figure 4.9, *e*). The conversion of **2** to **31** was observed only when **2** was incubated with TpnL, F_{420}, and FGD (Figure 4.9, *f*, t_R ~ 23.4 min, and Figure B.28). An HPLC co-injection of the reconstituted reaction after 1-hour (Figure 4.9, *f-iii*) and **31** shows that **31** and the product formed in the TpnL activity assay co-elute (Figure 4.9, *h*) but a co-injection of the reconstituted 1-hour reaction with **2** shows that the two do not coelute (Figure 4.9, *g*). The results from this assay demonstrate that TpnL catalyzes the reduction of the dehydropiperidine ring of **2** to the piperidine ring in **31**. Both F_{420} and FGD are required for TpnL activity, indicating the need for $F_{420}H_2$ as

a hydride source for the reduction. While TpnL does utilize $F_{420}H_2$ as a cofactor to reduce thiostrepton A, we wondered if another common biological hydride donor such as NADH and NADPH could substitute for $F_{420}H_2$ in *S. laurentii*. TpnL activity was not observed in the presence of 600 μM NADH and 600 μM NADPH (Figure 4.10) consistent with the low binding affinity observed between the nicotinamide cofactors and TpnL (Figure 4.6). Further biochemical and structural studies will be required to determine if TpnL can utilize other cofactors such as $FMNH_2$/$FADH_2$, and if TpnL can accept other dehydropiperidine-containing compounds as substrates.

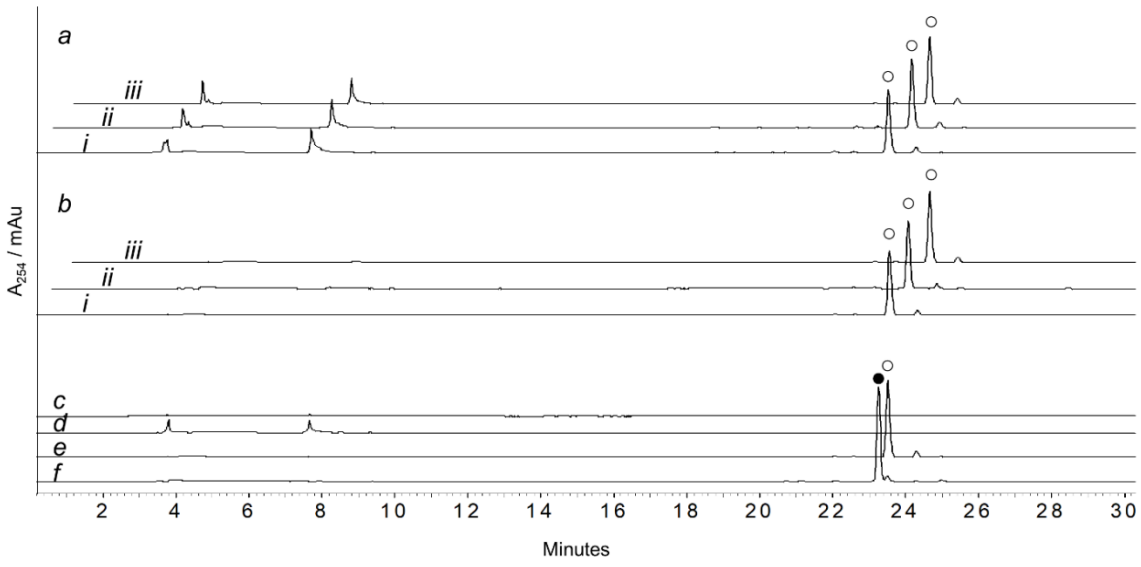

Figure 4.8: HPLC analyses of TpnL activity in (a) the absence of FGD and (*b*) the absence of F_{420}. Reactions incubated for (*i*) 0 min, (*ii*) 10 min, and (*iii*) 60 min. The standards of the reaction mixture are shown in (*c*) G6P, (*d*) F_{420}, (*e*) thiostrepton A **2**, and (*f*) thiostrepton A_a **31**. Absorbance was monitored at 254 nm. **2** is represented by (○) and (●) represents **31**.

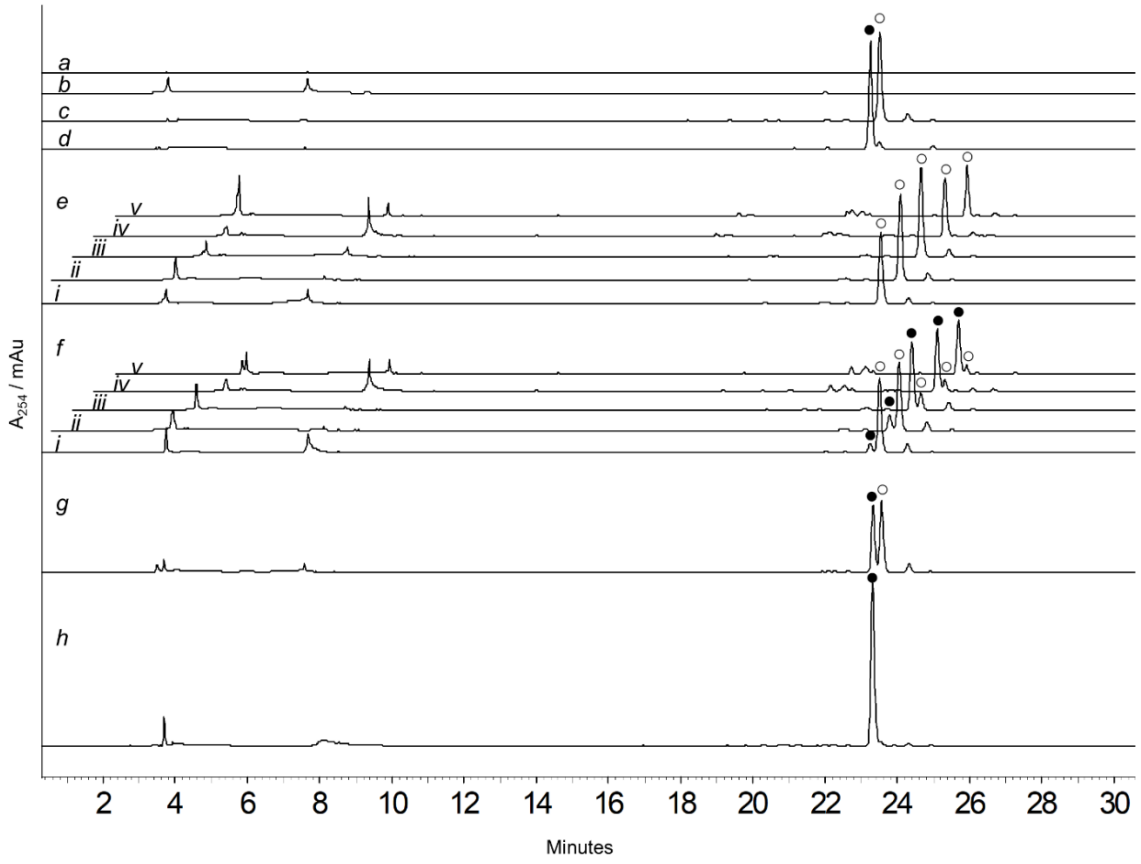

Figure 4.9: HPLC analyses of TpnL activity. The standards of the reaction components are shown in (*a*) G6P, (*b*) F_{420}, (*c*) thiostrepton A **2**, and (*d*) thiostrepton A_a **31**. Reactions (*e*) omitting TpnL and (*f*) containing TpnL incubated for (*i*) 0 min, (*ii*) 10 min, (*iii*) 60 min, (*iv*) 6 hours, and (*v*) 24 hours. (*g*) A co-injection of **2** and a 1-hour reaction with TpnL, and (*h*) a co-injection of **31** and a 1-hour reaction with TpnL. Absorbance was monitored at 254 nm. **2** is represented by (○) and (●) represents **31**.

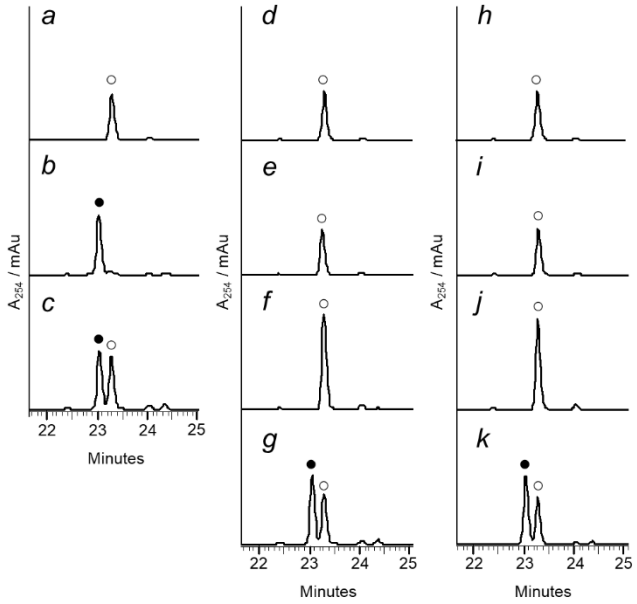

Figure 4.10: HPLC analyses of TpnL activity in the presence of nicotinamide cofactors. (*a*) Thiostrepton A **2**. (*b*) Thiostrepton A_a **31**. (*c*) A co-injection of **2** and **31**. (*d*) Reaction without TpnL or cofactor. (*e*) Reaction with 600 μM NADH. (*f*) A co-injection of the reaction with 600 μM NADH and **2**. (*g*) A co-injection of the reaction with 600 μM NADH and **31**. (*h*) Reaction without TpnL or cofactor. (*i*) Reaction with 600 μM NADPH. (*j*) A co-injection of the reaction with 600 μM NADPH and **2**. (*k*) A co-injection of the reaction with 600 μM NADPH and **31**. The reaction was incubated for 60 min. The absorbance at 254 nm was monitored. **2** is represented by (○) and **31** is represented by (●).

4.3.3 Kinetic assays of TpnL

To quantify **2** and **31** in the reaction, a calibration curve was prepared to compare the area under the HPLC peaks to the mass of **2** applied to the column (Figure 4.11). The calibration curve was applied to **31**, as well, assuming that the two compounds would share similar absorbances at 254 nm.[26-27]

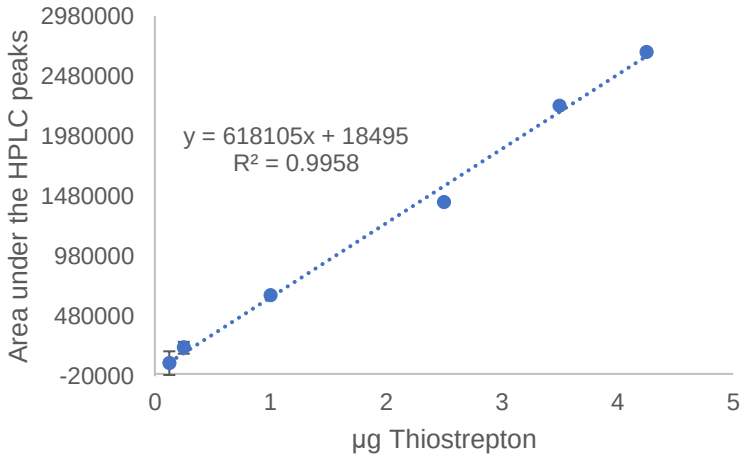

Figure 4.11: HPLC calibration curve for quantification of thiostrepton A **2** and A_a **31**.

To determine the kinetic parameters of TpnL, substrate concentration was varied between 0 and 20 µM thiostrepton A **2**, below the upper limit of solubility of **2** (21.88 ± 0.05 µM) under reaction conditions (50 mM Tris pH 7.5 and 10% DMSO). TpnL activity appears to be subject to substrate inhibition at concentrations greater than 2 µM **2** (Figure 4.12). To examine if the *in situ* generation of $F_{420}H_2$ could be limiting TpnL activity, F_{420} reduction by FGD was monitored during the time course of the TpnL assay, and was found to be unaffected by TpnL and **2** (Figure 4.13). An additional assessment of TpnL activity

using increased concentrations of F_{420} and FGD (from 10 µM F_{420} and 0.45 µM FGD to 20 µM F_{420} and 2 µM FGD) did not demonstrate a significant alteration of TpnL activity (Figure 4.12). The assay conditions examined here prevented a determination of K_M, but an apparent k_{cat}/K_M (2.80 x 10^4 $M^{-1}s^{-1}$) was derived from the linear region of substrate dependence on rate.

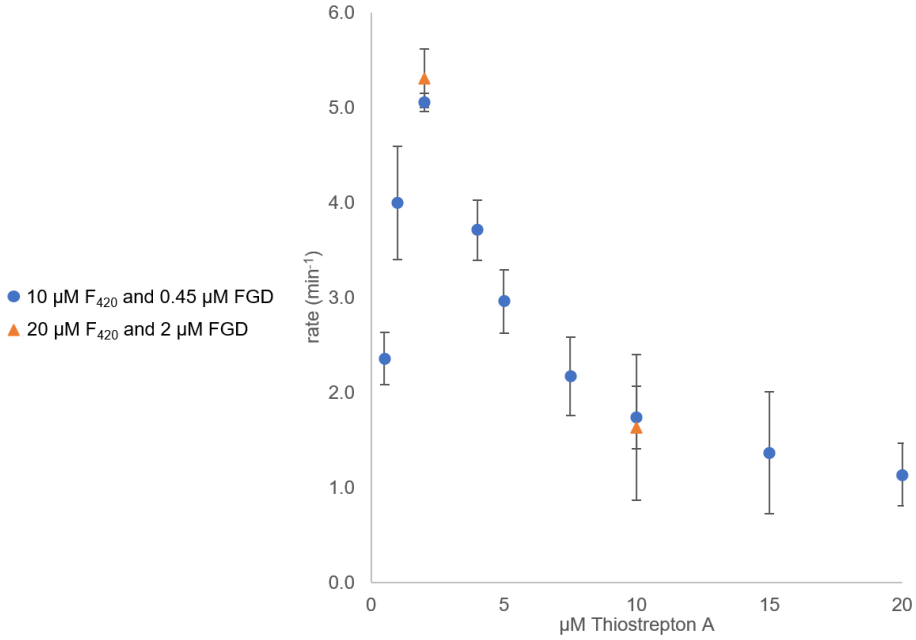

Figure 4.12: Dehydropiperidine reductase activity of TpnL with varying amounts of F_{420} and FGD. TpnL activity in the presence of 10 µM F_{420} and 0.45 µM FGD is shown by blue circles (●). Also included are two activity assays of TpnL in the presence of 20 µM F_{420} and 2 µM FGD, shown by orange triangles (▲) at two substrate concentrations, 2 and 10 µM thiostrepton A. The rate of moles thiostrepton A_a **31** produced per mole TpnL per min was plotted against thiostrepton A **2** concentration.

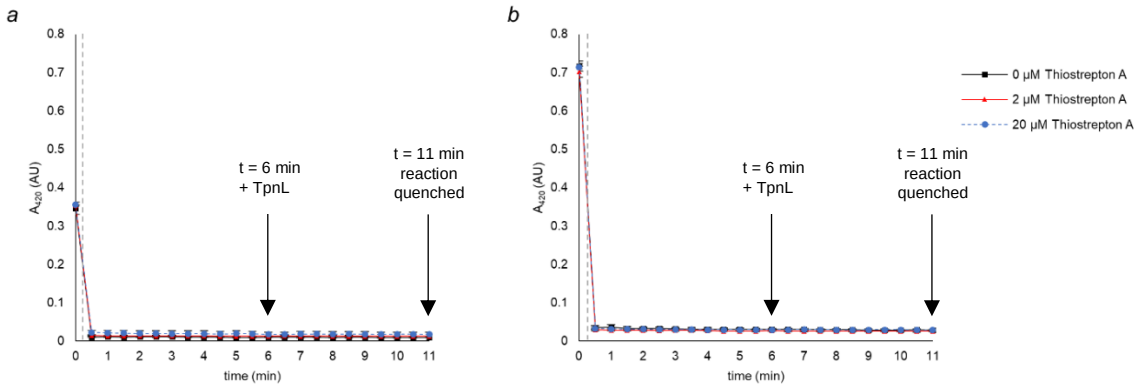

Figure 4.13: The reduction of F_{420} by F_{420}-dependent glucose-6-phosphate dehydrogenase (FGD) during the TpnL kinetic assay. (*a*) The reaction mixture containing 10 µM F_{420} and 0.45 µM FGD, the concentrations used for the kinetic analysis of TpnL. During the course of the TpnL reaction, at least 89% of the cofactor was in the reduced form, $F_{420}H_2$. (*b*) The reaction mixture containing 20 µM F_{420} and 2 µM FGD. During the course of the TpnL reaction, at least 90% of the cofactor was in the reduced form, $F_{420}H_2$. The reduction of F_{420} to $F_{420}H_2$ was monitored by the loss of absorbance at 420 nm.[28] Each condition was repeated in triplicate. The absorbance at 420 nm prior to the addition of FGD is shown at t = 0 min, FGD is added at t = 0.2 min (indicated by the vertical grey dashed line), TpnL is added at t = 6 min, and the TpnL kinetic assay is quenched at 11 min. The reduction of F_{420} in the absence of thiostrepton A **2** is shown with black squares (■), F_{420} reduction in the presence of 2 µM thiostrepton A **2** is shown with red triangles (▲), and F_{420} reduction in the presence of 20 µM thiostrepton A **2** is shown with blue circles (●).

The non-Michaelis-Menten behavior of TpnL activity may be a result of substrate inhibition or caused by non-ideal assay conditions. Temperature and pH may need optimization for future kinetic studies as it can affect the interactions of TpnL with its substrates, **2** and $F_{420}H_2$. The aqueous solubility of thiostrepton A is approximately 20 µM in 10% DMSO and 8 µM in 5% DMSO.[29] While the physiological concentration range of thiostrepton A **2** in *S. laurentii* or the corresponding substrate in *S. tateyamensis* is not known, its biological activities are in the sub-micromolar range.[26, 30] TpnL activity, however, appears to increase linearly with substrate concentration up to 2 µM, and, at concentrations above 2 µM, TpnL activity appears strongly and sharply inhibited by its

substrate. Under conditions tested, TpnL activity reaches its maximum (5.1 s^{-1}) at 2 μM thiostrepton A **2** and decreases nearly 5-fold (1.1 s^{-1}) by 20 μM thiostrepton A **2**. Further examination of TpnL activity is needed to fully explain its kinetic behavior.

4.3.4 F_{420} biosynthesis in *S. tateyamensis* and *S. laurentii*

TpnL is an F_{420}-dependent dehydropiperidine reductase involved in thiopeptin biosynthesis and it is expected that the deazaflavin cofactor is produced by the thiostrepton A_a **31** producer, *S. laurentii* HI1 and the thiopeptin (**13**-**16**) producer, *S. tateyamensis*. FbiABC are required for F_{420} biosynthesis and all three homologs were found in the *S. laurentii* genome (Figures 4.14-4.16). Two fragments of a protein that share homology to an F_0 synthase, FbiC was found in the draft genome assembly of *S. tateyamensis*. Primers were designed from the two FbiC-like fragments and a single 2.5 kb product was amplified from *S. tateyamensis* (Figure 4.17). This candidate FbiC from *S. tateyamensis* shows 63.1% identity and 75.8% similarity to the FbiC from *Mycobacterium bovis* and 76.2% identity and 84.2% similary to the candidate FbiC from *S. laurentii* (Figure 4.16). The aqueous cell extracts and the organic extracts of the cell cultures of *S. laurentii*, *S. laurentii* HI1, and *S. tateyamensis* were analyzed by LC-MS for positively and negatively charged ions of cofactor F_{420} with various glutamate tail lengths but F_{420} could not be identified (data not shown). Nonetheless, the presence of FbiABC in *S. laurentii* and FbiC in *S. tateyamensis* suggests that the two bacteria species produce cofactor F_{420}.

Figure 4.14: Alignment of FbiA (2-phospho-L-lactate transferase) amino acid sequences. M.bovis_FbiA: FbiA from *Mycobacterium bovis* BCG (Q7TWV4.1);[31] M.tuber_FbiA: a candidate FbiA from *Mycobacterium tuberculosis* H37Rv (WP_003417087.1);[31] and S.laur_FbiA: candidate FbiA from *S. laurentii* (BAU83677.1);[32] S.laur_FbiA shows 41.8% identity and 62.0% similarity to M.bovis_FbiA.

```
S.laur_FbiB       --MTPKGPTARFEVWALDGIPEVAPGDDLAKLIADASPGLADGDVLLVTSKIVSKAEGRV      58
M.tuber_FbiB      LTGPEHGSASTIEILPVIGLPEFRPGDDLSAAVAAAAPWLRDGDVVVVTSKVVSKCEGRL      60
M.bovis_FbiB      MTGPEHGSASTIEILPVIGLPEFRPGDDLSAAVAAAAPWLRDGDVVVVTSKVVSKCEGRL      60
                       :* :: :*:  : *:**. *****:  :* *:* * ****::****:***.***:

S.laur_FbiB       LAATDR--------EAAIDAETVRVVARRGPLRIVETRQGLVMAAAGVDASNTPSGTVLL      110
M.tuber_FbiB      VPAPEDPEQRDRLRRKLIEDEAVRVLARKDRTLITENRLGLVQAAAGVDGSNVGRSELAL      120
M.bovis_FbiB      VPAPEDPEQRDRLRRKLIEDEAVRVLARKDRTLITENRLGLVQAAAGVDGSNVGRSELAL      120
                  : * :         .  *: *:***:**:.   *.*.* *** ******.**.  . : *

S.laur_FbiB       LPEDPDASARRIRDGLRETLNVDVGVLVTDTFGRPWRNGLTDVAIGAAGVRVLDDLRGGT      170
M.tuber_FbiB      LPVDPDASAATLRAGLRERLGVTVAVVITDTMGRAWRNGQTDAAVGAAGLAVLRNYAGVR      180
M.bovis_FbiB      LPVDPDASAATLRAGLRERLGVTVAVVITDTMGRAWRNGQTDAAVGAAGLAVLRNYAGVR      180
                  ** ******  :* **** *.* *.*::***:** **** **.*:****: ** :  *

S.laur_FbiB       DAHGNGLNATITATADELAGAGDLVKGKIDGRPVAVVRGLSHLVKPEPEPESGDAPVAEA      230
M.tuber_FbiB      DPYGNELVVTEVAVADEIAAAADLVKGKLTATPVAVVRGFGVSD----------------      224
M.bovis_FbiB      DPYGNELVVTEVAVADEIAAAADLVKGKLTATPVAVVRGFGVSD----------------      224
                  * :** * .* .*.***:*.*.******: . *******:.

S.laur_FbiB       EGAAEAEGARALVRVAADDMFRLGTSEAVR----EAVTLRRTVRDFTDEPVDPGSVRRAV      286
M.tuber_FbiB      ----DGSTARQLLRPGANDLFWLGTAEALELGRQQAQLLRRSVRRFSTDPVPGDLVEAAV      280
M.bovis_FbiB      ----DGSTARQLLRPGANDLFWLGTAEALELGRQQAQLLRRSVRRFSTDPVPGDLVEAAV      280
                      :.. ** *:* .*:*:* ***:**:.    :*  ***:** *: :**  . *. **

S.laur_FbiB       AAAVTAPAPHHTTPWRFVLLESEASRTRLLDAMRDAWIADLRADGKTEESVAKRVKRGDV      346
M.tuber_FbiB      AEALTAPAPHHTRPTRFVWLQTPAIRARLLDRMKDKWRSDLTSDGLPADAIERRVARGQI      340
M.bovis_FbiB      AEALTAPAPHHTRPTRFVWLQTPAIRARLLDRMKDKWRSDLTSDGLPADAIERRVARGQI      340
                  * *:******** * *** *:: * *:**** *:* * :** :**   ::: :** **::

S.laur_FbiB       LRRAPYLIVPCLVMDGAHHYGDARRDAAEREMFVVAAGAGVQNLLVALAAEQLGSAWVSS      406
M.tuber_FbiB      LYDAPEVVIPMLVPDGAHSYPDAARTDAEHTMFTVAVGAAVQALLVALAVRGLGSCWIGS      400
M.bovis_FbiB      LYDAPEVVIPMLVPDGAHSYPDAARTDAEHTMFTVAVGAAVQALLVALAVRGLGSCWIGS      400
                  *  ** :::* ** **** * ** *  **: **.**.**.** ******.. ***.*:.*

S.laur_FbiB       TMFCRDVVRGVLGLPGDWDPMGAVAVGRPAAAPKERPARQAAEFIEVR          454
M.tuber_FbiB      TIFAADLVRDELDLPVDWEPLGAIAIGYADEPSGLRDPVPAADLLILK          448
M.bovis_FbiB      TIFAADLVRDELDLPVDWEPLGAIAIGYADEPSGLRDPVPAADLLILK          448
                  *:*. *:**. *.** **:*:**:*:*        *    **::: ::
```

Figure 4.15: Alignment of FbiB (coenzyme F_{420}:L-glutamate ligase) amino acid sequences. M.bovis_FbiB: FbiB from *Mycobacterium bovis* BCG (Q7TWV3.1);[31] M.tuber_FbiB: FbiB from *Mycobacterium tuberculosis* H37Rv (P9WP79.1);[33] S.laur_FbiB: a candidate FbiB from *S. laurentii* (BAU83678.1).[32] S.laur_FbiB shows 51.9% identity and 67.0% similarity to M.bovis_FbiB.

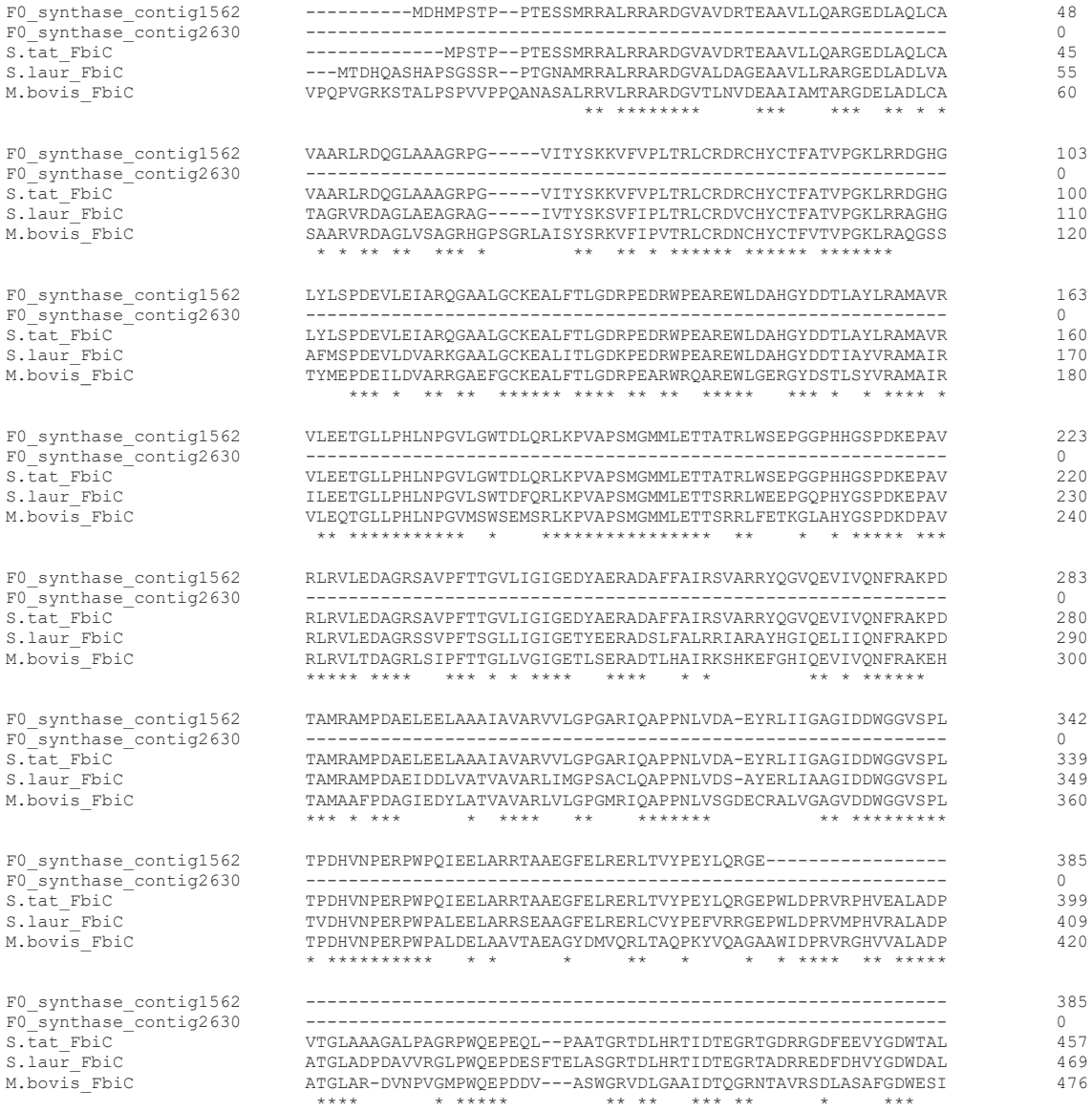

Figure 4.16: Alignment of amino acid sequences of FbiC (F_0 synthase) from *Mycobacterium* species with candidate F_0 synthases from *S. tateyamensis* and *S. laurentii*. M.bovis_FbiC: FbiC from *Mycobacterium bovis* BCG (WP_003406167);[34] S.laur_FbiC: a FbiC from *S. laurentii* (BAU84049.1);[32] two potential fragments of a protein, F0_synthase_contig1562 and F0_synthase_contig2630, encoded in the *S. tateyamensis* draft genome that is/are a candidate FbiC; and S.tat_FbiC: a PCR product that was amplified from *S. tateyamensis* using sequences from F0_synthase_contig1562 and F0_synthase_contig2630. S.tat_FbiC shows 63.1% identity and 75.8% similarity to M.bovis_FbiC, and 76.2% identity and 84.2% similary to S.laur_FbiC. S.laur_FbiC shows 61.6% identity and 73.6% similarity to M.bovis_FbiC.

```
F0_synthase_contig1562      ------------------------------------------------------------          385
F0_synthase_contig2630      ----------------------RAALAVAADDPTRLTDDQALALFAAEGEALDALCAVAD          38
S.tat_FbiC                  REQVA------AIPPARLPGDVRAALAVAADDPTRLTDDQALALFAAEGEALDALCAVAD          511
S.laur_FbiC                 REAAAPGLVPDVLAPERIDADTREALAVAADDPTRLTDAQALTLLHADGPALDALCRVAD          529
M.bovis_FbiC                REQVHELA---VRAPERIDTDVLAALRSAERAPAGCTDGEYLALATADGPALEAVAALAD          533
                            **           * *   *   **  *   *   **   * *  * * ** *    **

F0_synthase_contig1562      ------------------------------------------------------------          385
F0_synthase_contig2630      AVRRDAVGETVTYCVTRNINFTNVCYTGCRFCAFAQRRTDADAYTLSLDQVADRAEQAWQ          98
S.tat_FbiC                  AVRRDAVGETVTYCVTRNINFTNVCYTGCRFCAFAQRRTDADAYTLSLDQVADRAEQAWQ          571
S.laur_FbiC                 DVRKSVVGDEVTYLVTRNINFTNVCYTGCRFCAFAQRRTDADAYTLSLEQVADRAAQAWD          589
M.bovis_FbiC                SLRRDVVGDEVTFVVNRNINFTNICYTGCRFCAFAQRKGDADAYSLSVGEVADRAWEAHV          593
                              *   **  **  * ******* *************  ***** **   *****

F0_synthase_contig1562      ------------------------------------------------------------          385
F0_synthase_contig2630      VGATEVCMQGGIHPDLPGTAYFDIARAVKERVPGMHVHAFSPMEVVNGAARTGLSIRDWL          158
S.tat_FbiC                  VGATEVCMQGGIHPDLPGTAYFDIARAVKERVPGMHVHAFSPMEVVNGAARTGLSIRDWL          631
S.laur_FbiC                 VGAVEVCMQGGIHPDLPGTAYFDIARAVKERVPGIHVHAFSPMEVVNGASRTGLSIREWL          649
M.bovis_FbiC                AGATEVCMQGGIDPELPVTGYADLVRAVKARVPSMHVHAFSPMEIANGVTKSGLSIREWL          653
                             ** ******** * ** * * *  **** ***  *********  **    ***** **

F0_synthase_contig1562      ------------------------------------------------------------          385
F0_synthase_contig2630      TAAQQAGLDTIPGTAAEILDDEVRWVLTKGKLPAATWVEVVSTAHELGIRSSATMMYGHV          218
S.tat_FbiC                  TAAQQAGLDTIPGTAAEILDDEVRWVLTKGKLPAATWVEVVSTAHELGIRSSATMMYGHV          691
S.laur_FbiC                 TAAKEAGLDSIPGTAAEILDDEVRWVLTKGKLPTATWTEVVTTAHELGIRSSSTMMYGHV          709
M.bovis_FbiC                IGLREAGLDTIPGTAAEILDDEVRWVLTKGKLPTSLWIEIVTTAHEVGLRSSSTMMYGHV          713
                                 **** ***********************   * * * **** * *** *******

F0_synthase_contig1562      ------------------------------------------------------------          385
F0_synthase_contig2630      DTPAHWLGHLRLLAGIQQRTGGFTEFVTLPFIHTNAPVYLAGIARPGPTHRDNRAVVAMA          278
S.tat_FbiC                  DTPAHWLGHLRLLAGIQQRTGGFTEFVTLPFIHTNAPVYLAGIARPGPTHRDNRAVVAMA          751
S.laur_FbiC                 DQPRHWLGHLRTLARIQQRTGGFTEFVTLPFVHTNAPVYLAGIARPGPTIRDNRAVTAMA          769
M.bovis_FbiC                DSPRHWVAHLNVLRDIQDRTGGFTEFVPLPFVHQNSPLYLAGAARPGPSHRDNRAVHALA          773
                            * * **  **  *  ** ********* *** * * * **** *****  ****** * *

F0_synthase_contig1562      ------------------------------------------------------------          385
F0_synthase_contig2630      RLLLHPHIPNIQTSWVKLGAAGAAEMLRSGANDLGGTLMEETISRMAGSAYGSYKSVRDL          338
S.tat_FbiC                  RLLLHPHIPNIQTSWVKLGAAGAAEMLRSGANDLGGTLMEETISRMAGSAYGSYKSVRDL          811
S.laur_FbiC                 RLLLHPYIPNIQTSWVKLGTEGAAEMLRSGANDLGGTLMEETISRMAGSSYGSYRSIRDL          829
M.bovis_FbiC                RIMLHGRISHIQTSWVKLGVRRTQVMLEGGANDLGGTLMEETISRMAGSEHGSAKTVAEL          833
                            *  **  *  *********      **  * ******************  **      *

F0_synthase_contig1562      ------------------------------------------------          385
F0_synthase_contig2630      EAIAAAAGRPARQRTTTYGEVPPE------------------------          362
S.tat_FbiC                  EAIAAAAGRPARQRTTTYGEVPPE------------------------          835
S.laur_FbiC                 AAIAEAAGRPSRLRTTLYGEVPEERQRAARDSDGHLPELLPLLPAEDGA          878
M.bovis_FbiC                VAIAEGIGRPARQRTTTYALLAA------------------------          856
                             ***   *** * *** *
```

Figure 4.16 (continued)

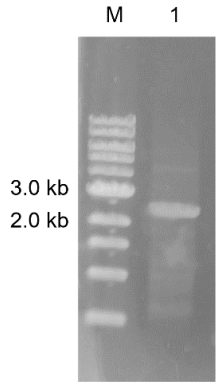

Figure 4.17: PCR amplification of a candidate F_0 synthase in *S. tateyamensis*. Primer pair HI24F/HI24R were used. (M) 1 kb molecular weight ladder and (1) *S. tateyamensis*.

4.3.5 Identification of potential thiopeptide biosynthetic gene clusters colocalized with TpnL

An *in silico* search for TpnL homologs in the NCBI database revealed potential thiopeptide biosynthetic gene clusters colocalized with a putative $F_{420}H_2$-dependent reductase (Figure 4.18). Two of these clusters appear to be capable of producing close structural homologs to **13**-**16**, identified in *Amycolatopsis saalfeldensis* DSM 44993 (*A. saalfeldensis*) and *Micromonospora carbonacea* DSM 43168 (DSM 43168). The TpnL homolog identified in *A. saalfeldensis* (SEO90151.1) shares 70% sequence identity (78% similarity) to TpnL. The associated gene cluster is identical in composition and organization to the *tpn* cluster, including homologs of *tpnMN* that are proposed to be involved in thioamidation of the peptide backbone (Figure 4.18 and Table 4.1). The core peptide sequence encoded in the *A. saalfeldensis* cluster (ASSSSCTTCICTCSCSS; SEO89922.1) is very similar to the sequence in TpnA and the thiostrepton precursor peptide TsrA.[35] The putative thiopeptide biosynthetic gene cluster in DSM 43168 differs in organization from the *tpn* and *S. saalfeldensis* clusters, but does contain a full set of *tpn*/*tsr*-like genes (Figure 4.18 and Table 4.2), and also encodes homologs of TpnLMN, with the TpnL-like protein (SCF235261.1) bearing 52% identity (64% similarity) to TpnL. The core peptide sequence in DSM 43168 (SCF23644.1) differs from the thiopeptin sequence only at the first residue, is identical to the thiostrepton amino acid sequence, and is identical to that predicted for Sch 18640 **1** (IASASCTTCICTCSCSS). Thus far, **1** has only been isolated from *Micromonospora arborensis*, and it is likely that DSM 43168 is another producer of this metabolite.[36] The gene clusters identified in *A. saalfeldensis* and

DSM 43168 may therefore be involved in the generation of thioamidated series *a* and *b* thiopeptides, similar to the complex of **13**-**16** produced by *S. tateyamensis*.

In fact, work by Mitchell and coworkers was released at the time of this writing demonstrating that *A. saalfeldensis* produces saalfelduracin (**34**, Figure 4.19), a thioamidated series *a* thiopeptide.[37] Unlike the thiopeptins which were isolated as a complex containing both dehydropiperidine and piperidine rings, only a piperidine-containing **34** was isolated.[26, 37-38] Mitchell and coworkers utilized a bioinformatic approach that focused on homologs of the YcaO-TfuA pair found in biosynthetic gene clusters of thioamidated metabolites to identify the thiopeptide gene cluster in *A. saalfeldensis* as a potential thioamidated thiopeptide producer. Therefore, a similar bioinformatic approach identifying TpnL-like proteins may be useful in the identification of yet unknown series *a* and series *c* (discussed below) thiopeptide biosynthetic gene clusters as previously unavailable genomes are sequenced and become available in the database.

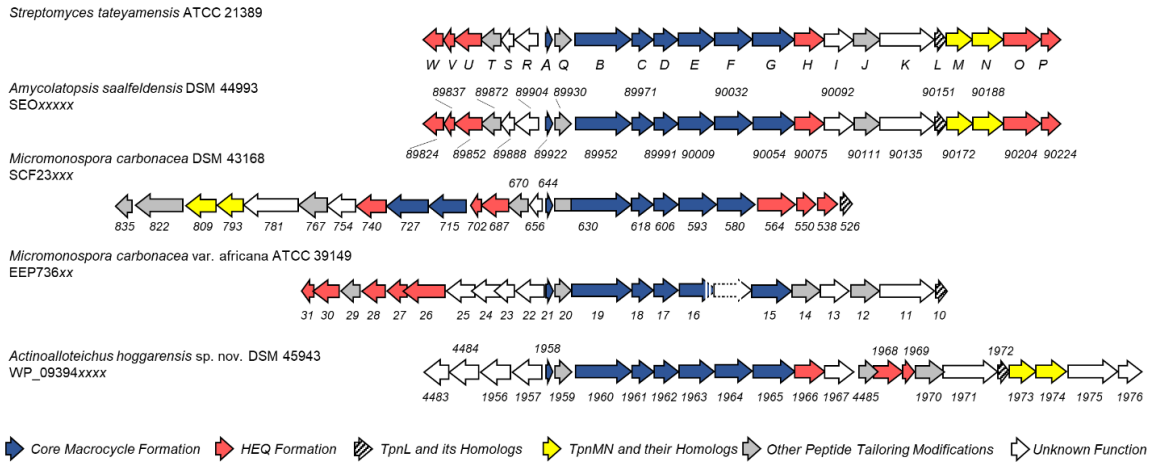

Figure 4.18: The thiopeptin biosynthetic gene (*tpn*) cluster and possible thiopeptide biosynthetic gene clusters containing a homolog of *tpnL*. Two *orf*s in *Micromonospora carbonacea* var. africana ATCC 39149 are based on incomplete nucleotide data in the NCBI database are shown with dashes and dotted lines. The accession numbers are indicated below each species and the range of values are abbreviated by the "*x*" in the accession number. The individual *orf*s are labeled according to the abbreviated accession numbers.

Table 4.1: Deduced functions of the open reading frames in the predicted thiopeptide biosynthetic gene cluster in *Amycolatopsis saalfeldensis* DSM 44993.

NCBI Accession Number	Description of Deduced Protein	Tsr or Tpn Homolog[a]
SEO89824.1	2-Methyl-L-tryptophan aminotransferase	TpnW (60/70)
SEO89837.1	SnoaL-like cyclase	TsrS (ACN52308.1; 67/77)
SEO89852.1	3-(2-Methylindolyl)pyruvate dehydrogenase	TsrQ (ACN52307.1; 66/78)
SEO89872.1	Carboxymethyltransferase	TsrP (ACN52306.1; 63/71)
SEO89888.1	Hypothetical protein	TsrO (ACN52305.1; 41/60)
SEO89904.1	α/β-Hydrolase fold family protein	TpnR (61/74)
SEO89922.1	Thiopeptide precursor peptide	TsrA (ACN52291.1; 76/84)
SEO89930.1	Thiopeptide macrocyclase	TsrB (ACN52292.1; 65/74)
SEO89952.1	LanB-type dehydratase glutamylation domain subunit	TsrC (ACN52293.1; 51/63)
SEO89971.1	LanB-type dehydratase glutamate elimination domain subunit	TsrD (ACN52294.1; 60/74)
SEO89991.1	Thiopeptide [4+2] cyclase	TsrE (ACN52295.1; 74/84)
SEO90009.1	Thiazoline dehydrogenase	TsrF (ACN52296.1; 58/65)
SEO90032.1	F-protein-leader peptide binding protein	TsrG (ACN52297.1; 51/59)
SEO90054.1	F-protein dependent cyclodehydratase	TsrH (ACN52298.1; 61/69)
SEO90075.1	4-(1-Hydroxyethyl)quinoline-2-carboxylic acid epoxygenase	TsrI (ACN52299.1; 58/66)
SEO90092.1	Adenylyltransferase	TsrJ (ACN52300.1; 64/71)
SEO90111.1	Isoleucine hydroxylase	TsrK (ACN52301.1; 56/66)
SEO90135.1	LanB-type dehydratase glutamylation domain subunit	TsrL (ACN52302.1; 46/56)
SEO90151.1	Flavin/deazaflavin oxidoreductase	TpnL (66/75)
SEO90172.1	YcaO domain-containing protein	TpnM (77/84)
SEO90188.1	TfuA-like protein	TpnN (72/80)
SEO90204.1	Tryptophan methyltransferase	TsrM (ACN52303.1; 63/73)
SEO90224.1	4-Acetyl-quinoline-2-carboxylic acid reductase	TsrN (ACN52304.1; 53/63)

[a]NCBI accession numbers and % identity/similarity are given in parentheses.

Table 4.2: Deduced functions of the open reading frames in the predicted thiopeptide biosynthetic gene cluster in *Micromonospora cabonacea* DSM 43168.

NCBI Accession Number	Description of Deduced Protein	Tsr or Tpn Homolog[a]
SCF23835.1	Carboxylesterase	TsrU (ACN52310.1; 51/64)
SCF23822.1	Amidotransferase	TsrT (ACN52309.1; 68/77)
SCF23809.1	TfuA-like protein	TpnN (57/65)
SCF23793.1	YcaO domain-containing protein	TpnM (66/74)
SCF23781.1	LanB-type dehydratase glutamylation domain subunit	TsrL (ACN52302.1; 47/56)
SCF23767.1	Isoleucine hydroxylase	TsrK (ACN52301.1; 56/68)
SCF23754.1	Adenylyltransferase	TsrJ (ACN52300.1; 60/69)
SCF23740.1	4-(1-Hydroxyethyl)quinoline-2-carboxylic acid epoxygenase	TsrI (ACN52299.1; 56/65)
SCF23727.1	F-protein dependent cyclodehydratase	TsrH (ACN52298.1; 60/69)
SCF23715.1	F-protein-leader peptide binding protein	TsrG (ACN52297.1; 41/51)
SCF23702.1	SnoaL-like cyclase	TsrS (ACN52308.1; 58/75)
SCF23687.1	3-(2-Methylindolyl)pyruvate dehydrogenase	TsrQ (ACN52307.1; 67/81)
SCF23670.1	Carboxymethyltransferase	TsrP (ACN52306.1; 60/69)
SCF23656.1	Hypothetical protein	TsrO (ACN52305.1; 54/68)
SCF23644.1	Thiopeptide precursor peptide	TsrA (ACN52291.1; 80/91)
SCF23630.1[b]	Thiopeptide macrocyclase	TsrB (ACN52292.1; 54/66)
	LanB-type dehydratase glutamylation domain subunit	TsrC (ACN52293.1; 50/62)
SCF23618.1	LanB-type dehydratase glutamate elimination domain subunit	TsrD (ACN52294.1; 60/71)
SCF23606.1	Thiopeptide [4+2] cyclase	TsrE (ACN52295.1; 69/81)
SCF23593.1	Thiazoline dehydrogenase	TsrF (ACN52296.1; 56/63)
SCF23580.1	F-protein-leader peptide binding protein	TsrG (ACN52297.1; 51/58)
SCF23564.1	Tryptophan methyltransferase	TsrM (ACN52303.1; 66/75)
SCF23550.1	4-Acetyl-quinoline-2-carboxylic acid reductase	TsrN (ACN52304.1; 56/69)
SCF23538.1	2-Methyl-L-tryptophan aminotransferase	TpnW (31/40)
SCF23526.1	Flavin/deazaflavin oxidoreductase	TpnL (52/64)

[a]NCBI accession numbers and % identity/similarity are given in parentheses.
[b]The protein deposited to GenBank showed two Tsr homologs fused as one *orf*.

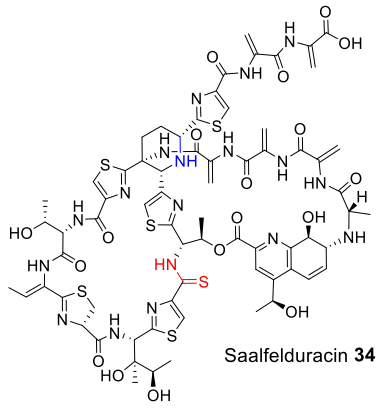

Figure 4.19: The structure of saalfelduracin **34**, a thioamidated series *a* thiopeptide isolated from *A. saalfeldensis* NRRL B-24474. The piperidine ring is in blue and the thioamide is in red.[37]

To date, only one dihydroimidazopiperidine-containing series *c* thiopeptide has been identified, Sch 40832 **3** (Figure 4.20) isolated from *Micromonospora carbonacea* var. africana ATCC 39149 (ATCC 39149).[39] The genome sequence of ATCC 39149 contains a candidate biosynthetic gene cluster for this unusual thiopeptide (Figure 4.18), and the precursor peptide found encoded in this locus (EEP73621.1) includes a match for a predicted Sch 40832 core peptide (TSSSSCTTCICTCSCSS). Like **2** and **13**-**16**, Sch 40832 houses a second, quinaldic acid-containing macrocycle, and the genes encoding HEQ biosynthetic enzyme homologs are present in the proposed cluster (Figure 4.18; Table 4.3). The structure reported for Sch 40832 **3** included a disaccharide tethered to the β-hydroxyl of Thr1, and a potential glycosyltransferase (EEP73625.1) is encoded in this cluster (Table 4.3). In addition, methylation of the Cys15 sulfur and the methylhydroxylation of the dihydroimidazopiperidine ring found in **3** may be accomplished by actions of a putative methyltransferase (EEP73623.1) and a cytochrome P450 (EEP73622.1), respectively, that are encoded in this cluster (Table 4.3). The role of a putative NAD(P)-dependent

oxidoreductase (EEP73624.1) is unclear, but it may be involved in the formation or maturation of the dihydroimidazopiperidine ring. A homolog of TpnL (EEP73610.1) is present in the ATCC 39149 cluster, but there do not appear to be any homologs to TpnMN, the proposed thioamidation YcaO-TfuA-like proteins. Accordingly, the reported structure of Sch 40832 includes a piperidine ring but lacks a thioamide.[39] The role of an $F_{420}H_2$-dependent reductase in the biosynthesis of a series *c* thiopeptide is not entirely clear. It could reduce a dehydropiperidine precursor, forming a nascent piperidine subjected to additional oxidative modifications elaborating the central nitrogenous ring into the dihydroimidazopiperidine scaffold. Alternatively, the TpnL homolog could mediate an entirely different reductive step in the maturation of a series *c* thiopeptide.

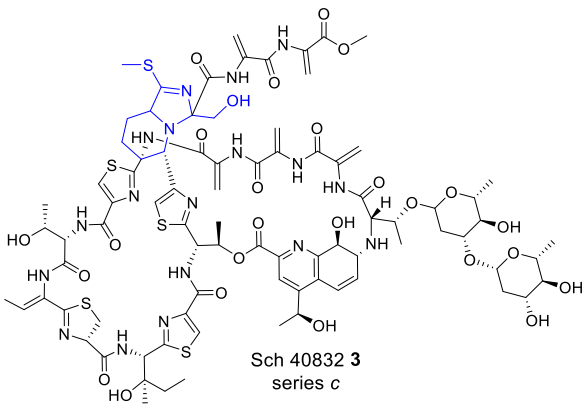

Figure 4.20: The structure of Sch 40832 **3**, a series *c* thiopeptide, produced by *Micromonospora cabonacea* var. africana ATCC 39149.[39] The dihydroimidazopiperidine ring is in blue.

Table 4.3: Deduced functions of the open reading frames in the predicted thiopeptide biosynthetic gene cluster in *Micromonospora carbonacea* var. africana ATCC 39149.

NCBI Accession Number	Description of Deduced Protein	Tsr or Tpn Homolog[a]
EEP73631.1	SnoaL-like cyclase	TsrS (ACN52308.1; 61/77)
EEP73630.1	3-(2-Methylindolyl)pyruvate dehydrogenase	TsrQ (ACN52307.1; 69/83)
EEP73629.1	Carboxymethyltransferase	TsrP (ACN52306.1; 55/65)
EEP73628.1	2-Methyl-L-tryptophan aminotransferase	TpnW (36/47)
EEP73627.1	4-Acetyl-quinoline-2-carboxylic acid reductase	TsrN (ACN52304.1; 48/62)
EEP73626.1	Tryptophan methyltransferase	TsrM (ACN52303.1; 59/68)
EEP73625.1	Glycosyltransferase	---
EEP73624.1	NAD(P)-dependent oxidoreductase	---
EEP73623.1	Methyltransferase	---
EEP73622.1	Cytochrome P450	---
EEP73621.1	Thiopeptide precursor peptide	TsrA (ACN52291.1; 65/78)
EEP73620.1	Thiopeptide macrocyclase	TsrB (ACN52292.1; 52/62)
EEP73619.1	LanB-type dehydratase glutamylation domain subunit	TsrC (ACN52293.1; 50/59)
EEP73618.1	LanB-type dehydratase glutamate elimination domain subunit	TsrD (ACN52294.1; 63/72)
EEP73617.1	Thiopeptide [4+2] cyclase	TsrE (ACN52295.1; 64/77)
EEP73616.1[b]	Thiazoline dehydrogenase	TsrF (ACN52296.1; 47/57)
Orf1[c]	F-protein-leader peptide binding protein	TsrG (ACN52297.1; 52/61)
EEP73615.1	F-protein dependent cyclodehydratase	TsrH (ACN52298.1; 56/64)
EEP73614.1	4-(1-Hydroxyethyl)quinoline-2-carboxylic acid epoxygenase	TsrI (ACN52299.1; 53/62)
EEP73613.1	Adenylyltransferase	TsrJ (ACN52300.1; 61/69)
EEP73612.1	Isoleucine hydroxylase	TsrK (ACN52301.1; 50/64)
EEP73611.1	LanB-type dehydratase glutamylation domain subunit	TsrL (ACN52302.1; 39/49)
EEP73610.1	Flavin/deazaflavin oxidoreductase	TpnL (50/61)

[a]NCBI accession numbers and % identity/similarity are given in parentheses.
[b]EEP73616.1 is deposited to GenBank with incomplete nucleotide sequence.
[c]A previously unannotated and *orf* with incomplete nucleotide sequence.

Actinoalloteichus hoggarensis DSM 45943 (*A. hoggarensis*) also identifies with a putative thiopeptide biosynthetic gene cluster harboring a TpnL-like protein, and contains many similarities to the components of the ATCC 39149 biosynthetic gene cluster (Figure 4.18, Tables 4.3 and 4.4). The *A. hoggarensis* core peptide (WP_093941958.1) is identical to the proposed Sch 40832 core peptide of ATCC 39149. Both *A. hoggarensis* and ATCC 39149 gene clusters encode a putative glycosyltransferase (WP_093941956.1/EEP73625.1), methyltransferase (WP_093941975.1/EEP73623.1), cytochrome P450 (WP_093941957.1/EEP73622.1), and an NAD(P)-dependent oxidoreductase (WP_093944483.1/ EEP73624.1), which may represent a set of enzymes required in the formation of series *c* thiopeptides. The *A. hoggarensis* cluster, however, also includes homologs to the proposed TpnMN thioamidating system. It is therefore possible that *A. hoggarensis* may generate another series *c* thiopeptide bearing a thioamide. In addition, the *A. hoggarensis* biosynthetic gene cluster contains additional encoded products (WP_093944484.1, WP_093941974.1, WP_093941976.1) not found in the ATCC 39149 biosynthetic gene cluster, which may be involved in additional modifications to the core peptide scaffold that is not found in the structure of Sch 40832 **3**.

Table 4.4: Deduced functions of the open reading frames in the predicted thiopeptide biosynthetic gene cluster in *Actinoalloteichus hoggarensis* sp. nov DSM 45943.

NCBI Accession Number	Description of Deduced Protein	Tsr or Tpn Homolog[a]
WP_093944483.1	Gfo/Idh/MocA family oxidoreductase	---
WP_093944484.1	NDP-hexose 2,3-dehydratase	---
WP_093941956.1	Glycosyltransferase	---
WP_093941957.1	Cytochrome P450	---
WP_093941958.1	Thiopeptide precursor peptide	TsrA (ACN52291.1; 70/88)
WP_093941959.1	Thiopeptide macrocyclase	TsrB (ACN52292.1; 60/72)
WP_093941960.1	LanB-type dehydratase glutamylation domain subunit	TsrC (ACN52293.1; 47/58)
WP_093941961.1	LanB-type dehydratase glutamate elimination domain subunit	TsrD (ACN52294.1; 57/71)
WP_093941962.1	Thiopeptide [4+2] cyclase	TsrE (ACN52295.1; 66/78)
WP_093941963.1	Thiazoline dehydrogenase	TsrF (ACN52296.1; 51/60)
WP_093941964.1	F-protein-leader peptide binding protein	TsrG (ACN52297.1; 45/54)
WP_093941965.1	F-protein dependent cyclodehydratase	TsrH (ACN52298.1; 52/62)
WP_093941966.1	4-(1-Hydroxyethyl)quinoline-2-carboxylic acid epoxygenase	TsrI (ACN52299.1; 55/65)
WP_093941967.1	Adenylyltransferase	TsrJ (ACN52300.1; 62/71)
WP_093944485.1	Carboxymethyltransferase	TsrP (ACN52306.1; 47/55)
WP_093941968.1	3-(2-Methylindolyl)pyruvate dehydrogenase	TsrQ (ACN52307.1; 54/69)
WP_093941969.1	SnoaL-like cyclase	TsrS (ACN52308.1; 52/68)
WP_093941970.1	Isoleucine hydroxylase	TsrK (ACN52301.1; 52/63)
WP_093941971.1	LanB-type dehydratase glutamylation domain subunit	TsrL (ACN52302.1; 40/48)
WP_093941972.1	Flavin/deazaflavin oxidoreductase	TpnL (45/60)
WP_093944486.1	YcaO domain-containing protein	TpnM (62/70)
WP_093941973.1	TfuA-like protein	TpnN (48/59)
WP_093941974.1	Peptidase	---
WP_093941975.1	FkbM family methyltransferase	---
WP_093941976.1	SGNH/GDSL hydrolase family protein	---

[a]NCBI accession numbers and % identity/similarity are given in parentheses.

Several other homologs of TpnL were identified in the NCBI database, only a few of which appear to be involved in thiopeptide biosynthesis. A phylogenetic analysis of TpnL was conducted alongside its homologs and established $F_{420}H_2$-dependent FDOR-Bs from *Mycobacterium* species and *Streptomyces rimosus*[1, 7, 9, 12-13, 40] The TpnL-like proteins affiliated with a known or predicted thiopeptide biosynthetic gene cluster are in a distinct clade from the other FDOR-B proteins (Figure 4.21). The two proteins that may be involved in biosynthesis of dihydroimidazopiperidine-containing (series *c*) thiopeptides form a separate subclade from the homologs identified from bacteria that are or may be involved in the biosynthesis of series *a* thiopeptides.

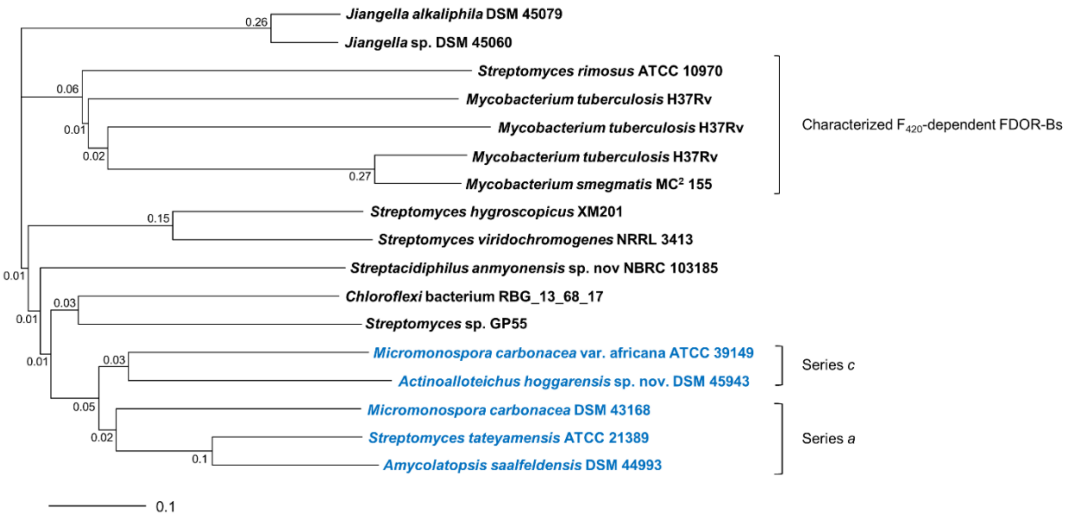

Figure 4.21: Phylogenetic tree of TpnL and other F_{420}-dependent FDOR-B homologs. TpnL homologs colocalized with predicted thiopeptide biosynthetic gene clusters are shown in blue, and other known and putative F_{420}-dependent FDOR-Bs are shown in black. The F_{420}-dependent FDOR-Bs from Actinobacteria that have been biochemically characterized are indicated with a bracket. The branch distances are indicated at the nodes and are based on the number of substitutions in the amino acid sequences between homologs, an indicator of genetic divergence. The scale bar represents ten amino acid substitutions per 100 amino acid residues. Accession numbers for the sequences used are listed in Table B.3.

4.4 Conclusions

A defining characteristic of thiopeptides is the core macrocycle linked through a nitrogenous heterocycle derived from two Dha residues *via* a formal [4+2] cycloaddition.[22] Series *d* thiopeptides utilize a dedicated pyridine synthase to catalyze this cyclization, followed by dehydration and elimination of the leader peptide.[41] A similar process might also lead to the core macrocycle of series *a* and *b* thiopeptides, although it is not yet understood how this permits retention of the N-terminal portion of the peptide and a more reduced ring system. There are, however, no obvious reductase candidates in either the **2** or siomycin biosynthetic gene clusters, leaving the origin of the dehydropiperidine ring enigmatic.[35, 42] Identification of TpnL as a dehydropiperidine reductase demonstrates that the series *a* thiopeptide piperidine originates from the reduction of a series *b* thiopeptide intermediate. TpnL does accept thiostrepton A **2**, a mature metabolite bearing both the core macrocycle and the quinaldic acid loop, as a substrate. It is not yet known, however, if TpnL would act upon a dehydropiperidine-containing intermediate in which the second, quinaldic acid-containing, macrocycle has not yet been installed.[43-44] The TpnL-dependent reduction shown here occurs independent of additional ancillary recognition elements such as the leader peptide, in contrast to many modifications in thiopeptide biosynthesis that do require the presence of the leader peptide.[22] A similar transformation is expected to be carried out by TpnL on a dehydropiperidine-containing biosynthetic intermediate of thiopeptin in *S. tateyamensis*. Gene deletion experiments of *tpnL* and other thiopeptide biosynthetic genes in *S. tateayamensis* or in *S. laurentii* HI1 (the *S. laurentii* strain that expresses TpnL), and a deletion experiment of the *tpnL* homolog in *A. saalfeldensis* are

needed to discern the exact timing of this modification in thiopeptide biosynthesis and substrate specificity of this enzyme.

The activity of TpnL appears to be subject to substrate inhibition by thiostrepton A at concentrations above 2 μM. A majority of F_{420} in the TpnL assay appears to be reduced during the course of the activity assay and increasing the concentration of available $F_{420}H_2$ did not alter the activity of TpnL. Further kinetic experiments that alter temperature and pH are needed to better describe the non-Michaelis-Menten behavior of TpnL activity. In addition, structural characterization of TpnL may reveal insights into the binding mode of the substrates with TpnL and the catalytic mechanism of the dehydropiperidine reduction. Kinetic and structural characterization of TpnL may help explain the apparent substrate inhibition that was observed.

A few TpnL homologs were found to colocalize with other predicted thiopeptide biosynthetic gene clusters. One of which was identified in *M. carbonacea* var. africana ATCC 39149, a known producer of the series *c* thiopeptide Sch 40832 **3**. The encoded core peptide sequence in this gene cluster matches the predicted core peptide sequence of Sch 40832 and it is likely that this gene cluster is involved in its biosynthesis. The role of the TpnL homolog in Sch 40832 biosynthesis is unclear and biosynthetic characterizations of the TpnL-like protein and other encoded products of the ATCC 39149 gene cluster are required.

There is a recent surge of interest in cofactor F_{420} for its involvement in mycobacterial virulence. Yet, our understanding of deazaflavin-dependent reactions is limited, especially in secondary metabolism. TpnL demonstrates the first known involvement of cofactor F_{420} in thiopeptide biosynthesis or RiPP biosynthesis. In addition

to TpnL, OxyR, the F_{420}-dependent reductase in oxytetracycline biosynthesis is one of the few characterized examples of F_{420} in secondary metabolism.[9] Discovery of novel F_{420}-dependent proteins may reveal additional chemical modifications that are attributed to this unusual coenzyme and the physiological relevance of F_{420}-dependent pathways.

4.5 References

1. Ahmed, F. H.; Carr, P. D.; Lee, B. M.; Afriat-Jurnou, L.; Mohamed, A. E.; Hong, N. S.; Flanagan, J.; Taylor, M. C.; Greening, C.; Jackson, C. J., Sequence-structure-function classification of a catalytically diverse oxidoreductase superfamily in mycobacteria. *J. Mol. Biol.* **2015**, *427*, 3554-3571.

2. Greening, C.; Ahmed, F. H.; Mohamed, A. E.; Lee, B. M.; Pandey, G.; Warden, A. C.; Scott, C.; Oakeshott, J. G.; Taylor, M. C.; Jackson, C. J., Physiology, biochemistry, and applications of F_{420}- and F_0-dependent redox reactions. *Microbiol. Mol. Biol. Rev.* **2016**, *80*, 451-493.

3. stHu, Y.; Jiang, F.; Guo, Y.; Shen, X.; Zhang, Y.; Zhang, R.; Guo, G.; Mao, X.; Zou, Q.; Wang, D. C., Crystal structure of HugZ, a novel heme oxygenase from *Helicobacter pylori*. *J. Biol. Chem.* **2011**, *286*, 1537-1544.

4. Biswal, B. K.; Au, K.; Cherney, M. M.; Garen, C.; James, M. N., The molecular structure of Rv2074, a probable pyridoxine 5'-phosphate oxidase from *Mycobacterium tuberculosis*, at 1.6 Å resolution. *Acta. Crystallogr. Sect. F Struct. Biol. Cryst. Commun.* **2006**, *62*, 735-742.

5. Canaan, S.; Sulzenbacher, G.; Roig-Zamboni, V.; Scappuccini-Calvo, L.; Frassinetti, F.; Maurin, D.; Cambillau, C.; Bourne, Y., Crystal structure of the conserved hypothetical protein Rv1155 from *Mycobacterium tuberculosis*. *FEBS Lett.* **2005**, *579*, 215-221.

6. di Salvo, M. L.; Contestabile, R.; Safo, M. K., Vitamin B_6 salvage enzymes: mechanism, structure and regulation. *Biochem. Biophys. Acta, Proteins Proteomics* **2011**, *1814*, 1597-1608.

7. Greening, C.; Jirapanjawat, T.; Afroze, S.; Ney, B.; Scott, C.; Pandey, G.; Lee, B. M.; Russell, R. J.; Jackson, C. J.; Oakeshott, J. G.; Taylor, M. C.; Warden, A. C., Mycobacterial $F_{420}H_2$-dependent reductases promiscuously reduce diverse compounds through a common mechanism. *Front. Microbiol.* **2017**, *8*, 1000.

8. Oyugi, M. A.; Bashiri, G.; Baker, E. N.; Johnson-Winters, K., Investigating the reaction mechanism of F_{420}-dependent glucose-6-phosphate dehydrogenase from *Mycobacterium tuberculosis*: kinetic analysis of the wild-type and mutant enzymes. *Biochemistry* **2016**, *55*, 5566-5577.

9. Wang, P.; Bashiri, G.; Gao, X.; Sawaya, M. R.; Tang, Y., Uncovering the enzymes that catalyze the final steps in oxytetracycline biosynthesis. *J. Am. Chem. Soc.* **2013**, *135*, 7138-7141.

10. Purwantini, E.; Mukhopadhyay, B., Conversion of NO_2 to NO by reduced coenzyme F_{420} protects mycobacteria from nitrosative damage. *Proc. Natl. Acad. Sci. U.S.A.* **2009**, *106*, 6333-6338.

11. Guo, Y.; Guo, G.; Mao, X.; Zhang, W.; Xiao, J.; Tong, W.; Liu, T.; Xiao, B.; Liu, X.; Feng, Y.; Zou, Q., Functional identification of HugZ, a heme oxygenase from *Helicobacter pylori*. *BMC Microbiol.* **2008**, *8*, 226.

12. Ahmed, F. H.; Mohamed, A. E.; Carr, P. D.; Lee, B. M.; Condic-Jurkic, K.; O'Mara, M. L.; Jackson, C. J., Rv2074 is a novel $F_{420}H_2$-dependent biliverdin reductase in *Mycobacterium tuberculosis*. *Protein Sci.* **2016**, *25*, 1692-1709.

13. Mashalidis, E. H.; Gittis, A. G.; Tomczak, A.; Abell, C.; Barry, C. E., 3rd; Garboczi, D. N., Molecular insights into the binding of coenzyme F_{420} to the conserved protein Rv1155 from *Mycobacterium tuberculosis*. *Protein Sci.* **2015**, *24*, 729-740.

14. Liu, Y.; Liu, J.; Tetzlaff, W.; Paty, D. W.; Cynader, M. S., Biliverdin reductase, a major physiologic cytoprotectant, suppresses experimental autoimmune encephalomyelitis. *Free Radic. Biol. Med.* **2006**, *40*, 960-967.

15. Barañano, D. E.; Rao, M.; Ferris, C. D.; Snyder, S. H., Biliverdin reductase: A major physiologic cytoprotectant. *Proc. Natl. Acad. Sci. U.S.A.* **2002**, *99*, 16093-16098.

16. Doré, S.; Takahashi, M.; Ferris, C. D.; Hester, L. D.; Guastella, D.; Snyder, S. H., Bilirubin, formed by activation of heme oxygenase-2, protects neurons against oxidative stress injury. *Proc. Natl. Acad. Sci. U.S.A.* **1999**, *96*, 2445-2450.

17. Bashiri, G.; Squire, C. J.; Baker, E. N.; Moreland, N. J., Expression, purification and crystallization of native and selenomethionine labeled *Mycobacterium tuberculosis* FGD1 (Rv0407) using a *Mycobacterium smegmatis* expression system. *Protein Expr. Purif.* **2007**, *54*, 38-44.

18. Bashiri, G.; Rehan, A. M.; Greenwood, D. R.; Dickson, J. M.; Baker, E. N., Metabolic engineering of cofactor F_{420} production in *Mycobacterium smegmatis*. *PLoS One* **2010**, *5*, e15803.

19. Bradford, M. M., A rapid and sensitive method for the quantitation of microgram quantities of protein utilizing the principle of protein-dye binding. *Anal. Biochem.* **1976**, *72*, 248-254.

20. Mahanta, N.; Liu, A.; Dong, S.; Nair, S. K.; Mitchell, D. A., Enzymatic reconstitution of ribosomal peptide backbone thioamidation. *Proc. Natl. Acad. Sci. U.S.A.* **2018**, *115*, 3030-3035.

21. Taylor, M. C.; Jackson, C. J.; Tattersall, D. B.; French, N.; Peat, T. S.; Newman, J.; Briggs, L. J.; Lapalikar, G. V.; Campbell, P. M.; Scott, C.; Russell, R. J.; Oakeshott, J. G., Identification and characterization of two families of $F_{420}H_2$-dependent reductases from Mycobacteria that catalyse aflatoxin degradation. *Mol. Microbiol.* **2010**, *78*, 561-575.

22. Hudson, G. A.; Zhang, Z.; Tietz, J. I.; Mitchell, D. A.; van der Donk, W. A., *In vitro* biosynthesis of the core scaffold of the thiopeptide thiomuracin. *J. Am. Chem. Soc.* **2015**, *137*, 16012-16015.

23. Zhang, Z.; Hudson, G. A.; Mahanta, N.; Tietz, J. I.; van der Donk, W. A.; Mitchell, D. A., Biosynthetic timing and substrate specificity for the thiopeptide thiomuracin. *J. Am. Chem. Soc.* **2016**, *138*, 15511-15514.

24. Cheeseman, P.; Toms-Wood, A.; Wolfe, R. S., Isolation and properties of a fluorescent compound, factor 420, from *Methanobacterium* strain M.o.H. *J. Bacteriol.* **1972**, *112*, 527-531.

25. Mohamed, A. E.; Ahmed, F. H.; Arulmozhiraja, S.; Lin, C. Y.; Taylor, M. C.; Krausz, E. R.; Jackson, C. J.; Coote, M. L., Protonation state of $F_{420}H_2$ in the prodrug-activating deazaflavin dependent nitroreductase (Ddn) from *Mycobacterium tuberculosis*. *Mol. Biosyst.* **2016**, *12*, 1110-1113.

26. Miyairi, N.; Miyoshi, T.; Aoki, H.; Kosaka, M.; Ikushima, H., Thiopeptin, a new feed additive antibiotic: microbiological and chemical studies. *Antimicrob. Agents Chemother.* **1972**, *1*, 192-196.

27. Ryan, P. C.; Lu, M.; Draper, D. E., Recognition of the highly conserved GTPase center of 23 S ribosomal RNA by ribosomal protein L11 and the antibiotic thiostrepton. *J. Mol. Biol.* **1991**, *221*, 1257-1268.

28. Bashiri, G.; Squire, C. J.; Moreland, N. J.; Baker, E. N., Crystal structures of F_{420}-dependent glucose-6-phosphate dehydrogenase FGD1 involved in the activation of the anti-tuberculosis drug candidate PA-824 reveal the basis of coenzyme and substrate binding. *J. Biol. Chem.* **2008**, *283*, 17531-17541.

29. Zhang, F.; Kelly, W. L., Saturation mutagenesis of TsrA Ala4 unveils a highly mutable residue of thiostrepton A. *ACS Chem. Biol.* **2015**, *10*, 998-1009.

30. Kelly, J.; Kutscher, A. H.; Tuot, I. F., Thiostrepton, a new antibiotic: tube dilution sensitivity studies. *Oral surgery, oral medicine, and oral pathology* **1959**, *12*, 1334-1339.

31. Choi, K. P.; Bair, T. B.; Bae, Y. M.; Daniels, L., Use of transposon Tn5367 mutagenesis and a nitroimidazopyran-based selection system to demonstrate a requirement for *fbiA* and *fbiB* in coenzyme F_{420} biosynthesis by *Mycobacterium bovis* BCG. *J. Bacteriol.* **2001**, *183*, 7058-7066.

32. Doi, K.; Fujino, Y.; Nagayoshi, Y.; Ohshima, T.; Ogata, S., Complete genome sequence of thiostrepton-producing *Streptomyces laurentii* ATCC 31255. *Genome Announc.* **2016**, *4*, e00360-16.

33. Bashiri, G.; Rehan, A. M.; Sreebhavan, S.; Baker, H. M.; Baker, E. N.; Squire, C. J., Elongation of the poly-γ-glutamate tail of F_{420} requires both domains of the F_{420}:γ-glutamyl ligase (FbiB) of *Mycobacterium tuberculosis*. *J. Biol. Chem.* **2016**, *291*, 6882-6894.

34. Choi, K. P.; Kendrick, N.; Daniels, L., Demonstration that *fbiC* is required by *Mycobacterium bovis* BCG for coenzyme F_{420} and F_0 biosynthesis. *J. Bacteriol.* **2002**, *184*, 2420-2428.

35. Kelly, W. L.; Pan, L.; Li, C., Thiostrepton biosynthesis: prototype for a new family of bacteriocins. *J. Am. Chem. Soc.* **2009**, *131*, 4327-4334.

36. Puar, M. S.; Ganguly, A. K.; Afonso, A.; Brambilla, R.; Mangiaracina, P.; Sarre, O.; MacFarlane, R. D., Sch 18640. A new thiostrepton-type antibiotic. *J. Am. Chem. Soc.* **1981**, *103*, 5231-5233.

37. Schwalen, C. J.; Hudson, G. A.; Kille, B.; Mitchell, D. A., Bioinformatic expansion and discovery of thiopeptide antibiotics. *J. Am. Chem. Soc.* **2018**, *140*, 9494–9501.

38. Hensens, O. D.; Albers-Schonberg, G., Total structure of the highly modified peptide antibiotic components of thiopeptin. *J. Antibiot.* **1983**, *36*, 814-831.

39. Puar, M. S.; Chan, T. M.; Hegde, V.; Patel, M.; Bartner, P.; Ng, K. J.; Pramanik, B. N.; MacFarlane, R. D., Sch 40832: a novel thiostrepton from *Micromonospora carbonacea*. *J. Antibiot.* **1998**, *51*, 221-224.

40. Manjunatha, U. H.; Boshoff, H.; Dowd, C. S.; Zhang, L.; Albert, T. J.; Norton, J. E.; Daniels, L.; Dick, T.; Pang, S. S.; Barry, C. E., 3rd, Identification of a nitroimidazo-oxazine-specific protein involved in PA-824 resistance in *Mycobacterium tuberculosis*. *Proc. Natl. Acad. Sci. U.S.A.* **2006**, *103*, 431-436.

41. Cogan, D. P.; Hudson, G. A.; Zhang, Z.; Pogorelov, T. V.; van der Donk, W. A.; Mitchell, D. A.; Nair, S. K., Structural insights into enzymatic [4+2] aza-

cycloaddition in thiopeptide antibiotic biosynthesis. *Proc. Natl. Acad. Sci. U.S.A.* **2017**, *114*, 12928-12933.

42. Liao, R.; Duan, L.; Lei, C.; Pan, H.; Ding, Y.; Zhang, Q.; Chen, D.; Shen, B.; Yu, Y.; Liu, W., Thiopeptide biosynthesis featuring ribosomally synthesized precursor peptides and conserved posttranslational modifications. *Chem. Biol.* **2009**, *16*, 141-147.

43. Li, C.; Zhang, F.; Kelly, W. L., Mutagenesis of the thiostrepton precursor peptide at Thr7 impacts both biosynthesis and function. *Chem. Commun.* **2012**, *48*, 558-560.

44. Zheng, Q.; Wang, S.; Duan, P.; Liao, R.; Chen, D.; Liu, W., An α/β-hydrolase fold protein in the biosynthesis of thiostrepton exhibits a dual activity for endopeptidyl hydrolysis and epoxide ring opening/macrocyclization. *Proc. Natl. Acad. Sci. U.S.A.* **2016**, *113*, 14318-14323.

CHAPTER 5: CONCLUSIONS AND OUTLOOK

The thiopeptin biosynthetic gene (*tpn*) cluster was identified in *Streptomyces tateyamensis* ATCC 21389 (*S. tateyamensis*), a producer of the antibiotic complex, thiopeptin (**13**-**16**).[1-2] To confirm the role of the *tpn* cluster in thiopeptin biosynthesis, the transaminase activity of TpnW was demonstrated *in vitro*. TpnW was able to convert 2-methyl-L-tryptophan to 3-(2-methylindolyl)pyruvate in the presence of aromatic α-keto acid donors. This transamination is the second step of HEQ biosynthesis, and HEQ is a component required to form the second macrocycle of thiopeptin. While most of the 23 open reading frames in the *tpn* cluster (*tpnA-W*) encode homologs of known thiopeptide biosynthetic proteins, the functions of TpnLMN were not immediately clear.[3] To confirm the involvement of the *tpn* cluster in thiopeptin biosynthesis and to investigate the roles of *tpnLMNR*, gene inactivation studies of *tpn*LMNR in *S. tateyamensis* were pursued. *S. tateyamensis,* however, was recalcitrant to genetic modifications. Neither the interspecies conjugation of *S. tateyamensis* with *E. coli* nor *S. tateyamensis* protoplast transformation were able to be optimized. In addition, thiopeptin production by *S. tateyamensis* became difficult to reproduce, making the results of the *S. tateyamensis* mutants difficult to interpret.

To circumvent obstacles encountered with genetic modifications to *S. tateyamensis*, TpnLMNR were expressed in *Streptomyces laurentii* ATCC 31255 (*S. laurentii*), a producer of thiostrepton A **2**, a thiopeptide antibiotic with a highly similar structure to thiopeptin.[4] *S. laurentii* HI1, a strain that expresses TpnL, produced thiostrepton A_a **31**, a piperidine-containing analog of **2**. The piperidine modification of thiostrepton A_a **31** did

not significantly alter either the aqueous solubility or antibacterial activities of the analog against the strains evaluated. *S. laurentii* HI6, a strain that coexpresses TpnMN, produced a metabolite with the same mass as a thioamidated thiostrepton analog **32**. Isolation and structural characterization of this metabolite is needed to confirm the thioamide modification that is predicted to be installed by TpnMN.

TpnL is homologous to enzymes of the flavin/deazaflavin oxidoreductase subgroup B (FDOR-B) and TpnL has a conserved lysine residue (K55) that is present in most F_{420}-dependent FDOR-Bs. Accordingly, TpnL was found to preferentially bind the deazaflavin cofactor F_{420} over flavin cofactors. TpnL activity was demonstrated in the presence of F_{420}, F_{420}-dependent glucose-6-phosphate dehydrogenase, glucose-6-phosphate, and thiostrepton A **2**. TpnL was able to reduce the dehydropiperine ring of **2** to the piperidine ring of thiostrepton A_a **31**. TpnL activity, however, appeared to be strongly inhibited by thiostrepton A **2** above 2 μM. While TpnL did accept **2**, a mature thiopeptide as a substrate, further characterization is required to determine if TpnL accepts a dehydropiperidine-containing biosynthetic intermediate in which the quindalic acid-containing macrocycle has not yet been installed. Gene inactivation studies in *S. laurentii* HI1 or heterologous expression of TpnL in *S. laurentii* mutants that have one or more thiostrepton biosynthetic genes inactivated may shed light on the timing of this modification and the substrate specificity of TpnL. Structural characterization of TpnL may reveal the binding mode of $F_{420}H_2$ and **2**, and possibly illuminate a structural mechanism for the substrate inhibition of TpnL activity.

TpnL homologs were found to colocalize with other predicted thiopeptide biosynthetic gene clusters. One of these clusters was identified in *M. carbonacea* var

africana, a known producer of Sch 40832, a series *c* thiopeptide. The encoded core peptide sequence in this gene cluster matches the predicted core peptide sequence of Sch 40832 and it is likely that this gene cluster is involved in its biosynthesis. A phylogenetic analysis of TpnL-like proteins showed that the TpnL homologs predicted to be involved in series *a* or series *c* thiopeptide biosynthesis formed their own separate clades. Therefore, genome mining for TpnL-like proteins may be useful in identifying series *a* and series *c* thiopeptide biosynthetic gene clusters as more microbial genomes become available on the database.

The characterization of TpnL as an $F_{420}H_2$-dependent dehydropiperidine reductase establishes the basis for a series *a* thiopeptide and TpnL is the first known instance of a F_{420}-dependent enzyme involved in the biosynthesis of ribosomally-translated and post-translationally modified peptides. Further characterization of TpnL will be needed to determine whether this reduction reflects the terminal step in series *a* thiopeptide biosynthesis or if the true biological substrate is an earlier intermediate. Regardless, TpnL represents a novel biosynthetic tool that may be useful in the development of additional thiopeptide metabolites.

5.1 References:

1. Miyairi, N.; Miyoshi, T.; Aoki, H.; Kosaka, M.; Ikushima, H., Thiopeptin, a new feed additive antibiotic: microbiological and chemical studies. *Antimicrob. Agents Chemother.* **1972**, *1*, 192-196.

2. Miyairi, N.; Miyoshi, T.; Aoki, H.; Kosaka, M.; Ikushima, H., Studies on thiopeptin antibiotics. I. Characteristics of thiopeptin B. *J. Antibiot.* **1970**, *23*, 113-119.

3. Kelly, W. L.; Pan, L.; Li, C., Thiostrepton biosynthesis: prototype for a new family of bacteriocins. *J. Am. Chem. Soc.* **2009**, *131*, 4327-4334.

4. Trejo, W. H.; Dean, L. D.; Pluscec, J.; Meyers, E.; Brown, W. E., *Streptomyces laurentii*, a new species producing thiostrepton. *J. Antibiot.* **1977**, *30*, 639-643.

APPENDIX A: PRIMERS, PLASMIDS, STRAINS, AND PROTEINS USED IN STUDY

Table A.1: Primers used in this study.

Primer	Sequence	Description
HI-1F	5'-TACAACCGCGAGCACGACT-3'	Primers for the amplification of a fragment of *tpnD* from the *S. tateyamensis* fosmid library.
HI-1R	5'-CTCGTACTCCTCCTCGAACG-3'	
HI-2F	5'-CTGCGGCTCTGGGTCTACT-3'	Primers for the amplification of a fragment of *tpnO* from the *S. tateyamensis* fosmid library.
HI-2R	5'-TGTTGTCGTGCTCGCTGT-3'	
HI-3F	5'-TCAACATGCACCTCTCGATG-3'	Primers for the amplification of a fragment of *tpnU* from the *S. tateyamensis* fosmid library.
HI-3R	5'-GCTGTAGGGGTGCATGGTT-3'	
HI-4F	5'-ATAAAGCTTGACTTGGTCAGCTCGTCCCAG-3'	Primers for the amplification of *tpnA* and flanking regions. The *Hin*dIII restriction sites are underlined.
HI-4R	5'-ATAAAGCTTAGCTCGTCCTCGGTCAGCTC-3'	
HI-5F	5'-GGCTGTAAAGAACTCAGTGATGGAGAGGTCTTTATCATGATTCCGGGGATCCGTCGACC-3'	Primers for the disruption of *tpnA* in pGM-tpnA. Underlined regions are homologous to *tpnA*. Regions that are not underlined are homologous to the *aac(3)IV/oriT* cassette of pIJ773.
HI-5R	5'-GTCCTCAACGGTGTGTCAGGAGCTGCAGCTGCAGGTGCATGTAGGCTGGAGCTGCTTC-3'	
HI-6F	5'-CATGTGATCACTCCCTGGTG-3'	Primers for the confirmation of *S. tateyamensis* HI1
HI-6R	5'-ATCAACTCGGCAAGATGCAG-3'	
HI-7F	5'-TCGATGGGCAGGTACTTCTC-3'	Primers for the confirmation of *S. tateyamensis* HI1
HI-7R	5'-GGTCCAGGTTCTCCAGCAT-3'	
HI-8F	5'-ATAAAGCTTCGGAGCTGCTGGCAGACCTG-3'	Primers for the amplification of *tpnL* and flanking regions. The *Hin*dIII restriction sites are underlined.
HI-8R	5'-ATAAAGCTTCCAACTGCCCTGCGTGTCCG-3'	
HI-9F	5'-ATGACCGCCGAAGCAGCTTTCGTCCCGATCCGCGCCGCGATTCCGGGGATCCGTCGACC-3'	Primers for the disruption of *tpnL* in pGM-tpnL. Underlined regions are homologous to *tpnL*. Regions that are not underlined are homologous to the *aac(3)IV/oriT* cassette of pIJ773.
HI-9R	5'-TCAGGCGACCTGCTCGGCGACGGCCGGCAGCCCGGCCTCTGTAGGCTGGAGCTGCTTC-3'	
HI-10F	5'-ATAAAGCTTGTGCCGCACAACGCCACCCT-3'	Primers for the amplification of *tpnM* and flanking regions. The *Hin*dIII restriction sites are underlined.
HI-10R	5'-ATAAAGCTTCGGTGATCCGCCACAGGTTGC-3'	
HI-11F	5'-CAGTTGGCGCAGCGTCAGTTCGAGCGGTGCGGGATCAGCATTCCGGGGATCCGTCGACC-3'	Primers for the disruption of *tpnM* in pGM-tpnM. Underlined regions are homologous to *tpnM*. Regions that are not underlined are homologous to the *aac(3)IV/oriT* cassette of pIJ773.
HI-11R	5'-CACCCGGACCACCGCGAGCTCCTCCCCGGGGGCGGTCAGTGTAGGCTGGAGCTGCTTC-3'	

Table A.1 (continued)

HI-12F	5'-ATAAAGCTTGTCACCGGACTGGACGTACT-3'	Primers for the amplification of *tpnN* and flanking regions. The *Hin*dIII restriction sites are underlined.
HI-12R	5'-ATAAAGCTTTCGGCGAAGGTGTAGTAGGT-3'	
HI-13F	5'-CACGAGGGCGTCCGGGTGGCCGGCGCGAGCAGCATGGGCATTCCGGGGATCCGTCGACC-3'	Primers for the disruption of *tpnN* in pGM-tpnN. Underlined regions are homologous to *tpnN*. Regions that are not underlined are homologous to the *aac(3)IV/oriT* cassette of pIJ773.
HI-13R	5'-TTGGCCAAGGCCCGTGAGCCCGCGGTCCCAGCAGGCGGTTGTAGGCTGGAGCTGCTTC-3'	
HI-14F	5'-ATAAAGCTTCTGCCTGCTGGATCAACTCGG-3'	Primers for the amplification of *tpnR* and flanking regions. The *Hin*dIII restriction sites are underlined.
HI-14R	5'-ATAAAGCTTCCGACCACCAGCGAGTACC-3'	
HI-15F	5'-ACACCGGTGCGGGTCAGCGCGGTGCTCTGCTCCCCGCCGATTCCGGGGATCCGTCGACC-3'	Primers for the disruption of *tpnR* in pGM-tpnR. Underlined regions are homologous to *tpnR*. Regions that are not underlined are homologous to the *aac(3)IV/oriT* cassette of pIJ773.
HI-15R	5'-GCCGGCGCTCGGCGAATAGTCGGACTGTTCGTTCCGGACTGTAGGCTGGAGCTGCTTC-3'	
HI-16F	5'-ATACATATGAGCGCTCCCACCGAA-3'	Primers for the amplification of *tpnA* for genetic complementation in *S. tateyamensis* HI1. The *Nde*I and *Eco*RI restriction sites are underlined.
HI-16R	5'-TAATATGAATTCTCAGGAGCTGCAGCTGCA-3'	
HI-17F	5'-GAGCAACTGGTGGCCGAC-3'	Primers for the amplification of *tpnW* and flanking regions.
HI-17R	5'-CACCTTCACCGACGAGGG-3'	
HI-18F	5'-ATACATATGTCGGCCGCCGCCGGG-3'	Primers for the amplification of *tpnW* for expression in *E. coli*. The *Nde*I and *Eco*RI restriction sites are underlined.
HI-18R	5'-ACATATGAATTCTCAACCGCTGACTGACGGGCAGTC-3'	
HI-19F	5'-CGACTCTAGGGAGCTCGGTA-3'	Primers for confirmation of *S. laurentii* HI0.
HI-19R	5'-TACCGCCTTTGAGTGAGCTG-3'	
HI-20F	5'-CATATGACCGCCGAAGCAGCT-3'	Primers for the amplification of *tpnL* for expression in *S. laurentii*. The *Nde*I restriction site is underlined.
HI-20R	5'-TGTACAATGCATCAGGCGACCTGCTCG-3'	
HI-21F	5'-CATATGACGGCCCAACAG-3'	Primers for the amplification of *tpnM* for expression in *S. laurentii*. The *Nde*I restriction site is underlined.
HI-21R	5'-TGTACAATGCATTCATCGGCCCTCCTCGG-3'	
HI-22F	5'-CATATGACCACGCACGTGTTC-3'	Primers for the amplification of *tpnN* for expression in *S. laurentii*. The *Nde*I restriction site is underlined.
HI-22R	5'-TGTACAATGCATTCATGACGGCTCCCTTC-3'	
HI-23F	5'-ATGCATGTGGGCTGCCTGATCCTG-3'	Primers for the amplification of *tpnR* for expression in *S. laurentii*.
HI-23R	5'-TGTACATCAGCTGGGGAAATGGCG-3'	
HI-24F	5'-ATTATACATATGACCGCCGAAGCAGCT-3'	Primers for the amplification of *tpnL* for expression in *E. coli*. The *Nde*I and *Hin*dIII restriction sites are underlined.
HI-24R	5'-ATAAAGCTTTCAGGCGACCTGCTCGGC-3'	
HI-25F	5'-ATGGACCACATGCCCAGCACGCC-3'	Primers for the amplification of an F_0-synthase candidate in *S. tateyamensis*.
HI-25R	5'-CCGCTCGGGCGGGACCTC-3'	

Table A.2: Strains and plasmids used in this study

Strain/Plasmid	Description	Reference or Source
E. coli strains		
BL21(DE3)	Host for protein expression	
BW25113/pKD46	Host for PCR-targeted disruption of a gene from a plasmid	[1]
EPI300	Host for inducing high copy number of a fosmid	Epicenter (Lucigen)
ET12567/pUZ8002	Host for conjugation with *Streptomyces* species	[2]
Streptomyces strains		
S. laurentii ATCC 31255	Wild type, thiostrepton A producer	ATCC
S. laurentii HI0	*S. laurentii* containing pSET1520	This study
S. laurentii HI1	*S. laurentii* containing pSET1520-tpnL	This study
S. laurentii HI2	*S. laurentii* containing pSET1520-tpnM	This study
S. laurentii HI3	*S. laurentii* containing pSET1520-tpnN	This study
S. laurentii HI4	*S. laurentii* containing pSET1520-tpnR	This study
S. laurentii HI5	*S. laurentii* containing pSET1520-tpnLM	This study
S. laurentii HI6	*S. laurentii* containing pSET1520-tpnMN	This study
S. laurentii HI7	*S. laurentii* containing pSET1520-tpnLMN	This study
S. tateyamensis ATCC 21389	Wild type, thiopeptin producer	ATCC
S. tateyamensis HI1	*S. tateyamensis tpnA* mutant	This study
Plasmids		
HI2B7	pCC1FOS fosmid containing a fragment (*tpnW-tpnJ*) of the *tpn* gene cluster	This study
HI2G2	pCC1FOS fosmid containing a fragment (*tpnF-tpnP*) of the *tpn* gene cluster	This study
JP8D9	pCC1FOS fosmid of the *S. laurentii* genomic fosmid library	[3]
pCC1FOS	Fosmid used for genomic library construction	Lucigen
pET28b(+)	Vector for protein expression in *E. coli*	Novagen
pET28b-tpnL	Plasmid for TpnL expression in *E. coli*	This study
pET28b-tpnW	Plasmid for TpnW expression in *E. coli*	This study
pGM160HKss	A derivative of pGM160HK, in which the ampicillin resistance gene was replaced by the spectinomycin-streptomycin resistance cassette. It is a conjugal and temperature-sensitive *E. coli-Streptomyces* shuttle vector	[4]
pGM-dtpnA	pGM-tpnA with an *aac(3)IV/oriT* inserted at *tpnA*	This study
pGM-dtpnL	pGM-tpnL with an *aac(3)IV/oriT* inserted at *tpnL*	This study
pGM-dtpnM	pGM-tpnM with an *aac(3)IV/oriT* inserted at *tpnM*	This study
pGM-dtpnN	pGM-tpnN with an *aac(3)IV/oriT* inserted at *tpnN*	This study
pGM-dtpnR	pGM-tpnR with an *aac(3)IV/oriT* inserted at *tpnR*	This study
pGM-tpnA	pGM160HKss containing *tpnA* and flanking regions	This study
pGM-tpnL	pGM160HKss containing *tpnL* and flanking regions	This study
pGM-tpnM	pGM160HKss containing *tpnM* and flanking regions	This study
pGM-tpnN	pGM160HKss containing *tpnN* and flanking regions	This study
pGM-tpnR	pGM160HKss containing *tpnR* and flanking regions	This study

Table A.2 (contined)

pSET1520	Derivative of pSET152 with a *ermE** and RBS of pET-series vector inserted into an MCS site	[5]
pSET1520-TpnL	Integrative plasmid for *tpnL* expression in *S. laurentii*	This study
pSET1520-TpnLM	Integrative plasmid for *tpnLM* expression in *S. laurentii*	This study
pSET1520-TpnLMN	Integrative plasmid for *tpnLMN* expression in *S. laurentii*	This study
pSET1520-TpnM	Integrative plasmid for *tpnM* expression in *S. laurentii*	This study
pSET1520-TpnMN	Integrative plasmid for *tpnMN* expression in *S. laurentii*	This study
pSET1520-TpnN	Integrative plasmid for *tpnN* expression in *S. laurentii*	This study
pSET1520-TpnR	Integrative plasmid for *tpnR* expression in *S. laurentii*	This study
pSET1520ss	Derivative of pSET152, with a *ermE** and RBS of pET-series vector inserted into MCS site, and apramycin resistance gene replaced by spectinomycin/streptomycin resistance gene	[6]
pSET1520ss-TpnA	pSET1520ss containing a functional *tpnA*	This study
pSC-B-amp/kan	A routine vector from StrataClone Blunt PCR Cloning Kit, for cloning a blunt-end PCR product	Agilent
pSC-B-tpnL	pSC-B-amp/kan containing *tpnL;* an *Eco*RI site is 3' to the stop codon of *tpnL*	This study
pTpnL	pSC-B-amp/kan containing *tpnL* and flanking regions	This study
pTpnM	pSC-B-amp/kan containing *tpnM* and flanking regions	This study
pTpnN	pSC-B-amp/kan containing *tpnN* and flanking regions	This study
pTpnR	pSC-B-amp/kan containing *tpnR* and flanking regions	This study
ptpnW	pSC-B-amp/kan containing *tpnW* and flanking regions	This study
ptpnW2	pSC-B-amp/kan containing *tpnW*	This study

Table A.3: NCBI accession numbers of proteins used to construct the TpnL homolog phylogenetic tree.

Source organism	Accession number	Homology to TpnL[a]
Actinoalloteichus hoggarensis sp. nov. DSM 45943	WP_093941972.1	45/60
Amycolatopsis saalfeldensis DSM 44993	SEO90151.1	70/78
Chloroflexi bacterium RBG_13_68_17	OGO13680.1	53/64
Jiangella alkaliphila DSM 45079	SDU67749.1	46/55
Jiangella sp. DSM 45060	SDT24520.1	45/56
Micromonospora carbonacea DSM 43168	SCF23526.1	53/62
Micromonospora carbonacea var. africana ATCC 39149	EEP73611.1	50/61
Mycobacterium smegmatis MC^2 155	YP_888093.1	19/29
Mycobacterium tuberculosis H37Rv	NP_217507.1	24/34
Mycobacterium tuberculosis H37Rv	WP_003898745.1	18/29
Mycobacterium tuberculosis H37Rv	WP_003899157.1	18/24
Streptacidiphilus anmyonensis sp. nov NBRC 103185	WP_042427374.1	52/60
Streptomyces hygroscopicus XM201	AQW53324.1	41/52
Streptomyces rimosus ATCC 10970	L8EYU3.1	22/28
Streptomyces sp. GP55	PKV74444.1	48/62
Streptomyces viridochromogenes NRRL 3413	KOG13857.1	32/50

[a] homology to TpnL is shown in % identity/similarity.

A.1 References

1. Datsenko, K. A.; Wanner, B. L. One-step inactivation of chromosomal genes in *Escherichia coli* K-12 using PCR products. *Proc. Natl. Acad. Sci. U.S.A.* **2000**, *97*, 6640-6645.
2. Gust, B.; Challis, G. L.; Fowler, K.; Kieser, T.; Chater, K. F. PCR-targeted *Streptomyces* gene replacement identifies a protein domain needed for biosynthesis of the sesquiterpene soil odor geosmin. *Proc. Natl. Acad. Sci. U.S.A.* **2003**, *100*, 1541-1546.
3. Kelly, W. L.; Pan, L.; Li, C. Thiostrepton biosynthesis: prototype for a new family of bacteriocins. *J. Am. Chem. Soc.* **2009**, *131*, 4327-4334.
4. Li, C.; Zhang, F.; Kelly, W. L. Heterologous production of thiostrepton A and biosynthetic engineering of thiostrepton analogs. *Mol. BioSyst.* **2011**, *7*, 82-90.
5. Palaniappan, N.; Alhamadsheh, M. M.; Reynolds, K. A. *cis*-$\Delta^{2,3}$-double bond of phoslactomycins is generated by a post-PKS tailoring enzyme. *J. Am. Chem. Soc.* **2008**, *130*, 12236-12237.
6. Rommel, K. R.; Li, C.; Kelly, W. L. Identification of a tetraene-containing product of the indanomycin biosynthetic pathway. *Org. Lett.* **2011**, *13*, 2536-2539.

APPENDIX B: SPECTRA

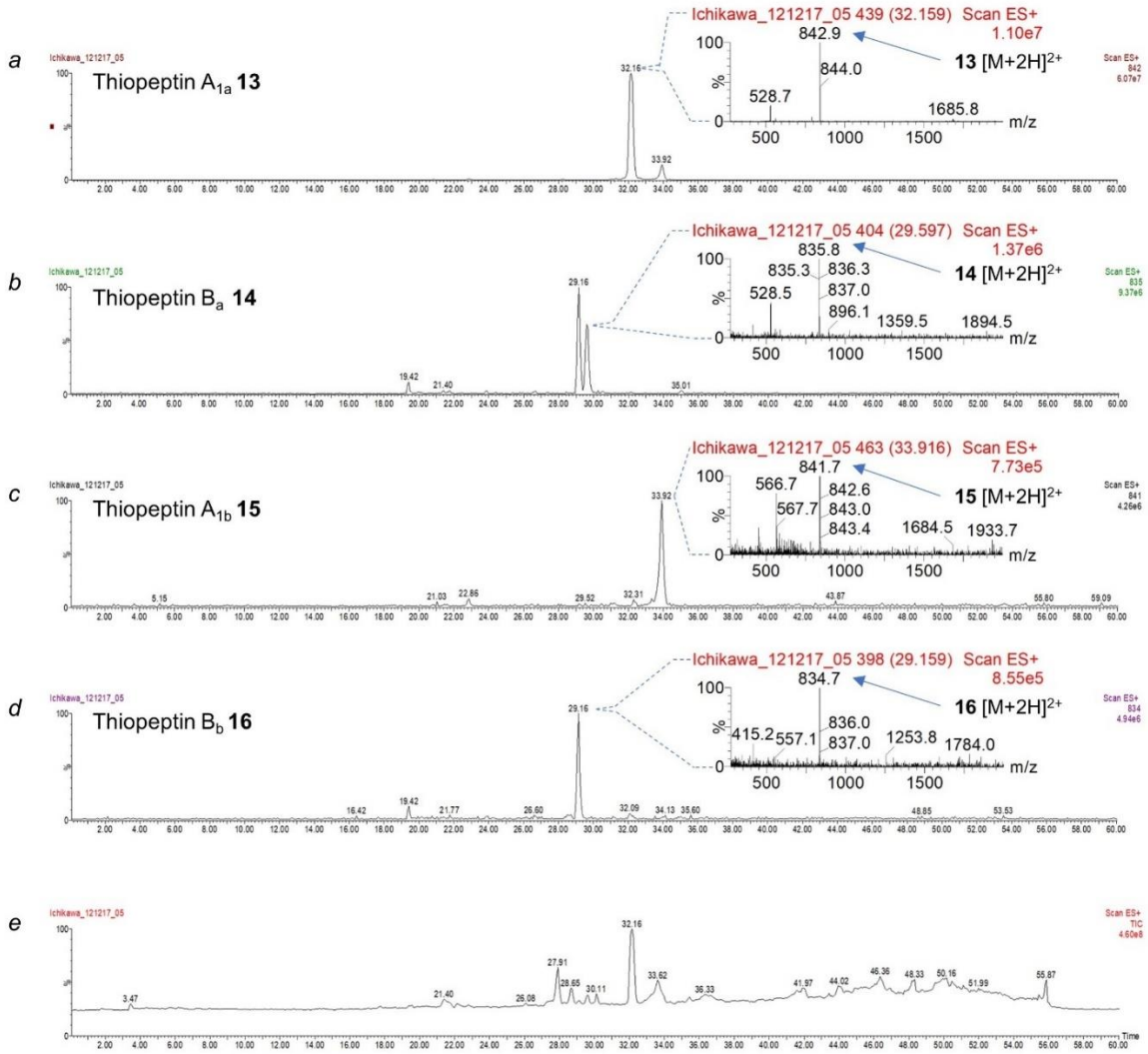

Figure B.1: HPLC-MS analysis of a crude culture extract from *S. tateyamensis.* (*a*) Extracted ion chromatogram of *m/z* 842 for thiopeptin A_{1a} **13** (calculated $[M+2H]^{2+}$ *m/z* = 842.2) and the mass spectrum at t_R = 32.16 min (inset). (*b*) Extracted ion chromatogram of *m/z* 835 for thiopeptin B_a **14** (calculated $[M+2H]^{2+}$ *m/z* = 835.2) and the mass spectrum at t_R = 29.60 min (inset). (*c*) Extracted ion chromatogram of *m/z* 841 for thiopeptin A_{1b} **15** (calculated $[M+2H]^{2+}$ *m/z* = 841.2) and the mass spectrum at t_R = 33.92 min (inset). (*d*) Extracted ion chromatogram of *m/z* 834 for thiostrepton B_b **16** (calculated $[M+2H]^{2+}$ *m/z* = 834.2) and the mass spectrum at t_R = 29.16 min (inset). (*e*) Total ion chromatogram of the crude culture extract from *S. tateyamensis*.

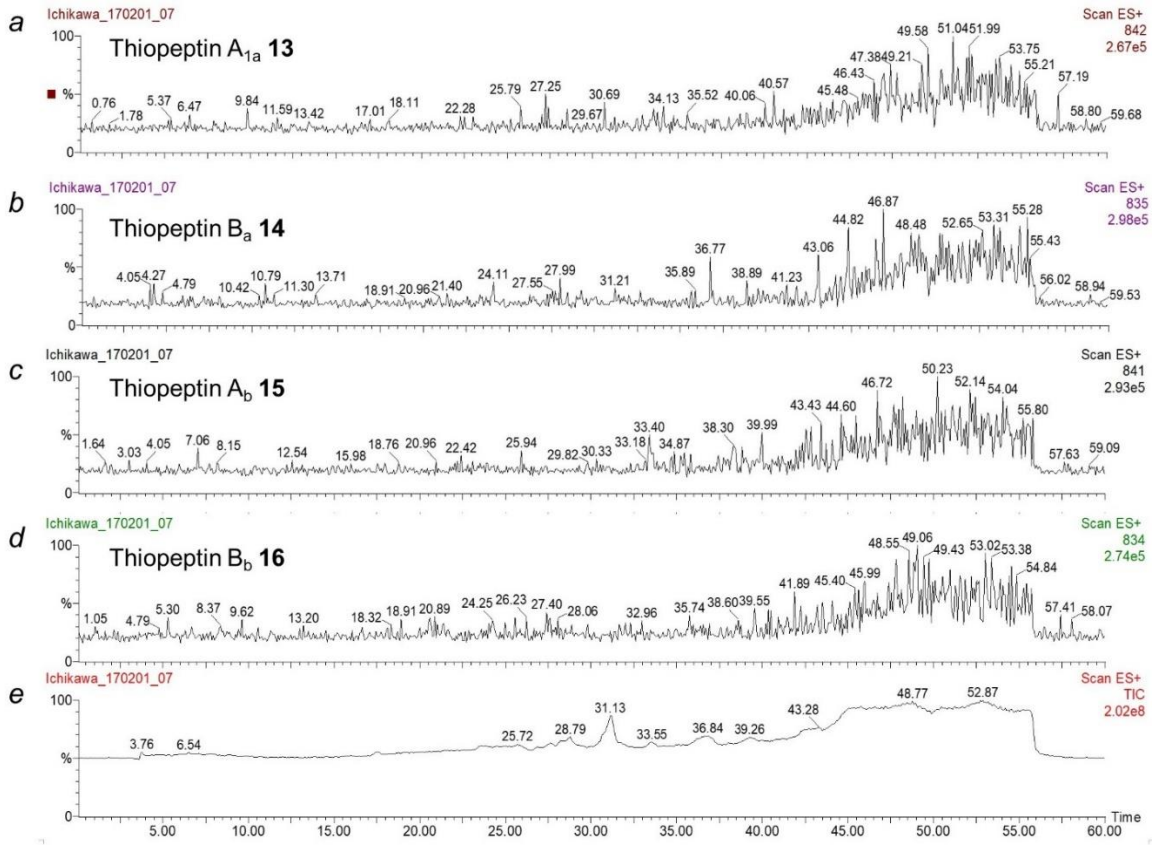

Figure B.2: HPLC-MS analysis of a crude culture extract from *S. tateyamensis* HI1. (*a*) Extracted ion chromatogram of *m/z* 842 for thiopeptin A_{1a} **13** (calculated $[M+2H]^{2+}$ *m/z* = 842.2). (*b*) Extracted ion chromatogram of *m/z* 835 for thiopeptin B_a **14** (calculated $[M+2H]^{2+}$ *m/z* = 835.2). (*c*) Extracted ion chromatogram of *m/z* 841 for thiopeptin A_{1b} **15** (calculated $[M+2H]^{2+}$ *m/z* = 841.2). (*d*) Extracted ion chromatogram of *m/z* 834 for thiostrepton B_b **16** (calculated $[M+2H]^{2+}$ *m/z* = 834.2). (*e*) Total ion chromatogram of the crude culture extract from *S. tateyamensis* HI1.

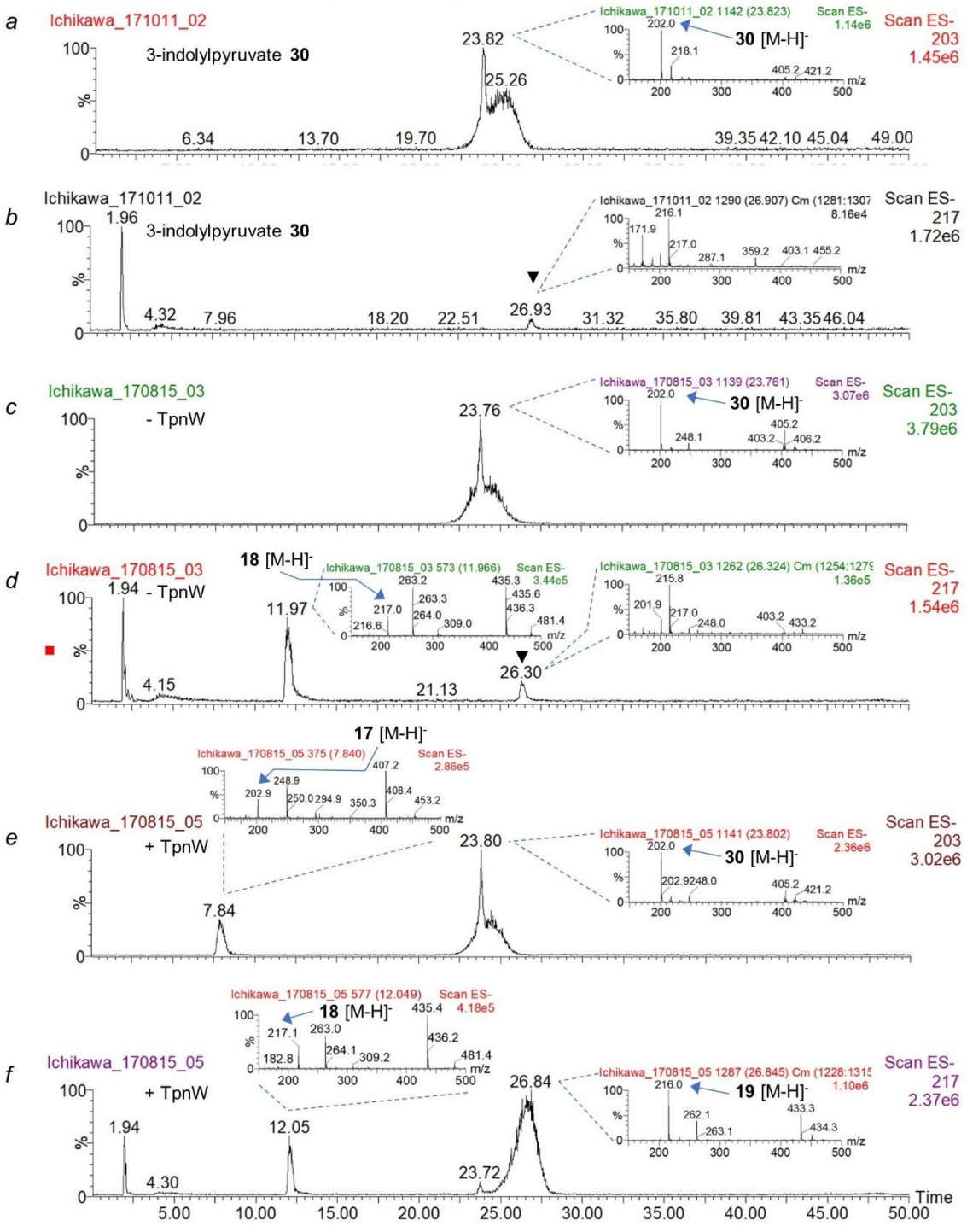

Figure B.3: HPLC-MS analyses of the *in vitro* reconstitution of TpnW transamination activity after 30 minute reaction time. (*a*) Extracted ion chromatogram of *m/z* 203 L-tryptophan **17** (calculated $[M\text{-}H]^-$ *m/z* = 203.1) and 3-indolylpyruvate **30** (calculated $[M\text{-}H]^-$ *m/z* = 202.1) and the mass spectrum at t_R = 23.82 min (inset) from the 3-indolylpyruvate **30** standard. (*b*) Extracted ion chromatogram of *m/z* 217 for 3-(2-methylindolyl)pyruvate

19 (calculated $[M-H]^-$ *m/z* = 216.1) and 2-methyl-L-tryptophan **18** (calculated $[M-H]^-$ *m/z* = 217.1) and the mass spectrum at t_R~26.93 min (inset) from the **30** standard. (*c*) Extracted ion chromatogram of *m/z* 203 and the mass spectrum at t_R = 23.76 min (inset) in the reaction mixture lacking TpnW. (*d*) Extracted ion chromatogram of *m/z* 217 and the mass spectrum at t_R = 11.97 min and t_R ~26.30 min (inset) in the reaction mixture lacking TpnW. (*e*) Extracted ion chromatogram of *m/z* 203 and the mass spectrum at t_R = 7.84 min and t_R ~23.80 min (inset) in the reaction mixture containing TpnW. (*f*) Extracted ion chromatogram of *m/z* 217 and the mass spectrum at t_R = 12.05 min and t_R ~26.84 min (inset) in the reaction mixture containing TpnW. The compound indicated by (▼) was observed in all reactions and has an identical *m/z* with **30** but has a slightly earlier t_R. ▼may be a contaminant, a degradation product, or an artifact of HPLC-MS analysis.

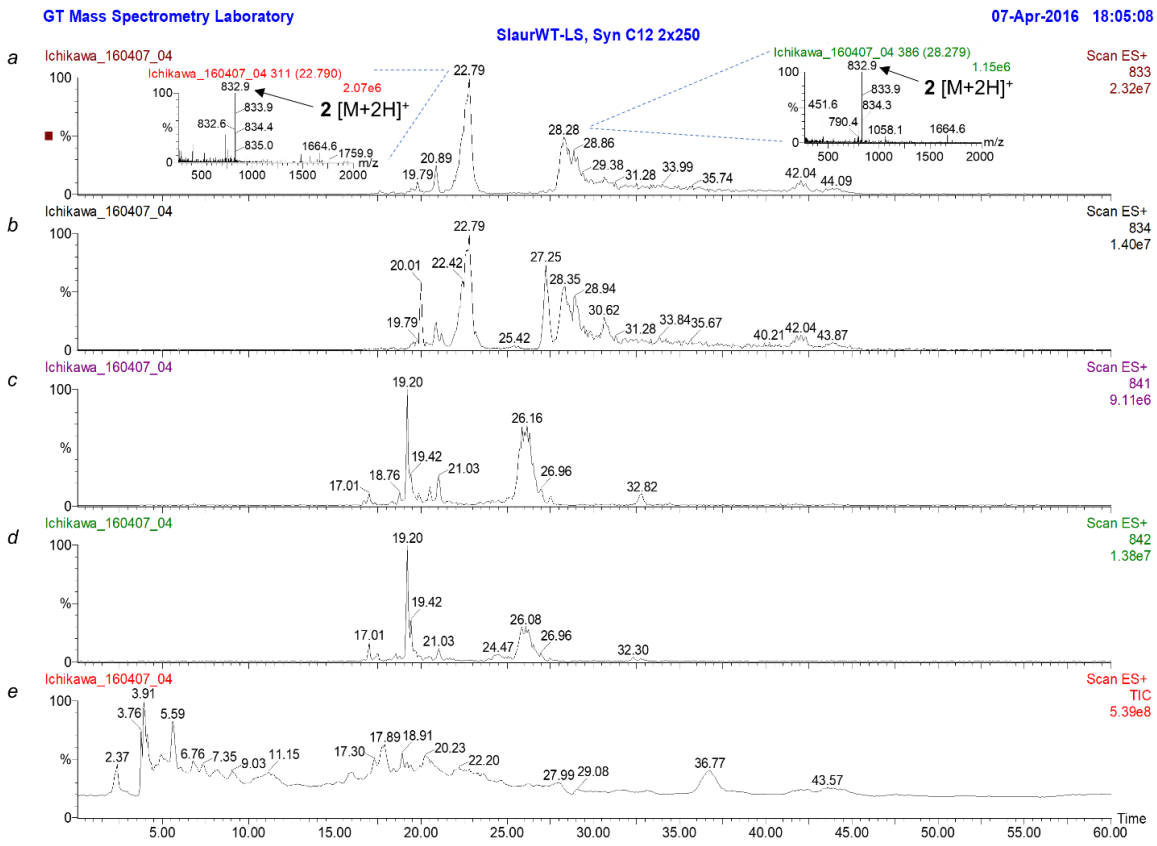

Figure B.4: HPLC-MS analyses of the crude culture extract from *S. laurentii*. (*a*) Extracted ion chromatogram of *m/z* 833 thiostrepton A **2** (calculated $[M+2H]^+$ *m/z* = 832.8) and the mass spectra at t_R = 22.79 min and t_R = 28.28 min (inset). (*b*) Extracted ion chromatogram of *m/z* 834 piperidine-containing thiostrepton analog **31** (calculated $[M+2H]^+$ *m/z* = 833.8). (*c*) Extracted ion chromatogram of *m/z* 841 thioamide-containing thiostrepton analog **32** (calculated $[M+2H]^+$ *m/z* = 840.7). (*d*) Extracted ion chromatogram of *m/z* 842 piperidine and thioamide-containing thiostrepton analog **33** (calculated $[M+2H]^+$ *m/z* = 841.8). (*e*) Total ion chromatogram of the crude culture extract from *S. laurentii*.

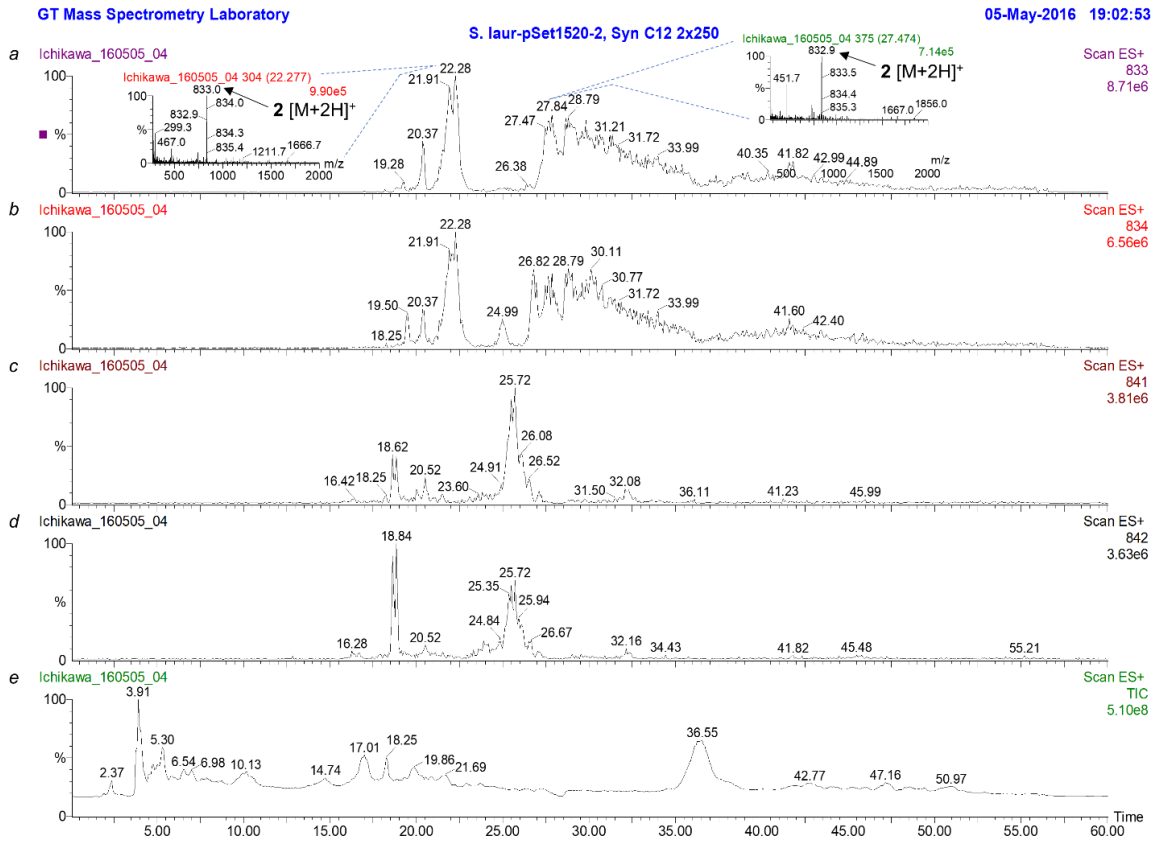

Figure B.5: HPLC-MS analyses of the crude culture extract from *S. laurentii* HI0, which houses the empty pSET1520 vector. (*a*) Extracted ion chromatogram of *m/z* 833 thiostrepton A **2** (calculated $[M+2H]^+$ *m/z* = 832.8) and the mass spectra at t_R = 22.28 min and t_R = 27.47 min (inset). (*b*) Extracted ion chromatogram of *m/z* 834 piperidine-containing thiostrepton analog **31** (calculated $[M+2H]^+$ *m/z* = 833.8). (*c*) Extracted ion chromatogram of *m/z* 841 thioamide-containing thiostrepton analog **32** (calculated $[M+2H]^+$ *m/z* = 840.7). (*d*) Extracted ion chromatogram of *m/z* 842 piperidine and thioamide-containing thiostrepton analog **33** (calculated $[M+2H]^+$ *m/z* = 841.8). (*e*) Total ion chromatogram of the crude culture extract from *S. laurentii* HI0.

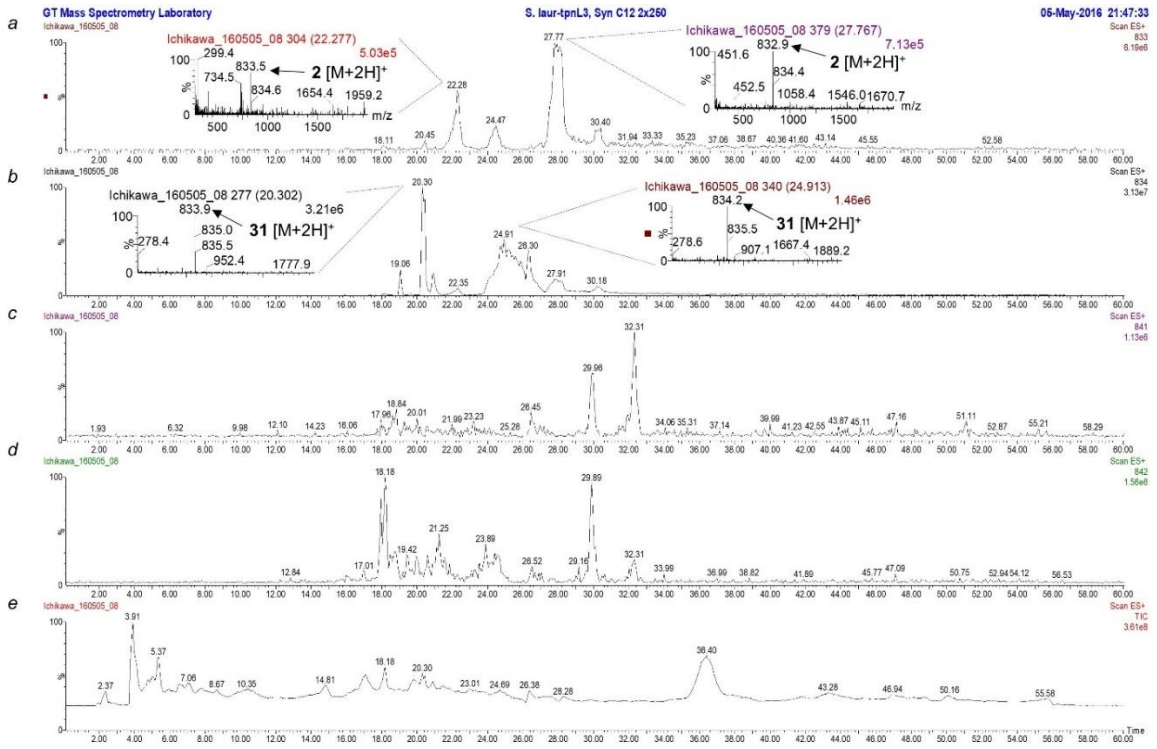

Figure B.6: HPLC-MS analyses of the crude culture extract from *S. laurentii* HI1, a strain that expresses TpnL. (*a*) Extracted ion chromatogram of *m/z* 833 thiostrepton A **2** (calculated $[M+2H]^+$ *m/z* = 832.8) and the mass spectra at t_R = 22.28 min and t_R = 27.77 min (inset). (*b*) Extracted ion chromatogram of *m/z* 834 piperidine-containing thiostrepton analog **31** (calculated $[M+2H]^+$ *m/z* = 833.8) and the mass spectra at t_R = 20.30 and t_R = 24.91 min (inset). (*c*) Extracted ion chromatogram of *m/z* 841 thioamide-containing thiostrepton analog **32** (calculated $[M+2H]^+$ *m/z* = 840.7). (*d*) Extracted ion chromatogram of *m/z* 842 piperidine and thioamide-containing thiostrepton analog **33** (calculated $[M+2H]^+$ *m/z* = 841.8). (*e*) Total ion chromatogram of the crude culture extract from *S. laurentii* HI2.

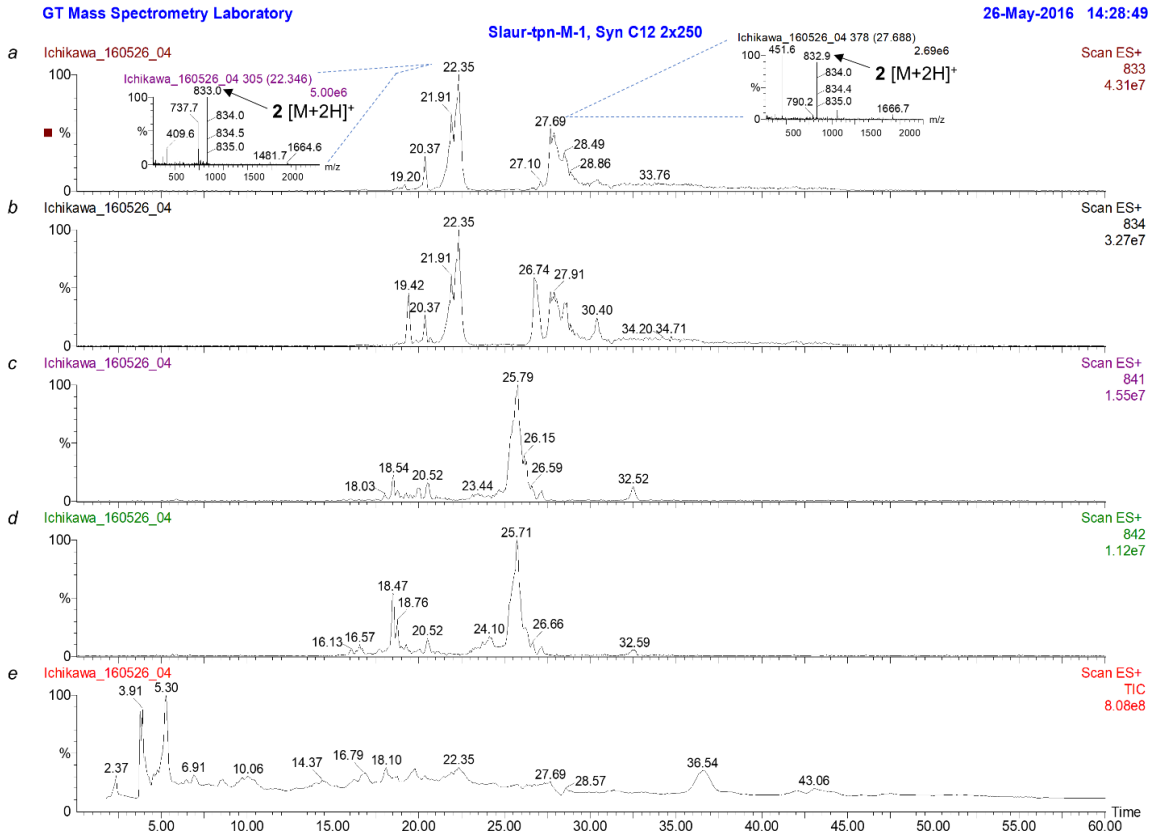

Figure B.7: HPLC-MS analyses of the crude culture extract from *S. laurentii* HI2, a strain that expresses TpnM. (*a*) Extracted ion chromatogram of *m/z* 833 thiostrepton A **2** (calculated $[M+2H]^+$ *m/z* = 832.8) and the mass spectra at t_R = 22.35 min and t_R = 27.69 min (inset). (*b*) Extracted ion chromatogram of *m/z* 834 piperidine-containing thiostrepton analog **31** (calculated $[M+2H]^+$ *m/z* = 833.8). (*c*) Extracted ion chromatogram of *m/z* 841 thioamide-containing thiostrepton analog **32** (calculated $[M+2H]^+$ *m/z* = 840.7). (*d*) Extracted ion chromatogram of *m/z* 842 piperidine and thioamide-containing thiostrepton analog **33** (calculated $[M+2H]^+$ *m/z* = 841.8). (*e*) Total ion chromatogram of the crude culture extract from *S. laurentii* HI2.

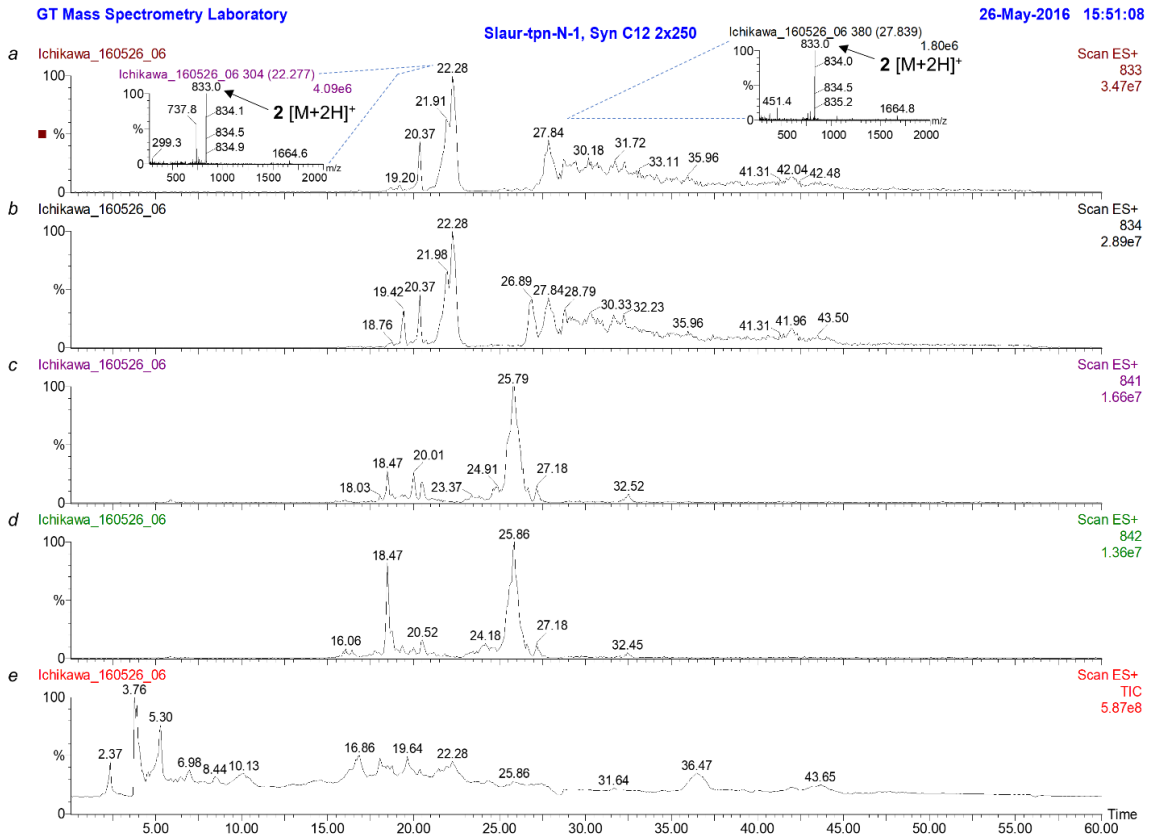

Figure B.8: HPLC-MS analyses of the crude culture extract from *S. laurentii* HI3, a strain that expresses TpnN. (*a*) Extracted ion chromatogram of *m/z* 833 thiostrepton A **2** (calculated $[M+2H]^+$ *m/z* = 832.8) and the mass spectra at t_R = 22.28 min and t_R = 27.84 min (inset). (*b*) Extracted ion chromatogram of *m/z* 834 piperidine-containing thiostrepton analog **31** (calculated $[M+2H]^+$ *m/z* = 833.8). (*c*) Extracted ion chromatogram of *m/z* 841 thioamide-containing thiostrepton analog **32** (calculated $[M+2H]^+$ *m/z* = 840.7). (*d*) Extracted ion chromatogram of *m/z* 842 piperidine and thioamide-containing thiostrepton analog **33** (calculated $[M+2H]^+$ *m/z* = 841.8). (*e*) Total ion chromatogram of the crude culture extract from *S. laurentii* HI3.

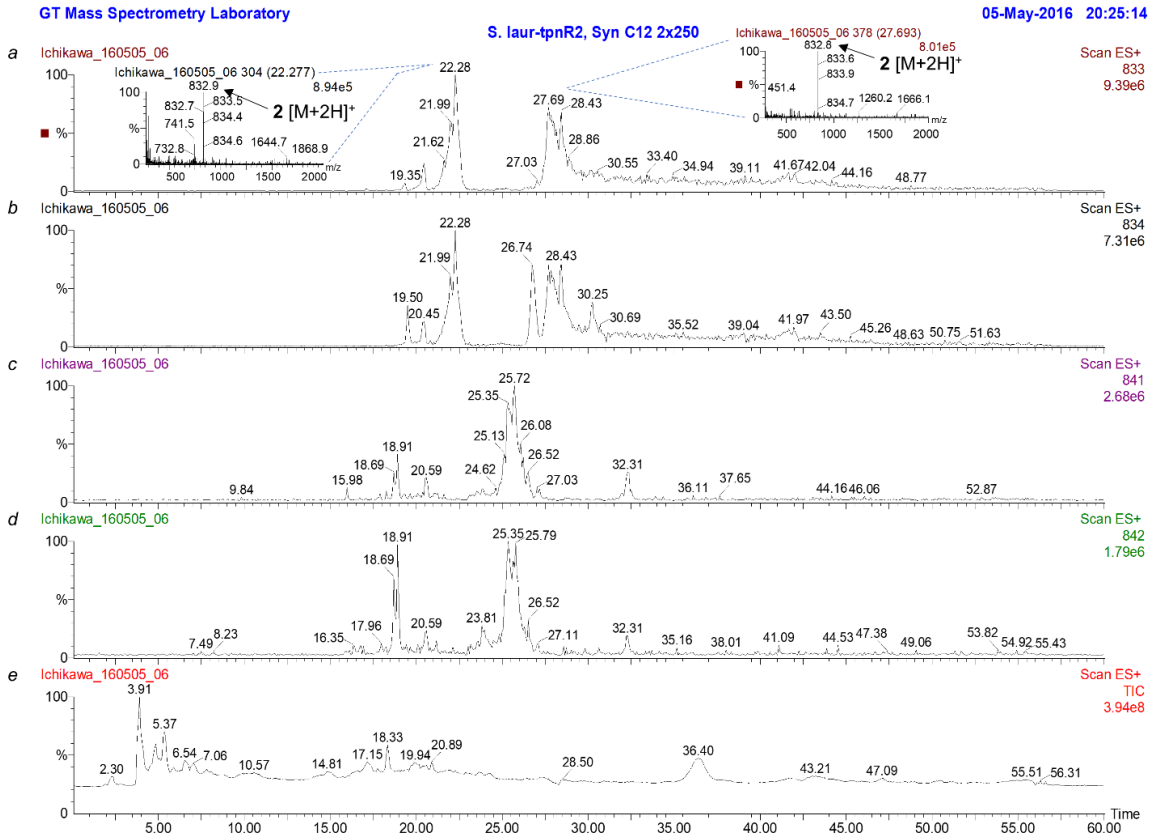

Figure B.9: HPLC-MS analyses of the crude culture extract from *S. laurentii* HI4, a strain that expresses TpnR. (*a*) Extracted ion chromatogram of *m/z* 833 thiostrepton A **2** (calculated $[M+2H]^+$ *m/z* = 832.8) and the mass spectra at t_R = 22.28 min and t_R = 27.69 min (inset). (*b*) Extracted ion chromatogram of *m/z* 834 piperidine-containing thiostrepton analog **31** (calculated $[M+2H]^+$ *m/z* = 833.8). (*c*) Extracted ion chromatogram of *m/z* 841 thioamide-containing thiostrepton analog **32** (calculated $[M+2H]^+$ *m/z* = 840.7). (*d*) Extracted ion chromatogram of *m/z* 842 piperidine and thioamide-containing thiostrepton analog **33** (calculated $[M+2H]^+$ *m/z* = 841.8). (*e*) Total ion chromatogram of the crude culture extract from *S. laurentii* HI4.

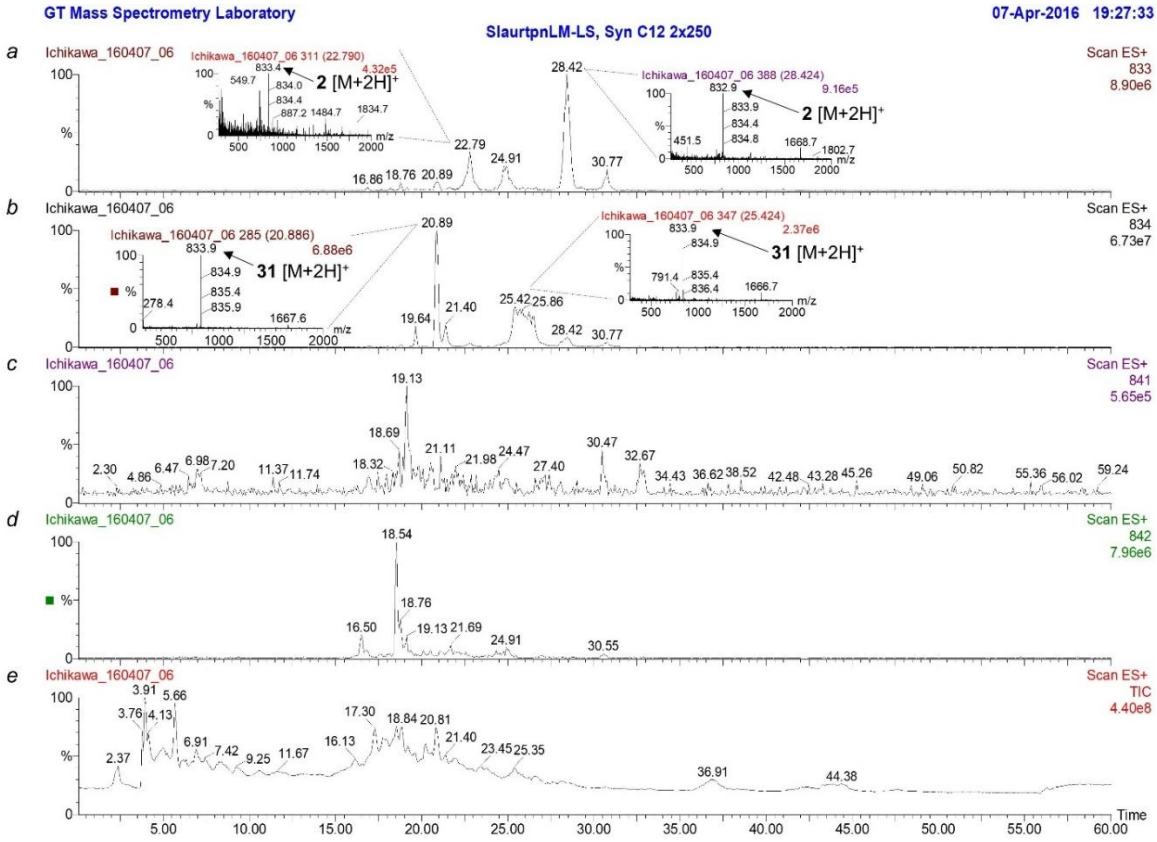

Figure B.10: HPLC-MS analyses of the crude culture extract from *S. laurentii* HI5, a strain that coexpresses TpnLM. (*a*) Extracted ion chromatogram of *m/z* 833 thiostrepton A **2** (calculated $[M+2H]^+$ *m/z* = 832.8) and the mass spectra at t_R = 22.79 min and t_R = 28.42 min (inset). (*b*) Extracted ion chromatogram of *m/z* 834 piperidine-containing thiostrepton analog **31** (calculated $[M+2H]^+$ *m/z* = 833.8) and the mass spectra at t_R = 20.89 min and t_R = 25.42 min (inset). (*c*) Extracted ion chromatogram of *m/z* 841 thioamide-containing thiostrepton analog **32** (calculated $[M+2H]^+$ *m/z* = 840.7). (*d*) Extracted ion chromatogram of *m/z* 842 piperidine and thioamide-containing thiostrepton analog **33** (calculated $[M+2H]^+$ *m/z* = 841.8). (*e*) Total ion chromatogram of the crude culture extract from *S. laurentii* HI5.

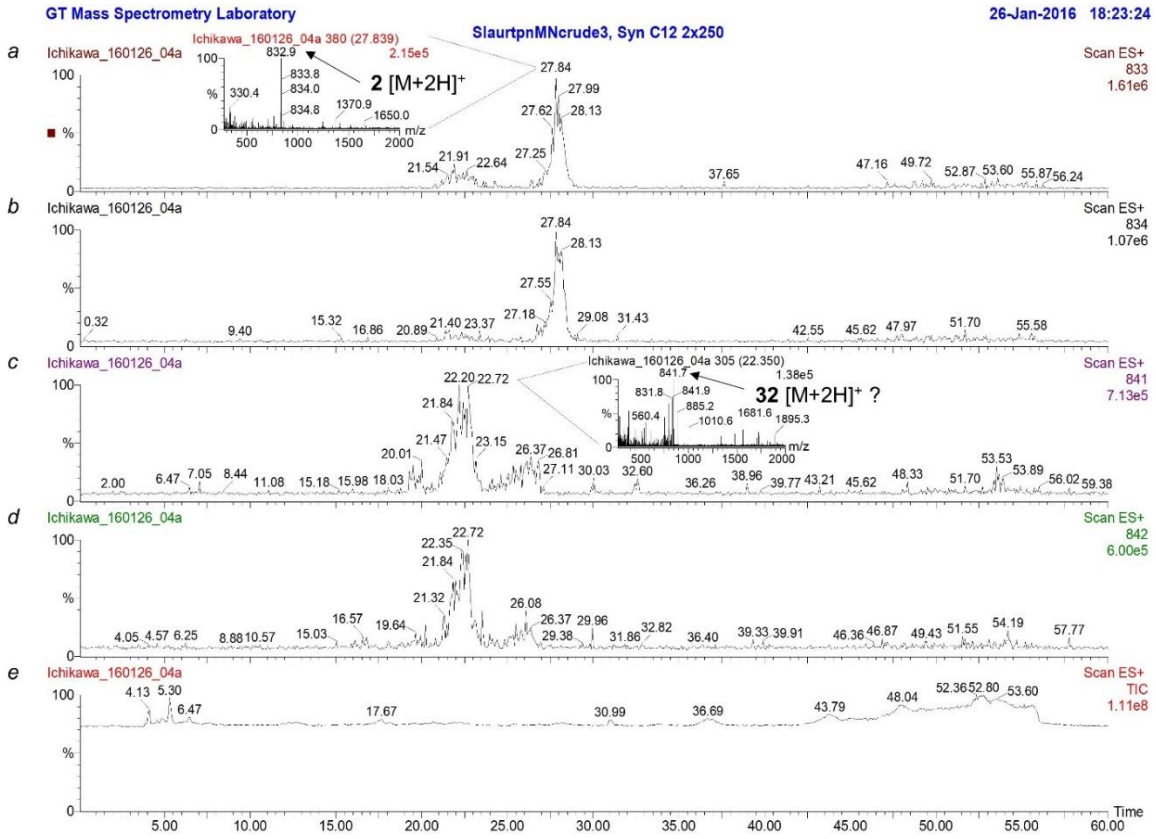

Figure B.11: HPLC-MS analyses of the crude culture extract from *S. laurentii* HI6, a strain that coexpresses TpnMN. (*a*) Extracted ion chromatogram of *m/z* 833 thiostrepton A **2** (calculated $[M+2H]^+$ *m/z* = 832.8) and the mass spectrum at t_R = 27.84 (inset). (*b*) Extracted ion chromatogram of *m/z* 834 piperidine-containing thiostrepton analog **31** (calculated $[M+2H]^+$ *m/z* = 833.8). (*c*) Extracted ion chromatogram of *m/z* 841 thioamide-containing thiostrepton analog **32** (calculated $[M+2H]^+$ *m/z* = 840.7) and the mass spectrum at t_R = 22.35 (inset). (*d*) Extracted ion chromatogram of *m/z* 842 piperidine and thioamide-containing thiostrepton analog **33** (calculated $[M+2H]^+$ *m/z* = 841.8). (*e*) Total ion chromatogram of the crude culture extract from *S. laurentii* HI6.

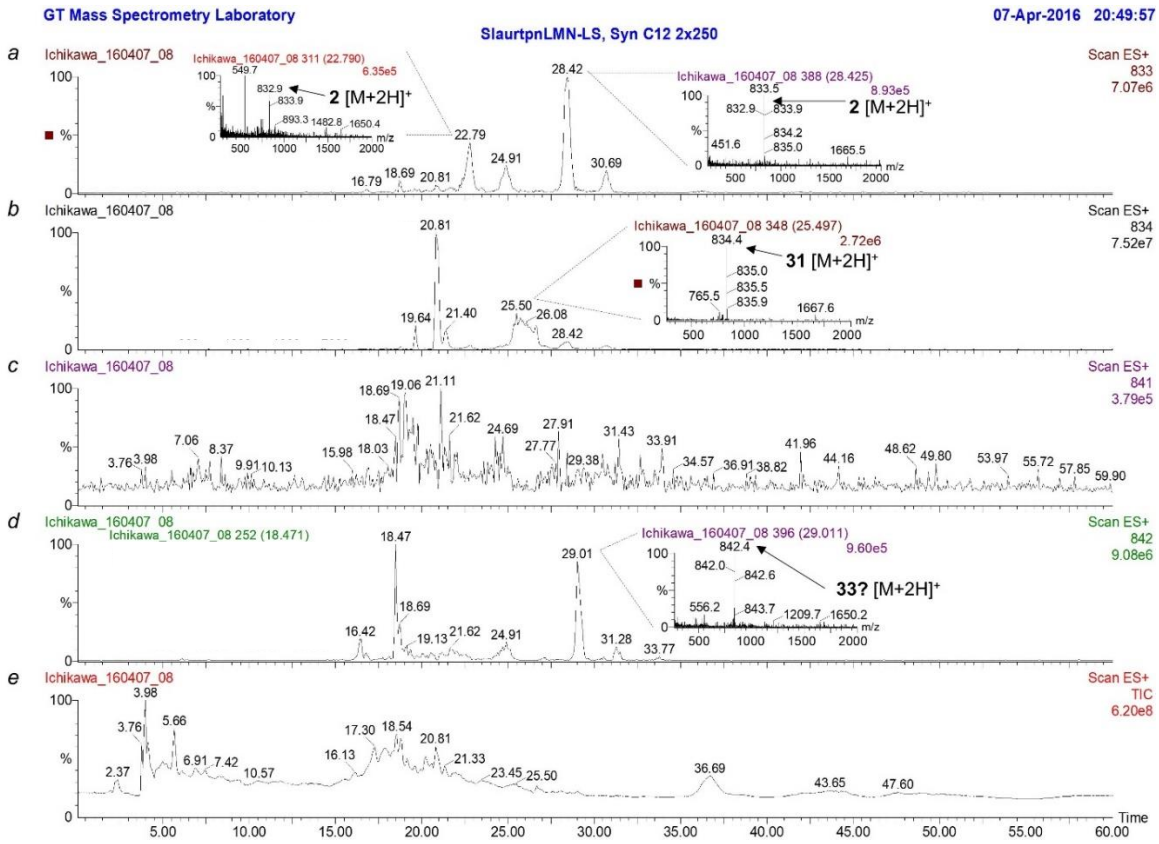

Figure B.12: HPLC-MS analyses of the crude culture extract from *S. laurentii* HI7, a strain that coexpresses TpnLMN. (*a*) Extracted ion chromatogram of *m/z* 833 thiostrepton A **2** (calculated $[M+2H]^+$ *m/z* = 832.8) and the mass spectra at t_R = 22.79 and t_R = 28.43 min (inset). (*b*) Extracted ion chromatogram of *m/z* 834 piperidine-containing thiostrepton analog **31** (calculated $[M+2H]^+$ *m/z* = 833.8) and the mass spectra at t_R = 20.81 and t_R = 25.50 min (inset). (*c*) Extracted ion chromatogram of *m/z* 841 thioamide-containing thiostrepton analog **32** (calculated $[M+2H]^+$ *m/z* = 840.7). (*d*) Extracted ion chromatogram of *m/z* 842 piperidine and thioamide-containing thiostrepton analog **33** (calculated $[M+2H]^+$ *m/z* = 841.8) and the mass spectrum at t_R = 29.01 min (inset). (*e*) Total ion chromatogram of the crude culture extract from *S. laurentii* HI7.

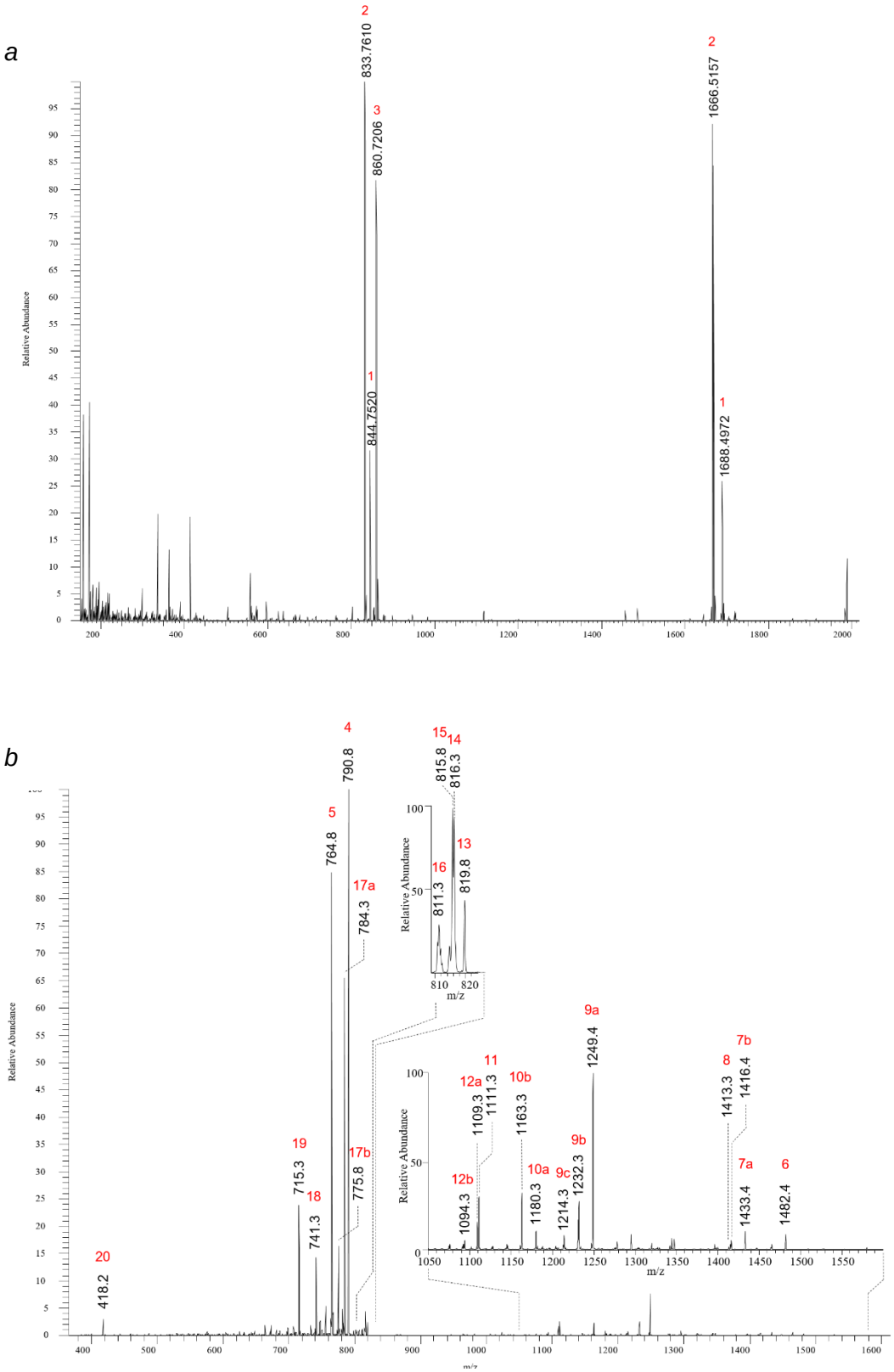

Figure B.13: MS analyses of thiostrepton A_a **31**. (*a*) ESI-MS analysis of thiostrepton A_a **31**. (*b*) ESI-MS/MS analysis parent ion *m/z* 833.8.

Table B.1: Key ions and fragments in ESI-MS and ESI-MS/MS of thiostrepton A_a **31**.

Fragment	Expected	Observed
1. $[M+Na]^+$	1688.4977	1688.4972
$[M+Na+H]^{2+}$	844.7528	844.7520
2. $[M+H]^+$	1666.5158	1666.5157
$[M+2H]^{2+}$	833.7618	833.7610
3. $[M+Mn]^{2+}$	860.7269	860.7206
4. $[M\text{-Dha3-OH}+2H]^{2+}$	790.8	790.8
5. $[M\text{-Dha17-Dha16}+2H]^{2+}$	764.8	764.8
6. $[M\text{-Ile1-Ala2}+H]^+$	1482.4	1482.4
7a. $[M\text{-Q}+H]^+$	1433.4	1433.4
7b. $[M\text{-Q-OH}+H]^+$	1416.4	1416.4
8. $[M\text{-Ile1-Ala2-Dha3}+H]^+$	1413.4	1413.3
9a. $[M\text{-Q-Ile1-Ala2}+H]^+$	1249.3	1249.4
9b. $[M\text{-Q-Ile1-Ala2-OH}+H]^+$	1232.3	1232.3
9c. $[M\text{-Q-Ile1-Ala2-OH-H}_2\text{O}+H]^+$	1214.3	1214.3
10a. $[M\text{-Q-Ile1-Ala2-Dha3}+H]^+$	1180.3	1180.3
10b. $[M\text{-Q-Ile1-Ala2-Dha3-OH}+H]^+$	1163.3	1163.3
11. $[M\text{-Q-Ile1-Ala2-Dha3-Dha17}+H]^+$	1111.3	1111.3
12a. $[M\text{-Q-Ile1-Ala2-Dha3-Ala4}+H]^+$	1109.3	1109.3
12b. $[M\text{-Q-Ile1-Ala2-Dha3-Ala4-OH}+H]^+$	1094.3	1094.3
13. $[M\text{-CO}+2H]^{2+}$	819.8	819.8
14. $[M\text{-OH-H}_2\text{O}+2H]^{2+}$	816.3	816.3
15. $[M\text{-2H}_2\text{O}+2H]^{2+}$	815.8	815.8
16. $[M\text{-CO-OH}+2H]^{2+}$	811.3	811.3
17a. $[M\text{-Ile1(CO)-Ala2}+2H]^{2+}$	784.2	784.3
17b. $[M\text{-Ile1(CO)-Ala2-OH}+2H]^{2+}$	775.7	775.8
18. $[M\text{-Ile1(CO)-Ala2-Dha3-OH}+2H]^{2+}$	741.2	741.3
19. $[M\text{-Ile1(CO)-Ala2-Dha3-Dha17}+2H]^{2+}$	715.2	715.3
20. $[Q\text{+Ile1+Ala2}+H]^+$	418.2	418.3

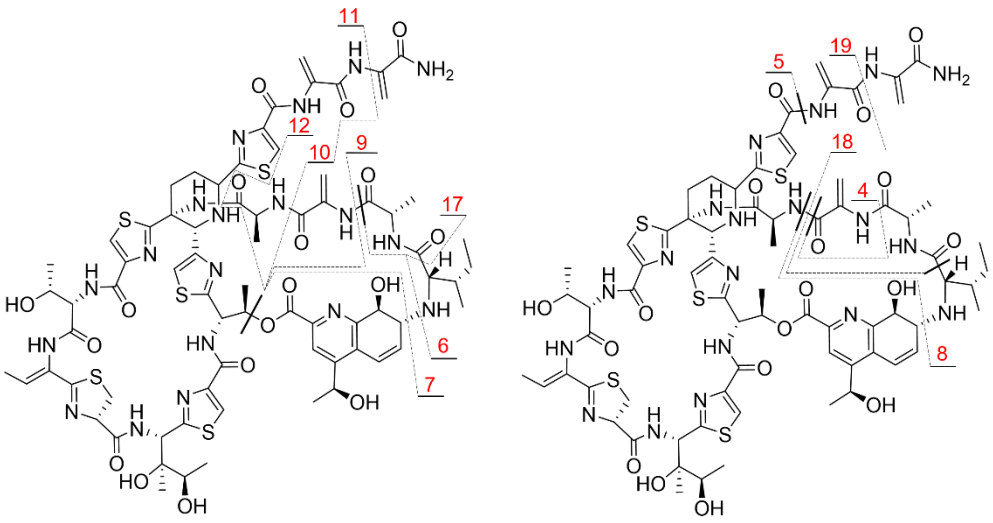

Figure B.14: The proposed structures of fragments of thiostrepton A_a **31** following MS/MS of parent ion *m/z* 833.8.

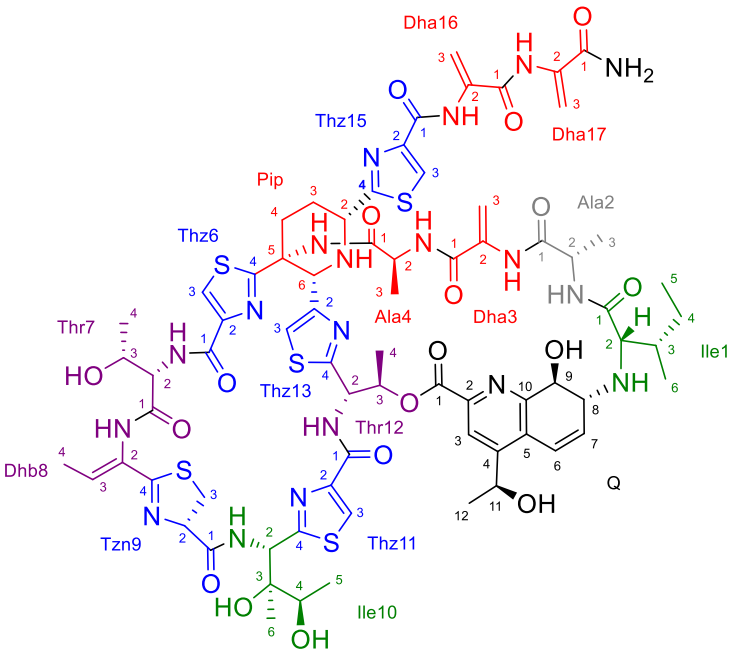

Figure B.15: Structure and numbering system used for thiostrepton A_a **31**.

Table B.2: ^{1}H and ^{13}C NMR assignments of thiostrepton A_a **31**.

Position	δ_c [ppm]; mult.	δ_H [ppm]; (mult, J in Hz)	HMBC[a]	COSY[b]
Ile1				
Ile1-1	173.7; C q			
Ile1-2	65.6; CH	3.12 (t, 4.6)	Ile1-1; Ile1-3; Ile1-4; Q-8	Ile1-3; Ile1-NH
Ile1-3	37.8; CH	1.76-1.73 (m)		Ile1-2; Ile1-4-H_A; Ile1-4-H_B; Ile1-6
Ile1-4	24.0; CH_2	H_A: 1.41-1.37 (m)	Ile1-3; Ile1-5; Ile1-6	Ile1-3; Ile1-4-H_B; Ile1-5
		H_B: 1.21-1.13 (m)	Ile1-2; Ile1-3; Ile1-5; Ile1-6	Ile1-3; Ile1-4-H_A; Ile1-5
Ile1-5	11.5; CH_3	0.81 (t, 7.3)	Ile1-3; Ile1-4	Ile1-4-H_A; Ile1-4-H_B
Ile1-6	15.7; CH_3	0.92 (d, 6.7)	Ile1-2; Ile1-3; Ile1-4	Ile1-3
Ile1-NH		2.39 (br s)		Ile1-2; Q-8
Ala2				
Ala2-1	172.3; C q			
Ala2-2	48.6; CH	4.48 (m)	Ala2-1	Ala2-3; Ala2-NH
Ala2-3	18.1; CH_3	1.27 (d, 7.0)	Ala2-1; Ala2-2	Ala2-2
Ala2-NH		8.53 (d, 4.2)	Ile1-1; Ala2-2	Ala2-2
Dha3				
Dha3-1	164.3; C q			
Dha3-2	135.7; C q			
Dha3-3	108.5; CH_2	H_A: 5.66 (s)	Dha3-1; Dha3-2	
		H_B: 5.51 (s)	Dha3-1	
Dha3-NH		7.91 (s)		
Ala4				
Ala4-1	172.0; C q			
Ala4-2	49.1; CH	4.60 (br s)		Ala4-3; Ala4-NH
Ala4-3	16.6; CH_3	1.30 (d, 8.1)	Ala4-1; Ala4-2	Ala4-2
Ala4-NH		8.45 (br s)		Ala4-2
Pip				
Pip-2	56.8; CH	4.68-4.66 (m)		Pip-3-H_A; Pip-3-H_B
Pip-3	28.1; CH_2	H_A: 2.12-2.08 (m)	Pip-5	Pip-2; Pip-3-H_B; Pip-4-H_A; Pip-4-H_B
		H_B: 1.70-1.65 (m)	Pip-2	Pip-2; Pip-3-H_A; Pip-4-H_A; Pip-4-H_B
Pip-4	30.6; CH_2	H_A: 3.06-3.02 (m)	Pip-2; Pip-6	Pip-3-H_A; Pip-3-H_B; Pip-4-H_B
		H_B: 2.63-2.58 (m)		Pip-3-H_A; Pip-3-H_B; Pip-4-H_A
Pip-5	60.5; C q			
Pip-5-NH		9.43 (br s)		
Pip-6	65.9; CH	4.76 (br s)		Pip-NH
Pip-NH		4.05 (br s)	Pip-5	Pip-2; Pip-3-H_A; Pip-6
Thz6				
Thz6-1	159.7; C q			
Thz6-2	148.6; C q			
Thz6-3	124.7; CH	8.00 (s)	Thz6-1; Thz6-2; Thz6-4	
Thz6-4	173.7; C q			
Thr7				
Thr7-1	168.1; C q			
Thr7-2	56.7; CH	4.63 (dd, 7.5, 4.3)	Thr7-1; Thr7-3; Thr7-4	Thr7-3; Thr7-NH
Thr7-3	66.2; CH	4.01- 3.97 (m)		Thr7-2; Thr7-3-OH; Thr7-4
Thr7-3-OH		5.23 (d, 2.1)		Thr7-3
Thr7-4	17.0; CH_3	0.82 (d, 7.0)	Thr7-2; Thr7-3	Thr7-3
Thr7-NH		7.81 (br s)		Thr7-2
Dhb8				
Dhb8-2	129.9; C q			
Dhb8-3	134.9; CH	6.40 (q, 6.7)	Dhb8-2; Dhb8-4; Tzn9-4	Dhb8-4
Dhb8-4	13.9; CH_3	1.77 (d, 6.9)	Dhb8-2; Dhb8-3; Tzn9-4	Dhb8-3; Dhb8-NH
Dhb8-NH		9.21 (s)	Thr7-1	Dhb8-4
Tzn9				
Tzn9-1	170.9; C q			
Tzn9-2	77.6; CH	5.31 (t, 8.2)	Thz9-1; Thz9-4; Dhb8-2	Tzn9-3-H_A; Tzn9-3-H_B
Tzn9-3	35.2; CH_2	H_A: 3.65 (t, 10.2)	Tzn9-1; Tzn9-2; Tzn9-4	Tzn9-2; Tzn9-3-H_B
		H_B: 3.51-3.47 (m)	Tzn9-1; Tzn9-2	Tzn9-2; Tzn9-3-H_A
Tzn9-4	168.5; C q			

Ile10				
Ile10-2	57.4; CH	5.37 (d, 8.9)	Tzn9-1; Ile10-3; Ile10-4; Ile10-6; Thz11-4	Ile10-NH
Ile10-3	74.9; C q			
Ile10-3-OH		5.47 (br s)	Ile10-2; Ile10-3; Ile10-4; Ile10-6	
Ile10-4	67.8; CH	3.56 (dq, 5.8, 5.7)	Ile10-3	Ile10-4-OH; Ile10-5
Ile10-4-OH		4.70 (d, 3.0)	Ile10-5	Ile10-4
Ile10-5	16.5; CH_3	1.06 (d, 6.1)	Ile10-3; Ile10-4	Ile10-4
Ile10-6	17.5; CH_3	0.76 (s)	Ile10-2; Ile10-3; Ile10-4	
Ile10-NH		8.78 (br s)		Ile10-2
Thz11				
Thz11-1	160.1; C q			
Thz11-2	146.5; C q			
Thz11-3	127.2; CH	8.39 (s)	Thz11-1; Thz11-2; Thz11-4	
Thz11-4	167.9; C q			
Thr12				
Thr12-2	53.3; CH	5.60 (t, 5.4)		Thr12-3; Thr12-NH
Thr12-3	70.1; CH	5.48-5.45 (m)		Thr12-2; Thr12-4
Thr12-4	13.9; CH_3	0.68 (br s)		Thr12-3
Thr12-NH		7.89 (br s)		Thr12-2
Thz13				
Thz13-2	153.0; C q			
Thz13-3	118.7; CH	7.94 (s)	Thz13-4	
Thz13-4	165.1; C q			
Thz15				
Thz15-1	159.3; C q			
Thz15-2	148.2; C q			
Thz15-3	125.3; CH	8.36 (s)	Thz15-1; Thz15-2; Thz15-4	
Thz15-4	175.6; C q			
Dha16				
Dha16-1	162.0; C q			
Dha16-2	134.9; C q			
Dha16-3	104.9; CH_2	H_A: 6.34 (s)	Dha16-1; Dha16-2	Dha16-3-H_B
		H_B: 5.69 (s)	Thz15-1; Dha16-1	Dha16-3-H_A; Dha16-NH
Dha16-NH		9.89 (s)	Thz15-1; Dha16-1; Dha16-3	Dha16-3-H_B
Dhb17				
Dha17-1	165.1; C q			
Dha17-2	135.0; C q			
Dha17-3	105.8; CH_2	H_A: 6.04 (s)	Dha17-1; Dha17-2	Dha17-3-H_B
		H_B: 5.68 (s)	Dha17-1; Dha17-2	Dha17-3-H_A
Dha17-NH		9.39 (s)	Dha16-1; Dha17-1; Dha17-3	Dha17-3-H_A; Dha17-3-H_B
Dha17-NH_2		H_A: 7.94 (s)	Dha17-1	Dha17-NH_B
		H_B: 7.51 (s)	Dha17-1; Dha17-2	Dha17-NH_A
Q				
Q-1	164.3; C q			
Q-2	144.1; C q			
Q-3	121.5; CH	8.17 (s)	Q-1; Q-2; Q-5; Q-11	
Q-4	151.5; C q			
Q-5	127.0; C q			
Q-6	120.9; CH	6.86 (dd, 10.2, 1.0)	Q-4; Q-5; Q-8; Q-7; Q-9; Q-10	Q-7; Q-8
Q-7	135.2; CH	6.36-6.34 (m)	Q-5; Q-8; Q-9	Q-6; Q-8
Q-8	59.9; CH	3.51-3.47 (m)	Q-6; Q-7; Q-9	Ile1-NH; Q-6; Q-7; Q-9
Q-9	73.2; CH	4.68-4.66 (m)	Q-5; Q-7; Q-8; Q-10	Q-8; Q-9-OH
Q-9-OH		5.11 (s)	Q-8; Q-9; Q-10	Q-9
Q-10	156.0; C q			
Q-11	64.1; CH	5.08 (dq, 5.7, 5.5)	Q-2; Q-3; Q-4; Q-12	Q-11-OH; Q-12
Q-11-OH		5.59 (d, 4.2)	Q-4; Q-11; Q-12	Q-11
Q-12	24.6; CH_3	1.31 (d, 6.6)	Q-4; Q-11	Q-11

[a] HMBC correlations are from the proton to the indicated carbon.
[b] COSY correlations are from the proton to the proton attached to the indicated position.

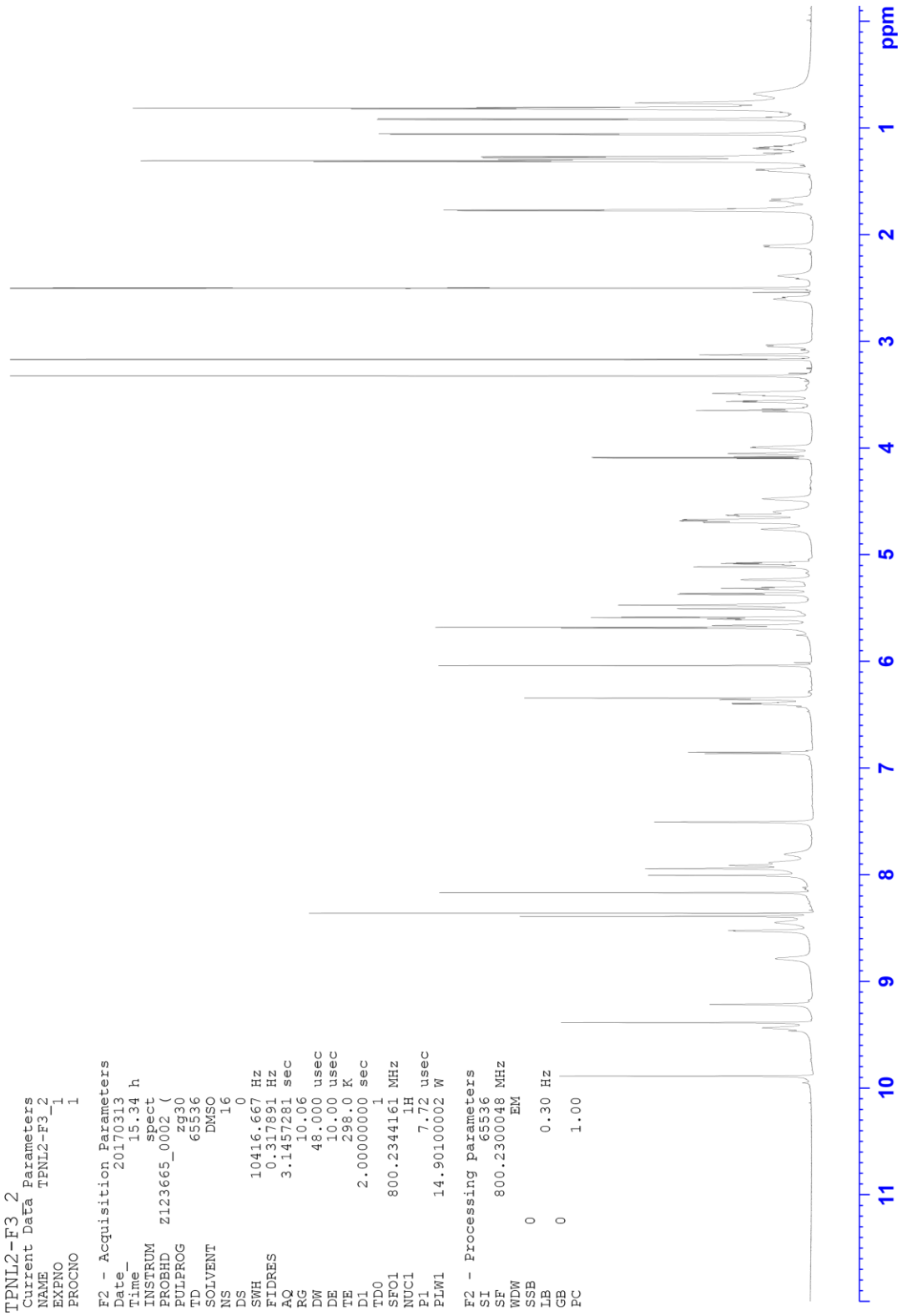

Figure B.16: ^{1}H NMR spectrum of thiostrepton A_a **31** (800 MHz, DMSO-d_6, 25 °C).

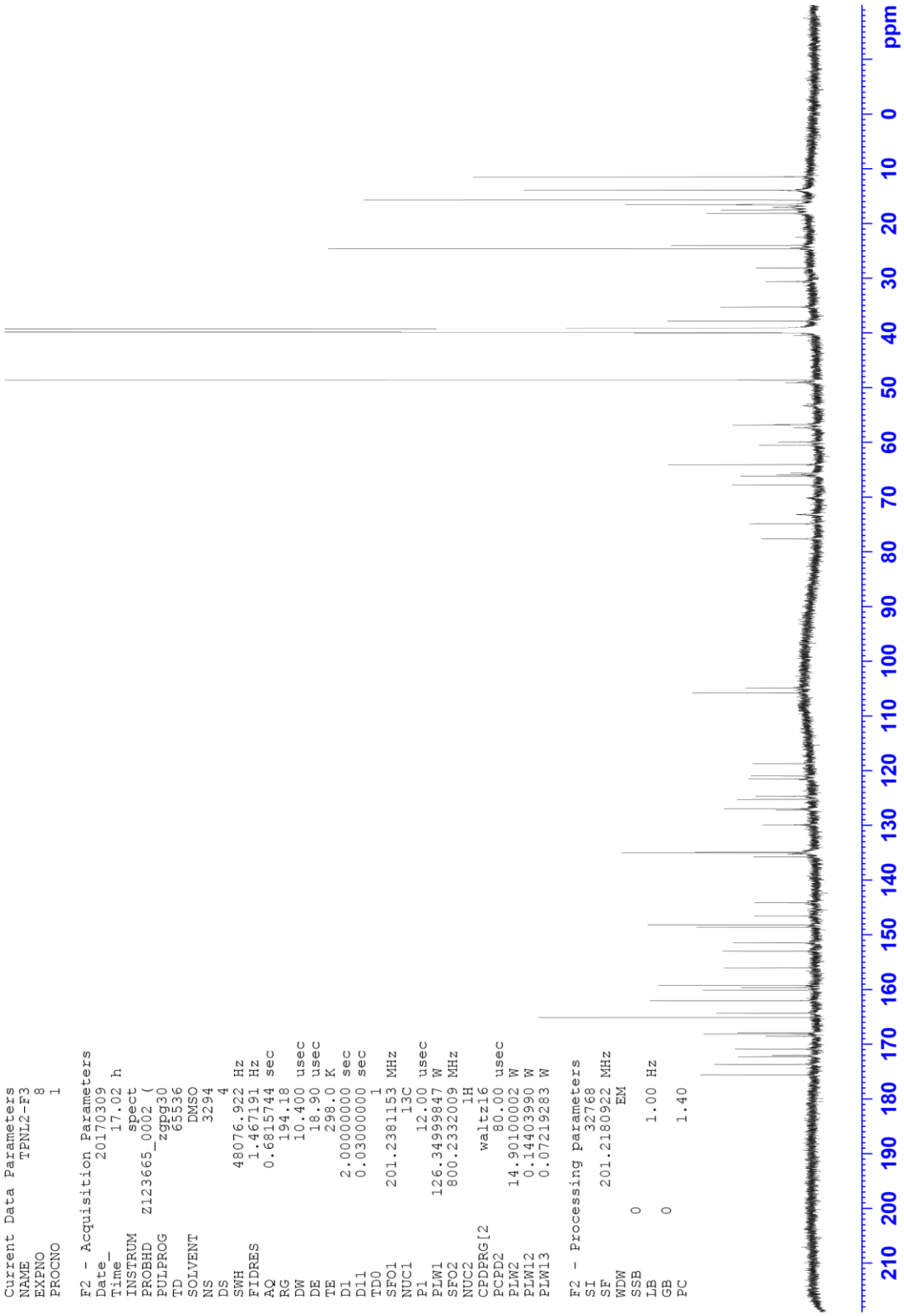

Figure B.17: ^{13}C NMR spectrum of thiostrepton A_a **31** (201 MHz, DMSO-d_6, 25 °C).

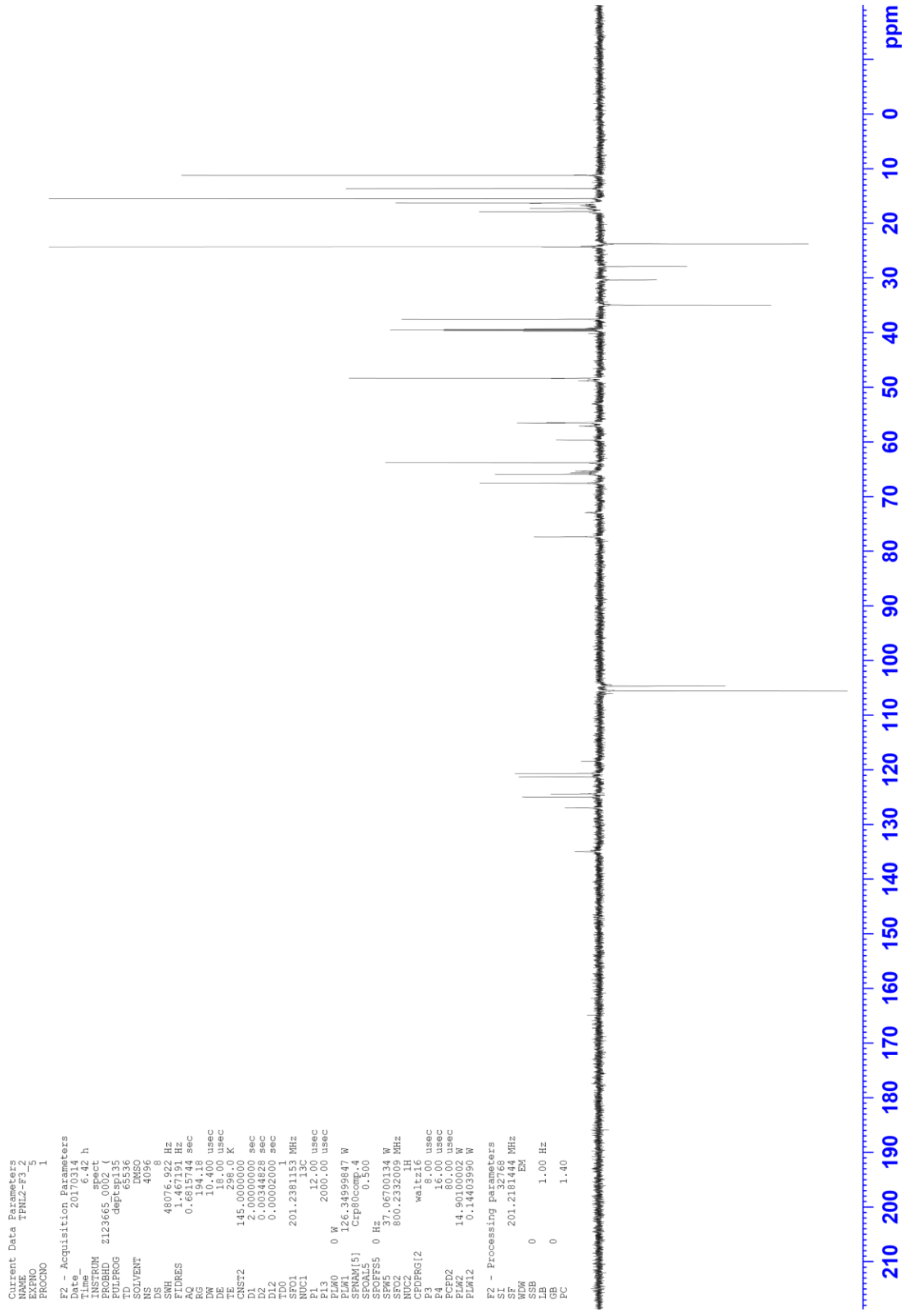

Figure B.18: DEPT-135 NMR spectrum of thiostrepton A_a **31** (201 MHz, DMSO-d_6, 25 °C).

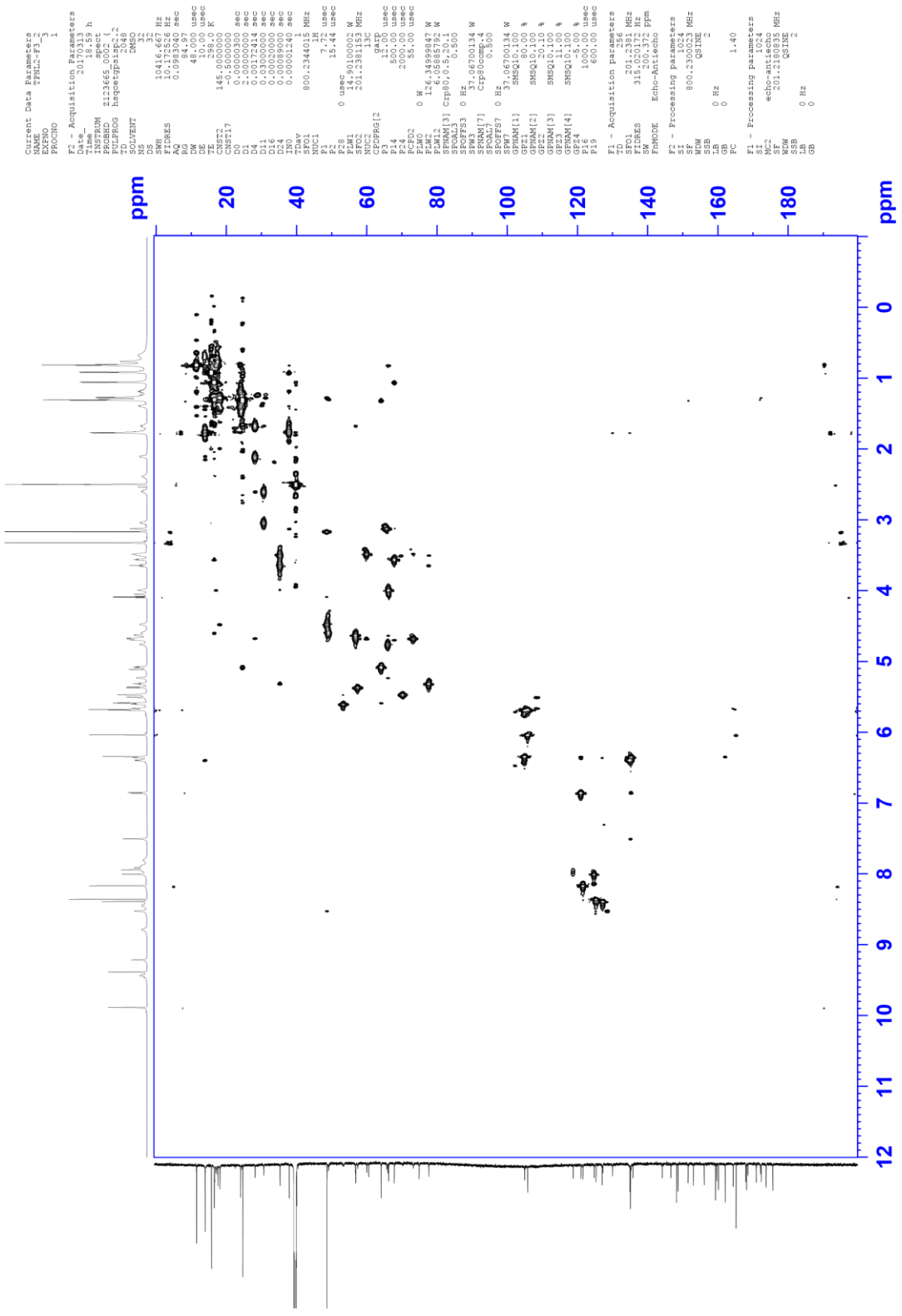

Figure B.19: gHSQC NMR spectrum of thiostrepton A_a **31** (800 MHz, DMSO-d_6, 25 °C).

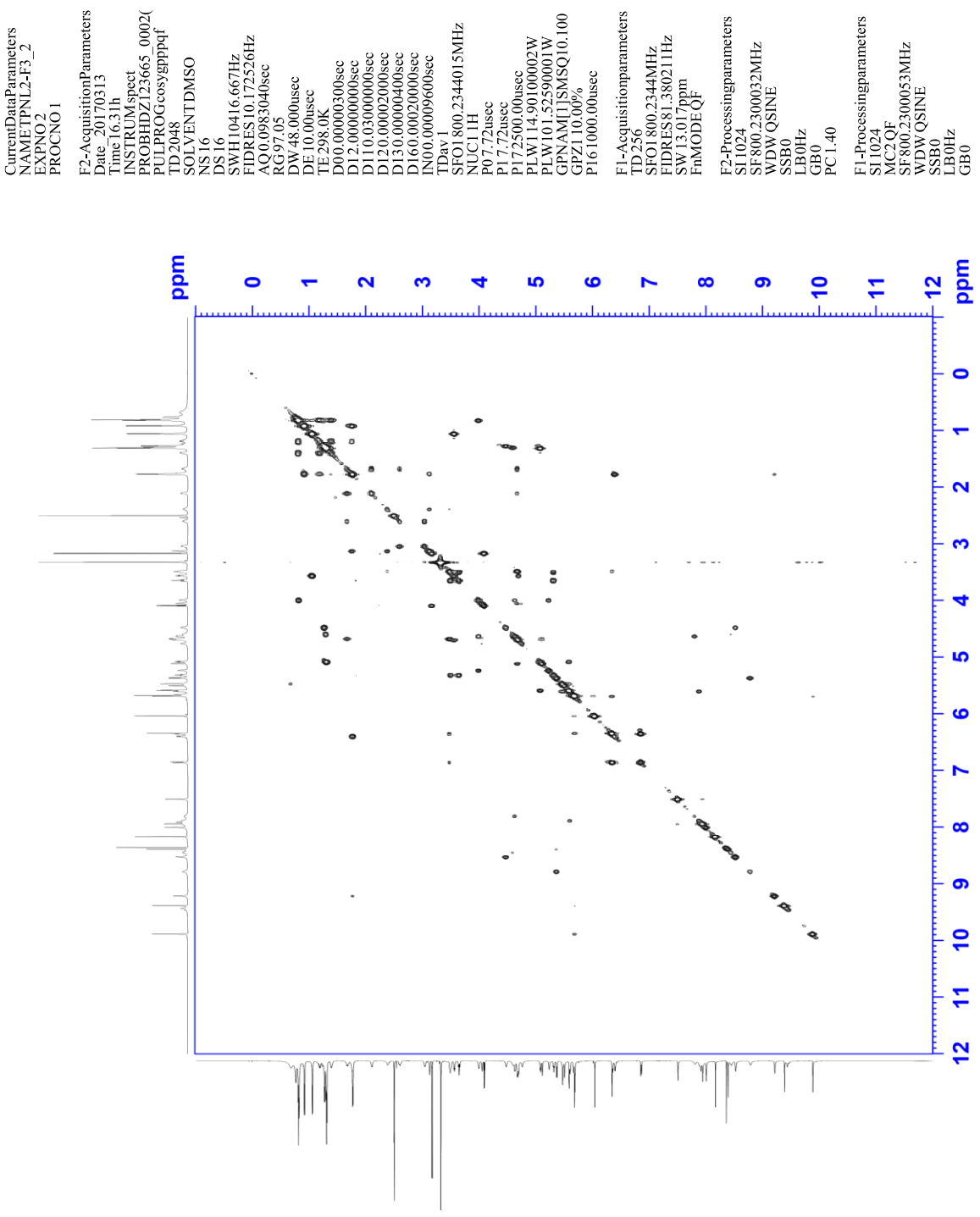

Figure B.20: gCOSY NMR spectrum of thiostrepton A_a **31** (800 MHz, DMSO-d_6, 25 °C).

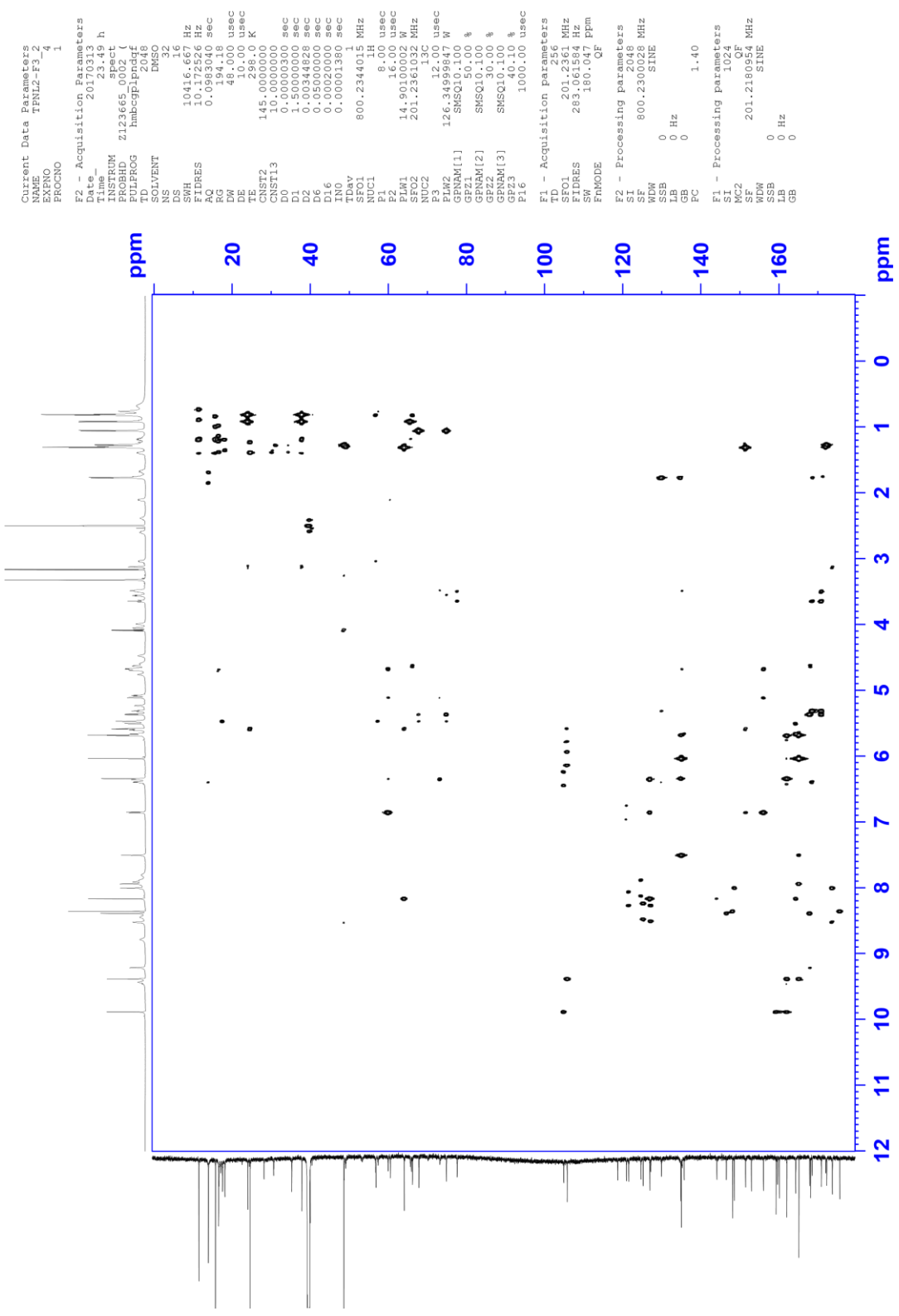

Figure B.21: gHMBC NMR spectrum of thiostrepton A_a **31** (800 MHz, DMSO-d_6, 25 °C).

Table B.3: ^{1}H-^{1}H ROESY correlations of the piperidine moiety of thiostrepton A_a **31**. Correlations used for the assignment of the configuration at Pip-2 is shown in blue.

	δ_H [ppm]; (mult, J in Hz)	**ROESY correlation**
Pip		
Pip-2	4.68-4.66 (m)	Pip-3-H_A; Pip-4-H_B; Pip-NH
Pip-3	H_A: 2.12-2.08 (m)	Pip-2-H; Pip-3-H_B; Pip-4-H_B
	H_B: 1.70-1.65 (m)	Pip-3-H_A; Pip-4-H_A
Pip-4	H_A: 3.06-3.02 (m)	Pip-4-H_B; Pip-3-H_B
	H_B: 2.63-2.58 (m)	Pip-2-H; Pip-3-H_A; Pip-4-H_A; Pip-6-H
Pip-5		
Pip-5-NH	9.43 (br s)	
Pip-6	4.76 (br s)	Pip-4-H_B; Pip-NH
Pip-NH	4.05 (bs s)	Pip-2-H; Pip-6-H

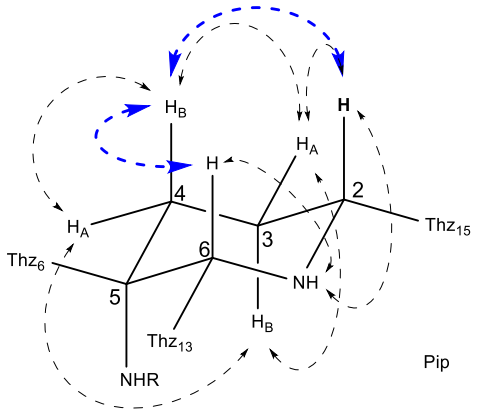

Figure B.22: The configuration of the piperidine moiety of thiostrepton A_a **31** overlaid with ROESY correlations. Correlations used for the assignment of the configuration at Pip-2 is shown in blue.

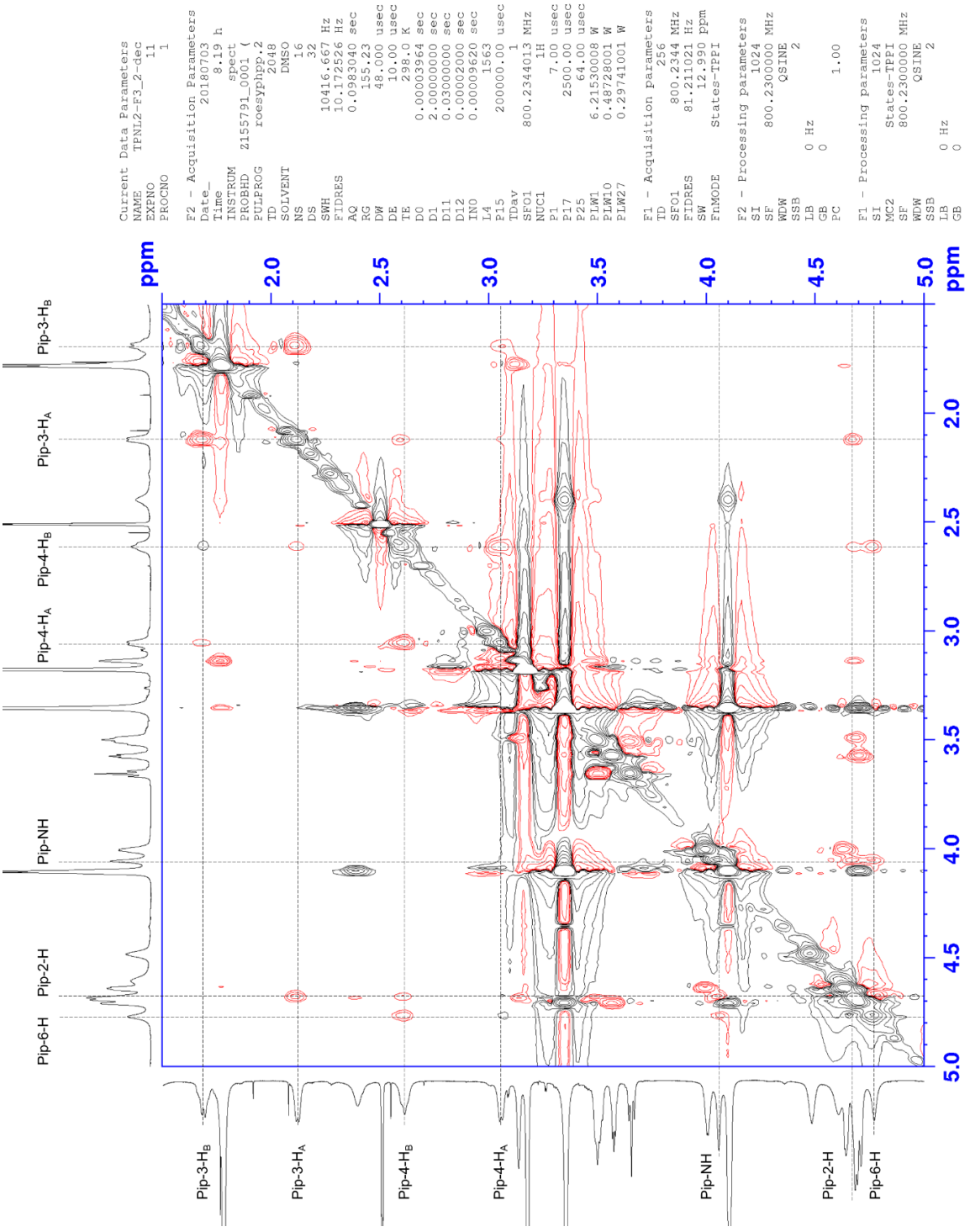

Figure B.23: ^{1}H-^{1}H ROESY NMR spectrum of thiostrepton A$_a$ **31** (800 MHz, DMSO-d_6, 25 °C). ^{1}H chemical shifts of the piperidine (Pip) moiety are indicated with dashed lines.

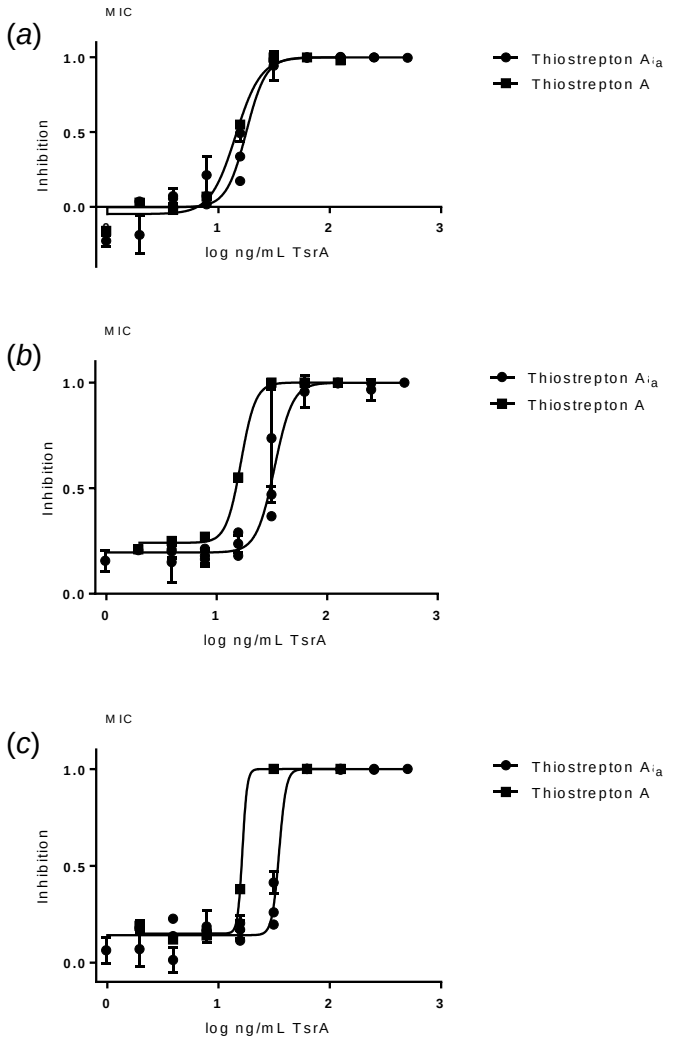

Figure B.24: Growth inhibition of *Bacillus* sp. by thiostrepton A **2** and A_a **31**. Results from three trials are shown. The MIC of thiostrepton A **2** was determined to be: (*a*) 0.0253 μg/mL, (*b*) 0.0231 μg/mL, and (*c*) 0.0182 μg/mL. The MIC of thiostrepton A_a **31** was determined to be: (*a*) 0.0278 μg/mL, (*b*) 0.0505 μg/mL, and (*c*) 0.0412 μg/mL.

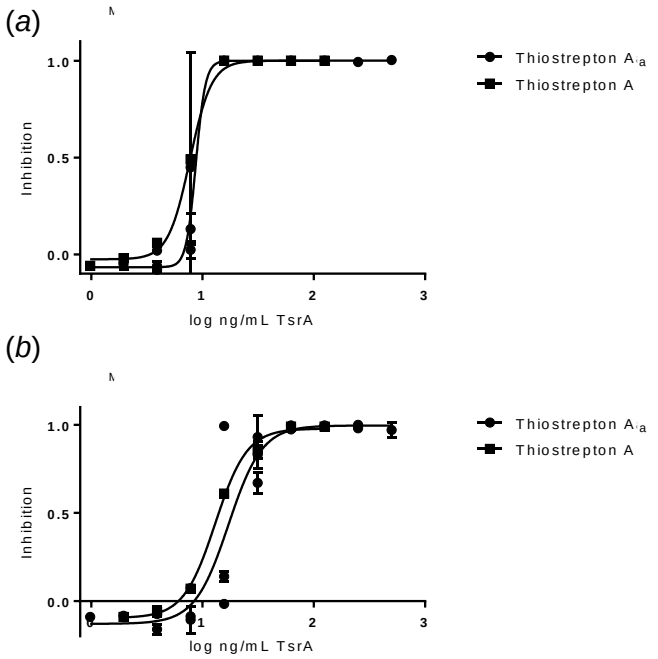

Figure B.25: Growth inhibition of vancomycin-resistant *Enterococcus faecium* (VRE) by thiostrepton A **2** and A_a **31**. Results from two trials are shown. The MIC of thiostrepton A **2** was determined to be: (*a*) 0.0126 μg/mL and (*b*) 0.0268 μg/mL. The MIC of thiostrepton A_a **31** was determined to be: (*a*) 0.0108 μg/mL,and (*b*) 0.0368 μg/mL.

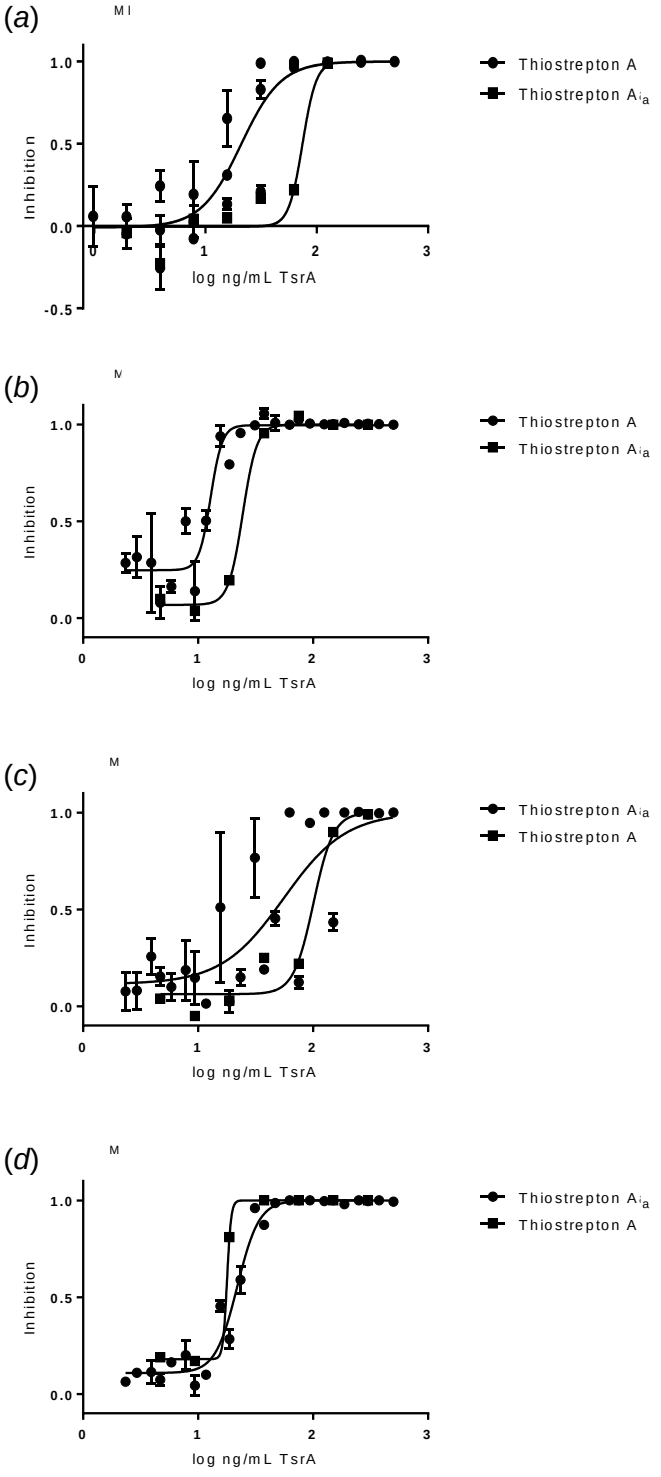

Figure B.26: Growth inhibition of methicillin-resistant *Staphylococcus aureus* (MRSA) by thiostrepton A **2** and A_a **31**. The MIC of thiostrepton A **2** was determined to be: (*a*) 0.0519 μg/mL, (*b)* 0.0166 μg/mL, (*c*) 0.1562 μg/mL, and (*d*) 0.0195 μg/mL. The MIC of thiostrepton A_a **31** was determined to be: (*a*) 0.1027 μg/mL, (*b*) 0.0334 μg/mL, (*c*) 0.2184 μg/mL, and (*d*) 0.0354 μg/mL.

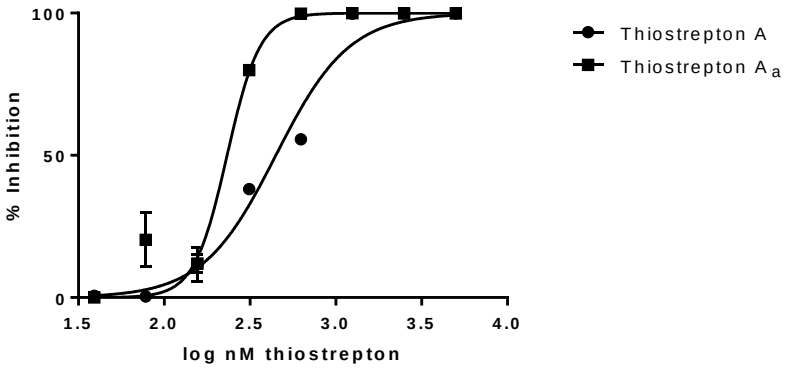

Figure B.27: Inhibition of prokaryotic ribosomal translation by thiostrepton A **2** and thiostrepton A_a **31**.

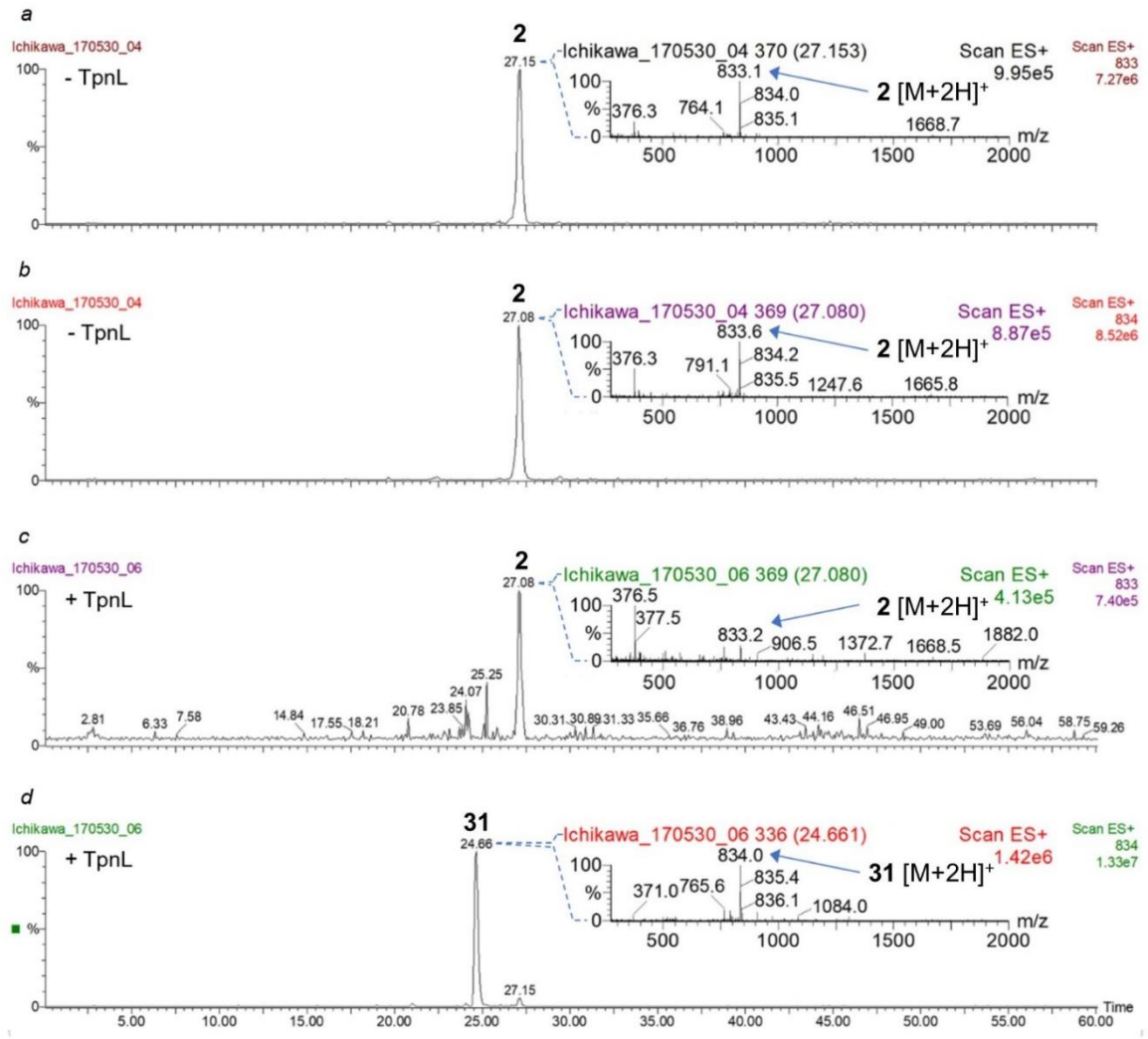

Figure B.28: HPLC-MS analyses of the *in vitro* reconstitution of TpnL activity after 1-hour incubation. (*a*) Extracted ion chromatogram of *m/z* 833 for thiostrepton A **2** (calculated $[M+2H]^{2+}$ *m/z* = 832.8) and the mass spectrum at t_R = 27.15 min (inset) of a reaction lacking TpnL. (*b*) Extracted ion chromatogram of *m/z* 834 for thiostrepton A_a **31** (calculated $[M+2H]^{2+}$ *m/z* = 833.8) and the mass spectrum at t_R = 27.08 min (inset) of a reaction lacking TpnL. (*c*) Extracted ion chromatogram of *m/z* 833 for thiostrepton A **2** and the mass spectrum at t_R = 27.08 min (inset) of a reaction containing TpnL. (*d*) Extracted ion chromatogram of *m/z* 834 for thiostrepton A_a **31** and the mass spectrum at t_R = 24.66 min (inset) of a reaction containing TpnL.